Factors that influence E. coli folate synthesis and their impact on C. elegans ageing

MAYNARD, CLAIRE,ALICE

FACTORS THAT INFLUENCE *E. COLI* FOLATE SYNTHESIS AND THEIR IMPACT ON *C. ELEGANS* AGEING

Claire A. Maynard

Submitted in accordance with the requirements

for the degree of Doctor of Philosophy

Department of Biosciences

Durham University

September 2017

ABSTRACT

Microbes can exert both positive and negative effects on animal health and longevity. The nematode worm, *Caenorhabditis elegans,* and its bacterial diet, *Escherichia. coli,* provide a simplified model to study animal-microbe interactions. Inhibiting *E. coli* folate synthesis has been found to increase *C. elegans* lifespan without any negative effects on either organism. Specifically disrupting worm folate uptake or metabolism was not found to influence lifespan and it was therefore hypothesized that a folate-dependent bacterial activity modulates ageing. This thesis aims to understand the factors that influence bacterial folate synthesis with the ultimate aim of understanding how bacterial folate affects *C. elegans* ageing.

Firstly, a folate-free defined media was developed in order to sensitively control bacterial folate synthesis and accurately measure bacterial and animal folate levels. *E. coli* folate was found to modulate *C. elegans* lifespan above the threshold for growth. Secondly, the impact of folic acid on bacterial folate synthesis was examined; LC-MS/MS detected degradation of folic acid into PABA-glu, where uptake of this folate precursor by *E. coli* AbgT boosted bacterial folate synthesis and was found to be responsible for decreasing *C. elegans* lifespan. This work highlighted a novel and harmful role of bacterial folate following folic acid supplementation.

An investigation into bacterial toxicity revealed a folate-dependent toxicity common to a pathogenic bacterium and the *E. coli* used here. The bacterial stress response transcriptional regulator, *rpoS,* was identified as a novel regulator of folate synthesis and a candidate mutant gene screen of the RpoS regulon for *C. elegans* longevity and low bacterial folate identified the *fic* gene as a possible mediator of folate-dependent toxicity. An examination into the timing of *E. coli* folate synthesis revealed a temporal window co-incident with exponential phase growth. Together, this work has provided several novel insights into the extrinsic and intrinsic factors that influence *E. coli* folate synthesis within the context of *C. elegans* ageing.

CONTENTS

LIST OF FIGURES

LIST OF ABBREVIATIONS

AbgA	p-aminobenzoyl-glutamate hydrolase subunit A
AbgB	p-aminobenzoyl-glutamate hydrolase subunit B
AbgT	para-aminobenzoyl glutamate transporter
ADC	4-amino-4-deoxychorismate
AMPK	AMP-activated protein kinase
cDNA	complementary strand DNA
CHES	N-cyclohexyl-2-aminoethanesulfonic acid
DHF	dihydrofolate
DHFR	dihydrofolate reductase
DHNP	7,8-Dihydro-D-neopterin
DHP	dihydropteroate
DHPS	dihydropteroate synthase
DM	defined media
DNA	deoxyribonucleic acid
DNase	deoxyribonuclease
dTMP	thymidine monophosphate
dUMP	deoxyuridine monophosphate
FEB	folate extraction buffer
FH	folate hydrolase
FPGS	folylpoly-γ-glutamate synthetase
GCPII	glutamate carboxypeptidase II
GF	germ free
GGH	g-glutamyl hydrolase
GI	gastrointestinal
GTP	guanine triphosphate
HEPES	2-[4-(2-hydroxyethyl)piperazin-1- yl]ethanesulfonic acid
HF	high fat
HGM	human gut microbiota
HPLC	high performance liquid chromatography
IBD	inflammatory bowel disease
IIS	insulin/insulin-like growth factor-1 signaling

LC-MS/MS	Ultra high performance liquid chromatography tandem mass spectrometry (here also indicating MRM)
LPS	lipopolysaccharide
MRM	multiple reaction monitoring
mRNA	messenger RNA
MS	mass spectrometry
mTOR	Mammalian target of rapamycin
MTX	methotrexate
NGM	Nematode growth medium
NTDs	neural tube defects
OD_{600}	optical density measured at 600nm
PABA	para-aminobenzoic acid
PabA	aminodeoxychorismate synthase component 2
PabB	aminodeoxychorismate synthase component 1
PabC	aminodeoxychorismate lyase
PAB-glu	para-aminobenzoyl- glutamate
PCFT	proton-coupled folate transporter
PCR	polymerase chain reaction
PEP	phosphoenolpyruvate
qPCR	quantitative real time PCR
RFC	reduced folate carrier
RNA	ribonucleic acid
RpoS	RNA polymerase sigma factor, RpoS
SHMT	serine hydroxymethyltransferase
SHMT	serine hydroxymethyltransferase
SMX	sulfamethoxazole
THF	tetrahydropteroyl glutamtic acid, or tetrahydrofolate
TLR	toll-like receptor
TNF-α	tumour necrosis factor α
WT	wild type

DECLARATION

I confirm that the original research described in this thesis is my own work. However, in the event that work was carried out by others, appropriate credit has been given within this thesis.

Some of the work within this thesis is published in:

Virk, B., Jia, J., Maynard, C.A., Raimundo, A., Lefebvre, J., Richards, S.A., Chetina, N., Liang, Y., Helliwell, N., Cipinska, M.*, et al.* (2016). Folate Acts in E. coli to Accelerate C. elegans Aging Independently of Bacterial Biosynthesis. Cell Rep *14*, 1611-1620 *these authors contributed equally

The work in this thesis was supported by the Biotechnology and Biological Sciences Research Council (BBSRC).

ACKNOWLEDGEMENTS

I would like to thank my supervisor, David Weinkove, for his support and encouragement throughout this PhD and for his lively approach to research. Thank you for helping to grow my confidence as a researcher and for making it fun at the same time. My thanks extends to the past and present members of the Weinkove lab for providing a creative and cooperative working environment. In particular, thank you to Sushmita Maitra, for your positive attitude and for teaching me all those invaluable things that you don't know you don't know. I would also particularly like to thank Ian Cummins, whose bioanalytical expertise with the LC-MS/MS, time and patience have helped pull this work together. Thank you to my secondary supervisor, Peter Chivers, for teaching me some microbiology skills in the early days and for useful discussions. Thank you to Jacalyn Green, the 'PABA Queen' whose insights have been invaluable. Thank you to Dana McGregor for all the qPCR tips. Formal thanks go to the BBSRC for providing the funding to make this project possible.

I would like to thank my parents, for their continued love and support, and to my siblings, Matthew and Olivia, for being the best role models a Bungry could hope for. To the past and present residents of the Kirkwood Sanctuary: Vanessa, Kasia, Sophie, Sanchita, Iain, Miriam and Olivia; thank you for providing equal measures of kindness, calm, madness and gin. I don't think I would have survived the last month without you.

Thank you to Durham for being a canny place to call home for the last seven years. It has provided a beautiful backdrop to mull over ideas and unexpected findings. Outings were always made more enjoyable when accompanied by Kath, with whom I have to thank for showing me that you always have room for one more hill; an attitude well applied to a PhD.

I must also thank the worms, who have always been there for me. Every day of the week. Finally, thanks go to the reader for taking the time to read this thesis; I do hope that you enjoy reading it and that it provides you with some interesting insights.

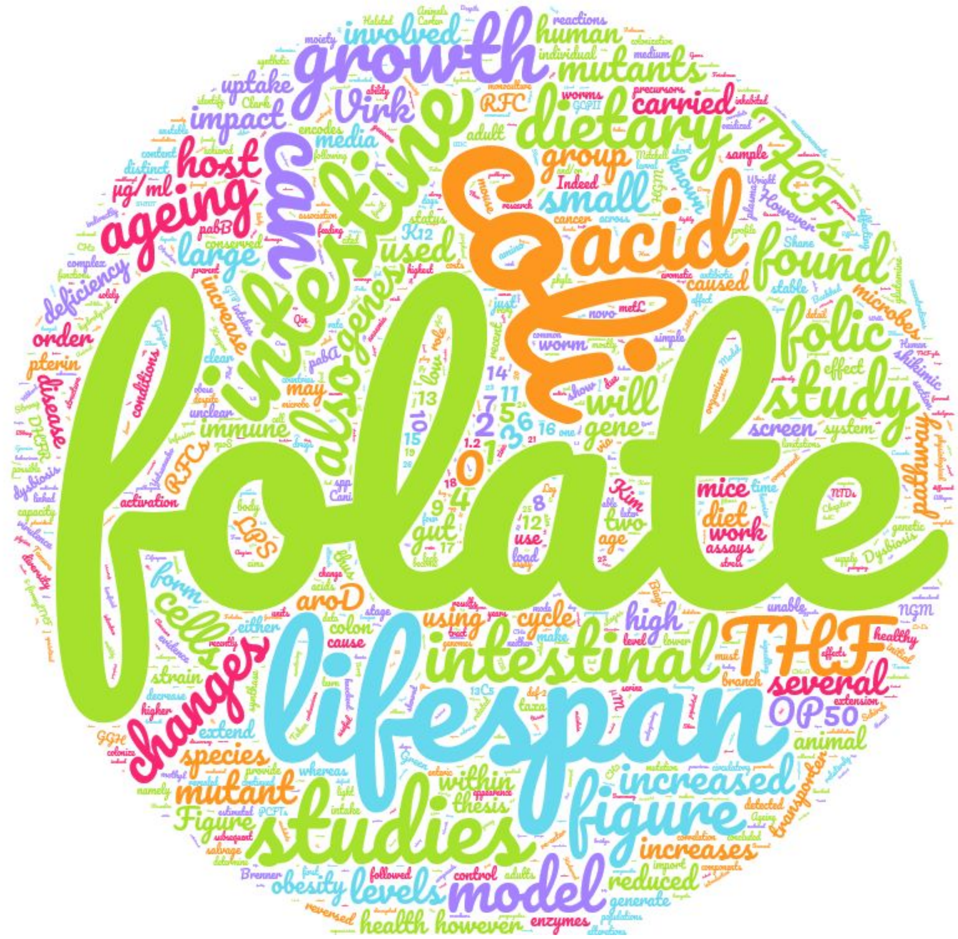
folate
lifespan
E. coli
acid
intestine
studies
growth
dietary
intestinal
THF
THFs
figure
model
ageing
found
folic
study
also
genes
changes
host
mutants
increased
cells
mutant
small
will
involved
impact
Virk
species
large
several
levels
increases
human
carried
group
known
high
pathway
transporter
animal
within
thesis
obesity
reduced
health
however
enzymes
generate
control
Figure
extend
strain
form
aroD
cycle
using
colon
diet
work
mice
gut
two
gene
screen
immune
deficiency
order
pterin
disease
conditions
uptake
media
used
status
K12
microbes
shikimic
caused
effect
system
increase
conserved
pabB
µg/ml
distinct
content
encodes
RFC
RFCs
LPS
OP50
worms
worm
precursors
medium
individual
reactions
sample
However
Indeed
cancer
adult
plasma
stable
simple
novo
metC
just
may
unclear
clear
pabA
activation
dysbiosis
Dysbiosis
NGM
unable
healthy
branch
taxa
extension
assays
age
use
load
time
Kim
Brenner
reversed
followed
adults
import
components
detected
species
salvage
subsequent
namely
whereas
provide
intake
PCFTs
cause
either
evidence
decrease
higher
GGH
colonize
complex
identify
Clark
moiety
Halsted
Carter
Animals
colonization
Shane
Wright
Mitchell
research
mouse
across
profile
genetic
supply
NTDs
Chapter
initial
effects
must
lower
level
make
stage
data
body
time
aromatic
antibiotic
affect
1.2
0
1
2
3
4
5
6
7
8
9
10
11
12
13
14
15
16
17
18
21

CHAPTER 1: INTRODUCTION

1.1 OVERVIEW

The thesis uses the well-established model organism, *Caenorhabditis elegans,* which is maintained in the laboratory in monoculture with a non-pathogenic strain of *Escherichia coli,* as an animal-microbe model to examine how bacterial folate affects animal ageing. Previous work discovered that inhibiting *E. coli* folate synthesis increases *C. elegans* lifespan (Virk et al., 2012), in a mechanism independent of worm folate metabolism and bacterial growth. This thesis combines a variety of microbiological, genetic and bioanalytical techniques in order to investigate the factors that influence bacterial folate synthesis, with the ultimate aim of understanding how bacterial folate affects *C. elegans* ageing.

The first section of this introductory chapter will discuss what is known about folates: synthesis, structure and function; bacterial folate synthesis in the microbiome; intestinal uptake and transport; health issues relating to folate deficiency and folate toxicity; and the methods used to quantify folates. The second section will discuss the composition and function of the human gut microbiome in relation to health, disease and ageing and the use of model organisms. The third section will introduce *C. elegans* as a model organism and discuss its use as a simplified model to study animal-microbe interactions and ageing. The final two sections will summarise the previous work carried out in the Weinkove laboratory and will discuss the key aims of this thesis.

1.2 FOLATE

The term 'folate' refers to a family of structurally related cofactors that donate and activate one-carbon units in a network of fundamental biosynthetic reactions known as one-carbon metabolism (Fox and Stover, 2008). Animals are unable to synthesize folate but can absorb plant-based dietary folate and folate synthesized by their intestinal microbiota (Visentin et al., 2014). Disruption to folate uptake, folate metabolism or inadequate dietary intake can cause folate deficiency, which is associated with several disorders and diseases (Lucock, 2000). Conversely, excess folate, which can be caused by folic acid supplementation, has also been associated with adverse health (Butterworth and Tamura, 1989; Kim, 2004; Shane, 2003). Despite being discovered as a family of essential vitamins over 70 years ago, the impact of both dietary and microbial folates on animal folate status and health and disease are not completely understood.

1.2.1 Structure and function

Folates are tripartite compounds (figure 1.1). The central aromatic compound, para-aminobenzoic acid (PABA), is linked by a methylene bridge to a pteridine ring, to form pteroic acid. The carboxyl group of PABA is conjugated to the amino group of an L-glutamic acid residue by a peptide bond. The active form of folate is reduced on its pteridine moiety to form tetrahydropteroyl glutamic acid, or tetrahydrofolate (THF) (Angier et al., 1948). THFs vary in one-carbon substitution at N5 (R1) and/or N10 (R2) nitrogen atoms of the pterin moiety, with either a methyl ($-CH_3$), formyl (-CH=O) methylene ($=CH_2$) or methenyl ($-CH_4$) group (figure 1.1) (Appling, 1991; Strong and Schirch, 1989). THFs are interconverted by the transfer and acceptance of these one-

carbon units in reactions catalysed by folate-dependent enzymes. These reactions are known collectively as one-carbon metabolism and facilitate the synthesis of purines, thymidylate, formylated methionyl-tRNA, the remethylation of homocysteine to methionine and the interconversion of glycine and serine (figure 1.2) (Fox and Stover, 2008).

THFs also vary in the length of their glutamate 'tail' which is formed enzymatically by gamma glutamyl bonds between the amino group and the carboxyl group of preceding glutamates (Qi et al., 1999; Turner et al., 1999). Polyglutamation increases the affinity of THFs as cofactors for folate-dependent enzymes and favours cellular retention (Egan et al., 1995; Schirch and Strong, 1989; Turner et al., 1999), whereas mono- and diglutamated THFs are favoured by transporters which facilitate intestinal and systemic transport (Baugh et al., 1971).

Folates are chemically unstable. Several studies have demonstrated that the methylene bridge linking PABA and pterin is prone to disassociation (in response to light, low pH, oxidation) to generate PABA-glu and pterin (De Brouwer et al., 2007; Gazzali et al., 2016; Gregory, 1989; Hanson and Gregory, 2011; Maruyama et al., 1978). PABA-glu can further disassociate to PABA and glutamate (Der-Petrossian et al., 2007; Thiaville et al., 2016). One-carbon substitution is thought to determine the stability of THFs; DHF and THF are the most unstable, followed by 5-methyl THF and 5-formyl THF is considered the most stable THF (Gregory, 1989; Hawkes and Villota, 1989). It is important to note that most of these studies have been carried out *in vitro* and little is known about the stability of THFs within cells.

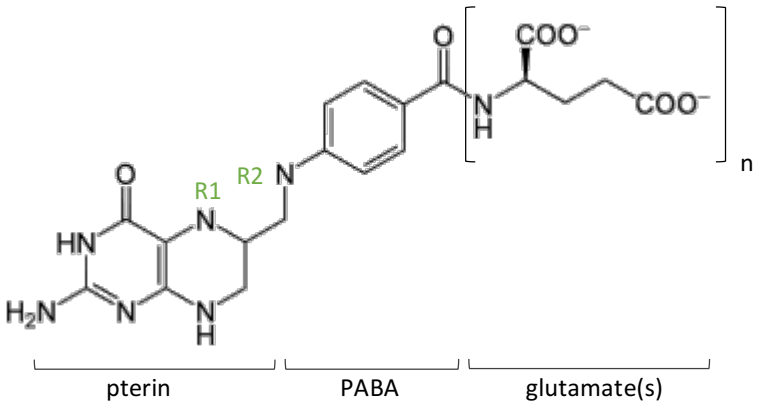

Tetrahydrofolate (THF)	R1	R2
5-methyl-THF	CH_3	H
5-formyl-THF	CHO	H
10-formyl-THF	H	CHO
5,10-methenyl-THF	=CH-	
5,10-methylene-THF	$-CH_2-$	

Figure 1.1 Structure of tetrahydrofolate (THF)

THFs are composed of pterin, PABA and glutamate. The pterin moiety is substituted at N5 (R1) and/or N10 (R2) nitrogen atoms with either a methyl ($-CH_3$), formyl (-CH=O) methylene ($=CH_2$) or methenyl ($-CH_4$) group. THFs also vary in the length of their glutamate 'tail', which varies in length depending on function.

1.2.2 Bacterial folate synthesis

1.2.2i Pathway of tetrahydrofolate synthesis

De novo folate synthesis does not occur in the animal kingdom. In bacteria such as *E. coli* that can synthesis folate, THF precursors are synthesized *de novo* in two separate branches: the PABA branch and the GTP/ pterin branch (Green and Matthews, 2007). The GTP/pterin branch synthesizes 6-hydroxymethyl-7,8-dihydropterin diphosphate (DHNDP) in a series of enzymatic steps using GTP as a precursor. The PABA branch synthesizes PABA in a two-step reaction from chorismate and glutamine. Chorismate itself is synthesized by the Shikimic acid pathway, which is responsible for the synthesis of aromatic amino acids and quinones, in addition to PABA (Green and Matthews, 2007) (figure 1.2).

The first reaction in the PABA branch is catalysed by the heterodimeric complex, 4-amino-4-deoxychorismate synthase, encoded by *pabA* and *pabB*, and forms the intermediate, 4-amino-4-deoxychorismate (ADC) (figure 1.2). PabA, a glutamine amidotransferase, hydrolyzes the ammonia group from glutamine, which is used by PabB along with chorismate, to form ADC (Green and Nichols, 1991). The second step is catalysed by aminodeoxychorismate lyase (PabC) (Green et al., 1992).

PABA and DHNDP are condensed enzymatically to generate dihydropteroate, by dihydropteroate synthase, which is then glutamylated to form dihydrofolate (DHF) and reduced to THF by dihdyrofolate reductase (DHFR) (figure 1.2) (Hoffbrand, 1975). Only DHFR is present in the animal kingdom.

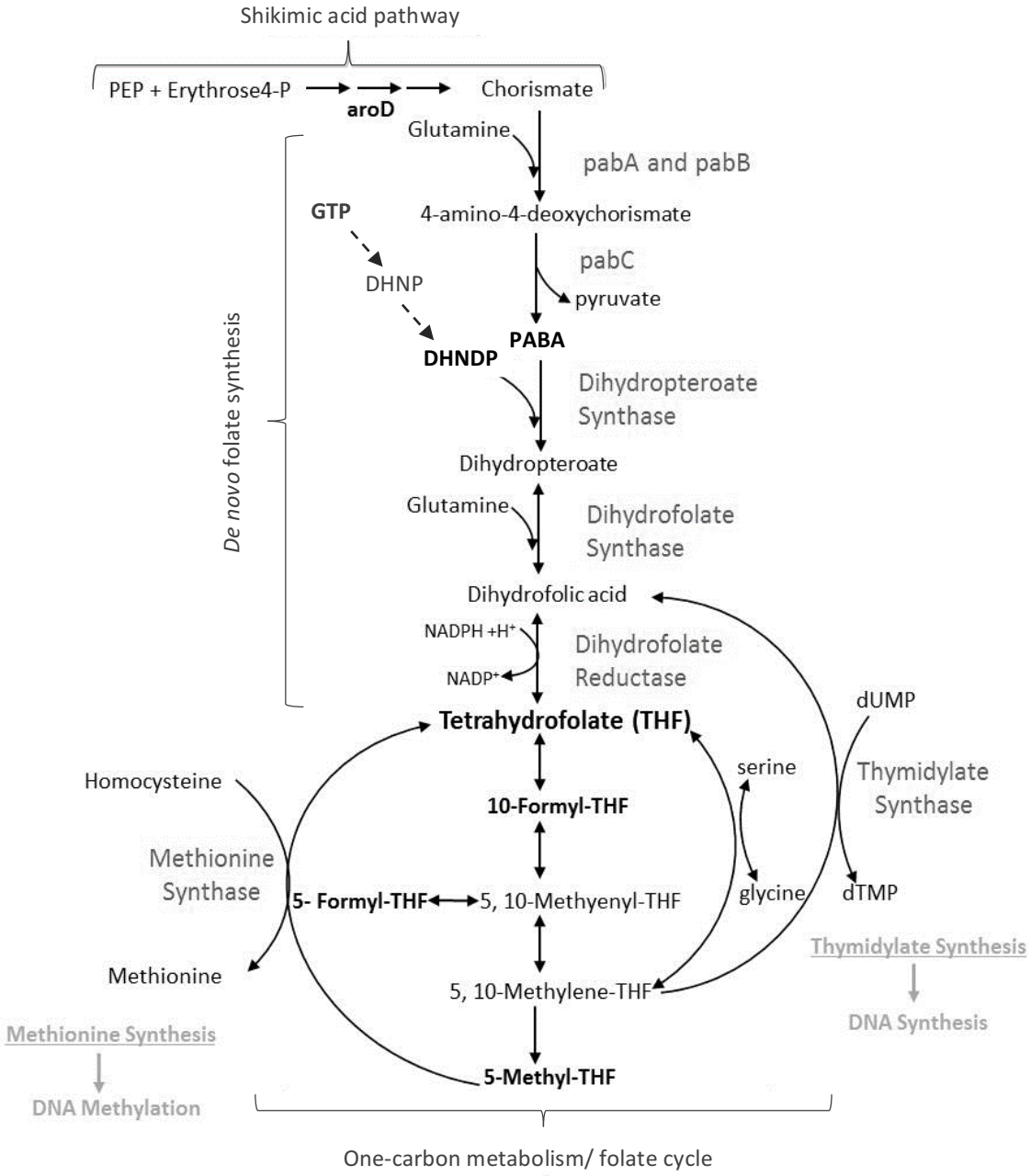

Figure 1.2 *E. coli* tetrahydrofolate synthesis and the one-carbon metabolism folate cycle. The folate precursors, para-aminobenzoic acid (PABA) (synthesized from chorismate and glutamine) and 6-hydroxymethyl-7,8-dihydropterin diphosphate (DHNDP) (synthesized from GTP) are conjugated to form dihydropteroate, which is glutamylated and reduced to form tetrahydrofolate. THF species are formed by the acceptance and transfer of one-carbon units in reactions that facilitate cellular biosynthesis and methylation. DHNP: 7,8-dihydroneopterin.

1.2.2 ii Bacterial folate uptake and salvage

The import and export of intact monoglutamated folates by bacteria is an established phenomenon (Shane and Stokstad, 1975), although in the vast majority of bacteria, transporters are yet to be identified. *E. coli* is unable to transport intact folate, but can use folate degradation and catabolism products, PABA or PABA-glu, as precursors for folate synthesis (Carter et al., 2007). PABA freely diffuses across biological membranes, but PABA-glu is transported via the specialized para-aminobenzoyl glutamate transporter, AbgT (Carter et al., 2007; Hussein et al., 1998). Once inside the cell, PABA-glu is cleaved by the heterodimeric glutamate carboxypeptidase protein, AbgA/B to generate free PABA that can be used for folate synthesis (Carter et al., 2007) (figure 1.3).

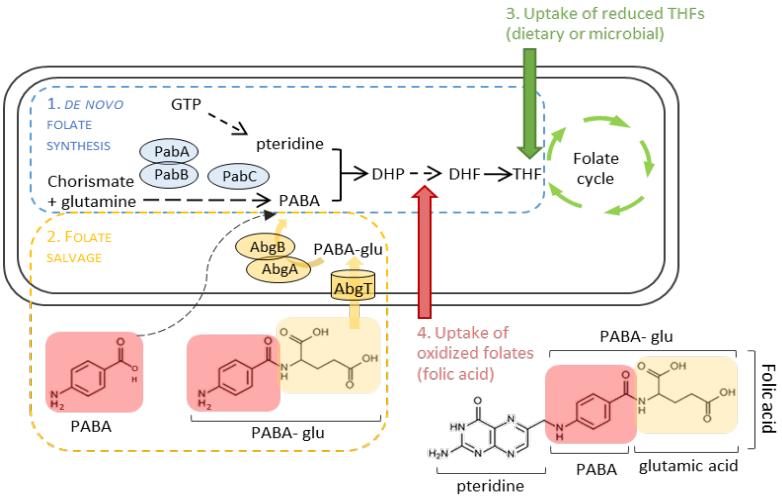

Figure 1.3 Diagram of a generalized bacterium illustrating the mechanisms via which bacteria can synthesize, import or salvage folate 1. *de novo* folate synthesis 2. Folate salvage of folate breakdown products, PABA and/ or PABA-glu 3. Uptake of exogenous THFs from dietary or microbial sources via transporters 3. Uptake of oxidized folates via transporters. *E. coli* is capable of pathways 1 and 2. PABA= para-aminobenzoic acid PABA-glu= PABA-glutamate; DHP= dihydropteroate; DHF= dihdyrofolate; THF= tetrahydrofolate

1.2.2iii Bacterial folate synthesis in the human intestine

In 1941, Mitchell and colleagues proposed that the compound they had isolated and concentrated from four tonnes of spinach leaves should be called 'folic acid' from the Latin, *folium*, meaning leaf. They also showed that this compound had vitamin activity in rats and suggested that it was likely to be synthesized by intestinal bacteria (Mitchell et al., 1941). *In vitro* studies followed which reported synthesis of 'folic acid' or folate by bacteria which normally inhabit the human intestine (Hutchings et al., 1941; Jukes and Stokstad, 1948; Lascelles and Woods, 1952; Miller and Rekate, 1944; Niven and Sherman, 1944). Subsequent *in vivo* animal studies indicated that folate synthesized by intestinal bacteria could compensate for induced dietary folate deficiency, although the role that coprophagy (the ingestion of faeces) played in rodent models here was unclear (Daft et al., 1963; Miller and Luckey, 1963).

Early studies in humans reported that folate synthesized by the colonic bacteria, where bacterial load is highest, exceeds dietary intake by 3-5 fold (Denko et al., 1946; Klipstein, 1967). More recent studies have verified that the human colon provides a large depot of absorbable monoglutamated folate which is indeed in excess of recommended dietary intakes (Kim et al., 2004; O'Keefe et al., 2009). Animal studies have demonstrated that folate can be incorporated into host tissues following infusion of [^{3}H] PABA, the bacterial folate precursor, into the cecum of conventionally raised rats (Rong et al., 1991) and piglets (Asrar and O'Connor, 2005). A similar study also using [^{3}H] PABA reported that bacterially synthesized folate in the small intestine also increases host folate status, as a result of bacterial overgrowth associated with

gastritis (Camilo et al., 1996). Together, these studies provide evidence that bacterially synthesized folate can be absorbed from the intestine and metabolized.

Recent advances in metagenomic technologies have enabled the folate synthesizing members of the human intestine to be identified. Magnusdottir et al. probed the B-vitamin synthetic capacity of 256 common human gut associated bacterial species (Magnusdottir et al., 2015). The complete *de novo* folate synthesis pathway was identified in 43% of bacterial genomes, including nearly all Bacteroidetes and most Fusobacteria and Proteobacteria, whereas folate synthesis was uncommon in Actinobacteria and Firmicutes genomes (Magnusdottir et al., 2015). Two similar studies focusing on intestinal-specific Lactobacilli and Bifidobacteria species revealed that most *Bifidobacterium* are able to synthesize folate *de novo,* whereas most *Lactobacillum* species only possess the enzymes involved in the later stages of folate synthesis and some only have DHFR (LeBlanc et al., 2013; Rossi et al., 2011). As all bacteria require folate to survive, this functional gap in the folate synthetic ability of gut microbes indicates a folate-dependent coevolution in the microbiota, suggesting that folate and precursors are actively exchanged between folate-synthesizers and folate-autotrophs, by the mechanisms outlined in figure 1.3.

1.2.3 Animal folate uptake and transport

1.2.3i Folate absorption in the intestine

There are two main folate carriers expressed in the gastrointestinal tract: the reduced folate carrier (RFC), which is expressed ubiquitously in the body and functions optimally at the higher pH of the large intestine (pH ~ 7.4) (Dixon et al., 1994; Dudeja

et al., 1997; Kumar et al., 1997); and the intestine-specific proton-coupled folate transporter (PCFT), which functions optimally at the lower pH of the proximal small intestine (pH ~ 5.5) (Qiu et al., 2006). At their optimal pHs, PCFT has a high affinity for both THFs (Km ~ 4 μM) and oxidized folates such as folic acid (Km ~ 1 μM), while RFC has a high affinity for THFs (K_t of 2–7 μM) and a low affinity for folic acid (K_i ~ 150–200 μM) (Dudeja et al., 2001; Matherly and Goldman, 2003; Whetstine et al., 2002; Zhao et al., 2009). It is generally accepted that dietary folates, like most micronutrients, are mainly absorbed in the small intestine by PCFT, where folate transporter expression is high and there are relatively few microbes competing with the host for absorption, whereas the majority of bacterially synthesized folate is absorbed in the large intestine by RFC (Balamurugan and Said, 2006) where microbial load is highest (figure 1.4) (Visentin et al., 2014).

The relative contributions of the small and large intestine to host folate status is unclear. The absorptive capacity of the large intestine has been examined by using infusion of a physiological dose of [$^{13}C_5$] 5-formylTHF into the cecum of patients undergoing colonoscopies (Aufreiter et al., 2009) and in a subsequent study by ingestion of [$^{13}C_5$] 5-formylTHF in a pH-sensitive enteric coated caplet by healthy adults (Lakoff et al., 2014). These two studies, carried out by the same group, monitored the appearance of plasma [$^{13}C_5$] 5-methylTHF formation by LC-MS/MS and concluded that the colon makes a significant contribution to host folate status (Aufreiter et al., 2009; Lakoff et al., 2014), but at an order of magnitude lower than the absorption of [$^{13}C_5$] 5-formylTHF across the small intestine as measured by similar studies (Wright et al., 2003; Wright et al., 2005).

Despite the large difference in the rate of absorption between the small and large intestine, the difference in net absorption is approximated to be much smaller due to the constant and excessive supply of bacterially synthesized folate in the large intestine, compared to the fluctuating supply in the small intestine. Furthermore, the transit time of material is estimated to be 20 times longer in the large intestine than the small intestine (Ghoshal et al., 2012; Kim, 1968).

1.2.3ii Folate deconjugation

Both PCFT and RFC preferentially import mono- and diglutamated folates (Halsted et al., 1986). As dietary and microbial folates are mostly polyglutamated derivatives, they must be deconjugated before they can be absorbed. In mammals, this is thought to be carried out by glutamate carboxypeptidase II (GCPII), which is expressed in the apical brush-border of the small intestine (Halsted et al., 1998). Monoglutamated folates can then be transported into enterocytes and exported vectorially across the enterocyte basolateral membrane into the hepatic portal vein (figure 1.4) (Wright et al., 2005). Monoglutamated 5-methyl THF is the main circulatory folate form and it is thought that dietary and microbial THFs are converted to 5-methyl THF in enterocytes (Pietrzik et al., 2010). It is not clear whether 5-methyl THF is exported by PCFTs or RFCs. The mechanism of uptake of the oxidized, synthetic monoglutamated folate supplement, folic acid, is not clear. Some studies suggests it is taken up in the small intestine by PCFT, but others indicate RFCs also play a role. It is not clear if folic acid is metabolized in enterocytes or in liver cells, to 5-methyl THF (Milman, 2012).

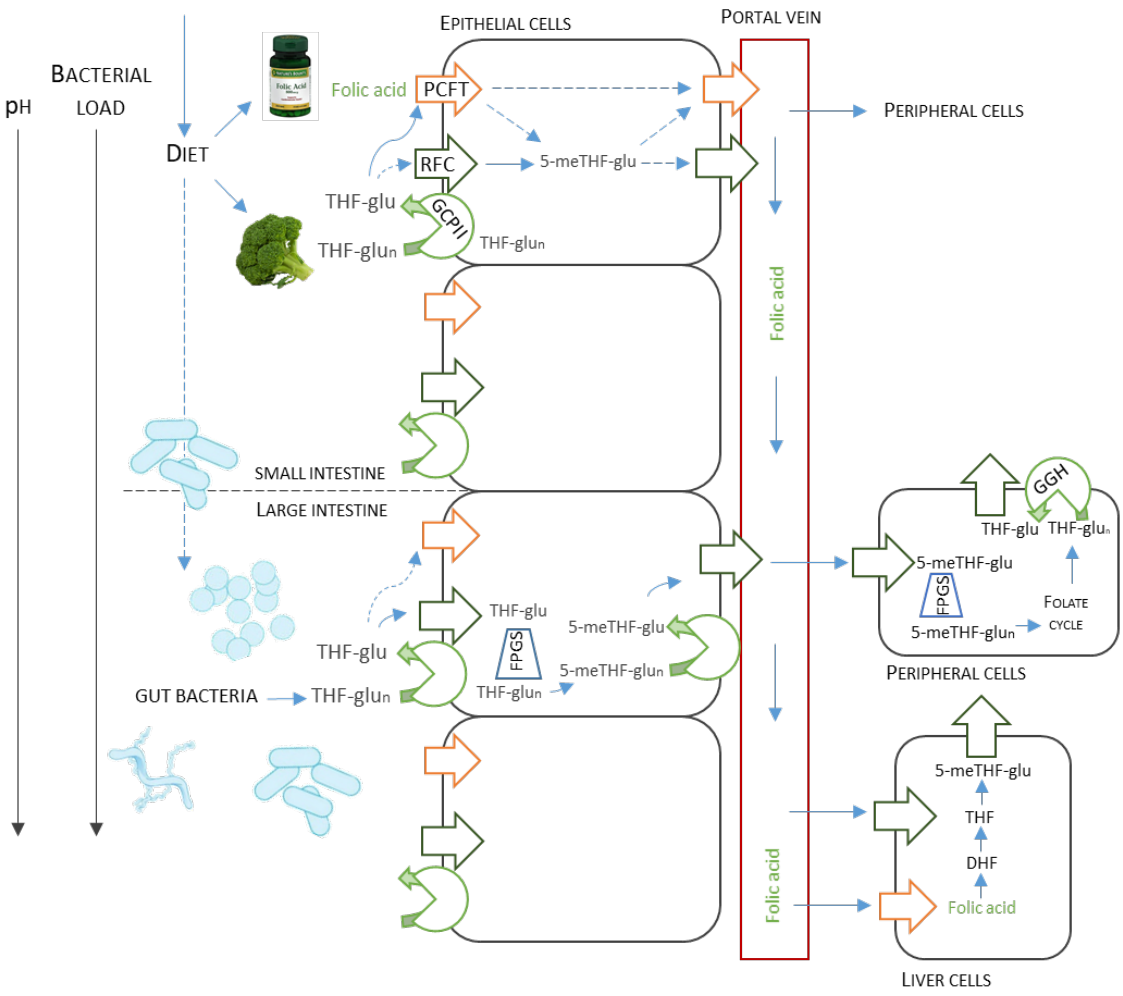

Figure 1.4 Model of intestinal uptake and metabolism of dietary and bacterial sources of folate. Animals obtain folate from their diet, intestinal bacterial and folate supplements, such as folic acid. The majority of dietary folates are absorbed in the small intestine by RFCs and PCFTs expressed in the apical membrane of the epithelium. These THFs are mostly polyglutamated and must be hydrolysed by GCPII into monoglutamated THFs before transport. Folic acid is monoglutamated and can be absorbed directly by PCFTs. Bacterial load is highest in the large intestine and bacterial folates synthesized here are thought to be transported by RFCs. The pH of the intestine increases proximally to distally, where pH favours PCFT function in the small intestine and RFC function in the large intestine. THFs are thought to beconverted into 5-methyl THF-glu in intestinal epithelial cells, before being exported (by either RFC or PCFT) into the hepatic portal vein. It is not clear whether folic acid

is metabolized in intestinal epithelial cells, but it is found in the liver after supplementation, where it is thought to be reduced by DHFR into THF and 5-methyl THF which can be exported to peripheral cells. Monoglutamated 5-methyl THF is transported into peripheral cells by RFCs, where it is polyglutamated by FPGS and converted into other THFs by enzymes in the folate cycle. THFs-glu_n are hydrolysed by GGH and exported by RFCs to re-enter circulation and be transported to other tissues. Dotted arrows indicate lower affinity of transporter. THF-glu, generic monoglutamted THF; THF-glu_n, generic polyglutamated THF; 5-meTHF-glu, 5-methylTHF; RFC, reduced folate carrier; PCFT, proton-coupled folate transporter; FPGS, folyl polyglutamate synthase; GCPII, glutamate carboxypeptidase II; GGH, gamma-glutamyl hydrolase.

1.2.3iii Folate polyglutmation

RFCs mediate the uptake of circulatory monoglutamated folate into systemic cells. Similarly to in enterocytes, FPGS activity then catalyzes the addition of subsequent glutamic acid residues to generate polyglutamated THFs, which are the preferred substrates for the folate-dependent enzymes involved in one-carbon metabolism (Allegra et al., 1987; Allegra et al., 1985; Schirch and Strong, 1989). Furthermore, THFs with glutamate chains where n>3, are no longer substrates for RFCs (Matherly and Goldman, 2003); FPGS activity therefore also aids cellular retention. In order to maintain a balance of THFs within the body, γ-glutamyl hydrolase (GGH) acts synergistically with FPGS to generate monoglutamated derivatives that can be exported out of cells to re-enter circulation (Egan et al., 1995; Garrow and Shane, 1993). See figure 1.4 for a model of folate uptake in the human intestine.

1.2.4 Folate deficiency and supplementation

1.2.4i Causes and effects

Failure to supply cells with sufficient THF cofactors has been associated with several health problems, including: anaemia, congenital birth defects such as neural tube defects (NTDs) (Hibbard, 1964; Hibbard et al., 1965), cardiovascular abnormalities and cancer (Bailey et al., 2015; Ebbing et al., 2009). As has been discussed, acquiring sufficient folate for one-carbon metabolism relies on a multitude of factors, including: dietary folate intake, intestinal folate biosynthesis, folate transporter efficiency, folate deconjugase and glutamation activity, and the activity of enzymes involved in one-carbon metabolism. Several of these processes can be disrupted by genetic

polymorphisms (Devlin et al., 2006; Fodinger et al., 2001; Winkelmayer et al., 2003), certain drugs (sulphonamides and anti-cancer drugs) (Goldberg, 1983; Halsted et al., 1981) and alcoholism (Tamura et al., 1981). Increased demand for folate during pregnancy can also exacerbate folate deficiency. Folate deficiency is therefore a multifactorial disorder, the pathogenesis of which is not completely understood (Boyles et al., 2006).

1.2.4ii Folic acid: supplementation and toxicity

In 1931, a substance in both Marmite and yeast that would later be identified as folic acid (Mitchell et al., 1941), was recognised by its ability to prevent megaloblastic anemia in pregnancy (Wills, 1931) (box 1). Following its synthesis in 1945 (Angier et al., 1945) and continued work by Wills during the Second World War, folic acid began to be used as a supplement to treat megaloblastic anaemia. The initial discovery of folic acid sparked the body of research concerning folates and their roles as cofactors in one-carbon metabolism.

Box 1. Who was Lucy Wills?

Lucy Wills *"is remembered as aristocratic, independent and radical in outlook, critical of established conservative medical and scientific committees. She rode to work on a bicycle rather than in a large car as did many of her colleagues" (Hoffbrand and Weir, 2001)*

In the early 90s, large-scale randomized trials of folic acid supplementation were carried out and together they concluded that folic acid supplementation before conception could reduce the risk of NTDs (1991; Berry et al., 1999; Czeizel et al., 1992) This led to the introduction of widespread folic acid fortification of grains

and cereals in 1998 in the US. Subsequent similar programmes were implemented in other countries, including Canada, Chile, South Africa and Jordan. Declines in the frequency of NTDs in these countries were reported (Imbard et al., 2013).

However, to date, no EU countries have adopted folic acid fortification programmes. This is because of uncertainties over whether an optimal dosage for an entire population can be achieved and concerns over folic acid toxicity (Butterworth and Tamura, 1989). Indeed, folic acid supplementation has been linked to several health complications, including: zinc deficiency caused by impaired absorption in the intestine (Milne et al., 1984); progression of neurological damage in megaloblastic anaemia due to masking of the signs of B12 deficiency (Selhub et al., 2009); and an increased risk of colon cancer (Cole et al., 2007; Kim, 2004). Furthermore, two mouse studies have reported that excessive folic acid supplementation may *disrupt* embryonic development (Marean et al., 2011; Pickell et al., 2011).

The association of folic acid supplementation with colorectal cancer is unclear; several independent meta-analyses have failed to reach a unanimous conclusion (Carroll et al., 2010), (Fife et al., 2011), (Qin et al., 2015). One epidemiological study has reported a temporal association between the introduction of folic acid fortification in the US and Canada with increased incidences of colon cancer (Mason et al., 2007); however, another study reported that incidences have continued to decline (Edwards et al., 2010).

1.2.5 Quantification of folates

Quantifying folate levels is important for clinicians and nutritionists; however, several factors make this intrinsically difficult. As described, folates exist as interconvertible THF derivatives and are unstable and sensitive to light, pH and temperature. In the 1930s, a microbiological assay was developed to measure the level of active folate within a given sample (Baker et al., 1959). The growth of the folate-auxotroph, *Lactobacillus casei,* is used as a readout, however the sample must be first hydrolysed by GGH in order to convert all polyglutamated folates into transportable monoglutamated folates. This assay therefore does not provide information on the polyglutamation profile and cannot differentiate between individual folate derivatives within a sample.

Protein binding assays were developed in the 1970s and 1980s as a more simple, rapid and effective means to measure folate levels within a sample. Later, automated assays were developed for use clinically and are still used today (Gregory, 1982). Whilst these assays are not sensitive to antibiotics and anti-folate drugs, they are subject to the same limitations as the microbiological assays and therefore cannot differentiate between specific folate derivatives (Shane et al., 1980). Nevertheless, the use of these assays has guided the recommended dietary intakes for folate and the concentrations of folate supplements. It is suggested that the insensitivity of these methods has led to over-estimations of recommended intakes (Ringling and Rychlik, 2017).

More recently, bioanalytical techniques using (ultra) high performance liquid chromatography (HPLC) coupled to mass spectrometry (MS) have been developed and made it possible to identify individual folate species within a sample (McDowell et al., 2008). Several LC-MS methods are outlined in the literature and differ in their chromatography mode (reversed phase or hydrophilic interaction chromatography), ionization mode (positive or negative) and mass spectrometry detection mode (MS-only or tandem MS) (Meadows, 2017). These methods are becoming more common, but require high initial set-up costs, expensive reagents and procedures are time-consuming. In light of this, the microbiological assay remains the method by which recommended dietary folate intakes are set. In this thesis, a LC-MS method coupled to a multiple reaction monitoring (MRM) technique has been used to achieve highly specific and sensitive folate detection in *E. coli* and *C. elegans* extracts. This will be described in more detail in Chapter 3.

1.3 THE HUMAN GUT MICROBIOME

Microbes have evolved to occupy nearly every ecological niche on Earth, including multicellular organisms (Lozupone and Knight, 2007).(Ebbing et al.) In humans, microbes inhabit the skin, the oral cavity and airways, the urogenital area and the gastrointestinal (GI) tract (Human Microbiome Project, 2012). These diverse and distinct communities consist of bacteria, archaea, fungi, viruses and protists, and are referred to as 'microbiotas', whilst their collective genomes within a defined ecosystem are termed 'microbiomes' (Lederberg and McCray, 2001; Marchesi and Ravel, 2015). Animals represent a nutrient rich and stable ecosystem for microbes to

thrive, and microbes benefit the host by digesting complex dietary carbohydrates, providing essential micronutrients, and supporting the development and function of the immune system (Marchesi et al., 2016). The human gut microbiota (HGM) is one of the most densely populated ecosystems on the planet, where the number of bacterial cells reaches up to 100 trillion cells in the colon and its genetic capacity is estimated to outnumber that of the human genome by 2 orders of magnitude (Qin et al., 2010).

1.3.1 Composition, structure and function

Recent advances in culture-independent sequencing technologies have enabled identification of the bacterial taxa which make up the HGM (Ebbing et al.; Human Microbiome Project, 2012). Studies agree that Firmicutes and Bateriodetes are the dominant phyla, followed by Proteobacteria and Actinobacteria (Human Microbiome Project, 2012; Ley et al., 2006; Yatsunenko et al., 2012). Over 1000 bacterial species have been associated with the HGM across different studies, with each individual predicted to host around 160 (Qin et al., 2010). Efforts to characterize the core bacterial constituents of a 'healthy' gut microbiota have been complicated by extensive interpersonal variation at species and strain level identified in these studies, however, metagenomic studies have suggested that the HGM is conserved at the functional level (Shafquat et al., 2014; Turnbaugh et al., 2009).

It has been proposed that the colonization of bacteria with specific functions into distinct spatial niches along the GI tract is driven by proximal- distal gradients of pH, oxygen, nutrient availability and the host secretion of antimicrobial peptides and bile

acids (Tropini et al., 2017). The small intestine is mainly inhabited by fast-growing facultative anaerobes that compete with host epithelial transporters for dietary nutrients (Donaldson et al., 2016). In contrast, the large intestine has a higher species diversity, is more densely populated (Booijink et al., 2010) and is inhabited by anaerobic species which metabolize the indigestible components of our diet, such as complex carbohydrates and oligosaccharides and generate easily absorbable, high energy short-chain fatty acids (Macfarlane and Macfarlane, 2003). As has been discussed, inhabitants of the colon synthesize essential amino acids and vitamins, including folate (Flint, 2012). Latitudinal microhabitats created by the secretion of mucin by the host epithelia play an important role in immune function (Pereira and Berry, 2017).

A healthy gut microbiota is also inhabited by a low abundance of enteric pathogens, or 'pathobionts'. Studies suggests that pathobionts are tolerated as they are directly suppressed by other beneficial or 'commensal' bacteria, and indirectly through the bacterial induction of host immune regulatory action (Kamada et al., 2013). The majority of pathobionts belong to families of the Proteobacteria phylum, particularly Enterobactericaeae (*E. coli, Yersinia spp., Salmonella spp., Shigella spp*.), and also Vibrionaceae (*Vibrio cholerae*) and Campylobacteriaceae (*Campylobacter spp*.) (Shin et al., 2015).

1.3.2 Dysbiosis and disease

Disruption to the spatial structure and composition of the healthy microbiota has been termed 'dysbiosis' (Tamboli et al., 2004). Dysbiosis can be caused by intrinsic

factors (genetics, disease, ageing) and extrinsic factors (dietary changes, antibiotic treatment, stress, smoking) and is associated with decreased bacterial diversity, where commensal bacteria decrease in abundance and the abundance of pathobionts increases (figure 1.5) (Mukhopadhya et al., 2012; Nagao-Kitamoto et al., 2016). Indeed, Proteobacteria have been coined the 'microbial signature of dysbiosis' in the microbiota (Shin et al., 2015)

Dysbiosis is associated with distinct changes in gut morphology, such as the breakdown of barrier function and the activation of host inflammatory immune signalling pathways (Vindigni et al., 2016). This is thought to create a favourable environment for the further colonization of enteric pathogens and the propagation and progression of pathogenesis (figure 1.5). Dysbiosis has been associated with several intestinal diseases, such as inflammatory bowel disease, colon and stomach cancer (Carding et al., 2015). There is increasing evidence that dysbiosis is also associated with extra-intestinal disorders, such as: obesity (Backhed et al., 2004; Ley et al., 2005), type II diabetes (Navab-Moghadam et al., 2017), cardiovascular disease (Fava et al., 2006) and even autism (Williams et al., 2011) and anorexia (Kleiman et al., 2015). There has been extensive work carried out to characterize the compositional changes in disease-associated microbiomes, however, descriptive studies have been unable to demonstrate a causal link between these changes and the progression of disease.

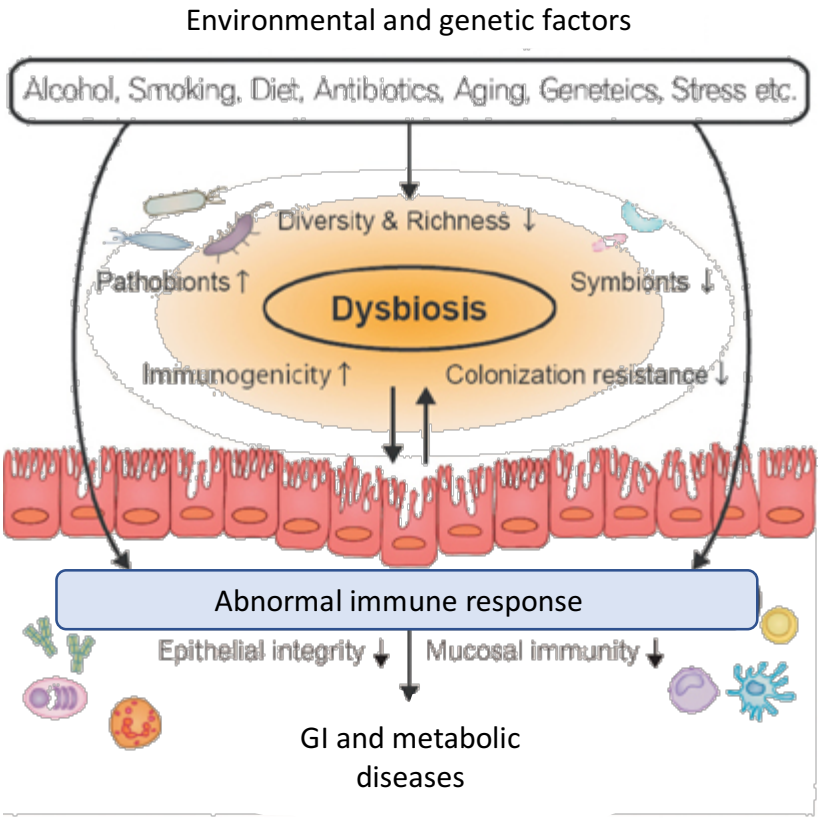

Figure 1.5 A schematic illustrating the model of how dysbiosis can cause disease. Several environmental and genetic factors can influence the composition of the gut microbiota either directly or indirectly by inducing host immune response pathways. This creates an environment where pathobionts bloom and become more abundant and symbionts become less abundant**.** These changes impair epithelial and mucosal integrity and activate an abnormal host immune response. This further propagates the changes in the microbiota and continued immune activation results in the pathogenesis of several diseases and disorders. Adapted from Nagao-Kitamoto et al. 2016.

1.3.2i Model organism case-study: mice, obesity and lipopolysaccharide (LPS)

Studies in mice have sought to investigate the host-microbe interactions that underpin disease progression in obesity. In 2004, it was found that the transfer of cecal microbiota from a healthy adult mouse into that of a germ free (GF) adult mouse caused a 60% increase in body fat content in the GF mouse (Backhed et al., 2004). Subsequent studies demonstrated that GF mice did not become obese on a high fat diet, whereas the control group with a conventional microbiota did (Backhed et al., 2007; Rabot et al., 2010). Obese mice on a HF diet and the obese mouse model (*ob/ob*) both show phylum-level microbiota changes associated with human obesity, namely: a reduction in Bacteroidetes and an increase in Firmicutes and Proteobacteria (Hildebrandt et al., 2009; Ley et al., 2005; Murphy et al., 2010; Turnbaugh et al., 2008).

One of the possible mechanisms by which this shift in gut bacteria may modulate obesity is by elevated levels of the bacterial gram-negative toll-like receptor (TLR) ligand, lipopolysaccharide A (LPS); activation of the TLR, TNF-α, by LPS mediates insulin resistance and is associated with obesity in mice and humans (Borst and Conover, 2005; Bouter et al., 2010). Cani et al. demonstrated that obese mice on a HF diet had increased levels of plasma LPS and that direct infusion of LPS into mice on a normal diet caused obesity (Cani et al., 2007). Furthermore, plasma LPS levels were reduced following antibiotic-treatment (Cani et al., 2008). Subsequent studies have indicated that this mechanism may be conserved in humans (Fei and Zhao, 2013; Lassenius et al., 2011). Here, a model organism approach has elucidated a microbial

molecular mechanism that assigns causality to the bacterial changes associated with obesity.

1.3.3 Dysbiosis and ageing

Ageing is associated with decreased intestinal motility (Madsen and Graff, 2004), increased intestinal permeability (Hollander and Tarnawski, 1985; Ma et al., 1992; Tran and Greenwood-Van Meerveld, 2013), chronic low-level inflammation, known as 'inflamm-ageing' (Franceschi, 2007; Guigoz et al., 2008), dietary changes (Flint et al., 2008) and increased antibiotic use (Augustine and Bonomo, 2011). Studies have found that the composition of the microbiota also changes with age, where the relatively stable adult microbiota begins to lose both stability and diversity with old age (Yatsunenko et al., 2012).

Metagenomic cohort studies have aimed to identify characteristic changes in the elderly microbiome. A study of a cohort of Northern Italian centenarians reported increased abundance of Proteobacteria and other changes in dominant phyla compared to a control group of younger adults (Biagi et al., 2010). These changes were also associated with increases in circulating pro-inflammatory markers and were only reported in centenarians and not in a group of older adults with an average age of 70 (Biagi et al., 2010). A more recent study by the same group found that an increase in 'health-associated' taxa, such as *Bifidobacteria* in extremely long-living people (Biagi et al., 2016). In contrast to the earlier Biagi et al. study, an Irish study reported increased abundance of Bacteroides and distinct changes in other dominant phyla in adults over 65 years of age (Claesson et al., 2011) and found that both diet

and antibiotic use were key predictors of shifts in microbiome composition. This study also positively correlated increased levels of pro-inflammatory circulatory markers with measures of frailty and comorbidity (Claesson et al., 2012). These studies consistently report that ageing is associated with both reduced diversity and increased interpersonal variability in microbiota composition (Yatsunenko et al., 2012).

Together, these studies indicate that age-related changes in the composition of the gut microbiota are inextricably linked to the increased inflammatory status associated with age (Buford, 2017). It is therefore unsurprising that microbiota composition in the elderly shares a similar profile to patients with diseases and disorders associated with inflammation, such as IBD and obesity (Franceschi and Campisi, 2014). However, it is unclear from these metagenomic descriptive studies whether the compositional changes described are a cause or consequence of ageing.

1.3.3i Model organism case study: fruit flies, intestinal barrier dysfunction and ageing

The fruit fly, *Drosophila melanogaster,* has proved to be a useful model to study host-microbe interactions in ageing, as the fly hosts up to approximately just 30 bacterial taxa (Broderick and Lemaitre, 2012) and it has a shorter lifespan and cheaper husbandry costs compared to mice. Moreover, studies have characterized age-associated intestinal cellular alterations in ageing flies, which are associated with an increased load of intestinal microbes (Broderick et al., 2014; Buchon et al., 2009; Rera et al., 2011). In 2015, Clark et al. demonstrated that specific age-related changes in

microbiota composition, namely an increase in the abundance of *Gammaproteobacteria* and a decrease in the proportion of *Firmicutes*, activates host pro-inflammatory immune signalling pathways which leads to cellular changes and compromised intestinal barrier integrity (Clark et al., 2015). These changes were found to prompt further dysbiosis, namely expansion of *Alphaproteobacteria,* which caused further immune activation. These changes were found to be primary cause of ageing. This study therefore provides evidence that microbiota alterations actively promote age-related intestinal dysfunction by prompting immune activation, which then further propagates pathogenesis (Clark et al., 2015). In mice, increased intestinal membrane permeability, or 'leaky gut' has been cited as a possible mechanism by which LPS may translocate from the intestine into the plasma (Cani et al., 2008).

1.4 *CAENORHABDITIS ELEGANS* AS A MODEL ORGANISM

In this thesis, the nematode worm, *C. elegans,* which is maintained in the laboratory on a monoculture of *E. coli* as a 'food source'*,* is used as a read-out to investigate a specific aspect of bacterial metabolism, namely folate synthesis. This section will introduce *C. elegans* as a model organism and outline the research related to using *C. elegans* as a model to study ageing. This will be followed by a review of more recent work which discusses the nature of the relationship between *C. elegans* and *E. coli,* with the aim of persuading the reader that *C. elegans-E. coli* is a useful model system to study animal-microbe interactions.

1.4.1 Why *C. elegans*?

C. elegans was introduced as a model organism in 1963 by Sydney Brenner, who

recognized the need to simplify biological systems in order to make fundamental discoveries about cell biology (Brenner, 1974). *C. elegans* are small (about 1mm in length) transparent organisms that can be maintained in large numbers in the laboratory using simple techniques and inexpensive equipment. *C. elegans* are mostly self-fertilizing hermaphrodites and can lay between 300-350 eggs within a short reproductive window: males will make up only a small proportion of the progeny, but if a male mates with a hermaphrodite, the progeny will be 50:50 . The *C. elegans* lifespan is short and temperature dependent, developing from an egg through 4 larval stages (L1-L4) within just 3 days at 25 °C (figure 1.6). The average adult lifespan is only around 12-15 days at 25 °C, thus lending itself to ageing studies. Worms can be frozen at -80 °C and revived after several years, thus facilitating the storage of transgenic strains (Brenner, 1974).

Indeed, *C. elegans* are extremely tractable genetically and biochemically. It is relatively simple to knockdown a gene by RNAi (microinjection of feeding) (Fire et al., 1991) and knockout strains can be obtained from the gene knockout consortium at the CGC (*C. elegans* Genetics Center). More recently, CRISPR/ Cas 9 genome editing has been established in *C. elegans* and provides a simple way to specifically knockout genes of interest (Frokjaer-Jensen, 2013 #960). The *C. elegans* genome is fully sequenced and annotated, with studies showing that 60- 80% of human genes have orthologs in *C. elegans* (Kaletta and Hengartner, 2006). Indeed, out of the 17 known signal transduction pathways in humans, 12 are conserved in *C. elegans* (Lai et al., 2000). Together, these characteristics make the worm an extremely useful model organism to investigate diverse aspects of biology.

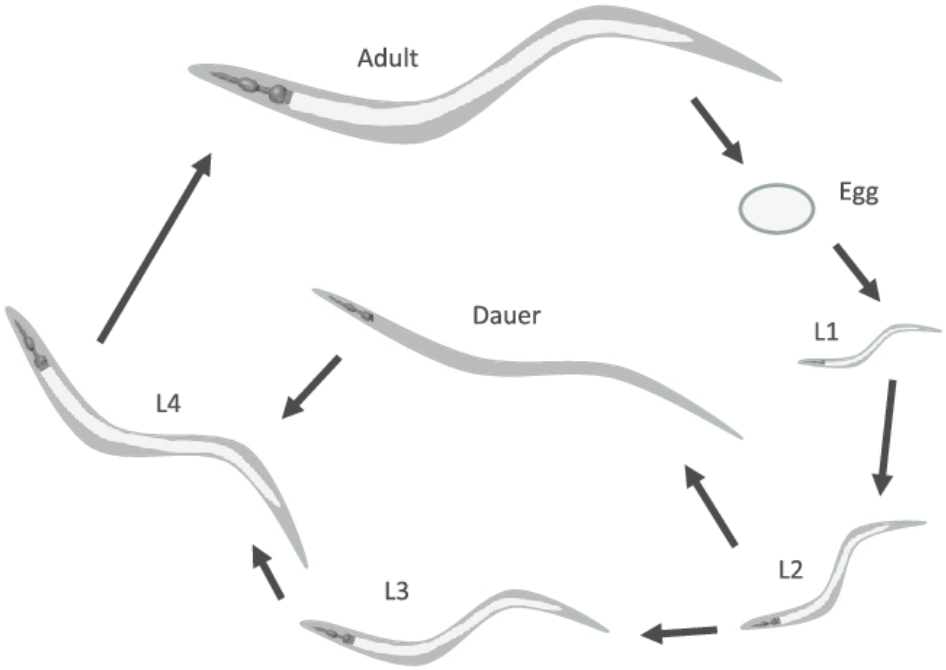

Figure 1.6. Life cycle of *C. elegans*. *C. elegans* develop from a fertilized egg, through four developmental larval stages (L1-L4) before becoming a young adult and then a gravid (egg-laying) adult (hermaphrodites only). At 25 °C when maintained on *E. coli*, this entire life cycle takes just 3 days. *C. elegans* can enter a state known as dauer formation at L2 stage, in response to crowding, starvation or high temperatures. *C. elegans* can remain in dauer stage for up to four months and can re-enter L4 stage when adverse conditions are cleared. Worms can also arrest at the L1 larval stage. Image taken from (Clark and Hodgkin, 2014).

1.4.3 *C. elegans* as a model to study ageing

Ageing is the accumulation of cellular defects over time which cause tissue damage and deterioration and increase the likelihood of mortality. Ageing within populations is characterized by a high degree of heterogeneity (Kirkwood et al., 2005). Likewise, in isogenic *C. elegans* populations, despite highly controlled dietary and environmental conditions, heterogeneity in ageing is a defining feature (Kirkwood and Finch, 2002). *C. elegans* show several physiological and physical changes which positively correlate with physiological age, including: reduced motility, decreased rate of pharyngeal pumping (feeding mechanism), accumulation of lipofuscin, appearance of vacuole-like structures and intestinal tissue disruption (Klass, 1977). With their short lifespan, low husbandry costs and the ability to maintain over one hundred animals on a single petri dish, *C. elegans* is a fantastic model to study ageing.

In 1983, a method to screen for long-lived *C. elegans* mutants was reported and isolated eight mutants that likely extended lifespan by restricting the calorie intake of the worm (Klass, 1983). A few years later, Friedman and Johnson identified the *age-1* long-lived mutant ((Friedman and Johnson, 1988a, b). In 1993, the Kenyon laboratory discovered the *daf-2* mutant and its dependence on *daf-16,* thus identified the role of the insulin/insulin-like growth factor-1 signaling (IIS) pathway in lifespan modulation (Kenyon et al., 1993). This pathway has since been found to be involved in ageing in conserved mechanisms in *Drosophila* (Clancy et al., 2001) and mice (Bluher et al., 2003; Holzenberger et al., 2003). Polymorphisms in these genes have also been associated with longevity in humans (Suh et al., 2008). Subsequent research

using *C. elegans* has uncovered other conserved pathways which can be targeted to modulate ageing, including: the target of rapamycin (mTOR), sirtuin and AMPK signalling pathways (Uno and Nishida, 2016). Thus, many fundamental insights into the mechanisms underpinning mammalian ageing have been gleaned from studies using *C. elegans* (Kenyon, 2010).

1.4.4 Living in a bacterial world

1.4.4i E. coli as C. elegans diet

In the laboratory, *C. elegans* are conventionally maintained on a peptone-based growth medium (NGM), which supports the growth and proliferation of a 'lawn' of the *E. coli* B-strain, OP50 (Brenner, 1974). Other *E. coli* strains are also commonly used as a *C. elegans* food source, such as the K12 strain, MG1655. *C. elegans* is solely dependent on *E. coli* for all the macro- and micronutrients required for growth, development and reproduction. *C. elegans* feed by sucking in bacterial cells with a specialized organ called the pharynx, which then grinds up cells and pumps them into the intestine. The pumping and peristaltic mechanisms ensure that cell debris passes through the intestine efficiently, nutrients are absorbed, and the remainder is swiftly defecated (Kim and Mylonakis, 2012), with an estimated transit time of 3-10 minutes in young worms (Avery and Shtonda, 2003).

1.4.4ii E. coli as C. elegans microbiota

OP50 and the other *E. coli* strains used in *C. elegans* studies are lab-adapted *E. coli* strains which are unable to colonize the *C. elegans* intestine or establish a stable association (Browning et al., 2013). Only in older worms, when the pharynx and the

peristaltic muscles deteriorate, and defences breakdown, do bacterial cells accumulate in the intestine (Garigan et al., 2002). Thus, *C. elegans* does not constitute a 'host' in the conventional sense, nor *E. coli* a 'microbiota'. Nevertheless, *C. elegans* swim in a sea of bacterial cells and secreted bacterial metabolites for the duration of their lifetime and are therefore in constant intimate contact with their bacterial 'diet'.

In the wild, however, three recent independent studies have suggested that *C. elegans* have a stable associated microbiota in their natural habitat (Berg et al., 2016; Dirksen et al., 2016; Samuel et al., 2016), where they are found on rotting fruit and plant material (Barriere and Felix, 2005; Felix and Braendle, 2010). These studies reported similarities, despite different geographical collection sites: all studies identified Proteobacteria, particularly gram-negative *Enterobactericeae* as the most abundant taxa and two identified significant abundances of Bacteriodetes and Firmicutes (Dirksen et al., 2016; Samuel et al., 2016). However, others in the field remain sceptical about whether these identified taxa constitute a microbiota or are simply the bacteria that predominate in the *C. elegans* natural habitat, and were associated with the worm at the time of collection (Zhang et al., 2017).

1.4.4iii E. coli as a C. elegans pathogen

Maintenance of *C. elegans* on axenic media compromises fitness, as discussed, but also results in a significant increase in lifespan (Croll et al., 1977). This may reflect the impact of sub-optimal nutrition, and thus dietary restriction, or it may be due to the removal of toxic bacterial factors that are detrimental to *C. elegans* longevity. Indeed, *C. elegans* are long-lived on heat-killed or antibiotic-treated *E. coli* (in which cells are

alive but not proliferating) (Garigan et al., 2002; Gems and Riddle, 2000) and Leanerts et al. demonstrated that the developmental phenotypes could not be rescued, nor lifespan reversed, by supplementation of the required dietary components into the axenic medium (Leanerts et al. 2008). Together, these studies indicated that the nutritional content of *E. coli* is uncoupled from its impact on lifespan.

In line with this hypothesis was the observation that *C. elegans* were longer-lived on the gram-positive soil bacterium, *Bacillus subtilis*, compared to on *E. coli* OP50, but no differences in developmental rate or reproduction were found (Garsin et al., 2003). This suggested that the two bacterial species have similar macronutrient content and lifespan is modulated by an *E. coli*- specific component. A subsequent study found that *C. elegans* on OP50 show higher expression of the stress-response gene, *sod-3,* compared to on *B. subtilis* (Sanchez-Blanco and Kim, 2011). The same group also showed that worms express the antimicrobial gene, *lys-8*, 5-fold higher when fed live OP50 compared to UV- killed OP50 (Hahm et al., 2011). Another study investigated the impact of the growth medium on *E. coli,* and found that *C. elegans* lived significantly shorter when OP50 was cultured on a rich agar growth medium compared to NGM. The authors cited an unknown change in bacterial metabolism and/or increase in pathogenic behaviour (Garsin et al., 2001).

The notion that *E. coli* has a mild pathogenic effect on *C. elegans* was supported by the discovery of an OP50 mutant, *ubiG*, which increased *C. elegans* lifespan (Larsen and Clarke, 2002). This mutant disrupted bacterial respiration and caused delayed intestinal bacterial accumulation, without affecting nutritional content (Saiki et al.,

2008). Together with the observation that accumulation of *E. coli* in the intestine is a biomarker of *C. elegans* ageing (Garigan et al., 2002), it was hypothesized that the proliferative capacity of live *E. coli* in the *C. elegans* intestine is mildly pathogenic to *C. elegans* (Portal-Celhay et al., 2012).

Several recent studies have challenged this hypothesis by tracking individual worms, rather than heterogeneous populations, and finding no correlation between bacterial intestinal accumulation and mortality (Han et al., 2017; Virk et al., 2016). As previously discussed, the Henderson lab found that neither OP50 nor the K12 strain were able to colonize the *C. elegans* intestine, and only upon restoration of the O-antigen component of K12 LPS, were *E. coli* cells able to colonize the intestine and kill *C. elegans* at rates similar to pathogenic bacteria (Browning et al., 2013).

1.4.5 *C. elegans- E. coli* as a simplified animal-microbe model

Together, these studies support the model that *E. coli* is both the diet and a mild pathogen of *C. elegans,* but not a microbiota in the conventional sense. Manipulations to *E. coli* metabolism and physiology in this simplified animal-microbe model system therefore provide a means to explore how specific bacterial genes, pathways or metabolites affect animal health, fitness and longevity (figure 1.7) (Cabreiro and Gems, 2013; Kim, 2013).

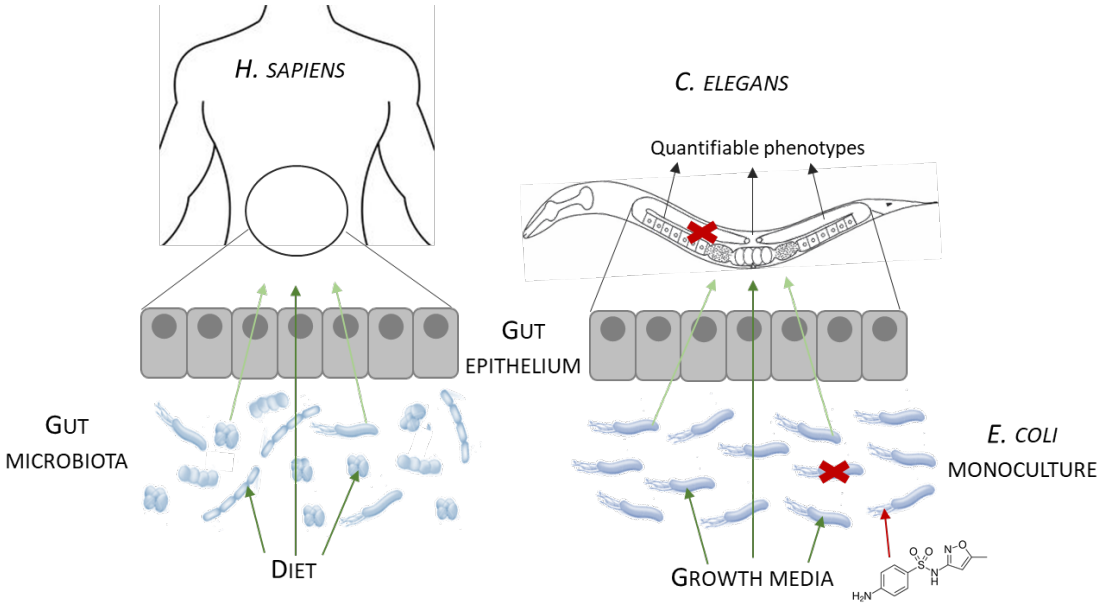

Figure 1.7 Schematic model of the *C. elegans- E. coli* animal-microbe system. *C. elegans* are maintained on a monoculture of *E. coli*, upon which they are almost solely dependent on for micro- and macronutrients. *C. elegans* can also take up some dietary components from the growth media directly. *E. coli* growth, proliferation and metabolism are dependent on the growth media and thus the growth media both directly and indirectly affects *C. elegans.* Constituents of the growth media can be chemically defined and altered. *E. coli* and *C. elegans* can be genetically manipulated (red crosses) and xenobiotics can be added to the growth media. The impact of these manipulations can be quantified by monitoring several *C. elegans* phenotypes.

1.5 BACKGROUND WORK

The following sections detail the work carried out in the Weinkove laboratory that identified *E. coli* folate synthesis as a determinant of *C. elegans* longevity (Virk et al., 2012). This work will be described in considerable detail as it provides the background for the aims of this thesis.

1.5.1 A serendipitous *aroD* mutant extends *C. elegans* lifespan

A spontaneous mutation in the *E. coli* RNAi strain, HT115 (DE3) was found to extend lifespan of the long-lived *C. elegans* mutant, *daf-2.* This mutant strain had a growth defect on minimal media. A screen for growth complementation was conducted and sequence analysis identified a mutation in the *aroD* gene. *aroD* gene encodes 3-dehydroquinate dehydratase, an essential enzyme in the shikimic acid pathway. The shikimic acid pathway is involved in the biosynthesis of several aromatic compounds, including PABA (figure 1.8a). Lifespan was extended on an *aroD* deletion strain from the Keio collection, BW25113 (K12) and reversed with supplementation of shikimic acid and PABA into NGM (figure 1.8b). Plasmid complementation of the *aroD* gene restored normal wild-type lifespan. The *aroD* mutant did not show any growth defects compared to WT *E. coli.* Together, this provided strong evidence that the *aroD* gene and disruption to the shikimic acid pathway was mediating *C. elegans* longevity (Virk et al., 2012).

1.5.2 Inhibiting folate synthesis with a sulfonamide extends *C. elegans* lifespan without inhibiting bacterial growth

The sulfonamide drug, sulfamethoxazole (SMX), is a structural mimic and competitive inhibitor of PABA (box 2) (Seydel, 1968). Virk et al. found that SMX increased *C. elegans* longevity in a dose-dependent manner, between 1 μg/ml to 256 μg/ml (figure 1.8c). Bacterial growth was monitored and surprisingly, no significant bacteriostatic effect was observed (figure 1.8e). SMX did not have any effect on *C. elegans* development or fecundity (data not shown here) and therefore lifespan extension was not found to have a negative trade-off (Virk et al. 2012).

Box 2. What are sulfonamides?

- The first systematically used antibiotics
- Structural analogs of PABA and therefore competitive inhibitors of dihydropteroate synthase (DHPS)
- Bacteriostatic: inhibit growth and proliferation of bacteria

Sulfonanilimide PABA

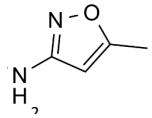

R group of sulfamethoxazole (SMX)

In order to determine whether this effect was folate-specific, 250 μM PABA was added into the growth media and longevity on SMX was completely reversed. SMX was unable to extend the lifespan of *C. elegans* maintained on OP50 transformed with the sulfonamide-resistant plasmid, R26 (figure 1.8d). Together, this indicated that E. coli folate synthesis is responsible for modulating lifespan (Virk et al. 2012).

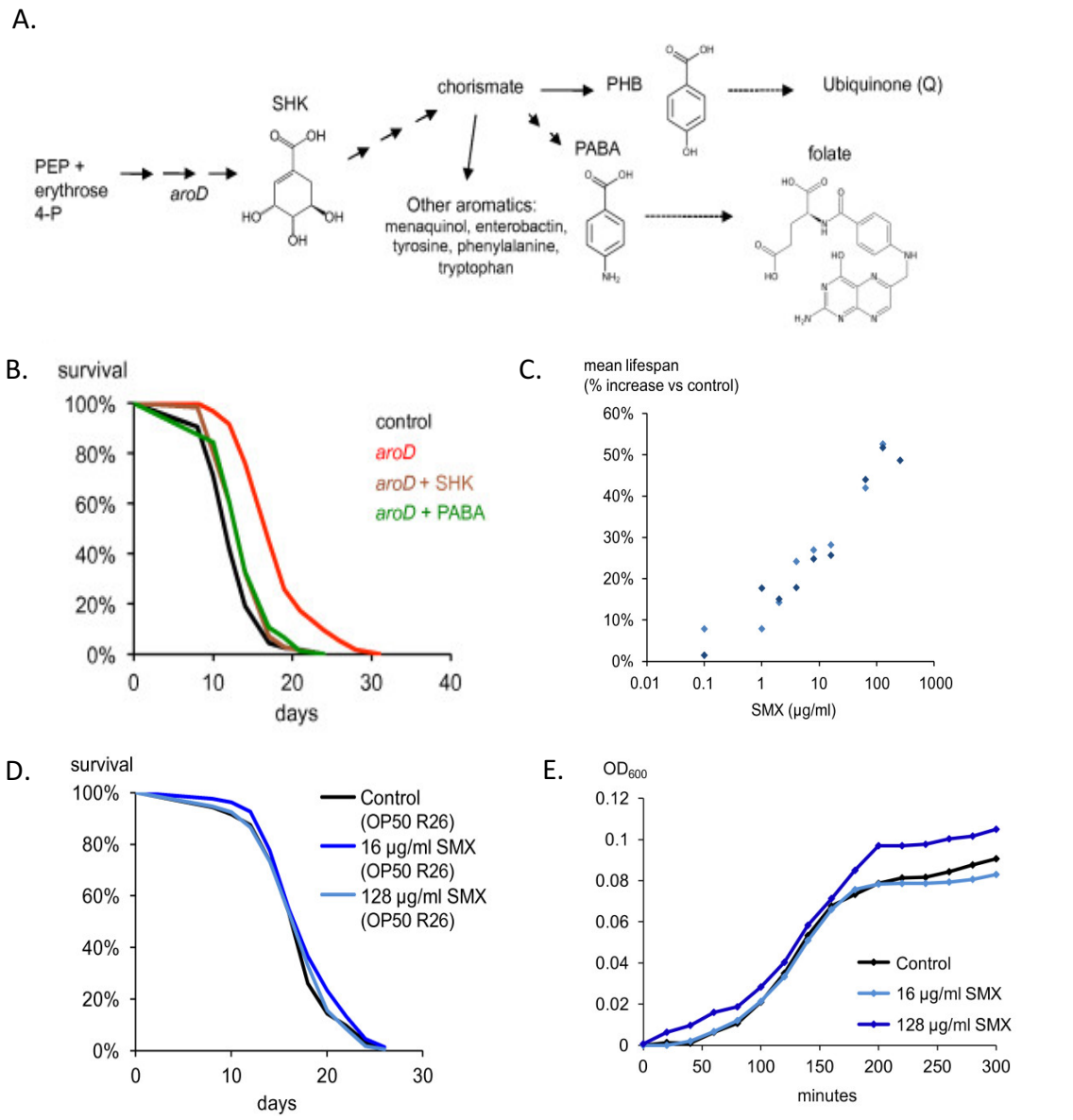

Figure 1.8 Summary of background work demonstrating that inhibiting *E. coli* folate synthesis extends *C. elegans* lifespan without negatively affecting bacterial growth a) schematic of the shikimic acid pathway b) lifespan of *C. elegans* on *aroD* mutant is reversed with PABA and not shikimic acid c) *C. elegans* mean lifespan increases with increasing [SMX] d) *C. elegans* lifespan is not increased on sulfonamide resistant OP50 in the presence of SMX e) *E. coli* growth is not affect by concentrations of SMX that extend lifespan. Taken from Virk et al. 2012.

1.5.3 Inhibiting folate synthesis lowers folates in both *E. coli* and *C. elegans*

As SMX did not cause a growth defect in either bacteria or the worm, it was verified that SMX did indeed decrease folate levels in both *E. coli* and *C. elegans*. Folate extraction methods were optimised from published literature protocols (Garratt et al., 2005; Lu et al., 2007) and samples were analysed by LC-MS. The equipment used in this study was not as sensitive as that which can be achieved today, and only the most abundant folate derivatives could only just be detected: 5/10-formyl THF-glu_3 (in *E. coli*) and 5-methyl THF-glu_5 (in *C. elegans*) (figure 1.9)

In *E. coli* treated with 128 µg/ml SMX-treated, 5/10-formyl THF-glu_3 folate could not be detected; the threshold for detection was 2 µg/ml (figure 1.9a). In *C. elegans* on SMX-treated *E. coli,* levels of 5-methyl THF-glu_5 were significantly lower at just 1 µg/ml SMX, compared to non-supplemented conditions; levels were further decreased at 4 µg/ml SMX, after which further decreases were indistinguishable (figure 1.9b) (Virk et al. 2012). Together, these data indicate that despite not affecting *E. coli* or *C. elegans* growth or development, SMX-treatment significantly decreased folate levels in both organisms. However, the LC/MS data collected here was limited and signals obtained were noisy and close to the limit of detection. A more accurate detection method is required to provide a more complete picture of the folate profile of both *E. coli* and *C. elegans*.

A.

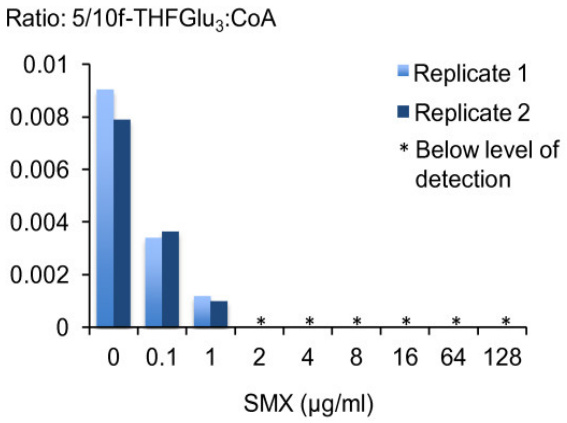

B.

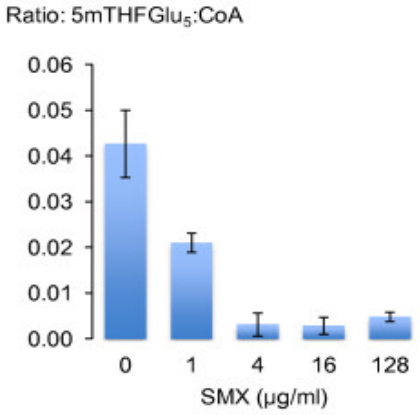

Figure 1.9 LC-MS detection of *E. coli* and *C. elegans* folate in response to SMX a) 5/10-formyl THF-glu$_3$ was detected in *E. coli* at 0.1 and 1 µg/ml SMX, and levels were below the level of detection above this concentration b) 5-methyl THF-glu$_3$ was detected in *C. elegans* up to 128 µg/ml. Levels were normalized to levels of co-enzyme A as an internal standard. Taken from Virk et al. 2012.

1.5.4 Folate-dependent lifespan extension: animal or microbe?

As folates seemed to be lowered in both *E. coli* and *C. elegans* on conditions that extend lifespan, it was unclear whether the mechanism underpinning longevity was dependent on animal or microbe folates, or both. It was important to distinguish this as any intervention which targets folate synthesis must ensure that animal folate levels are sufficient. Caloric restriction was ruled out as neither *aroD,* nor SMX, affected bacterial growth. Furthermore, the initial *aroD* mutation extended *C. elegans* lifespan in a *daf-2* mutant background. However, the lack of dietary folate, a specific folate or a folate-dependent micronutrient, could induce a specific dietary-restriction which increases lifespan. Alternatively, inhibition of folate synthesis may prevent *E. coli* accumulation in the *C. elegans* intestine with age, a phenomenon which is widely thought to accelerate ageing. More subtly, folate-dependent alterations in bacterial metabolism may either promote a beneficial activity, or attenuate a toxic one, which increases *C. elegans* lifespan. The experiments carried out to test these possibilities are detailed below.

1.5.4i C. elegans folates do not impact lifespan

Folate supplementation into NGM in a form which was presumed to be directly absorbed by *C. elegans* (folinic acid/ 5-formyl THF-glu_1) did not decrease lifespan in an SMX background. Also, the lifespan of a *C. elegans* folate-uptake mutant, *gcp-2.1 (ok1004),* which does not show any abnormal developmental phenotypes, was not long-lived. Disruption of the *C. elegans* folate cycle by methotrexate (MTX), which targets the DHFR enzyme, also did not impact lifespan. Together, these results

suggested that neither folate supplementation nor folate deficiency impact *C. elegans* lifespan, and thus the possibility that lack of dietary folate extends lifespan, was ruled out (Virk et al., 2016). However, *C. elegans* folate measurements were not carried out to substantiate these claims as the LC-MS facility was not accessible at this time; this will be addressed in this thesis in Chapter 5, using a more sensitive detection method.

1.5.4ii Reduced intestinal accumulation does not underpin lifespan extension

The possibility that the inhibition of folate synthesis increases lifespan by decreasing intestinal bacterial load was addressed by quantifying the fluorescence of GFP-tagged OP50 in the *C. elegans* lumen after day 5 of adulthood. Individual animals were separated into 'high' and 'low' accumulation cohorts and lifespans carried out on SMX and control conditions. Lifespan was dictated solely by SMX treatment, with no significant impact of 'high' or 'low' accumulation. In the untreated control condition, approximately 50% of recently dead worms showed no visible accumulation. SMX was found to delay accumulation, but did not prevent it. Overall, it was concluded that intestinal accumulation cannot be attributed to the lifespan extension on SMX. This has since been endorsed by a similar study which found no correlation between intestinal colonization of *E. coli* mutants and their lifespan-extending effects on *C. elegans* (Han et al., 2017).

1.5.4iii A screen of 1000+ E. coli mutants for C. elegans longevity revealed novel genes which influence lifespan and are involved in virulence in pathogenic microbes

In order to further understand how *E. coli* influences *C. elegans* lifespan, the Weinkove laboratory conducted a screen of over 1,000 *E. coli* K12 deletion mutants from the Keio collection. These mutants are constructed by replacing the open-reading frame of individual genes with a kanamycin resistance gene, flanked by FLP recognition sites (Baba et al., 2006). On these mutants, bacterial *C. elegans* longevity was not found to correlate to bacterial growth. Following several rounds of screening, only 9 mutants were identified to robustly increase lifespan (figure 1.10). Encouragingly, two of the genes identified were *pabA* and *pabB* which encode the heterodimeric enzymatic complex, 4-amino-4-deoxychorismate synthase, responsible for PABA synthesis (figure 1.2). Three of the mutants, *metL*, *ihfA*, and *ihfB*, caused a distinct change in the biophysical properties of the bacterial 'lawn' and altered the feeding and movement of *C. elegans.* The other mutants identified, *ompA , znuB, tatC* and *rpoS* did not change the appearance of the bacteria on the agar plates and were therefore focused on.

Briefly, *ompA* is an abundant outer membrane transporter(Smith et al., 2007); *znuB* encodes part of the ZnuABC zinc transporter, which facilitates uptake of low concentrations of zinc (Patzer and Hantke, 1998); *tatC* encodes a component of the twin arginine translocation pathway, which transports folded proteins to the periplasm (Sargent et al., 2001); and *rpoS* encodes the global stress response sigma factor, responsible for the transcription of several hundred genes involved in responses to abiotic stress (Dong et al., 2008).

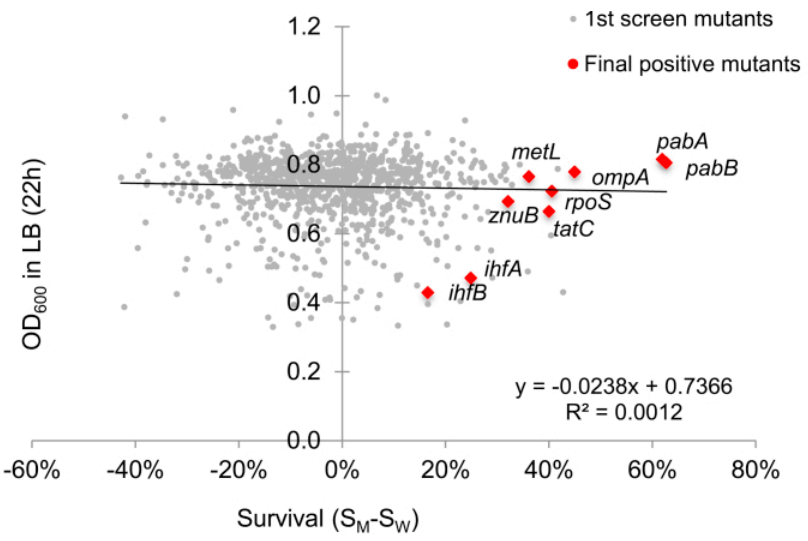

Figure 1.10 Screen for *E. coli* mutants that robustly extend *C. elegans* lifespan revealed 9 genes where longevity did not depend on reduced bacterial growth. Of the 1000+ *E. coli* mutants tested, overall there was not correlation between the growth the mutant strains in LB and *C. elegans* survival at day 11 or 12. The mutants that increased lifespan after the fourth round of the screen are indicated. Taken from Virk et al. 2016.

Interestingly, a common factor of the genes isolated in the screen, including *pabA* and *pabB,* is that they reduce virulence when mutated in pathogenic bacteria (Brown and Stocker, 1987; Chimalapati et al., 2011; Dong and Schellhorn, 2010; Gabbianelli et al., 2011; Ochsner et al., 2002). *E. coli* strains used for *C. elegans* culture do not have known virulence factors, however, it was hypothesized that the genes isolated in the screen might regulate other, as yet unidentified, factors with a milder but chronic effect on their hosts. The role of the *rpoS* gene in *E. coli* folate synthesis, toxicity and *C. elegans* lifespan will be explored in Chapter 7.

1.5.4 iv Mutations in (most) E. coli folate cycle genes did not extend lifespan

In order to determine whether a specific folate or by-product of the folate cycle was responsible for *C. elegans* lifespan, lifespan assays were carried out on mutants of genes involved in the folate cycle. Of the 23 non-essential genes involved in the folate cycle or related reactions, only a small significant effect on lifespan on the *glyA* mutant was observed. *glyA* encodes serine hydroxymethyltransferase (SHMT) (Shen et al., 1997) and uses 5,10-methylene THF as a methyl donor to convert glycine to serine and also catalyzes the reverse reaction, using THF. SHMT also converts 5-methenyl THF to 5-formyl THF. *metL,* which was identified in the screen, is involved in two steps in the methionine biosynthesis pathway (Zakin et al., 1983). No other genes involved in methionine biosynthesis had any impact on lifespan. Due to the 'watery' consistency of the *metL* lawn cited, *metL* was disregarded as having any biochemical impact on longevity. Virk *et al* therefore hypothesized that folate synthesis, not the folate cycle, is responsible for *C. elegans* lifespan (Virk et al. 2012).

1.5.5 Summary of background work and limitations to the study

Virk et al. identified *E. coli* folate synthesis as a target to extend *C. elegans* lifespan. This was achieved genetically *(aroD, pabA, pabB* mutants) and pharmacologically (SMX) without affecting bacterial growth or *C. elegans* health. LC-MS detection identified one folate species in both *E. coli* and *C. elegans* that was significantly decreased in response to SMX, however LC-MS measurements were limited due to lack of sensitivity. No impact of limiting or supplementing *C. elegans* folate on lifespan was found, indicating that a bacterial folate-dependent process underpins lifespan, however, LC-MS measurements were not carried out under these conditions. Efforts

to identify an *E. coli* folate-dependent process responsible for lifespan increase eliminated several hypotheses but did not illuminate a mechanism. An *E. coli* K12 mutant gene screen for *C. elegans* longevity isolated genes involved in virulence in pathogenic microbes (including *pabA* and *pabB*), but it was not clear whether folate synthesis was acting via this mechansism in *E. coli* to shorten *C. elegans* lifespan.

1.6 AIMS OF THESIS

The initial aims of this PhD are to address the limitations of the previous study by developing a more controlled and sensitive model system in order to control and accurately detect folate levels in the media, the microbe and the worm. This optimised system will then be used to understand the factors that influence *E. coli* folate synthesis, both extrinsically and genetically, with the ultimate aim of understanding how bacterial folate synthesis and one-carbon metabolism affect *C. elegans* health and longevity. This thesis therefore takes an *E. coli*–centric view, where *C. elegans* lifespan (and development, reproduction and behaviour) will be used as a phenotypic read-out in response to perturbations that influence bacterial folate synthesis.

2.1 STRAINS

2.1.1 *C. elegans* strains

Strain	Genotype	Source/Origin
N2	wild type	(Brenner, 1974)
SS104	*glp-4(bn2)*	(Beanan and Strome, 1992)
UF208	wild type	(Virk et al., 2016)
UF209	*gcp-2.1(ok1004)*	(Virk et al., 2016)

2.1.2 *E. coli* strains

Strain	Genotype	Plasmid	Characteristics	Source
OP50	wild-type	n/a	ura^-	(Brenner, 1974)
BW25113	wild-type	pGreen 0029	kan^r	(Baba et al., 2006)
JW3323-1	*ΔpabA*	n/a	kan^r	"
JW5437-1	*ΔrpoS*	n/a	kan^r	"
JW1253-1	*ΔtrpB*	n/a	kan^r	"
JW3686-7	*ΔtnaA*	n/a	kan^r	"
JW0912-1	*ΔompF*	n/a	kan^r	"
JW3325-1	*ΔyhfG*	n/a	kan^r	"
JW0554-1	*ΔompT*	n/a	kan^r	"
JW1023-1	*ΔcsgD*	n/a	kan^r	"
JW0230-1	*Δcrl*	n/a	kan^r	"
JW0940-6	*ΔompA*	n/a	kan^r	"
JW5181-1	*ΔhlyE*	n/a	kan^r	"
JW2203-1	*ΔompC*	n/a	kan^r	"
JW1736-1	*ΔastA*	n/a	kan^r	"
JW5571-1	*ΔbipA*	n/a	kan^r	"
JW2284-6	*ΔlrhA*	n/a	kan^r	"
JW5702-4	*Δcrp*	n/a	kan^r	"

JW1653-1	*Δcfa*	n/a	kan^r	"
JW3484-1	*ΔgadX*	n/a	kan^r	"
JW5571-1	*ΔbipA*	n/a	kan^r	"
JW2449-4	*ΔtktB*	n/a	kan^r	"
JW4338-1	*ΔosmY*	n/a	kan^r	"
JW1488-7	*ΔgadB*	n/a	kan^r	"
JW3474-5	*Δslp*	n/a	kan^r	"
JW1912-1	*ΔmysB*	n/a	kan^r	"
JW3480-2	*ΔgadE*	n/a	kan^r	"
JW1653-1	*Δcfa*	n/a	kan^r	"
JW1477-1	*ΔosmC*	n/a	kan^r	"
JW3221-5	*ΔcsrA*	n/a	kan^r	"
JW3485-1	*ΔgadA*	n/a	kan^r	"
JW2448-4	*ΔtalA*	n/a	kan^r	"
JW2755-3	*ΔrelA*	n/a	kan^r	"
JW3879-1	*ΔsodA*	n/a	kan^r	"
JW1886-1	*ΔotsB*	n/a	kan^r	"
JW3323-1	*Δfic*	n/a	kan^r	"
JW1736-1	*ΔastA*	n/a	kan^r	"
JW5702-4	*Δcrp*	n/a	kan^r	"
JW5437-1	*ΔrpoS*	n/a	kan^r	"
JW2284-6	*ΔlrhA*	n/a	kan^r	"
JW5822-1	*ΔabgT*	n/a	kan^r	"
CM*abgTpabA*	*ΔabgT ΔpabA*	n/a	n/a	This study
CM1/puc19*	WT	pUC19‡, pGreen 0029	kan^r, amp ^{r}	This study
CM2/puc19*	*ΔpabA*	pUC19	kan^r, amp ^{r}	This study
CM3/puc19*†	*ΔabgTΔpabA*	pUC19	kan^r, amp ^{r}	This study
CM1/pJ128*	WT *(abgT* OE)	pJ128‡, pGreen 0029	kan^r, amp ^{r}	This study
CM2/pJ128*	*ΔpabA (abgT* OE)	pJ128	kan^r, amp ^{r}	This study
CM3/pJ128*†	*ΔabgTΔpabA (abgT* OE)	pJ128	kan^r, amp ^{r}	This study

*Derived from BW25113 or relevant mutant strain

† *ΔabgTΔpabA* double mutant strain made by P1 transduction (section 2.X)

‡ pUC19 and pJ128 plasmids were obtained with thanks from Jacalyn Green's laboratory, Northwestern University, Chicago.

2.2 GENERAL SOLUTIONS

LB (Luria Bertolani broth) (10.0g/l Tryptone (95039, Sigma-Aldrich), 5.0g/l Yeast Extract (Y1625, Sigma-Aldrich), 10.0g/l NaCl, to distilled water and mixed thoroughly.

M9 buffer (7.37g/l $Na_2HPO_4.2H_2O$ (≥99.0%, Sigma-Aldrich), 3.00g/l KH_2PO_4 (≥99.0%, Sigma-Aldrich), and 5.00g/l NaCl (≥99.0%, Sigma-Aldrich), to distilled water, stirred until dissolved. Solutions were divided into 250ml aliquots and autoclaved at 121°C for 20 minutes sterilise.

2.3 PLATE PREPARATION

2.3.1 Nematode Growth Media (NGM) plate preparation

NGM was prepared by adding 3.00g/l NaCl, 2.50g/l Peptone (70171, Sigma-Aldrich) and 20.0g/l Agar (05038, Sigma Aldrich) to distilled water. The media was then autoclaved at 121°C for 20 minutes to sterilise. Once the autoclave cycle had completed, the media was cooled to 55°C at which point, 1ml/l of Cholesterol (≥99.0%, SigmaAldrich) (from 5mg/ml cholesterol solution dissolved in ethanol), 1ml/l of 1M $CaCl_2$ (≥96.0%, Sigma-Aldrich), 1ml/l of 1M $MgSO_4$ (≥99.5%, Sigma-

Aldrich) and 25ml/l of 1M KH_2PO_4 (pH 6.0) were added aseptically in a flow cabinet. 15 ml NGM was aliquoted into 60 mm plates and left to dry. Plates were stored at 4-5 °C for up to three weeks and used for *C. elegans* maintenance.

2.3.2 Defined Media (DM) plate preparation

Defined media was prepared by adding 3.00g/l NaCl, and 18.0g/l high-purity agar (56763, Sigma Aldrich) to distilled water. The media was autoclaved at 121°C for 20 minutes and cooled to 55°C. The following constituents were added aseptically in a flow cabinet: 1ml/l of Cholesterol (≥99.0%, Sigma-Aldrich) (from 5mg/ml cholesterol solution dissolved in ethanol), 1ml/l of 1M $MgSO_4$ (≥99.5%, Sigma-Aldrich) and 25ml/l of 1M KH_2PO_4 (pH 6.0). 20.3 ml/l of an amino acid solution (see below), 0.2ml/l of a trace metal solution† and 10 nM B12 were also added in the flow cabinet. Antibiotics and additional components were added at this stage if required‡. 15 ml DM was aliquot into 60 mm plates and left to solidify. Plates were stored at 4-5 °C and used within 2-3 days. DM was used for all experimental procedures in this thesis unless otherwise stated.

2.3.2i Amino acid solution for defined media

Amino acid	g/ 750ml
Alanine	1.0643
Arginine	0.9698
Aspartic acid	1.3365
Cysteine	0.0765
Glutamic acid	2.2455
Glycine	2.5605
Histidine	0.2115
Isoleucine	0.3510

Leucine	0.6345
Lysine	0.6930
Methionine	0.1643
Phenylalanine	0.4118
Proline	1.5480
Serine	0.6323
Threonine	0.4005
Tryptophan	0.0428
Tyrosine	0.2385
Valine	0.47025

2.3.2ii Trace metal solution for defined media†

2000 x trace metals solution was made up using the stock solutions of individual metals as detailed below. Except for FeCl3, stock solutions of were autoclaved and stored at room temperature. Used at 0.2x.

2000 x trace metals			MW	1 x conc.
36 ml distilled, sterilized water				
50 ml	0.1 M	FeCl3 in ~0.12 M HCl	270.3	50 µM Fe
2 ml	1 M	CaCl2	110.99	20 µM Ca
1 ml	1 M	MnCl2-4H2O	197.91	10 µM Mn
1 ml	1 M	ZnSO4-7H2O	287.56	10 µM Zn
1 ml	0.2 M	CoCl2-6H2O	237.95	2 µM Co
2 ml	0.1 M	CuCl2-2H2O	170.486	2 µM Cu
1 ml	0.2 M	NiCl2-6H2O	237.72	2 µM Ni
2 ml	0.1 M	Na2MoO4-2H2O	241.98	2 µM Mo
2 ml	0.1 M	Na2SeO3-5H2O	263.03	2 µM Se
2 ml	0.1 M	H3BO3	61.83	2 µM B

2.3.2iii Antibiotic and folate solutions added to defined media‡

100 x stock solutions of antibiotics (kanamycin, 25 mg/ml; carbenicillin, 50 mg/ ml) and folates were made before adding the appropriate volume into DM after all other

constituents had been added. Antibiotic solutions were dissolved in distilled water and aliquot into 1.5 ml Eppendorf tubes and stored at -20 ºC for several weeks. Folic acid (16.203, Schircks), folinic acid (96.220, Schircks), PABA-glu (16.701, Schircks), PABA (≥99.0%, Sigma-Aldrich), and SMX (S7507, Sigma-Aldrich) solutions were dissolved in minimum concentrations of NaOH (1 mM- 100 mM) and were not stored after use. All stock solutions were filter sterilised using a 0.2µm filter.

2.4 PREPARATION OF LB BACTERIAL CULTURES

5 ml of sterile LB was pipetted aseptically into a sterile 10 ml falcon tube. A sterile pipette tip was used to inoculate the LB with *E. coli* from a stock culture stored at -80ºC. Tubes were then incubated overnight at 37°C in an orbital shaker (Stuart SSL1 Lab-scale orbital shaker) at 220rpm. LB bacterial cultures used to seed NGM plates for worm maintenance were stored at 4 ºC for a maximum of one week. LB cultures were also used to inoculate DM cultures for experimental procedures (see below), and were used the following day and not stored for further use.

2.5 PREPARATION OF DM BACTERIAL CULTURES

DM cultures were used for all experimental procedures carried out on DM plates. 3 ml of sterile DM was pipetted aseptically into a sterile 10 ml falcon tube. A sterile pipette tip was used to inoculate the DM with 30 µl of an LB overnight culture. Tubes were incubated as described above, but for a set time of 18 hours. Strict stipulations with protocol here have been optimised in order to ensure minimum and controlled carryover of nutrients from LB.

2.6 SEEDING NGM AND DM PLATES WITH *E. COLI*

Agar media in plates was seeded with 100µl of bacterial culture using a repeat pipette dispenser under sterile conditions. The plates were incubated at 25°C for 2 days before use *C. elegans* were transferred. DM plates were always seeded with DM cultures. NGM plates were always seeded with LB cultures.

2.7 MEASURING BACTERIAL GROWTH

2.7.1 Agar media

E. coli seeded onto agar DM (*C. elegans* experimental conditions) was removed by pipetting 1ml M9 onto the plate and a glass spreader was used to scrape of the bacterial lawn. The bacterial suspension was pipetted into a 1.5 ml Eppendorf and the volume was recorded. Tubes were vortex vigourously in order to obtain a homogenised solution. 100 µl was taken and diluted with 900 µl M9 in a cuvette. A spectrophotometer was used to read bacterial growth at 600 nm. Bacterial growth was calculated by multiplying OD_{600} by the volume of the sample.

2.7.2 Liquid 96-well microtiter plates

In order to measure bacterial growth over time and test a range of experimental conditions simultaneously, a liquid growth assay was developed. 96-well round-bottom microtiter plates (Greiner) were used. Wells were filled to 200 µl with DM containing appropriate supplement and were inoculated to a starting OD_{600} of 0.001 of an overnight DM culture. The plate was incubated at 37°C with continuous shaking in a Synergy H4 Hybrid Multi-Mode Microplate Reader. Readings were taken every 5

minutes for ~18-22h to give kinetic growth curves. Mean growth curves were created using readings from at least 3 replica wells in each case.

2.8 *C. ELEGANS* STRAIN MAINTENANCE

C. elegans populations were maintained on NGM plates seeded with OP50 *E. coli.* When the *E. coli* had been used up and animals had starved, ~ 1 cm^3 sections of agar with starved worms were cut using a sterile scalpel blade and placed onto NGM agar plates with 'fresh' OP50 (seeded two days previously). This enables starved worms to re-enter development.

2.9 OBTAINING SYNCHRONISED POPULATIONS OF *C. ELEGANS*

2.9.1 Bleaching (carried out on NGM)

Gravid unstarved worms were subjected to bleaching as a method to obtain a synchronized and sterile population of eggs. Four plates were used per worm strain. 1ml M9 was used to wash worms off each plate and washings from two plates were pooled into a 1.5 ml Eppendorf tubes. Gravid worms were left to settle and excess M9 was carefully removed, leaving approximately 200µl. 125µl of bleach solution (7:8 sodium hypochlorite (425044, Sigma-Aldrich) and 4M NaOH respectively) was added to each tube and the tubes were shaken continuously by hand for approximately 3 minutes, until the solutions became uniformly cloudy and worm definition was lost. At this point, 1 ml M9 was added to each tube and centrifuged for 1.5 mins at 3000 rpm in a Spectrafuge 24D bench top centrifuge (Jencons-PLS). The supernatant was removed, leaving approximately 20-40µl in

the tube and 1 ml fresh M9 was added to wash the eggs and remove traces of bleach. The pellet was dissasociated by shaking and c centrifuged again as before. The supernatant was again removed and 1 ml M9 added again. Tube were again centrifuged and the supernatant was removed as before – leaving 20-40 µl. The pellet was resuspended by shaking and 5 µl pipetted onto a seeded agar plate in order to rougly quantify the number of eggs within each tube and normalize volumes pipetted onto plates between tubes. Approximately 50-200 eggs were pipetted onto each plate. NGM plates were used for bleaching.

2.9.2 Egg-lay (carried out on DM)

Populations of worms obtained by bleaching are not used directly for experimental analysis due to potentially adverse effects of bleaching on fitness. Eggs obtained from bleaching are raised until gravid and an egg-lay is performed in order to again gain synchronized populations for experiments. Egg-lays are carried out on DM plates. 3-5 gravid worms are transferred onto seeded DM plates, where the number of replicates per condition depends on the experiment being carried out: for lifespan assays, 4-5 plates are used for each condition to obtain sufficient numbers of worms. Plates are incubated overnight at 20 °C (15 °C if using temperature sensitive SS104 for lifespan analysis) and gravid worms are removed from the plates after ensuring that sufficient eggs have been laid. Egg-lays were set up either in the late afternoon and worms removed early the next morning (overnight egg-lay) or set-up early in the morning and removed in the later afternoon (day time egg-lay). Worms were then incubated at the temperature appropriate for further analysis.

2.10 DEVELOPMENTAL ASSAY: BODY LENGTH QUANTIFICATION

C. elegans body length at L4 stage was used to measure development. Following egg-prep, an egg-lay onto the appropriate experimental condition was carried out. Gravid adults were removed and plates were incubated at 25 °C for 2.5 days until L4 stage. Plates were imaged using a 1.0x PLANAPO lens and 4.0x magnification and captured using a digital microscope camera with a CCD (charge-coupled device) sensor. ImageJ was used to measure *C. elegans* body length. A randomly-offset 10x 8 grid overlay was applied to each image and each square assigned a grid reference. A random number generator was used to arbitrarily select squares and any worms falling within this square were measured. Those worms that occupied two squares or more were discounted. A total of 40 worms were measured for condition. Measurements were made using the freehand line tool by tracing a line along the extent of the *C. elegans* body axis (figure 2.1). Measurements were converted from pixels to mm, where at this magnification, 1 pixel= 0.011mm. Measurements were carried out blinded.

2.11 DEVELOPMENTAL ASSAY: FECUNDITY ASSAY

Following bleaching, an egg-lay onto the appropriate experimental condition was carried out. Plates were incubated at 25°C for 3 days until worms developed into young adults. 10 individual worms were transferred onto 10 separate plates per condition*. Once worms began laying eggs they were transferred to freshly

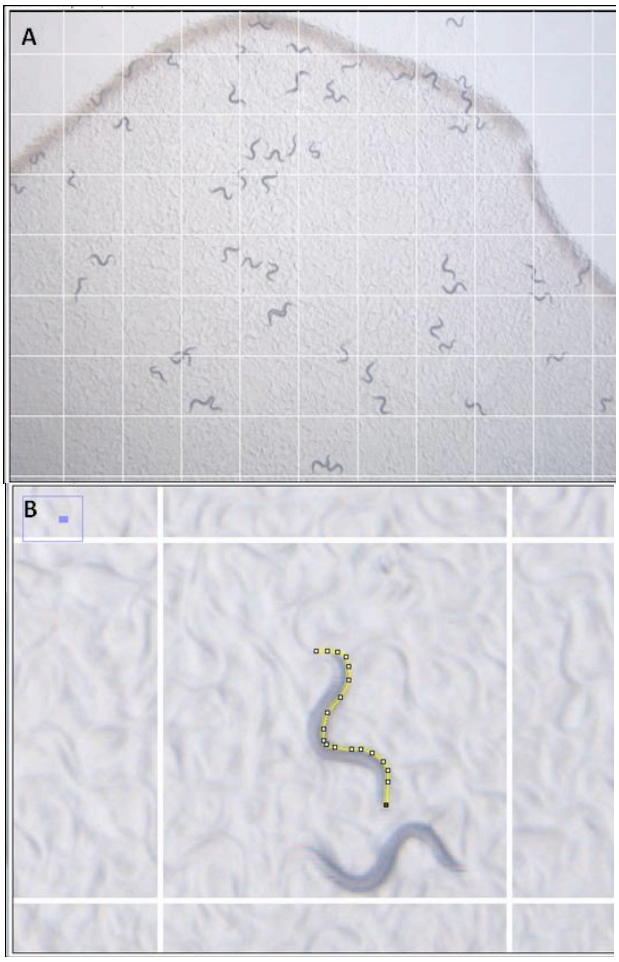

Figure 2.1 Representative images obtained for body length measurement

ImageJ was used to measure *C. elegans* body length a) to reduce bias in measuring, a randomly-offset 10x 8 grid overlay was applied to each image and each square assigned a grid reference. A random number generator was used to arbitrarily select squares and any worms falling within this square were measured b) measurements were made using the freehand line tool by tracing a line along the *C. elegans* body axis.

seeded plates each day. Plates with eggs were maintained at 25°C for 24 hours to allow the larvae to develop and the number of viable progeny was counted*. plates per condition. Unhatched eggs were also counted and recorded separately.

*fecundity assay carried out at SJTU (Chapter 7) used 3 worms per plate and 5 replicates

2.12 C. ELEGANS LIFESPAN ANALYSIS

Lifespan experiments were performed using the *glp-4(bn2)* SS104 *C. elegans* strain. This strain was used as it sterile at 25°C and therefore eliminates the complication of progeny production during lifespan analysis. The full procedure for a lifespan analysis is detailed in figure 2.2, using the techniques previously outlined in this chapter. Egg-prep and egg-lay procedures are carried out at 15°C, where the latter is on DM. OP50 carryover from NGM at this stage is minimized as OP50 cannot survive on DM as it does not contain uracil, and the majority of DM plates contained 25 μg/ ml kanamycin due to the requirements of the *E. coli* strains used.

Plates are shifted to 25 °C following the egg-lay when worms reach L3/ early L4 stage. The following day, L4 worms (as distinguished here by appearance of the lumen of the uterus as a clear crescent), 25 animals are transferred onto seeded DM plates, with 5 plates per condition, so n~ 125 worms for each lifespan condition. Plates are maintained at 25 °C for the duration of the lifespan. Worms are counted after 7 days incubation, where this is recorded as day 7 of adulthood,

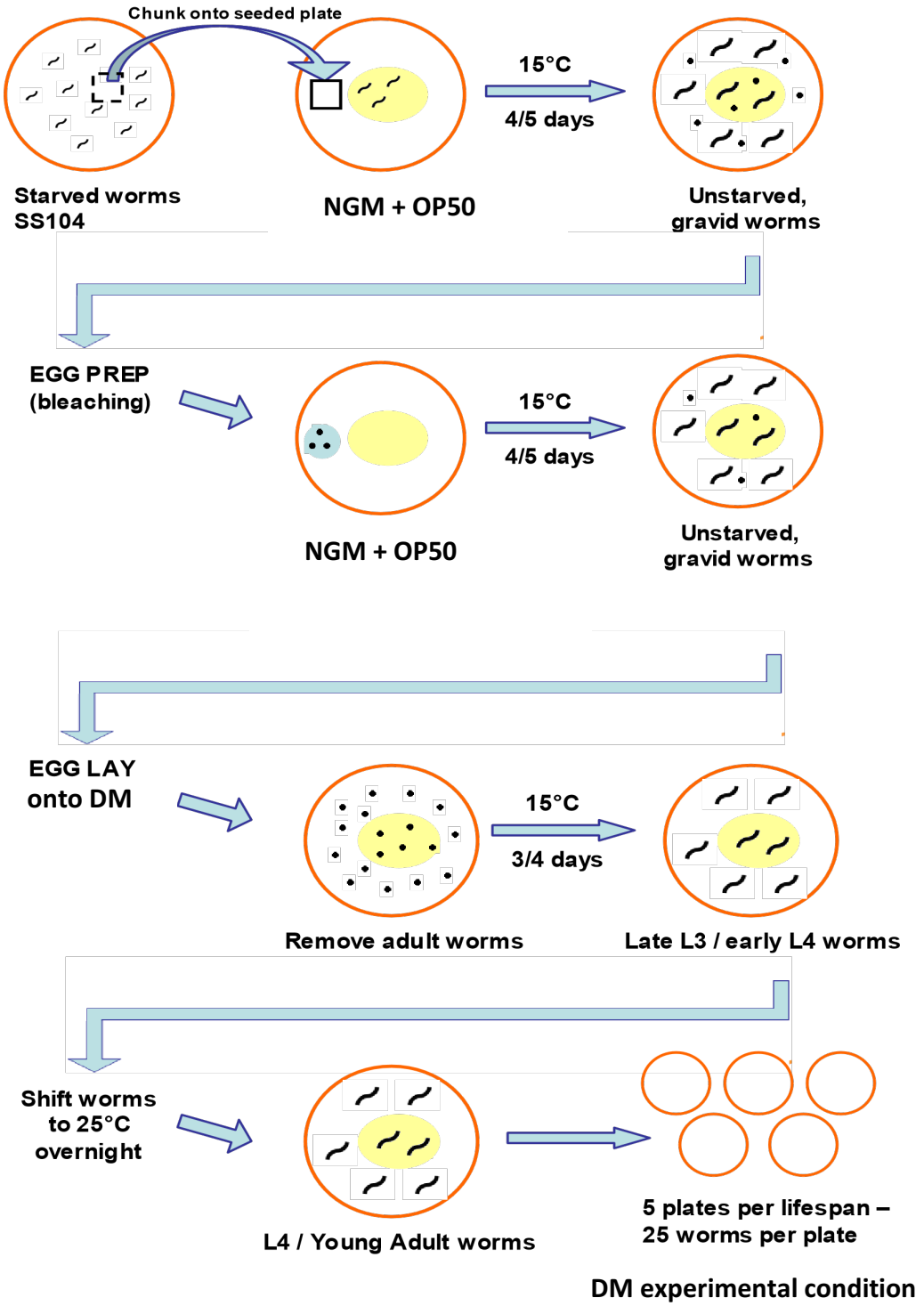

Figure 2.2. Diagrammatic representation of the lifespan protocol. Lines represent *C. elegans*, black dots represent *C. elegans* eggs, blue dot containing black dots represents *C. elegans* eggs from bleaching protocol. Adapted from Marjanne Bourgeois, a Master's student in the Weinkove laboratory.

and then counted every other day for remainder of the lifespan. Worms are scored as alive, dead or censored. At days 7 and 14, worms are transferred onto freshly seeded plates in order to ensure sufficient 'food.' If plates developed contamination, all the animals on the plate were censored, although this was rare due to the presence of kanamycin. See supplementary table 1 for full details of all lifespan experiments carried out in this thesis, including statistical analyses.

2.13 FOLATE EXTRACTION AND LC-MS/MS

2.13.1 Folate extraction for *E. coli*

100 µl *E. coli* DM culture were seeded onto DM plates of the experimental condition. Two plates per replicate were required and 4-5 replicates per condition were carried out. Plates were incubated for four days (unless otherwise stated) at 25 °C before the folate extraction procedure was carried out. *E. coli* was removed from the two plates within a replicate using a sterile glass spreader and 2 ml sterile M9, and bacterial solution was pipetted into a 1.5 ml Eppendorf tube; sample volume was recorded. Tubes were vortexed vigorously in order to obtain a homogenised solution. 100 µl of sample was removed and diluted 1:10 with M9 in a plastic cuvette and OD_{600} was measured and recorded. Eppendorf tubes were kept on ice.

Eppendorfs were centrifuged for 8 minutes at 4000 rpm in a chilled centrifuge. Supernatant was discarded and excess was removed by dabbing inverted tubes on a paper towel. Tubes were snap frozen in liquid nitrogen. Samples can be stored at -80 °C at this stage if necessary. A specific amount (see below) of 90:10 ice cold methanol:

folate extraction buffer (50mM HEPES, 50mM CHES, 0.5% w/v ascorbic acid, 0.2M DTT, pH 7.85 with NaOH), spiked with MTX-glu_6 as an internal standard, was added to each tube and vortexed vigorously until the pellet was dissolved. Samples were left on ice for 15 minutes and then centrifuged for 15 minutes at full speed in a chilled centrifuge. Supernatant was decanted and transferred to a fresh Eppendorf tube. 20 µl supernatant was aliquot into vials for LC-MS/MS analysis, or stored at -80°C.

Volume of folate extraction buffer was calculated by:

$$Vol.extraction\ buffer\ (\mu l) = sample\ vol.\ (ml) \times OD_{600} \times 37.5$$

2.13.2 Folate extraction for *C. elegans*

An overnight egg-lay at 20°C was carried out onto DM seeded 9cm plates (of the experimental condition) in order to gain a large synchronized population of worms (~200) (four plates per replicate, with four replicates per condition). Plates were stored at 25°C for 2 days to allow worm development to L4/ young adulthood. Worms were washed off the agar with 3ml sterile M9, pooled into 50 ml falcon tubes, and allowed to settle before removing the supernatant to 5 ml. To remove remaining bacteria, worms were again washed with M9, allowed to re-settle, and the supernatant removed to 1 ml. Worms were transferred to 1.5 ml Eppendorf tubes, gently centrifuged (2000rpm) for 10 seconds and pellet volumes estimated and recorded.

The supernatant was removed before adding 1ml of folate extraction buffer (50mM HEPES, 50mM CHES, 0.5% w/v ascorbic acid, 0.2M DTT, pH 7.85 with

NaOH) spiked with MTX-glu_6 as an internal standard, and the samples vortexed and gently centrifuged (2000rpm) for 10 seconds. Supernatant removal and addition of folate extraction buffer was repeated, and worms left in an FEB volume of twice the pellet volume. Procedures described thus far were carried out on ice and in chilled centrifuges.

Proteinase K was added to a final concentration of 500 µg/ml, samples vortexed, and shaken vigorously at 37°C for 60-90 minutes to lyse worm cells. Tubes were covered with aluminium foil due to light sensitivity of folates. A volume of ice-cold methanol equal to that in the Eppendorf tube was added to lyse remaining cells, samples vortexed, and centrifuged (13000rpm) at 4°C for 10 minutes. 20 µl supernatant was aliquot into vials for LC-MS/MS analysis, or stored at -80°C.

2.13.3 Tandem liquid chromatography-mass spectrometry (LC-MS/MS) analysis

The methodology was based on published literature (Lu et al., 2007) and parameters were optimised by Ian Cummins in the Durham University Biosciences Department,. Folates were detected by multiple reaction monitoring (MRM) analysis using a SCIEX QTRAP 6500 instrument. MRM conditions for 5-methylTHF-glu_3 and formyTHF-glu_3 were optimised by first infusing these standards (Schircks) into the instrument, and were applied to other folates using MRM transitions previously described (Lu et al., 2007). Folate identity was confirmed by performing enhanced product ion scans of relevant folates and comparing fragment spectra with known standards.

In ESI+ mode the QTRAP 6500 was interfaced with a Shimadzu Nexera UHPLC system. Samples were separated using a Thermo PA2 C18 column (2.2µm, 2.1x100mm) with a gradient of 0.1% formic acid in water (mobile phase A) and acetonitrile (mobile phase B). Samples were maintained at 4^0C and 2µl aliquots injected. The column was maintained at 40^0C with a flow rate of 200µl/min, starting at 2% B, held for 2 minutes, with a linear gradient to 100% B at 7 minutes, held for 1 minute, before a 7 minute re-equilibration step at 2% B, necessary for consistent retention times. The QTRAP switching valve controlled eluate flow to the mass spectrometer, allowing analysis between 4-8 minutes to minimise instrument contamination. Folates were quantified from the mass spectrometry traces using Analyst software. See figure 2.3 for elution profiles of *C. elegans* 5-methyl-THF-glu_{1-6} detected by LC-MS/MS.

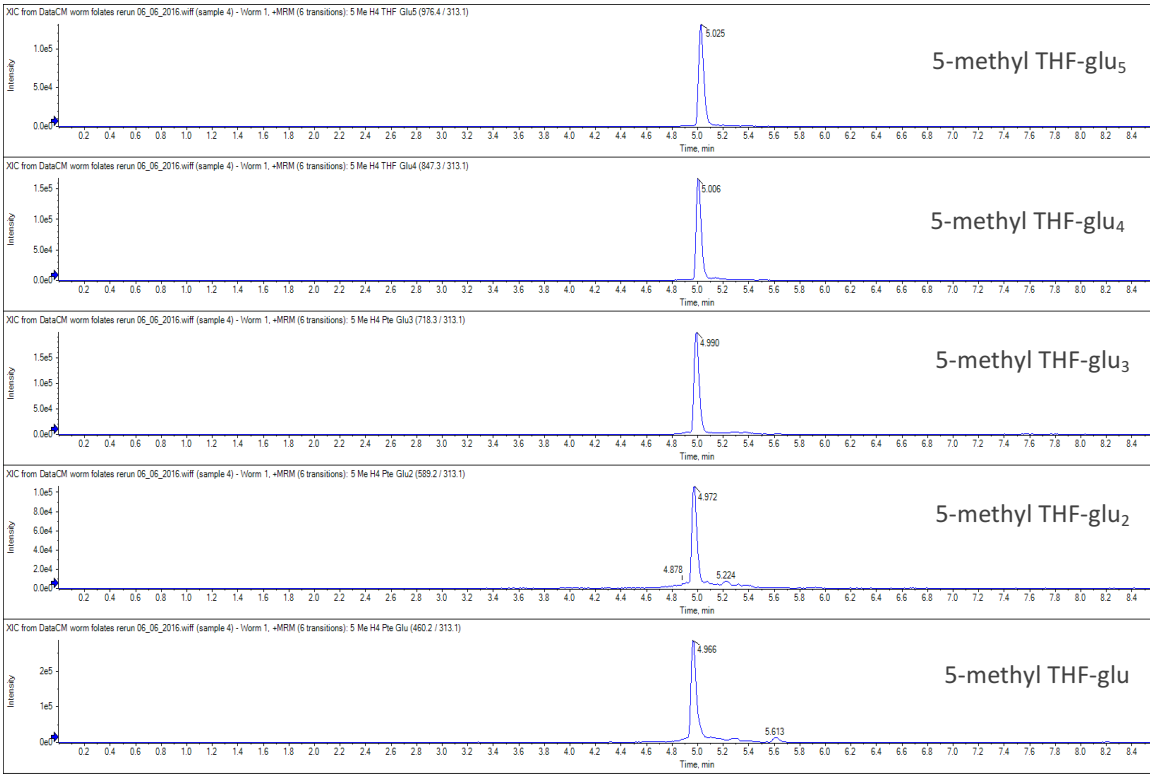

Figure 2.3 Separation of polyglutamated folates by LC-MS/MS with detection by multiple reaction monitoring (MRM) –$glu_{1\text{-}5}$ derivatives of 5-methylTHF in a *C. elegans* extract as an example of the specificity and sensitivity of the detection method.

2.14 PROCEDURE FOR QUANTITATIVE REAL TIME PCR

2.14.1 Extraction of bacterial RNA

DM plates were seeded with a DM culture and incubated for the required period at 25 ^{o}C. Two plates were required per extraction, with four replicates per condition. 2ml of 2:1 stabilization mixture (2 volumes Qiagen RNAprotect bacteria reagent: 1 volume M9) was pipetted onto the two plates and bacteria was removed carefully using a glass spreader and pipetted into a 1.5 ml Eppendorf tube. Tubes were mixed by vortexing for 30 secs and incubated at room temperature for 5 mins. Volume was recorded. 100 µl of sample was taken and diluted 1:10 (with M9) in a plastic cuvette. OD_{600} was measured and the required sample volume was calculated to obtain 7.5 x 10^8 cells was calculated as below:

$$Required\ sample\ volume = \frac{7.5}{80 \times OD_{600}}$$

The appropriate amount of material was pipetted into a new Eppendorf tube and samples were centrifuged for 10 mins at 3000 x g. Supernatant was decanted and residual supernatant was carefully removed by dabbing inverted tube onto a paper towel. The enzymatic lysis of the bacteria was carried by incubation with 200 µl of TE buffer (30 mM Tris. Cl, 1 MM EDTA, pH 8.0) containing 1 mg/ ml lysozyme. Samples were vortexed for 30 secs before incubation for 5 mins, with vortexing every minute for 10 secs. β-mercaptoethanol was added to a lysate buffer to inactivate RNases in the lysate and samples were precipitated using 96-100% ethanol. RNA was purified from the bacterial lysate using Qiagen RNeasy mini spin columns according to the manufacturer's directions. RNA was eluted using RNase-free water. Samples were

subjected to off-column DNase treatment using Turbo DNA-free kit (Invitrogen). RNA purity and concentration was quantified using the NanoDrop™ 8000 Spectrophotometer.

2.14.2 Reverse transcription of RNA to cDNA

Taqman reverse transcriptase reagents (Applied Biosystems/ Life Technologies) were used to generate cDNA. A master mix was prepared as below, mixed and briefly centrifuged before adding aliquoting and adding random hexamers and template RNA into separate PCR tubes.

Component	20 ul-rxn	Final concentration
DEPC-treated water	to 20 µl	-
10X RT Buffer	2.0 µl	1X
25 mM MGCl2	1.4 µl	1.75 mM
10 mM dNTP mix (2.5 mM each)	4.0 µl	0.5 mM each
100 mM DTT	1.0 µl	5.0 mM
Rnase inhibitor (20 U/ uL)	1.0 µl	1.0 U/ µl
Multiscribe RT (50 U/ uL)	1.0 µl	2.5 U/ µl
Mixed and briefly centrifuged:		
50 µM random hexamers	1.0 µl	2.5 µM
Template RNA	varies	1 µg

PCR tubes were capped tightly, mixed and briefly centrifuged before using a bench top thermocycler to complete the following incubation programme:

Temperature	Time
25°C	10 minutes
37°C	30 minutes
95°C	5 minutes
4°C	indefinitely

Samples were stored at - 20°C until use for qPCR.

2.14.3 Quantitative real-time PCR (RT-qPCR)

Products were detected using SYBR green fluorescence using SensiFast SYBR Lo-Rox kit (Bioline) in reactions set-up as below:

Component	20 ul-rxn	Final concentration
DEPC-treated water	3.4 µl	-
SYBR	10 µl	1x
Fwd primer	0.8 µl	400 nM
Rev primer	0.8 µl	400 nM
cDNA (1:50)	5 µl	20 ng

qPCR reactions were carried out using the Bioline micPCR v2.2 thermocycler. Using the parameters outlined below:

Step	Temperature	Time
Initial hold	95°C	2 mins
Cycle x 40		
Denaturation	95°C	5 secs
Annealing	60°C	10 secs
Extension	72°C	10 secs

Primers for qPCR were designed to have similar annealing temperatures.

1:50 was chosen as optimal cDNA concentration after running several dilutions of pooled WT cDNA (1:5, 1:10, 1:50, 1:100, 1:500) against the primer pairs for the two reference genes, *rrsA* and *mdoG,* and all the primer pairs for all the genes of interest (*pabA, rpoS, fic, abgT*). A no template control was included here, as standard with all reactions. The standard curves are shown in figure 2.4, where primer efficiencies have been calculated and fall within 90-110%.

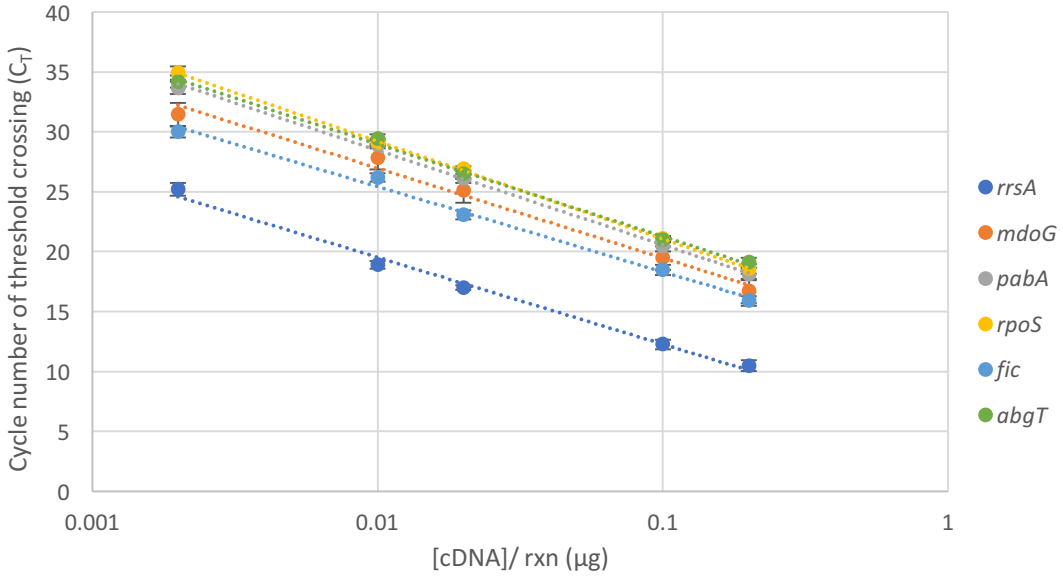

Gene	R^2	Gradient	Primer efficiency (%)
rrsA	0.9926	-3.153	107.57
mdoG	0.9879	-3.257	102.78
pabA	0.9978	-3.428	95.76
rpoS	0.998	-3.54	91.64
fic	0.9934	-3.091	110.63
abgT	0.9978	-3.347	98.964

Figure 2.4 Standard curves demonstrating primer efficiency in pooled WT cDNA

Gene expression was normalized to the expression of the *rrsA* transcript and used to calculate $\log_2$ fold-change using the ΔΔct method (Nolan et al. 2006). Values given are the averages of three replicate RNA extractions.

2.14.4 Primers for qPCR

Primers were designed using ApE - A Plasmid Editor Version 1.17. Primers were designed to give products ~200 bp.

Primer	Sequence (5' > 3')	Tm [°C]
rrsA fwd	GAATGCCACGGTGAATACGTT	57.9
rrsA rev	ACCCACTCCCATGGTGTGA	58.8
mdoG fwd	GCAATTGATACCGCCTTGC	56.7
mdoG rev	TTCGACTGCACATCCACAAC	57.3
pabA fwd	ACTTTACCGCCAAATGCCTG	57.3
pabA rev	TGGTTAAGCGCAACGATGC	56.7
rpoS fwd	TGGACCATGAACCAAGTGC	56.7
rpoS rev	TCGTCATCTTGCGTGGTATC	57.3
fic fwd	TCCAGGCCTTGATATCATGC	57.3
fic rev	AGCGCCGTCATTTCGTAAG	56.7
abgT fwd	AGCCACATTTCTTCCGATGC	57.3
abgT rev	CATTTGCGGATTGAACGCAG	57.3

2.15 ASSEMBLING NEW *E. COLI* K12 STRAINS BY P1 PHAGE TRANSDUCTION

The *abgTpabA* double mutant was created using the single mutants from the KEIO collection, *abgT* (JW5822-1) and *pabA* (JW3323-1). Several other mutants were also made for the Weinkove laboratory but have not been cited in this thesis. The method here consists of three steps: 1. Removal of the kanamycin marker from the 'recipient' strain 2. Preparation of phage lysate of 'donor' strain 3. P1 Phage transduction.

2.15.1 Removal of the kanamycin marker from KEIO strains

In KEIO strains, the kanamycin resistance gene alleles are flanked by FRT (FLP recognition target) sites. If FLP recombinase is expressed, the kanamycin resistance gene is eliminated through the deletion by homologous recombination at FRT sites. This was achieved using the pCP20 plasmid: an Ampicillin^R and Chloamphenicol^R plasmid with temperature-sensitive replication and constitutive expression of FLP recombinase. pCP20 was transformed into competent cells (see section 2.3) of the

strain containing the kanamycin gene to be removed (recipient strain). Cells were plated onto LB/amp plates and incubated overnight at 30 °C. 5 colonies were picked and streaked onto on an LB plate without selection and incubated for 18 hours at 43 °C in order to eliminate the plasmid. 20 single colonies were picked from each of the 5 colonies streaked and were patched (twizzle pipette tip with colony in LB) onto 3 separate plates (LB, LB/kan, LB/amp) and incubated over night at 37 °C. Select clones which grow on LB only, and thus have lost both pCP20 and the kanamycin resistance gene.

2.15.2 Preparation of phage lysate

An overnight culture of donor strain (grown with selection for the marker to be transduced (25 μg/ml kanamycin)) was diluted 1:100 in fresh LB supplemented with 10-25 mM MgCl2, 5 mM CaCl2, and 0.1-0.2% glucose (1 mL per lysate). Cultures were incubated 37 ˚C for 1-2 hr. When cells reached early log-phase, 40 μL of P1 phage lysate was added to the culture and continue growing at 37 ˚C. Cultures were monitored for 1–3 hr until cellular debris was visible in the tube, indicating that cells had lysed. Several drop of chloroform (50-100 μL) were added to the lysate and vortexed. Lysates were centrifuged (15 minutes, 3000 x g) to remove debris and the supernatant was transferred to a fresh tube. A few drops of chloroform were added and lysates were stored at 4 ˚C.

2.15.3 P1 phage transduction

An overnight LB culture of recipient strain (with kan marker removed) was pelleted by centrifugation (2 min, 6000 rpm) and resuspended in 1/5- 1/3 of the harvested

culture volume in fresh LB + 100 mM $MgSO_4$ + 5 mM $CaCl_2$. 100 uL (for each reaction) of transducing P1 lysate was incubated (caps open) for 37 ˚C for ~30 minutes to allow excess chloroform to evaporate from the phage stock. During this time, resuspended recipient strain cells were incubated at 37 ºC. Four conditions were set up (A-D) by adding the recipient cells to the tubes with phage. Contents were mixed rapidly after addition. A. 100 µL undiluted P1 lysate + 100 µL recipient cells B. 100 µL 1:10 diluted P1 lysate + 100 µL recipient cells C. 100 µL LB + 100 µL recipient cells D. 100 µL undiluted P1 lysate + 100 µL LB. LB used here was LB + 100 mM $MgSO_4$ + 5 mM $CaCl_2$.

Tubes were incubated at 37 ˚C for 30 min. 200 µL 1 M Na-Citrate (pH 5.5) was added and then 1 mL LB (normal LB) and incubated at 37 ˚C for 1 hr to allow expression of the antibiotic resistance marker. Cells were centrifuged for 5 min at 6000 rpm and resuspended in 100 µL LB supplemented with 100 mM Na-Citrate (pH 5.5). Cells were vortexed before plating onto LB/ kan plates and incubated at 37 ºC overnight. Colonies were picked and restreaked on LB/kan plates spread with 100 µL of 1 M citrate (pH 5.5) in order to obtain isolate colonies free from phage. Colonies were tested for the absence of the recipient mutant gene by diagnostic PCR (section 2.16)

2.15.4 Preparation of competent cells and transformation

An overnight culture of the appropriate strain was diluted 1:100 in fresh LB. OD_{600} was monitored until ~0.5-0.7. Cultures were places in ice water for 15 minutes and then pelleted by centrifugation in a chilled centrifuge for 5 minutes, 5000 rpm. The supernatant was removed and cells were resuspended in 1/ 10 of the original volume in TSS solution (10% (w/v) PEG 8000, 5% (v/v) DMSO, 30 mM $MgCl_2$, pH 6.5).

50 µL cells per transformation were aliquot into separate tubes and incubated on ice for 10 minutes, followed by room temperature incubation for 10 minutes and ice again for 10 minutes. Plasmid DNA was added (<1 µl) and heat shocked for 60 seconds at 42 ºC. Cells were places on ice for 10 minutes. 900 µl LB was added and cells were incubated with shaking at 37 ºC for 1 hours. 100 µl cells were plated onto LB plate containing appropriate marker. 50 µg/ml ampicillin and 25 µg/ml kanamycin was required for pUC19 and pJ128 transformations.

2.16 COLONY DIAGNOSTIC PCR

This technique was carried out in order to ensure that the mutants created by P1 transduction contained the desired mutations. Individual colonies were picked carefully with a pipette tip from an LB plate and twizzled in 5 µl of distilled H2O in the bottom of a PCR tube. The tip was them dropped into a 15ml Falcon tube for overnight culture. 20 µl reactions were set up as followed:

Component	Volume	Final concentration
dH_2O	3.8 µl	-
Master Mix Promega	10 µl	2x
Gene primer(s)	0.4 µl	400 nM
Kanamycin (K2) primer	0.4 µl	400 nM
Colony in dH_2O	5 µl	-

The K2 primer is specific to the kanamycin resistance gene and will give a product of ~891-1025 bp with a gene specific external primer if the gene is knocked out.

PCR reactions were carried out as outlined below:

Step	Temperature	Time
Denaturation	94 °C	25 secs
Annealing	51 °C	30 secs
Elongation	72 °C	30 secs
Extension	72 °C	10 minutes
Hold	4 °C	indefinitely

2.17 AGAROSE GEL ELECTROPHORESIS

10 µl of each sample was loaded into wells of a 1% agarose (MB1200, Melford) gel. Gels were run for approximately 20 minutes at 110V and PCR products were visualised with ethidium bromide.

2.18 STATISTICAL ANALYSIS

Statistical analysis of *C. elegans* lifespan assays was carried out using the statistical software JMP Pro 12.2 8.0.2. Survival function was estimated using the Kaplan-Meier estimator. This accounts for right-censoring (when worms are censored and withdrawn from the assay). Statistical significance was determined by the non-parametric statistical tests: Log-Rank and Wilcoxon. In the text, test statistics from Log-Rank tests have been cited. Full statistical analysis of lifespan data can be seen in supplementary table 1.

Student's *t* tests have been used to compare means between two different samples. Test statistics have been quoted in the text where appropriate.

CHAPTER 3: DEVELOPING METHODS TO CONTROL AND MEASURE *E. COLI* FOLATE IN THE *C. ELEGANS- E. COLI* MODEL SYSTEM

3.1 INTRODUCTION

In our model system, *C. elegans* is almost entirely dependent on *E. coli* for all macro- and micronutrients, including folate. Bacterial synthesis of these dietary components is itself dependent on the constituents of the growth media. The growth media therefore indirectly impacts *C. elegans* health by altering *E. coli* metabolism. The growth media conventionally used for *C. elegans* assays, NGM, is a soy peptone-based media consisting of a homogenised mixture of peptides, amino acids, vitamins, trace metals and fatty acids. It is likely to contain sources of folate and/ or folate precursors.

In order to understand how bacterial folate synthesis is modulating lifespan, we must be able to sensitively control and accurately measure the process. The constituents of the growth media must therefore be defined. This chapter outlines the development of a chemically defined media for use in *E. coli- C. elegans* research and the characterisation of bacterial and animal phenotypes on said media. This media will also facilitate sensitive bioanalytical techniques, thus enabling accurate quantification of both *E. coli* and *C. elegans* folate levels by LC-MS/MS. An alternative *in vivo* method to analyse *E. coli* folate status is also developed and characterized here. Using these methods, the aim is to determine and distinguish between the folate levels which support *E. coli* growth, and that which is 'excessive' and has a negative impact on *C. elegans* lifespan.

3.1.1 Development of a chemically defined media

A Master's student working in the Weinkove laboratory, Noel Helliwell (NH), began creating a folate-free chemically defined media. NH replaced the peptone constituent of NGM with individually defined amino acids and trace metals, and replaced the normal agar with 'high-purity' agar (see Chapter 2). NH reported that the media supported normal *E. coli* growth, but did not characterize *C. elegans* phenotypes. The first section of this chapter outlines further optimisation of this media, which will be referred to as defined media (DM), hereafter, and characterizes *E. coli* and *C. elegans* phenotypes on DM in order to establish it as a chemically controllable alternative to NGM.

3.1.2 LC-MS/MS: a highly sensitive method to detect specific folate species

A high performance liquid chromatography QTRAP mass spectrometry facility (referred to as LC-MS/MS hereafter) was installed in the Durham University Biosciences Department towards the end of this PhD research period. QTRAPs use multiple reaction monitoring (MRM) to obtain a high level of selectivity and sensitivity and can detect specific compounds in a sample within the picomole range (figure 3.1).

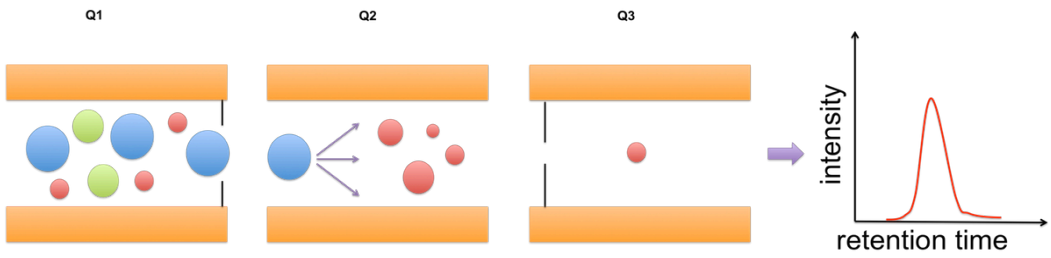

Figure 3.1. Diagrammatic representation of the LC-MS/MS QTRAP. QTRAPS have three separation modules or quadropoles, Q1-Q3: Q1 is set to select a specific 'precursor ion' of known mass, where it is then fragmented in Q2; the 'product ion' is selected in Q3 and detected. This is known as multiple reaction monitoring and is capable of highly specific and sensitive detection.

LC-MS/MS settings were optimized for folate detection by Ian Cummins in the Durham Biosciences Bioanalytics facility based on parameters set out in the literature (Lu et al., 2007) (see Chapter 2, section 2.13.3). This method differs from the previous detection method (LC-MS) used by the Weinkove laboratory, where the former method scanned all peaks within a sample and selected only the most abundant for fragmentation and quantification.

3.1.3 *C. elegans gcp-2.1* mutant: a phenotypic bioassay to detect *E. coli* folate status

Due to the insensitivity of the LC-MS technique used in the previous study (Virk et al. 2012) and the lack of a replacement facility for the first half of this PhD research period, there was a need to develop an alternative method to measure bacterial folate. It was hypothesized that in a genetically susceptible background, *C. elegans* life-traits which have a high demand for folate, such as development and reproduction, could be sensitized to low levels of dietary/ *E. coli* folate. Quantification of these phenotypes would act as a readout of the bacterial folate status. Furthermore, as this is an *in vivo* quantification method, it acts as a readout of functional folate levels.

Work carried out by Bhupinder Virk (BV), a PhD student in the Weinkove laboratory, sought to restrict *C. elegans* folate uptake by knocking out the gene thought to be responsible for the deconjugation of polyglutamated folates in the intestine, thus generating monoglutamated folates for absorption. A BLASTp search revealed a *C. elegans* protein, encoded for by the R57.1 gene, with 35% sequence identity to the mammalian glutamate carboxypeptidase protein, GCPII (see Chapter 1 for more information on GCPII). Two other glutamate carboxypeptidase genes, C35C5.2 and C35C5.11 were also identified, but as R57.1

had been identified in a study using an intestine specific promoter to probe for intestinally-expressed genes (Pauli et al., 2006), it was carried forward for further research. R57.1, C35C5.2 and C35C5.11 were named *gcp-2.1, gcp-2.2* and *gcp-2.3,* respectively, by the Weinkove group.

BV out-crossed the *gcp-2.1* mutant strain obtained from the *C. elegans* Genetics Gentre (CGC) to wild-type to create the *gcp-2.1(ok1004)* strain. This strain contains a <TCTCTTCTTTTCCGAAAGTGGTGACGTCATTTATC> insertion and a functional 1523bp deletion in the *gcp-2.1* gene (*gcp-2.1* (*ok1004)*), which is located on the X chromosome. Phenotypic analysis revealed that this strain had no development defects or survival differences compared to the wild-type parent strain, however, on SMX-treated *E. coli*, *gcp-2.1* mutants had stunted developmental growth at L4 stage and were sterile. The phenotype was rescued with a transgene containing a genomic fragment including the *gcp-2.1* gene. This chapter details the further characterization of the *gcp-2.1* strain as a bioassay to detect low *E. coli* folate levels.

3.2 CHAPTER AIMS

- Aim 1: Optimize the defined media and establish it as an alternative to NGM
- Aim 2: Use defined media to sensitively detect the folate thresholds for bacterial growth and lifespan modulation
- Aim 3: Characterize the *gcp-2.1 (ok1004)* strain and develop it as a phenotypic assay of bacterial folate status

3.3 RESULTS

3.3.1 Establishing defined media as a suitable alternative to NGM

DM was optimised by NH for *E. coli* growth, however, when the media began to be used for *C. elegans* assays, several issues became apparent. Namely, plate drying and 'cracking', the presence of crystalline deposits, and a lack of vitamin B12. These issues were resolved relatively simply and are detailed here. Lower agar percentages (from 2%) were trialed and 1.7% agar was found to mitigate the issue with plate cracking, which was proving a particular problem during incubation at 25°C over the course of lifespan assays. Omitting the addition of 1 mM $CaCl_2$ post-autoclaving (as standard with NGM) was found to solve the issue of the crystalline deposits in the media, which was likely due to excessive calcium in the media: this was an oversight as $CaCl_2$ is also included in the trace metal solution. 10 nM B12 was added to the media as it is an essential requirement for both *E. coli* and *C. elegans*. Following this optimization, *E. coli* growth and several *C. elegans* life-traits were monitored on DM.

3.3.1i Defined media supports wild-type E. coli growth

The wild-type *E. coli* K12 parental strain, BW25113, transformed with a kanamycin resistance plasmid, pGreen, is used here for all experiments, unless otherwise stated, and referred to hereafter as WT *E. coli.* Growth of WT *E. coli* on NGM and DM solid agar (with and without 10 nM B12) was measured by OD_{600} after 24, 48 and 72 hours of growth (see Chapter 2, section 2.7.1). Bacterial growth on DM, regardless of B12, was not significantly different to growth on NGM (figure 2.2). This is consistent with the preliminary work carried out by NH and indicates

that the manipulations made to optimize DM do not alter its ability to support bacterial growth.

3.3.1ii Defined media supports C. elegans development, fecundity and lifespan

Previous work did not carry out a phenotypic analysis of *C. elegans* life-traits on DM. Here, body length at L4 stage, fecundity and lifespan on DM are compared to

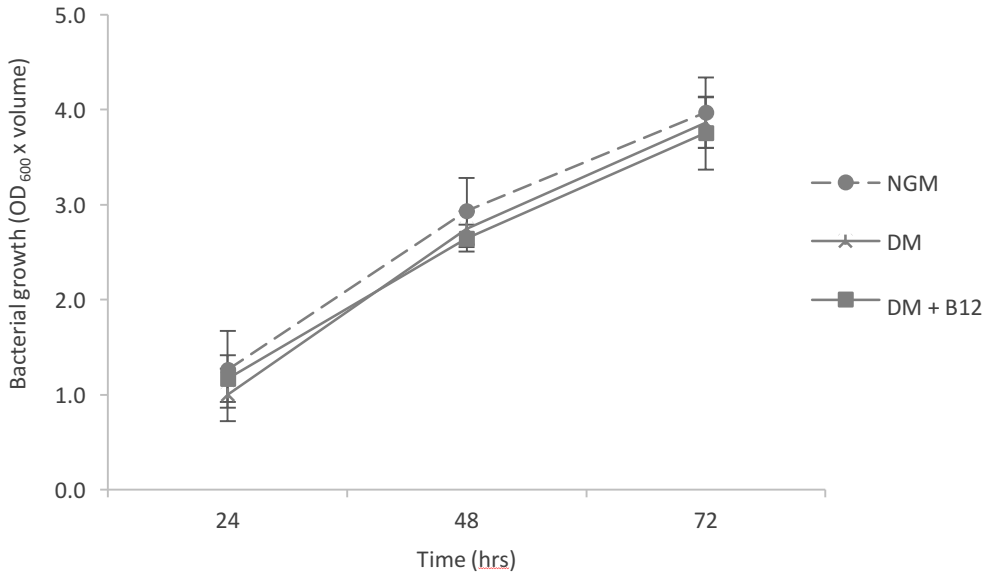

Figure 3.2 Defined media supports wild-type *E. coli* growth similarly to on NGM

WT *E. coli* was seeded onto DM agar plates and incubated at 25 ˚C. Bacterial growth was measured at 24, 48 and 72 hours after seeding (see Chapter 2, section 2.9). Error bars represent standard deviation over 10 replicate plates per condition.

on NGM. The wild type *C. elegans* Bristol N2 strain was used to conduct fecundity analysis and the temperature-sensitive sterile *glp-4* (SS104) strain was used for the development assay and all lifespan assays in this thesis (Chapter 2, section 2.12). Development was quantified by raising synchronized populations of worms from egg on stated growth media and measuring body length at L4 stage (2.5 days at 25°C) (see Chapter 2, section 2.9) (figure 3.3a). No significant difference in body length was observed in worms raised on DM, with or without B12, compared to NGM. These worms were transferred at day 1 of adulthood onto freshly seeded *E. coli* plates of the same condition they were raised on and the other two conditions (figure 3.3b), and lifespan assays were carried out (figure 3.3c).

As for all lifespans presented in this thesis, please see Supplementary table 1 for a full outline of experimental conditions, strains used, number of animals included in each condition, mean lifespans and statistical analysis (indexed by Chapter no., fig no.). Kaplan Meier survival curves are plotted using the statistical software JMP. The non-parametric statistical tests of survival, Log-rank and Wilcoxon, were used to test significance between two lifespan conditions. The result of Log-rank tests will be quoted in the text where appropriate.

It was found that if worms were raised on NGM and shifted to DM at day 1 of adulthood, mean lifespan was increased by 8.80% ($P=0.0254$) and if shifted to DM + 10 nM B12, mean lifespan was increased by 16.33%, ($P<0.0001$) compared to worms that remained on NGM (figure 3.3). If raised on DM and shifted to NGM for lifespan, survival was not statistically significant from that of worms on NGM throughout their lifespan, however, if maintained on DM for lifespan or shifted to

DM + B12, mean lifespan was increased by 8.57% (P=0.0351) and 12.46% (P=0.0067), respectively. Likewise, if raised on DM + B12 and shifted to NGM for lifespan, survival was not affected, however, a large increase in mean lifespan was measured when worms were maintained on DM + B12 (28.795) or shifted to DM (17.19%), where Log-rank P<0.0001, in both cases. Together this indicates that that DM in adulthood extends lifespan and that worms require B12 in both development and adulthood for optimal lifespan.

Fecundity analysis was carried out using the N2 WT strain. Synchronized populations of worms were raised from egg on stated condition until adulthood and individual gravid (egg-laying) hermaphrodites were transferred onto individual plates (n=10) where they were then transferred again onto a fresh plate each day for 4 days. Plates were incubated at 25 ˚C and viable progeny were counted 24 hours after the worm was removed (see Chapter 2, section 2.9.2). Interestingly, there was a significant reduction in the number of progeny produced on NGM compared to DM (± B12) on day 1 of egg-laying (figure 3.4). Overall, there was no significant difference in the total progeny produced over the egg-laying period in animals raised on NGM or DM, with or without supplemental B12.

Together, these data demonstrate that DM sufficiently supports *C. elegans* development, fecundity and lifespan in line with that observed on NGM. DM in adulthood and B12 during both development and adulthood increases survival compared to NGM. 10 nM B12 was added to DM for all subsequent experiments.

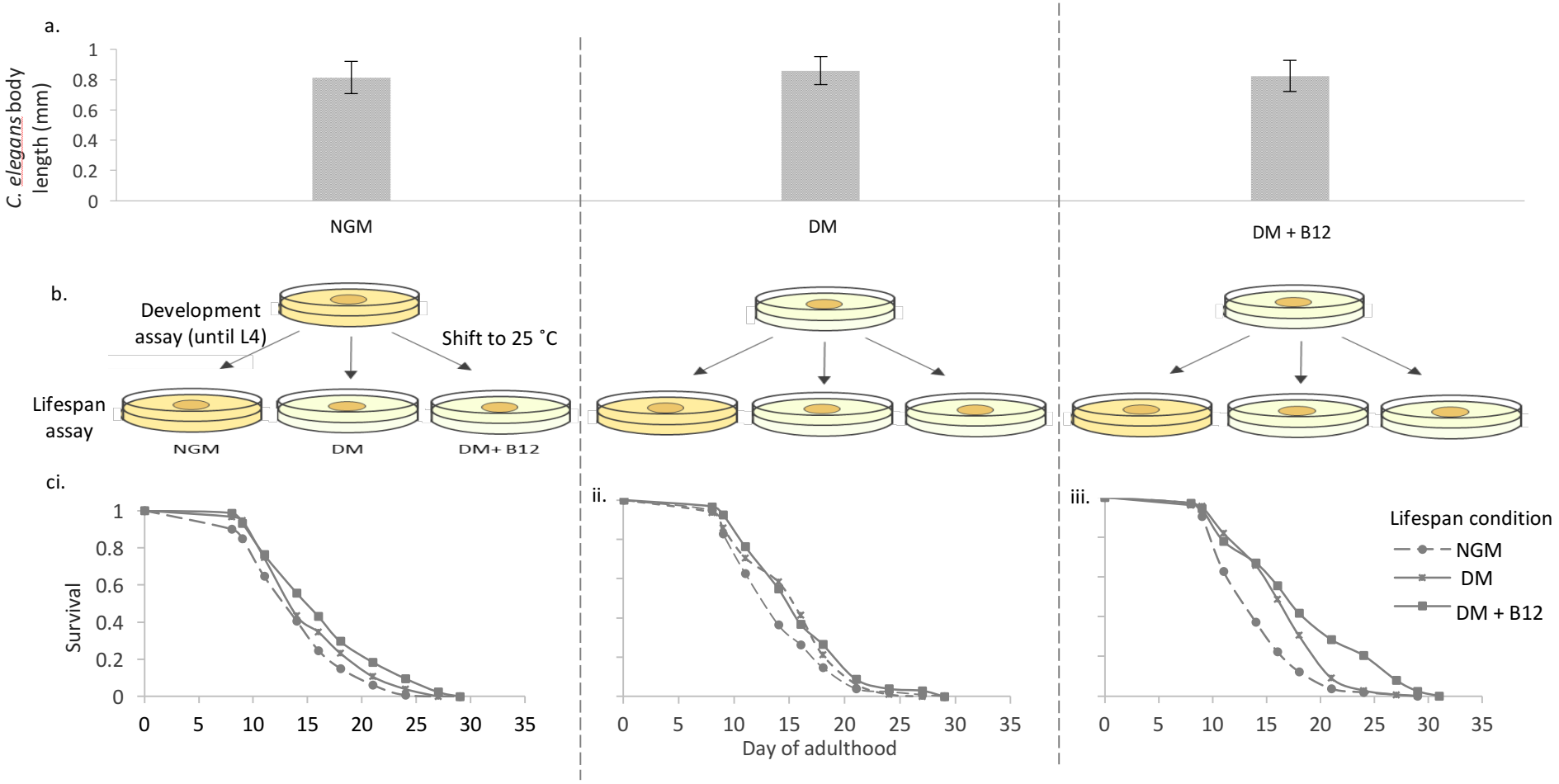

Figure 3.3 Development and lifespan analysis of *C. elegans* on NGM and DM± B12. *C. elegans* were raised on either NGM, DM or DM + B12 until L4 stage (at 15 ˚C) and a) body length was measured. Error bars represent standard deviation b) worms were then shifted to 25 ˚C for 24 hrs and transferred onto fresh plates of each of the three conditions for lifespan anlysis c) Kaplan Meier suvirval curves of worms raised on i. NGM ii. DM iii. DM + B12. See supplementary table 1 for full details of lifspan analysis.

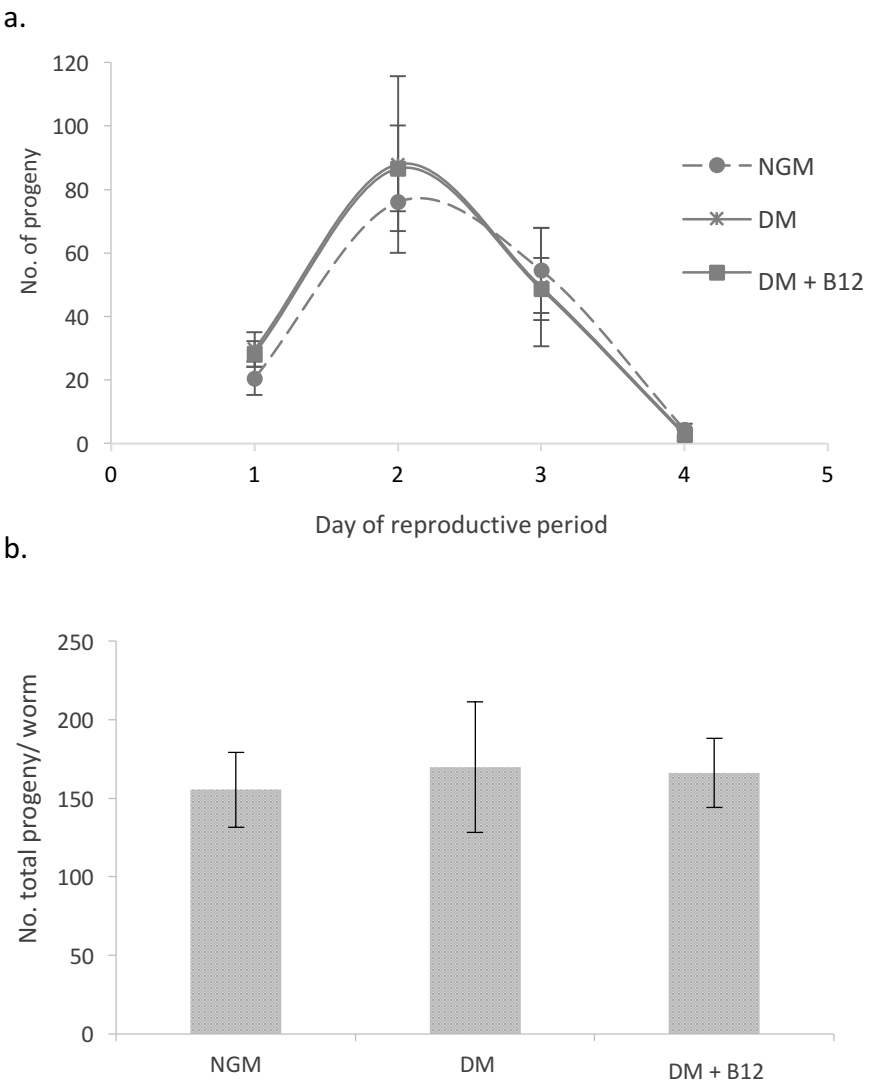

Figure 3.4 Fecundity analysis of *C. elegans* on NGM and DM± B12. *C. elegans* were raised on either NGM, DM or DM + B12 until L4 stage and individual worms were transferred onto plates for fecunity analysis a) number of viable progeny produced over four day reproductive window was monitored (n=10 worms per condition) b) total number of progeny produced by 10 worms over 4 days. Error bars represent standard deviation.

3.3.2 Using DM to examine *E. coli* folate threshold for growth and *C. elegans* lifespan modulation

In order to monitor how DM affects the growth of the *E. coli* folate-synthesis mutant, *pabA,* a 96-well microtiter plate assay was developed. Plates were incubated at 37 °C and OD_{600} monitored by a plate reader every 5 minutes (after shaking) for 20 hours (See chapter 2, section 2.7.2). Optimization of this assay was required as *pabA* growth was initially similar to WT (data not shown); it was hypothesized that *E. coli* cells carry over PABA from the initial culture in LB into the DM. An intermediate 'subculture' step from LB into an overnight DM culture was introduced in order to 'wash' the cells of PABA. This subculture was then used to inoculate the wells at OD_{600} =0.001 (figure 3.5b). This produced a robust and repeatable sensitized *pabA* baseline growth 'curve'. The need for these steps emphasizes the sensitivity of *E. coli* to small quantities of exogenous folate precursors.

The growth of WT *E. coli* and all *pab* mutants were assayed (figure 3.5a). This would ensure that limited *pabA* growth on DM was folate specific and not due to a folate-independent defect in this strain. Both *pabA* and *pabB* showed negligible growth in DM, whereas, despite an extended lag phase, the *pabC* mutant reached end-point growth in line with WT *E. coli* (figure 3.5a). This is consistent with the lifespan screen data from the Weinkove lab, where *pabA* and *pabB* mutants were found to significantly extend lifespan, but the *pabC* mutant did not.

3.3.2ii pabA mutant growth is sensitive to defined media and is rescued with PABA

The *pabA* mutant was focused on for all following experiments. The impact of the folate precursor, PABA, on *pabA* growth in DM was assayed by supplementing wells with varying concentrations of PABA. A dose-dependent growth response of *pabA* to PABA supplementation was observed (figure 3.5bi), where 50 nM PABA completely rescued *pabA* growth and a partial rescue in growth was observed with just 1 nM. Growth curves represent an average of 4 technical replicate wells. This assay was repeated several times with similar results.

In order to assess the impact of PABA on *pabA* growth under conditions used for *C. elegans* experiments, the assay was also carried out on agar DM (figure 3.5bii). Plates were incubated at 25 °C and OD_{600} was measured at 24, 48 and 72 hrs after 'seeding' the *E. coli* liquid DM sub-culture onto the agar DM. Again, a dose-dependent response to PABA was observed, but a 10-fold higher concentration was required here to rescue growth: 100 nM PABA completely restored growth, whereas1 nM PABA had a negligible effect (figure 3.5bii). Together these assays identify that the *pabA* mutant requires nanomolar quantities of PABA for growth.

3.3.2iii 1μM PABA reverses C. elegans longevity on pabA mutant on defined media

Having identified the lower folate threshold required to support *pabA* growth on DM, lifespan assays were carried out on the *pabA* mutant in order to determine the folate threshold which dictates *C elegans* lifespan. *C. elegans* were raised on DM plates seeded with DM subcultures of WT *E. coli* until adulthood and then transferred onto either *pabA* or WT seeded DM plates supplemented with a range of PABA concentrations. The lowest PABA concentration used was 100 nM so as to ensure *pabA* growth and eliminate a confounding effect of dietary restriction on

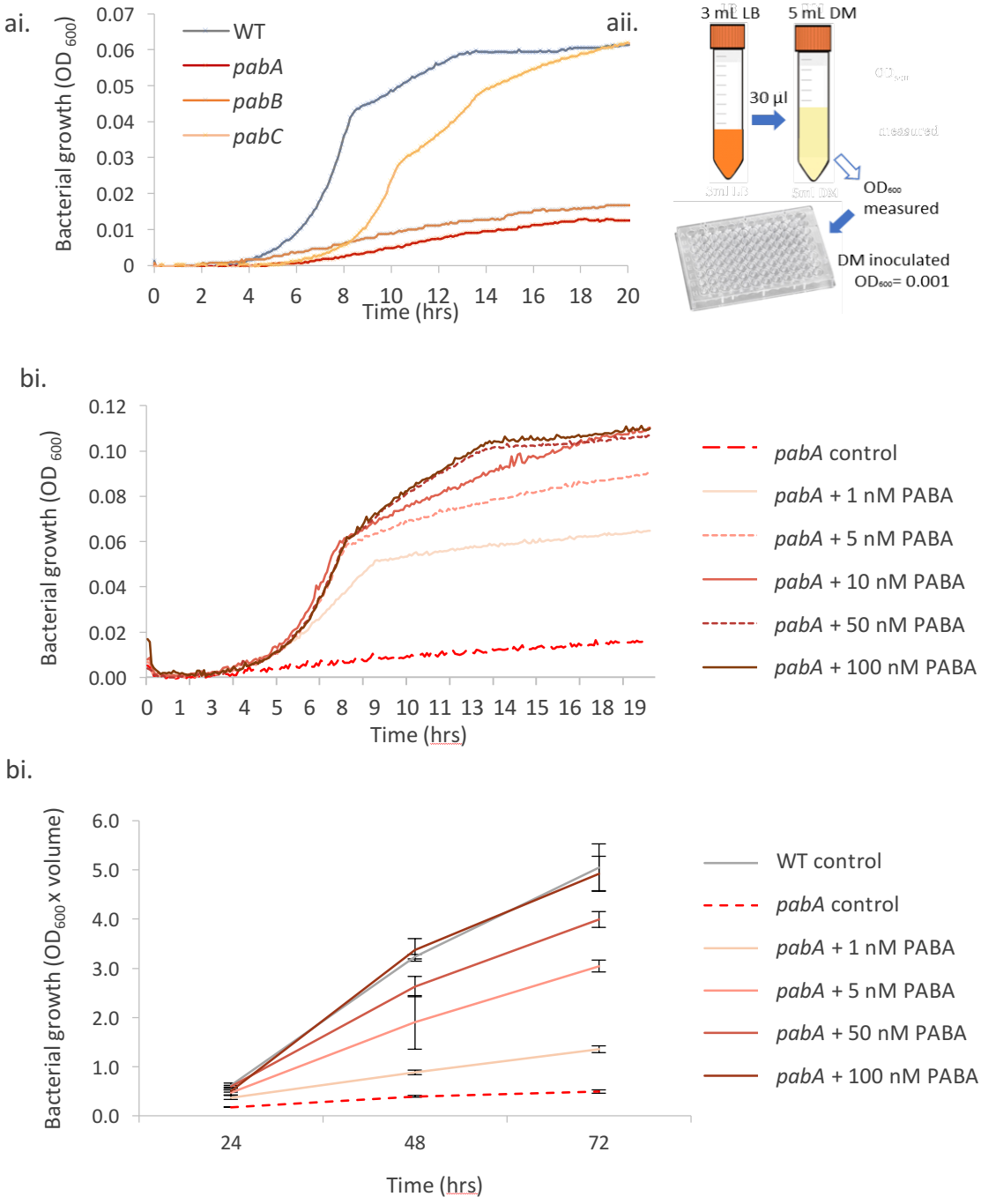

Figure 3.5 Growth of *pabA* strains on solid and liquid DM supplemented with PABA ai) growth of *pabA, pabB* and *pabC* in liquid conducted at 37 °C in microtiter plates and OD_{600} measured after shaking, every 5 mins for 19 hrs. each curve is the mean reading from 4 biological replicates aii) depicts experimental set-up. Growth of *pabA* supplemented with PABA was assessed in bi) liquid DM (37 °C) and bii) solid agar DM (25 °C). For solid agar assay, *E.* coli was washed off after 4 days growth, using sterile media at 24, 48 and 72 hrs. Error bars represent standard deviation over 5 biological replicates.

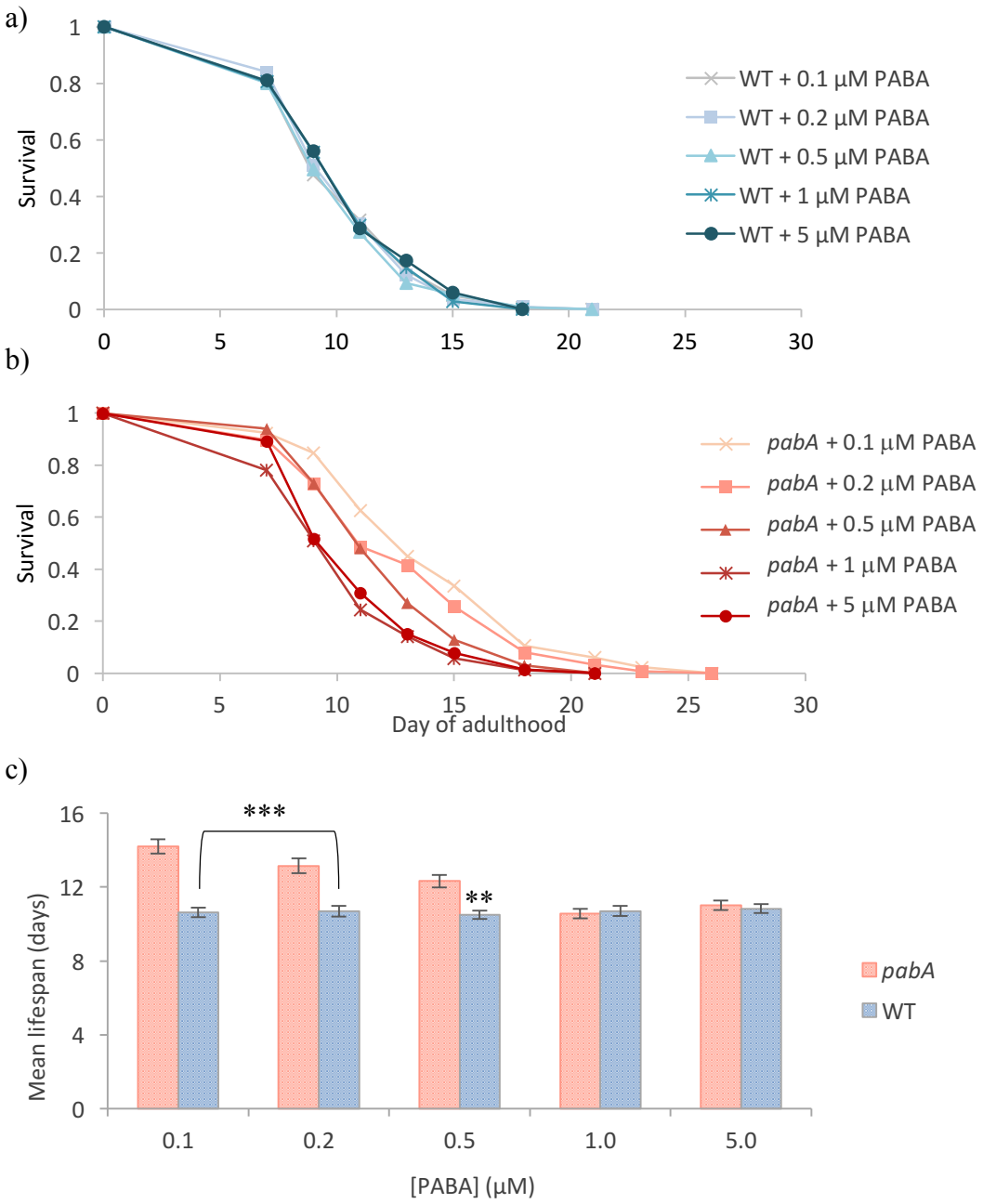

Figure 3.6. PABA reverses lifespan of *C. elegans* on *pabA* mutant *E. coli*. Temperature-sensitive *C. elegans* (*glp-4*) at L4 stage (n=150) were transferred onto DM solid agar plates supplemented with PABA and seeded with a) WT or b) *pabA E. coli* and incubated at 25 °C for the duration of their lifespan. Animals were transferred onto plates with 'fresh' *E. coli* at days 7 and 14 of adulthood. All plates contained 0.1 µM PABA to ensure sufficient bacterial growth c) Mean lifespan on each condition. Error bars represent standard error. Asterisks indicate the result of non-parametric Log-rank statistical analyses comparing indicated *pabA* condition to WT control (WT + 0.1 µM PABA), where **P<0.005, ***P<0.0001

lifespan. As nano/ micromolar concentrations of PABA are used here, any impact of PABA on *C. elegans* lifespan can be attributed to changes in *E. coli* metabolism as *C. elegans,* like all animals, lack the enzymatic machinery to metabolize PABA.

Figure 3.6 displays both the Kaplan-Meier survival curves and mean lifespans on each condition. PABA supplementation was not found to impact the lifespan of *C. elegans* fed WT *E. coli.* Mean lifespan of *C. elegans* on the *pabA E. coli* mutant on DM supplemented with 100 nM PABA was 33.36% higher compared to on WT *E. coli* on the same condition ($P<0.0001$). A dose-dependent reduction in *C. elegans* lifespan on the *pabA E. coli* mutant was observed between 0.2 μM-1 μM PABA, where lifespan was reverted to WT at 1 μM PABA. Higher concentrations of PABA did not further decrease lifespan. This lifespan assay demonstrates that supplementation of PABA into DM, above the threshold required to support *pabA E. coli* growth, acts to decrease *C. elegans* lifespan. Thus, the folate thresholds for bacterial growth (0.1 μM PABA) and that which reverses *C. elegans* lifespan (1 μM) on the *pabA E. coli* mutant are determined and distinguished between.

3.3.2iv PABA increases pabA folate levels in correlation with its impact on lifespan

Given the central hypothesis that *E. coli* folate synthesis shortens *C. elegans* lifespan, it was assumed from the previous data that PABA supplementation at 1 μM would increase folate synthesis and thus folate increase levels in the *pabA E. coli* mutant in line with the WT *E. coli* strain. In order to test this, the LC-MS/MS facility was used to detect levels of individual folates in the *pabA* mutant in response to PABA. Optimization of the extraction technique was carried out in order to prevent folate degradation, promiscuous interconversions and to obtain

maximum yield. Please see Chapter 2, section 2.13 for a full outline of the folate extraction protocol and LC-MS/MS detection.

The *pabA* mutant and WT *E. coli* were seeded onto DM agar plates supplemented with PABA at 0.1 μM, 1 μM, 10 μM and 100 μM. Folate extractions were carried out after 4 days growth at 25 °C. This was deemed an appropriate time point relevant to *C. elegans* experiments. Samples were normalized for growth prior to extraction. Signals were normalized to that of an internalized standard (MTX-glu_6) added to the extraction buffer in order to control for variability in MS sensitivity over the large number of samples analyzed. Tri-glutamated folates are presented here (figure 3.7)

In *pabA* mutant extracts with 0.1 μM PABA, levels of 5-methyl THF (P=0.002), 5-formyl THF (P<0.001), THF (P=0.002) and 5,10-methenyl THF (P<0.001) were detected at significantly lower levels compared to WT extracts with 0.1 μM PABA, as determined by Student's *t*-tests. However, 1 μM PABA significantly increased levels of all folates in *pabA* mutants extracts compared to *pabA* mutants with 0.1 μM PABA. Folate levels in *pabA* mutant extracts with 1 μM PABA were not significantly different compared to in WT extracts with 0.1 μM PABA (figure 3.7), however, as 1 μM PABA also markedly increased WT folate levels, folate levels in *pabA* mutant extracts with 1 μM PABA were significantly different compared to in WT extracts with 1 μM PABA. At 10μM PABA, all folate levels in *pabA* mutant extracts were detected at levels similar to WT. 100 μM PABA did not increase the folate levels further in either WT or *pabA* extracts.

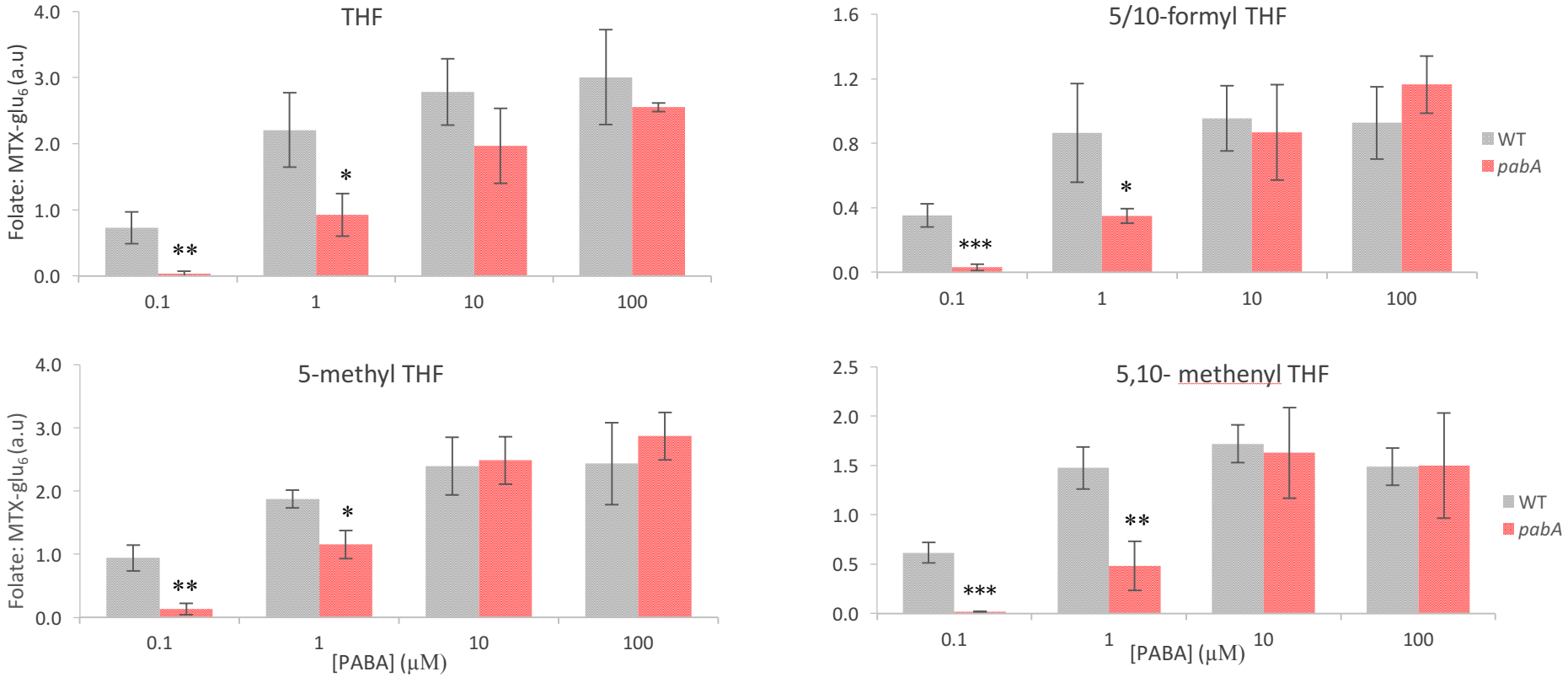

Figure 3.7. LC-MS/MS detection of folate species in WT and *pabA* supplemented with PABA. WT and *pabA E. coli* were seeded onto DM and incubated at 25 °C for 4 days. Samples were normalized for growth before extraction. Folate levels are expressed as a ratio of an internal MTX-glu$_6$ spike. Error bars represent standard deviation (4 biological replicates). Asterisks denote the result of Student's *t*-Tests, of *pabA* condition compared to relevant WT condition (same [PABA]), where * P<0.05 **P<0.005, ***P<0.001.

Together, this demonstrates that the impact of PABA on *C. elegans* lifespan on the *pabA* mutant is correlated to bacterial folate status, as a wild-type folate profile is restored in the *pabA* mutant at 1 μM PABA. The increase in folate levels above 1 μM PABA, in both WT and *pabA,* despite no further impact on lifespan, indicates that a folate-dependent activity within the 0.1 μM to 1 μM PABA window is responsible for lifespan modulation.

3.3.3 Characterizing the *C. elegans gcp-2.1* folate-uptake mutant strain as a biological read-out of *E. coli* folate status

The LC-MS/MS facility became available only towards the end of the research period. There was therefore a need to develop a method to assess bacterial folate status. As discussed, previous work carried out by BV in the Weinkove laboratory created the *gcp-2.1(ok1004)* and hypothesized that folate uptake in the intestine is disrupted due to knockout of the gene required for folate deconjugation. These claims were based on the observation that the *gcp-2.1* mutants strain has no abnormal phenotypes on NGM on WT *E. coli*, but it exhibits developmental and reproductive sensitivity to SMX-treated *E. coli.*

3.3.3i gcp-2.1 mutants show normal developmental phenotypes on NGM and DM

As this thesis uses DM, and the preliminary work was carried out on NGM, it was first tested whether the folate-free DM caused further *gcp-2.1* sensitivity. Body length and fecundity of *gcp-2.1* mutants and the wild-type parent strain were monitored, as previously described, on both DM and NGM seeded with WT *E. coli*

No significant difference in body length at L4 stage of *gcp-2.1* mutants on DM or NGM was found compared to the wild-type strain on either condition (figure 3.8a). Fecundity analysis revealed a slight delay in the reproductive period of both

mutant and wild-type strains on NGM compared to DM (figure 3.8bi,ii). This was also observed in N2 worms on NGM compared to DM (figure. 3.4a). The mean total number of eggs laid per worm was not statistically different across any of the conditions (figure. 8biii). This demonstrates that DM is capable of supporting normal development and reproduction of the *gcp-2.1* strain on WT *E. coli,* and is consistent with the ability of DM to support WT *E. coli* growth in line with that on NGM.

3.3.3ii gcp-2.1 mutants show stunted growth and sterility on pabA and SMX-treated E. coli

The previous work had not quantified the phenotypes of the *gcp-2.1* mutant strain on SMX-treated *E. coli.* In order to establish this strain as a reliable sensor of bacterial folate levels, quantification on both SMX and the *pabA* mutant needed to be carried out. WT and *pabA* mutant *E. coli* was seeded onto DM agar plates and WT was also seeded onto plates supplemented with 128 μg/ml SMX. 100 nM PABA was supplemented into the media in order to ensure bacterial growth. Synchronized populations of worms were obtained by egg-lay onto the stated condition, with 4 replicates per condition.

As shown in figure 3.9 the body length of the *gcp-2.1* mutant strain at L4 stage was reduced by over 50% on both the *pabA* mutant and on SMX compared to on control

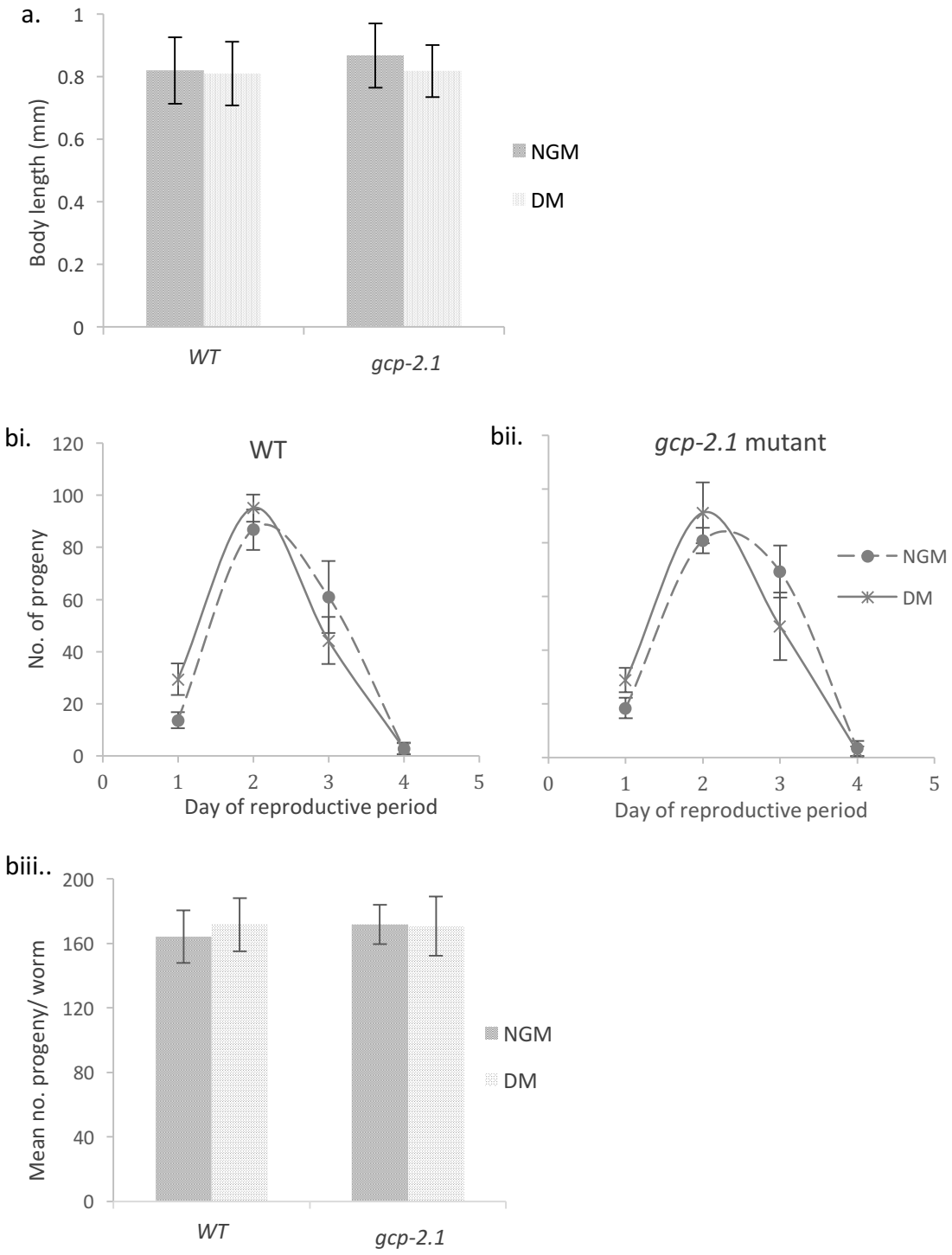

Figure 3.8 The *C. elegans gcp-2.1* mutant has normal developmental and reproduction on WT *E. coli* on NGM and DM. *gcp-2.1* mutants were raised from egg on NGM and DM seeded with WT *E. coli* and incubated at **2**5 °C until L4 stage when a) body length was measured and b) progeny produced of i) WT and ii) *gcp-2.1* mutants over a 4 day reproductive window was monitored iii) Total number of progeny produced by WT and *gcp-2.1* mutants. Error bars represent standard deviation of 10 worms per experimental condition.

WT *E. coli*. The wild-type *C. elegans* strain did not show a growth defect on these conditions (figure 3.9a). A fecundity analysis was not carried out as the number of eggs laid by the *gcp-2.1* strain on the sensitive conditions was negligible.

3.3.3ii PABA rescues the gcp-2.1 phenotype on pabA mutant E. coli

In order to verify that these phenotypes are folate-dependent, PABA was added into the media in order to rescue bacterial folate synthesis in the *pabA* mutant, and thus increase the amount of folate available to the *gcp-2.1* mutant. The *gcp-2.1* strain was raised on *pabA* mutant *E. coli* on DM agar plates supplemented with 0.1 μM, 0.2 μM, 0.5 μM and 1 μM PABA. A concentration-dependent increase in *gcp-2.1* body length with PABA was observed, where wild-type body length was restored at 1 μM PABA (figure 3.9b). This is consistent with the restoration of wild-type folate levels in the *pabA* mutant at this concentration (figure 3.7). Together, these data verify that the developmental phenotype of the *gcp-2.1* strain can be used as a readout of *E. coli* folate levels. Following this characterization, the *gcp-2.1* strain has been used throughout this thesis to test for genetic manipulations and extrinsic factors that modulate bacterial folate synthesis.

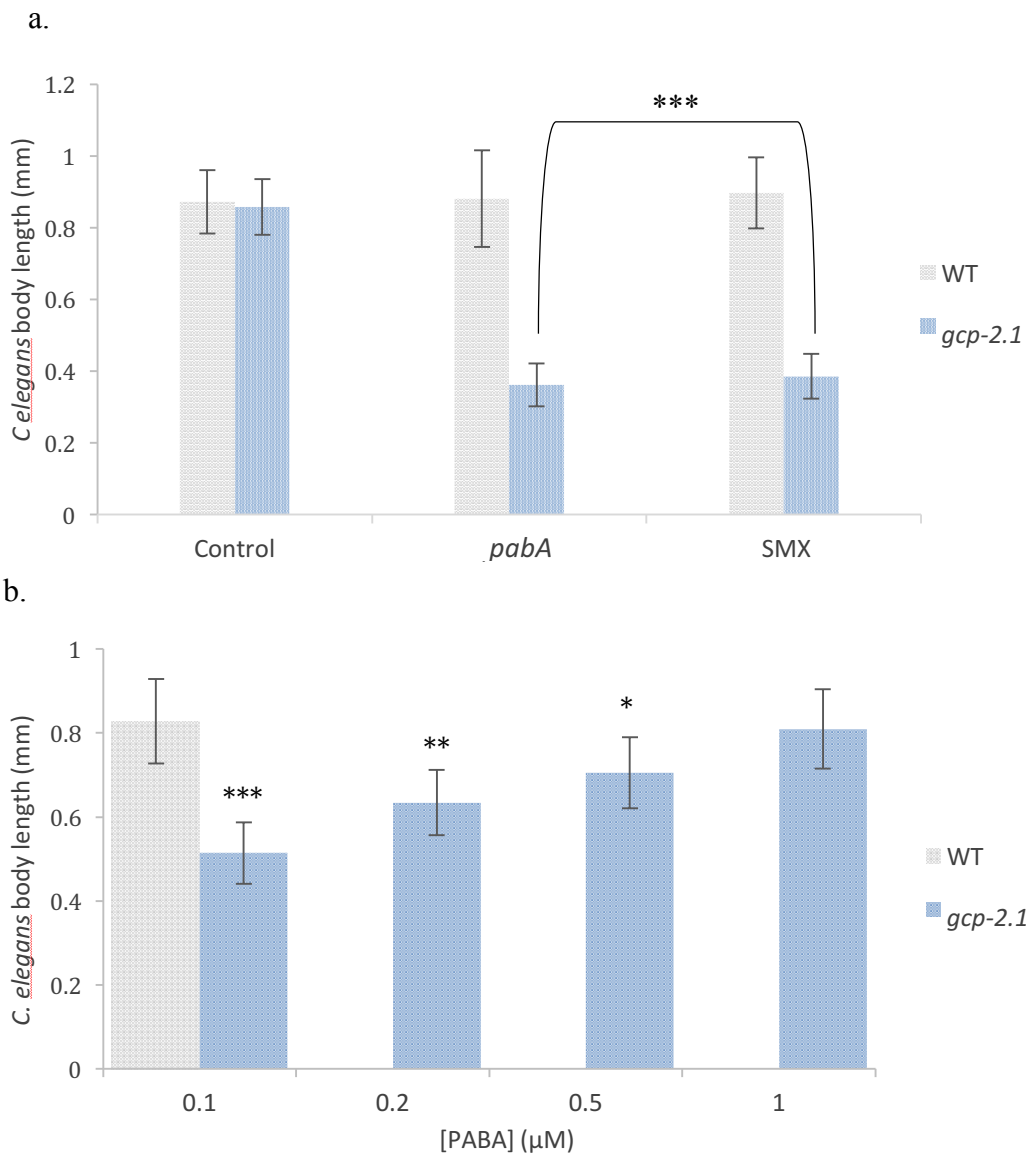

Figure 3.9. *C. elegans gcp-2.1* mutant has abnormal development on SMX and *pabA E. coli* but is rescued by PABA. WT and *gcp-2.1* mutants were synchronized by overnight egg-lay (20 °C) onto DM plates and incubated at 25 °C until L4 stage when body length was measured. *C. elegans* were maintained from egg on plates seeded with a) WT or *pabA* mutant *E. coli,* or onto plates seeded with WT *E. coli* containing 128 µg/ml SMX and on b) plates seeded with *pabA* mutant supplemented with PABA. All plates in (a) contained 0.1 µM PABA to ensure sufficient bacterial growth. Error bars represent standard deviation. Asterisks denote the result of Student's *t*- tests of denoted condition compared to a) WT *C. elegans* on same bacterial condition and b) WT worms on DM + 0.1 µM PABA, where ***P<0.005, **P<0.01 *<0.05.

3.4 DISCUSSION

3.4.1 Defined media is a chemically definable, highly controllable and effective replacement for NGM

Given that bacterial metabolism can be altered by its external environment, which in our controlled system is the NGM, and that here we are investigating a specific aspect of bacterial metabolism, it was essential to control the components of NGM that may be modulating bacterial folate synthesis. The first section of this chapter outlined the development of a folate-free, chemically defined media (DM) and demonstrated its capability to support normal *E. coli* growth and *C. elegans*, development, reproduction and lifespan. DM provides control over all components of the *E. coli* 'diet' by precisely defining concentrations of all amino acids and trace metals (see Chapter 2, section 2.3.2). This media may therefore be useful to other *C. elegans* laboratories, or indeed microbiology groups, interested in controlling bacterial metabolism and/ or altering specific aspects of the bacterial diet. LC-MS/MS detection of *E. coli* folates on DM was more sensitive and reliable compared to on NGM; DM therefore also provides a 'clean' platform for bioanalytical analyses.

3.4.2 Folates for one-carbon metabolism and beyond

Due to the confounding impact of bacterial folate precursors in the media, the previous study was unable to differentiate between the folate threshold required to support bacterial growth and that which shortens *C. elegans* lifespan. Here, the use of DM in combination with *E. coli* genetic manipulation has enabled control of *E. coli* folate levels in order to define these thresholds. The sensitized growth of the *pabA*

mutant on DM facilitated assays in which the effect of the folate precursor, PABA, on *E. coli* growth and *C. elegans* lifespan were distinguished: 0.1 μM PABA supported *pabA* growth (figure 3.5), whereas 1 μM PABA shortened *C. elegans* lifespan on *pabA* (figure 3.6). LC-MS/MS enabled highly sensitive detection of *E. coli* folates under these conditions, revealing that at 1 μM PABA, folate levels in *pabA* mutants were increased to wild-type levels (figure 3.7)

In previous work, only one folate species (5/10-formyl THF-glu_3) could be detected in *E. coli* under conditions that extend lifespan and signals were noisy and close to the threshold of detection. Here, low levels of bacterial folates have been sensitively detected by LC-MS/MS and it has been shown that the *pabA* mutant extends lifespan above the threshold for bacterial growth and that lifespan is reversed when these levels are restored to wild-type levels. The finding that folate levels continue to increase beyond this window, despite no effect on lifespan, provides a small target window for further investigation. This also makes it unlikely that PABA or folates themselves are directly toxic to *C. elegans,* as we would expect to see lifespan decline in response to increasing PABA/ folate levels. The data is more consistent with a threshold model whereby either a folate-dependent beneficial activity is promoted, or a harmful/ toxic activity is attenuated when folate levels are low (figure 3.10). This discrepancy will be addressed further in Chapter 8.

3.4.3 The *gcp-2.1* mutant strain provides a phenotypic readout of low *E. coli* folate levels

The characterization of a *C. elegans* folate uptake mutant strain, *gcp-2.1 (ok1004)* was described in this chapter with the aim of developing a novel method to assay *E. coli*

folate levels. The data is consistent with a model whereby *gcp-2.1* mutants are able to obtain sufficient monoglutamated folates from their bacterial diet on WT *E. coli,* however, when this level is decreased by inhibiting bacterial folates synthesis (*pabA* mutant, SMX-treatment), the monoglutamated portion of the diet is no longer sufficient to support a functional folate cycle, and a developmental folate deficiency is manifest (figure 3.11). Supplementation with the bacterial folate synthesis precursor, PABA, rescues this deficiency on the *pabA* mutant, likely due to the restoration of bacterial folate. This data is consistent with a role of GCP-2.1 in the *C. elegans* intestine, where it cleaves glutamates off polyglutamated *E. coli* folates to facilitate absorption. The folate profile of the *gcp-2.1* mutant strain will be analysed in further detail by LC-MS/MS in Chapter 5, alongside other *C. elegans* folate measurements which are relevant to the following chapters. Together, this data establishes the *gcp-2.1* strain as a phenotypic readout of *E. coli* folate.

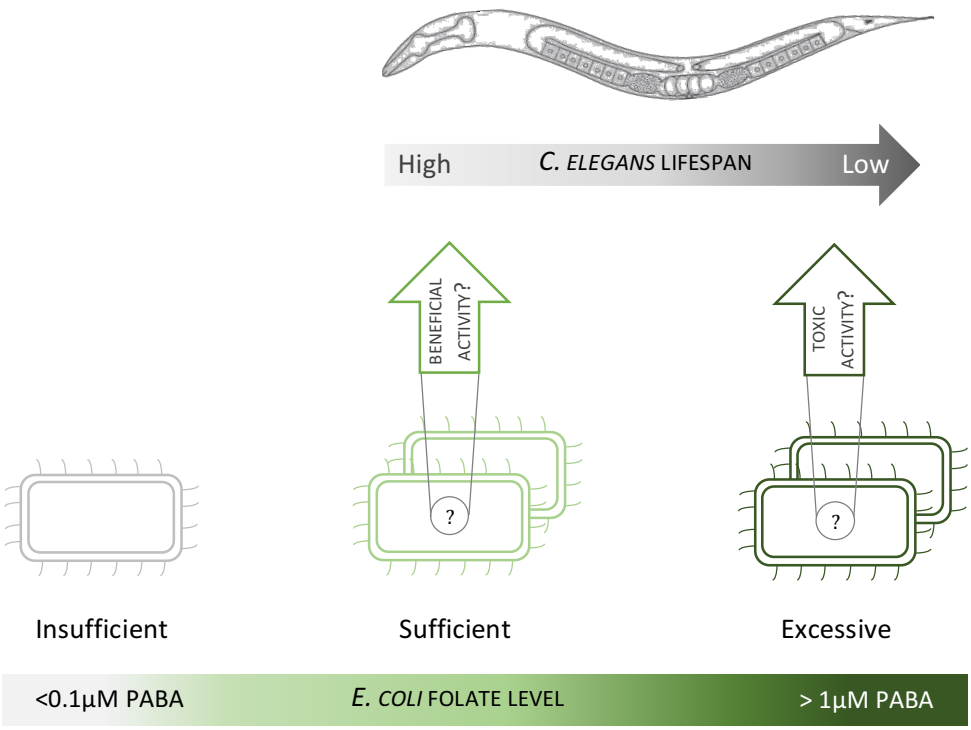

Figure 3.10 Model of the bacterial thresholds of folate which support growth and modulate *C. elegans* lifespan. When [PABA] < 0.1 µM, folate levels are insufficient to support bacterial growth. Above this threshold, bacterial growth is supported and *C. elegans* are long-lived when [PABA] <1 µM. Above this threshold, folate levels are excessive and *C. elegans* are short-lived. It is not clear whether folate has a beneficial effect on *C. elegans* lifespan at the 'sufficient' level, or a toxic effect when levels are excessive.

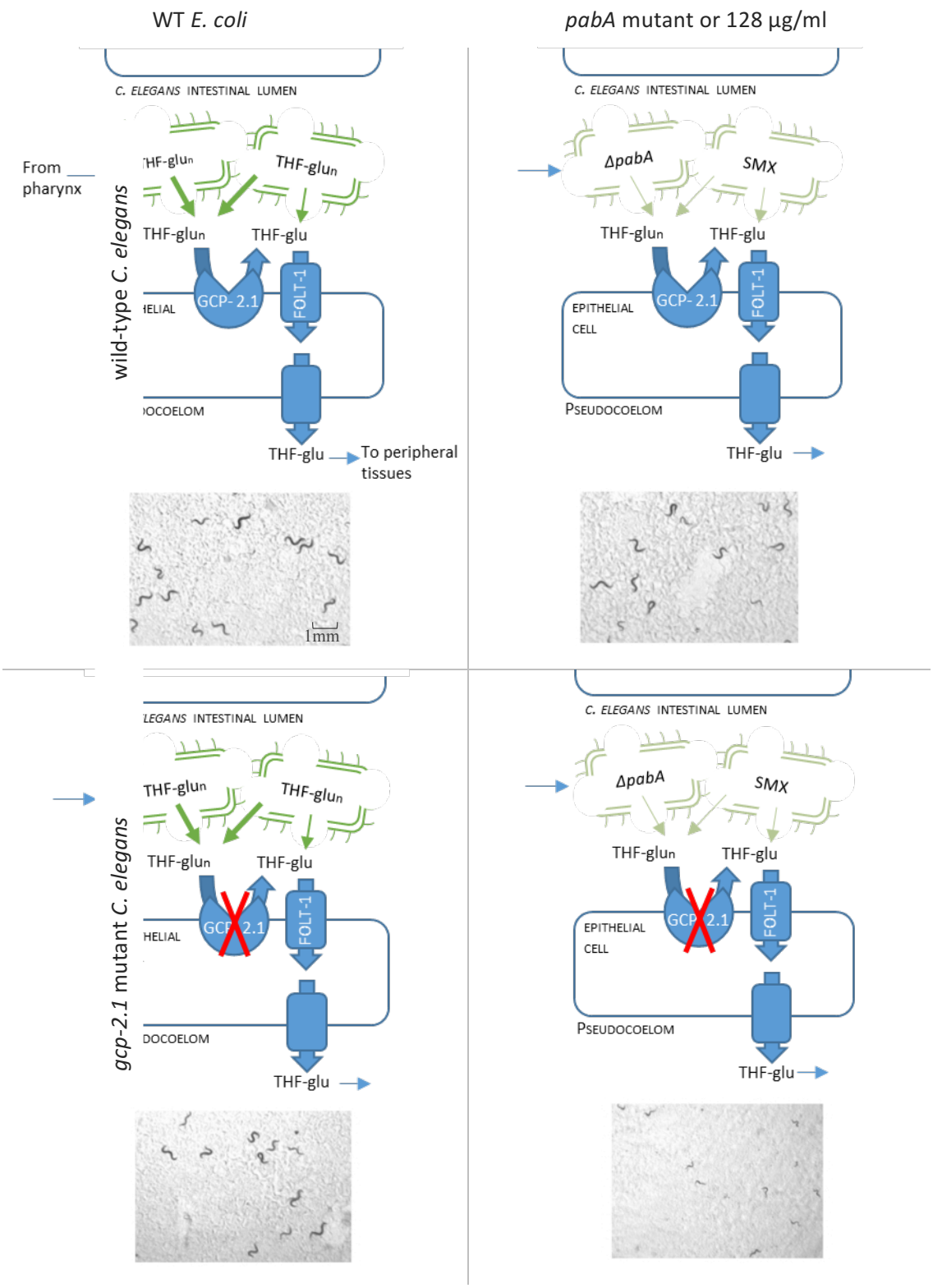

Figure 3.11 Model of the *gcp-2.1* mutant bioassay with representative images. Top left panel: wild-type worms obtain both THF-glu$_n$ and THF-glu from WT *E. coli.* THF-glu$_n$ are hydrolysed to

generate THF-glu which can be absorbed by *C. elegans* reduced folate carrier, FOLT-1. Monoglutamated THFs are transported to peripheral tissues to supply cells with cofactors for one-carbon metabolism. Top right panel: wild-type worms on folate-deficient bacteria have a limited supply of THF-glu_n and THF-glu but this is sufficient to support develoment. Bottom left panel: *gcp-2.1* mutant worms on WT *E. coli* receive sufficient THF-glu to support development. Bottom right panel: *gcp-2.1* mutant worms on folate-deficient *E. coli* do not receive sufficient THF-glu to support development. Representative images taken on plates ± 128 μg/ml SMX. THF-glu_n represents a general tetrahydrofolate with more than one glutamate residue. THF-glu represents a monoglutamated general tetrahydrofolate

CHAPTER 4. EXAMINING *C. ELEGANS* FOLATE STATUS UNDER CONDITIONS THAT INFLUENCE LIFESPAN

4.1 INTRODUCTION

Previous work in the Weinkove laboratory revealed that inhibiting *E. coli* folate synthesis with SMX decreased folate levels in *C. elegans* (Virk et al. 2012). In order to distinguish between the impact of bacterial and host folate status on lifespan, the Weinkove group carried out lifespan analyses under conditions where *C. elegans*' folate was specifically limited (*gcp-2.1* mutant) or supplemented (SMX + folinic acid). Neither intervention was found to alter lifespan, thus, it was hypothesized that worm folate status was not a determinant of lifespan. However, the folate status of *C. elegans* was not tested under these interventions. In this chapter, LC-MS/MS detection of *C. elegans* folate under these conditions is carried out in an attempt to verify this hypothesis. DM is used in order to eliminate any background sources of folate which may otherwise confound results.

4.2 CHAPTER AIMS

Using LC-MS/MS detection of *C. elegans* folates, this chapter aims to:

- Aim 1: Examine the folate status of the *C. elegans gcp-2.1* mutant
- Aim 2: Examine the impact of folinic acid on *C. elegans* folate levels

4.3 RESULTS

Considerable preliminary work was carried out to optimize the folate extraction protocol for *C. elegans* (data not shown). Previously, only 5-methylTHF-glu$_5$ could be

detected in *C. elegans* (Virk et al. 2012). Here, using the more sensitive LC-MS/MS technique, -glu_{1-5} derivatives of 5-methyl THF, 5/10-formyl THF and THF have been detected at reliable levels. Student's *t*-tests have been carried out here to determine significance between two folate species under different experimental conditions, and P values will be quoted in the text where appropriate. As with all LC-MS/MS measurements, levels of two different folate species cannot be directly compared, as the level here is an arbitrary unit and dependent on the ability of the compound to travel in the MS reaction chamber, which varies depending on compound. Absolute values can only be obtained when known concentrations of standards are infused into the LC-MS/MS.

4.3.1 Examining the folate profile of the *C. elegans gcp-2.1* mutant strain

In order to understand how the *gcp-2.1* mutation affects *C. elegans* folate levels, folate extractions on synchronized populations of L4/ young adult wild-type and *gcp-2.1* populations maintained on WT *E. coli* were performed in quadruplicate and samples were analyzed by LC-MS/MS (Figure 4.1). Despite normalizing for worm pellet volume between each condition, extractions on *gcp-2.1* worms on low folate *E. coli* were not included in the analysis due to lack of material. As standard, folate levels were normalized to that of an internal MTX-glu_6 spike added to the extraction buffer. As the *gcp-2.1* gene is predicted to be involved in polyglutamated folate deconjugation, LC-MS/MS parameters were optimized to detect –glu_{1-5} of all folate species.

4.3.1i gcp-2.1 mutation shifts folates towards polyglutamated derivatives

In *gcp-2.1* mutant extracts, levels of all mono- and diglutamated folates were detected at significantly lower levels than in WT extracts (with the exception of 5/10-formyl THF-glu_1): methyl THF –glu_1 (P=0.002) and –glu_2 (P=0.023), 5/10-formyl THF-glu_2 (P=0.047), THF-glu_1 (P=0.012) and THF-glu_2 (P=0.049) (figure 4.1). Unexpectedly, levels of -glu_3 and –glu_4 derivatives were significantly higher in the *gcp-2.1* extracts than in the WT extracts (with the exception of THF-glu_4): methyl THF –glu_3 (P=0.005) and –glu_4 (P=0.004), 5/10-formyl THF-glu_3 (P=0.041) and –glu_4 (P=0.023) and THF-glu_3 (P=0.028). Interestingly, the most significantly decreased folate in *gcp-2.1* mutant extracts was 5-methyl THF-glu_1 (P<0.001), the main circulatory folate form in mammals.

The overall pattern in figure 4.1 illustrates a shift towards polyglutmated THFs and a restricted supply of mono- and diglutamated folates in *gcp-2.1* mutants. As polyglutamted THFs are the required substrate for the enzymes that carry out one-carbon metabolism reactions, this may account for the lack of folate-deficiency in the *gcp-2.1* strain. This data provides an insight into the functional role of polyglutamation in *C. elegans*. Having gained a more complete picture of the folate status of the *gcp-2.1* mutant strain, the results are not consistent with the hypothesis that the *gcp-2.1* mutation lowers the levels status of the worm; its use as a mutant to demonstrate that worm folate status is not a determinant of lifespan is therefore questioned. This will be discussed in more detail.

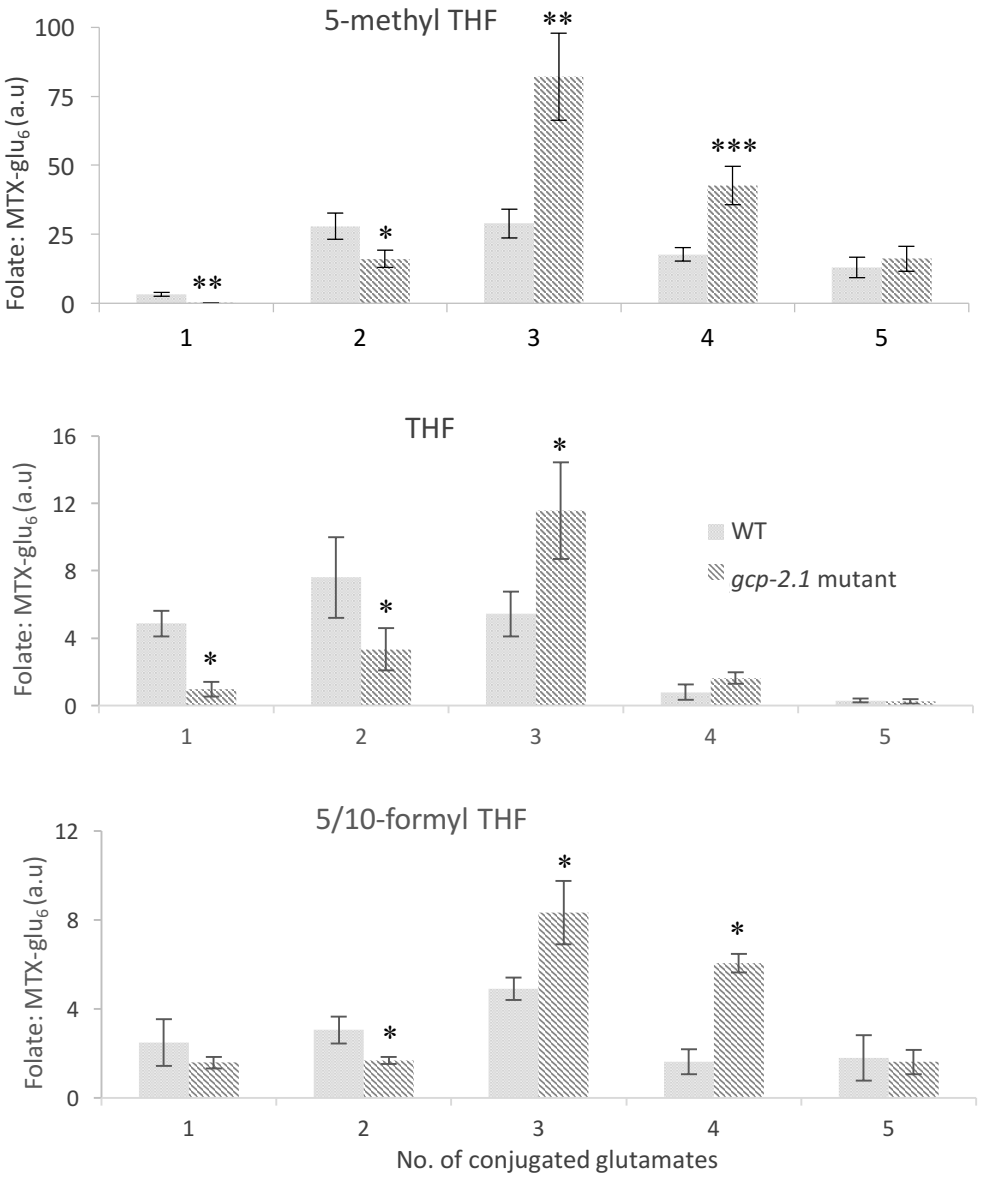

Figure 4.1. LC-MS/MS detects altered polyglutamtion profile in *gcp-2.1* mutant *C. elegans*. Synchronized populations of wild-type and *gcp-2.1* mutant *C. elegans* were raised on WT *E. coli* incubated at 25 °C until L4/ young adult stage. Folate extractions were normalized for volume and analyzed by LC-MS/MS. 5-methyl THF, 5/10-formyl THF and THF-glu_{1-5} were detected. Folate levels are expressed as a ratio of an internal MTX-glu_6 spike added to the extraction buffer. All plates contained 0.1 µM PABA. Error bars represent standard deviation over 4 biological replicates. Asterisks denote significance of Student's *t*-Test of folate level in *gcp-2.1* mutant compared to in WT worms, where *P<0.05, **P<0.01, ***P<0.005

4.3.2 Examining the impact of folinic acid on *C. elegans* folate

In order to test the hypothesis that folinic acid increases *C. elegans* folate status, folate extractions were carried out as previously described, on synchronized populations of L4/ young adult wild-type *C. elegans* on DM agar plates supplemented with 10 μM folinic acid on both WT *E. coli* and the *pabA* mutant. Non-supplemented conditions were included as controls. 10 μM folinic acid was chosen as it rescues the folate-deficiency of the *gcp-2.1* strain on *pabA* (Chapter 7, figure 7.12), but does not impact the lifespan of wild-type *C. elegans* on *pabA* (Chapter 7, figure 7.10) or on SMX-treated WT *E. coli* (Virk et al. 2016); it is therefore hypothesized that folinic acid must be supplementing *C. elegans* directly. Folate extractions were also carried out in parallel on folic acid supplemented conditions, with separate non-supplemented controls. Folinic acid extractions were carried out by Emma Williams, an undergraduate student working in the Weinkove laboratory under my supervision.

4.3.2i Folinic acid does not increase the folate status of wild-type C. elegans on either WT or pabA mutant E. coli

As shown in figure 4.2, in response to folinic acid, there was a significant increase in 5/10-formyl THF-glu_1 in *C. elegans* raised on both WT and *pabA* mutant *E. coli* ($P<0.001$, in both cases), most likely corresponding to uptake and accumulation of 5-formyl THF-glu_1 (folinic acid). Despite this, levels of all other folate derivatives remained unchanged in WT *E. coli* extracts. On the *pabA* mutant on non-supplemented conditions, 5-methyl THF-glu_1 ($P=0.005$), $-glu_2$ and $-glu_3$ ($P=0.002$, in both cases) and

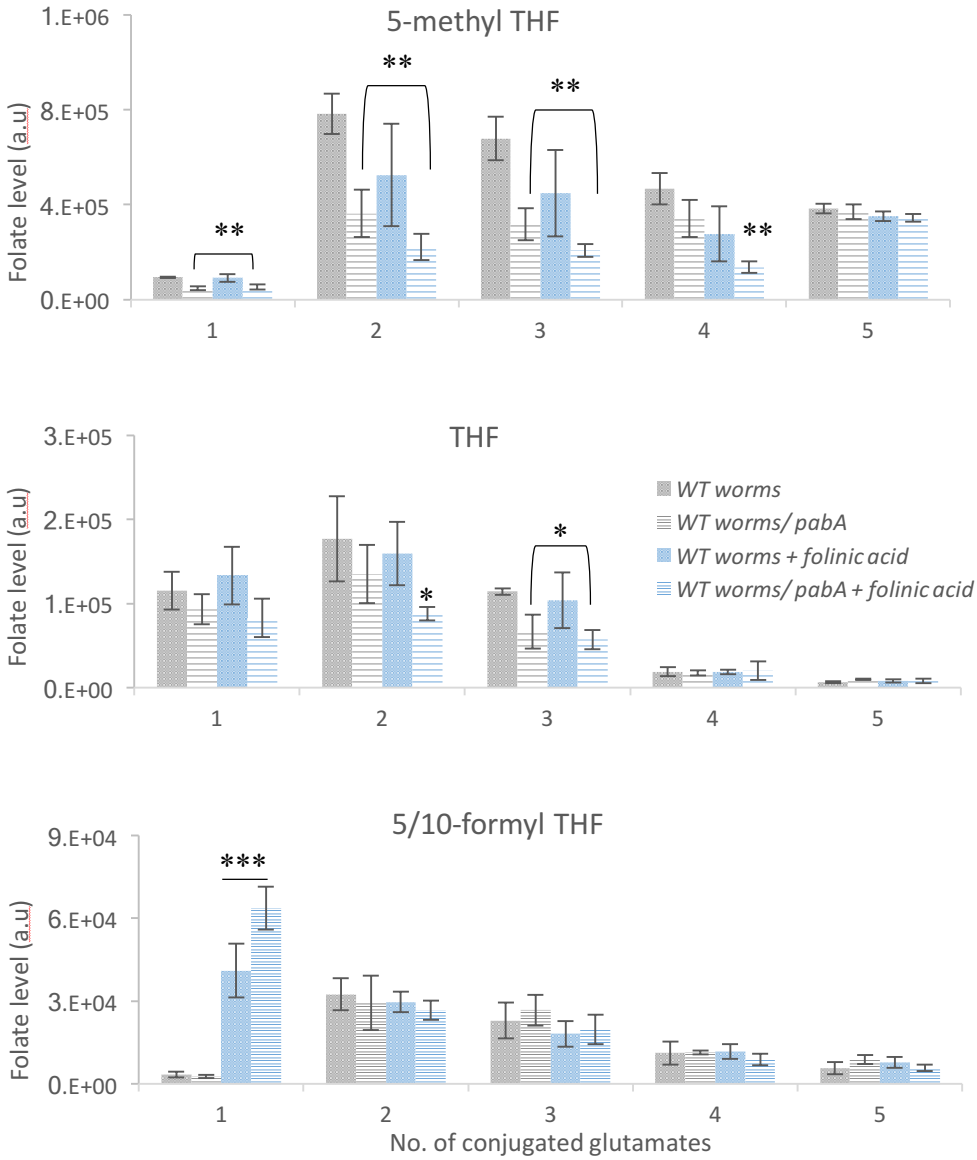

Figure 4.2. LC-MS/MS detects no impact of folinic acid on *C. elegans* folate levels Wild-type *C. elegans* were raised on WT or *pabA* mutant *E. coli* ± 10 µM folinic acid supplemented into the DM and folate extractions performed at L4/ young adult stage. All plates contained 0.1 µM PABA. Error bars represent standard deviation over 4 biological replicates. Asterisks denote significance of Student's *t*-Test of non-supplemented or folinic acid supplemented condition on *pabA E. coli* compared to on WT *E. coli*. For 5.10-formyl THF, asterisks denote significance of folinic acid supplemented conditions compared to non-supplemented conditions, where *P<0.05, **P<0.01, ***P<0.005.

THF-glu_3 (P=0.039) were significantly decreased compared to on WT *E. coli,* as was expected, however levels of all 5-formyl THF derivatives remained unchanged. Again, despite an increase in 5/10-formyl THF-glu_1 in response to folinic acid, *C. elegans* folate levels were not increased on the *pabA* mutant. 5-methyl THF-glu_{2-4} showed detectable *decreases* in the *pabA* mutant in response to folinic acid supplementation compared to on WT *E. coli* (P=0.006, 0.035, 0.040, <0.001, respectively), as did THF-glu_2 and -glu_3 (P=0.049, P=0.010, P=0.037, respectively).

5-methyl THF-glu_5 was not affected (figure 4.2). As folinic acid did not increase *C. elegans* folate status, these data also question the use of folinic acid supplementation as a means to demonstrate that worm folate status is not a determinant of lifespan. However, the increase in 5-formyl THF-glu_1 provides relatively clear evidence that folinic acid is indeed taken up by the worm, so the data may perhaps be limitations of only looking at folate levels at a single time point.

In the folic acid non-supplemented control (figure 4.3), only 5-methyl-glu_1 (P=0.024) was significantly decreased on *pabA* compared to on WT *E. coli.* Similarly to folinic acid, levels of 5-methyl THF-glu_{1-4} (P<0.001, in all cases) and THF-glu_{1-3} (P=0.024, P=0.012, P=0.001, respectively) were significantly decreased in response to folic acid on *pabA.* Again, 5-methyl THF-glu_5 was not affected. Notably, levels of 5/10-formyl THF were not affected under any condition (figure 4.3). The unexpected decrease in *C. elegans* folate levels in response to both folinic and folic acid on *pabA* mutant *E. coli* will be discussed.

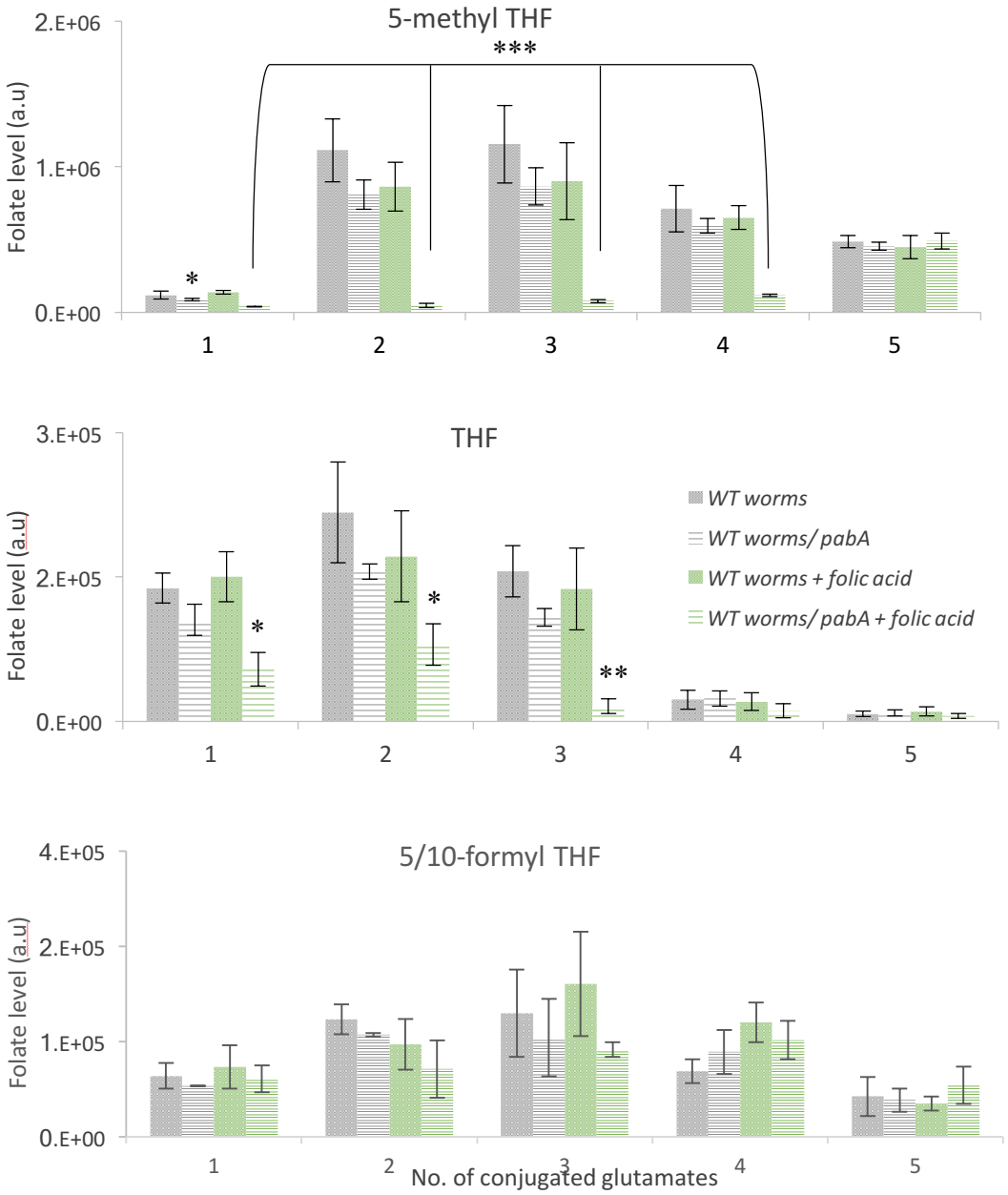

Figure 4.3: LC-MS/MS detects no impact of 10 µM folic acid on folate levels or glutamation in wild-type *C. elegans*. Wild-type *C. elegans* were raised on WT or *pabA* mutant *E. coli* ± 10 µM folic acid supplemented into the DM and folate extractions performed at L4/ young adult stage. Error bars represent standard deviation over 4 biological replicates. All plates contained 0.1 µM PABA. Asterisks denote significance of Student's *t*-Test of non-supplemented or folic acid supplemented condition on *pabA E. coli* compared to on WT *E. coli*., where *P<0.05, **P<0.01, ***P<0.005.

4.3.2ii Folinic acid increases the folate status of gcp-2.1 mutants

As discussed, the data that suggested folinic acid supplements *C. elegans* was based on the rescue of the *gcp-2.1* mutant strain on the *pabA* mutant (Chapter 7, 7.12). Folate extractions of *gcp-2.1* mutants supplemented with 10 μM folinic acid were therefore carried out as a positive control, alongside the extractions on wild-type *C. elegans*, as presented above. To clarify, the wild-type extractions presented in figure 4.4 here are the same as those in figure 4.2. Folate extractions of *gcp-2.1* mutants supplemented with 10 μM folic acid were also carried out as a negative control (figure 4.5), as this concentration did not have an appreciable impact on *gcp-2.1* body length (Chapter 7, figure 7.12) The wild-type extractions in figure 4.5 are the same as in figure 4.3. Separate wild-type control *C. elegans* extractions were carried out for the folic extractions, but were performed within the same experiment as the folinic acid extractions.

In *gcp-2.1* extracts, significant increases were detected in 5-methyl THF-glu_3 (P=0.050) and –glu_4 (P=0.002), 5/10-formyl THF-glu_4 (P=0.038) and THF-glu_3 (P=0.007) and –glu_4 (P=0.049) in response to folinic acid. This suggests that it is taken up more effectively in this strain compared to in wild-type worms (figure 4.3). Indeed, the accumulation of 5/10-formylTHF-glu_1 following folinic acid supplementation was lower in *gcp-2.1* extracts compared to WT extracts (although difference was not significant, P=0.060), suggesting that more of this mono-glutamate folate source may be used up in *gcp-2.1* mutants than in wild-type worms. As expected, folic acid did not increase levels of any folates in the wild-type strain or the *gcp-2.1* mutant (figure 4.4).

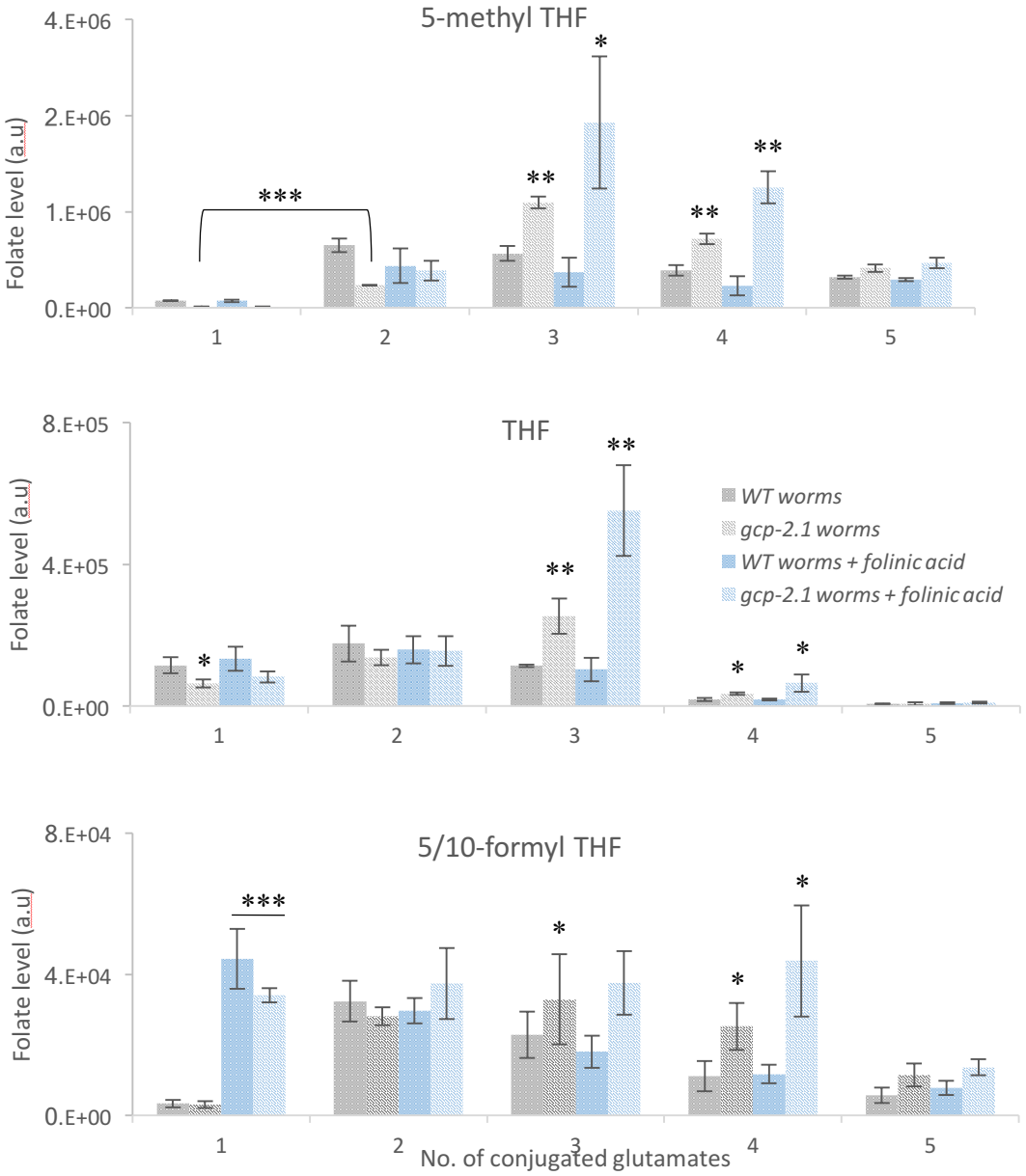

Figure 4.4: LC-MS/MS detects 10 µM folinic acid increases glutamation of *gcp-2.1* mutant *C. elegans*. Wild-type and *gcp-2.1* mutant *C. elegans* were raised on WT *E. coli* ± 10 µM folinic acid supplemented into the DM and folate extractions performed at L4/ young adult stage. Error bars represent standard deviation over 4 biological replicates. All plates contained 0.1 µM PABA. Asterisks denote significance of Student's *t*-Test of either *gcp-2.1* mutants compared to WT worms or *gcp-2.1* mutants + folinic acid compared to non-supplemented *gcp-2.1* mutants, where *P<0.05, **P<0.01, ***P<0.005

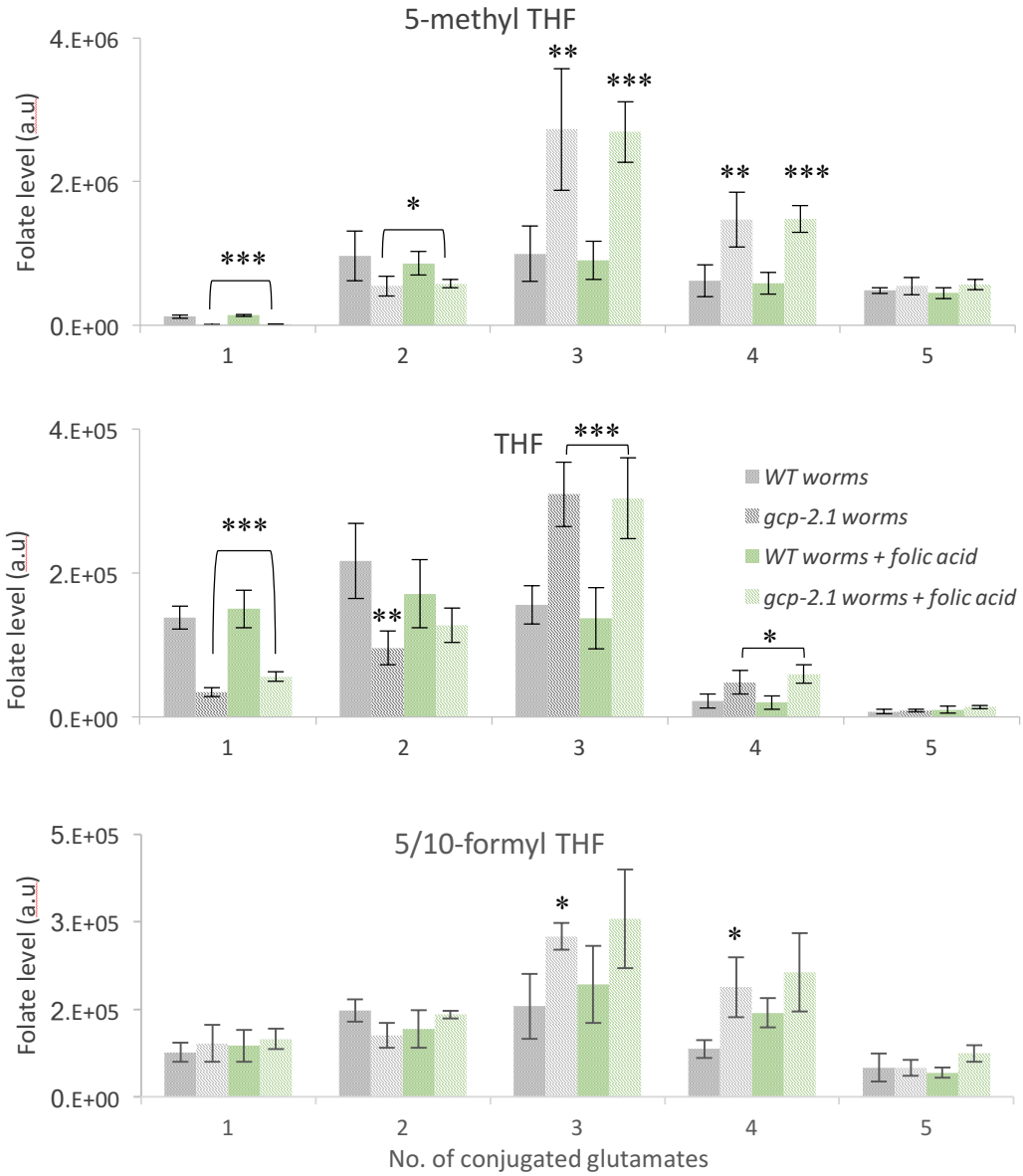

Figure 4.5: LC-MS/MS detects no impact of 10 µM folic acid on folate levels in *gcp-2.1* mutant *C. elegans*. Wild-type and *gcp-2.1* mutant *C. elegans* were raised on WT *E. coli* ± 10 µM folic acid supplemented into the DM and folate extractions performed at L4/ young adult stage. Error bars represent standard deviation over 4 biological replicates. Asterisks denote significance of Student's *t*-Test of either *gcp-2.1* mutants compared to WT worms or *gcp-2.1* mutants + folic acid compared to non-supplemented *gcp-2.1* mutants, where *P<0.05, **P<0.01, ***P<0.005

This experiment also provided further clarification of the folate status of the *gcp-2.1* strain: 5-methyl-glu_1 and $-glu_2$ ($P<0.001$, in both cases) and THF-glu_1 ($P=0.007$) were significantly lower and 5-methylTHF-glu_3 ($P=0.010$) and $-glu_4$ ($P=0.008$); 5/10-formyl THF-glu_3 ($P=0.015$) and $-glu_4$ ($P=0.019$) and THF-glu_3 ($P=0.003$) and $-glu_4$ ($P=0.011$) were significantly higher in *gcp-2.1* extracts in the folinic acid controls compared to WT (figure 4.4). Likewise, in the folic acid controls, a similar pattern in *gcp-2.1* polyglutmation was observed (figure 4.5).

4.4 DISCUSSION

C. elegans folate extractions had been performed previously in the Weinkove lab, however, only 5-methyl THF-glu_5 could be detected close to the level of detection. Here, following optimisation of the extraction protocol, this chapter presents the first LC-MS/MS analysis of the polyglutamated derivatives of *C. elegans* 5-methyl THF, 5/10-formylTHF and THF. This was carried out to test the hypotheses that specifically supplementing or limiting *C. elegans* folate does not affect lifespan. As discussed, this was based on two observations, namely: that although folinic acid supplements the *C. elegans gcp-2.1* mutant, it does not decrease (wild-type) *C. elegans* lifespan on either SMX-treated WT *E. coli* or the *pabA* mutant; and that although the *gcp-2.1* mutant shows a folate deficiency on both SMX-treated WT *E. coli* and the *pabA* mutant, it does not have an increased lifespan on wild-type *E. coli.*

The hypothesis that *C. elegans* folate status does not affect lifespan was therefore based on the two assumptions that: 1. folinic acid supplements *gcp-2.1* mutants and

wild-type worms similarly and 2. the *gcp-2.1* mutant strain has low folate levels on wild-type *E. coli.* The data collected here does not support these two assumptions. Firstly, we find evidence that folinic acid increases folate levels in *gcp-2.1* mutants, but not in wild-type worms on WT *E. coli,* and that on *pabA E. coli,* folinic acid *decreases* levels of the detectable folates in wild-type worms. In the *gcp-2.1* mutant strain, folate levels were not uniformly lowered as was expected; only $-glu_1$ and $-glu_2$ derivatives were lowered, whereas $-glu_3$ and $-glu_4$ derivatives were markedly increased. Thus, the use of these two lifespan conditions as examples of where *C. elegans* folate status is specifically supplemented or restricted, is not substantiated here.

It is possible, however, that results may be confounded by technicalities with the experimental procedure. In both cases, folate extractions were only carried at only one time-point (L4/ young adult stage) on populations synchronized by egg-lay onto the stated condition. This was done to ensure that large populations and sufficient extraction material was obtained. However, when carrying out lifespan assays, *C. elegans* are transferred onto the stated conditions only at L4/ young adult stage. It is likely that the folate profile will fluctuate with developmental stage and into adulthood. Extractions should be repeated with time-points during development and into adulthood and on conditions where worms are only transferred at L4/ young adult stage. This may reveal folate-flux through the system which could not be detected at a single time-point.

4.4.1 *C. elegans* folate status does not correlate with lifespan

Despite these limitations, the data presented in this chapter are consistent with the hypothesis that *C. elegans* folate status does not correlate with lifespan. *C. elegans* folate levels are decreased on the *pabA* mutant when supplemented with 10 μM folic acid, however lifespan is partially shortened on this condition. Moreover, 10 μM folinic acid has a similar effect on *C. elegans* folate levels on *pabA* as folic acid, however lifespan is not affected on this condition. The decrease in worm folate levels on the *pabA* mutant in response to folic and folinic acid is puzzling and requires further investigation. The phenomena may perhaps be explained by sequestration of folate in forms which are less available to *C. elegans* in the *pabA* mutant (protein bound). Indeed, the effect is more pronounced in response to folic acid, suggesting that uptake by *E. coli* may be confounding the results here. Although this was not the focus of this chapter, *C. elegans* folate extractions on the *abgTpabA* mutant may provide further insight into this conundrum.

4.4.2 *gcp-2.1* folate profile: insights into the role of folate polyglutamation in folate deficiency

It was previously hypothesized that *gcp-2.1* was expressed solely in the *C. elegans* intestine, similarly to the mammalian glutamate carboxypeptidase gene, folate hydrolase (FH), acting to deconjugate *E. coli* polyglutamated THFs to generate mono-glutamated THFs for uptake and transport (see Chapter 1). Thus, *gcp-2.1* deletion would act to create a functional folate deficiency on conditions where the monoglutamated folate pool provided by *E. coli* was decreased (SMX treatment and

pabA deletion). If this was the case, we would expect to see a decrease in all folates in the *gcp-2.1* strain. However, the shift towards polyglutamated folates, which are generally considered to be intracellular derivatives of the vitamin, indicates that *gcp-2.1* may also have a role in cellular export of folates, in a similar role to mammalian GGH (see Chapter 1). Indeed, this is consistent with the finding by E. Williams that mutants of the other *C. elegans* genes encoding glutamate carboxypeptidase genes (*gcp-2.2* and *gcp-2.3*), do not exhibit folate deficiency on SMX-treated or *pabA* mutant *E. coli* (data not shown). In order to verify localisation of GCP-2.1 GFP transcriptional and translational *gcp-2.1/* GCP-2.1 fusions were attempted but were not successful. Expression of *gcp-2.2* was detected in two tail neurons and *gcp-2.3* in the secretory system following the creation of fusion constructs and transgenic lines by an undergraduate project student, Alex Crisp.

In humans, GGH acts in opposition with the FPGS enzyme, where the latter polyglutamylates folates that have been transported into cells by RFC in order to increase their affinity for folate dependent enzymes and prevent their export (see Chapter 1, section 1.2.3). A BLASTn search search revealed a *C. elegans* gene (F25B5.6) with similar nucleotide scaffolds to human FPGS. Expression of a GFP translational F25B5.6 fusion construct has been detected in the pharynx, intestine and hypodermis in *C. elegans* (Dupuy et al., 2007). Thus, if GCP-2.1 is involved in cellular export, knockout would be expected to 'trap' THFs as polyglutamates (figure 4.6). It would be interesting to examine the *C. elegans* folate profile in F25B5.6 knock-out or knock-down mutants in order to characterize the opposing functions of GCP-2.1 and FPGS. It would be expected that inhibition of FPGS activity would shift the folate

profile toward mono- and glutamated derivatives, and perhaps cause a folate-deficiency due to a lack of suitable derivatives for enzymes involved in one-carbon metabolism.

4.4.3 *E. coli* provides folates in excess of that required by *C. elegans* for one carbon metabolism

The data collected here is consistent with the hypothesis made by Virk et al. in 2012 that *E. coli* provides folates in excess of that required by *C. elegans* to support a functional folate cycle (Virk et al. 2012). For example, in the *pabA* mutant, bacterial folate levels are very low (Chapter 3), however, the *C. elegans* folate status on this strain is only mildly affected, and worms show no phenotypic abnormalities.

It would be interesting to examine whether adaptive mechanisms in worms are compensating for the decreased dietary supply of folate. Indeed, animal studies have reported that an increase in FPGS activity in response to dietary folate deficiency, which acts to shift the folate glutamation equilibrium towards polyglutamation and increase cofactors available for one-carbon metabolism (Ifergan and Assaraf, 2008; Mendelsohn et al., 1996). Increased expression of cellular and intestinal folate transporters (RFCs and PCFTs) is also a well reported and recognized adaptive response to folate deficiency (Ifergan and Assaraf, 2008) and has also been demonstrated in *C. elegans* (Ortbauer et al., 2016).

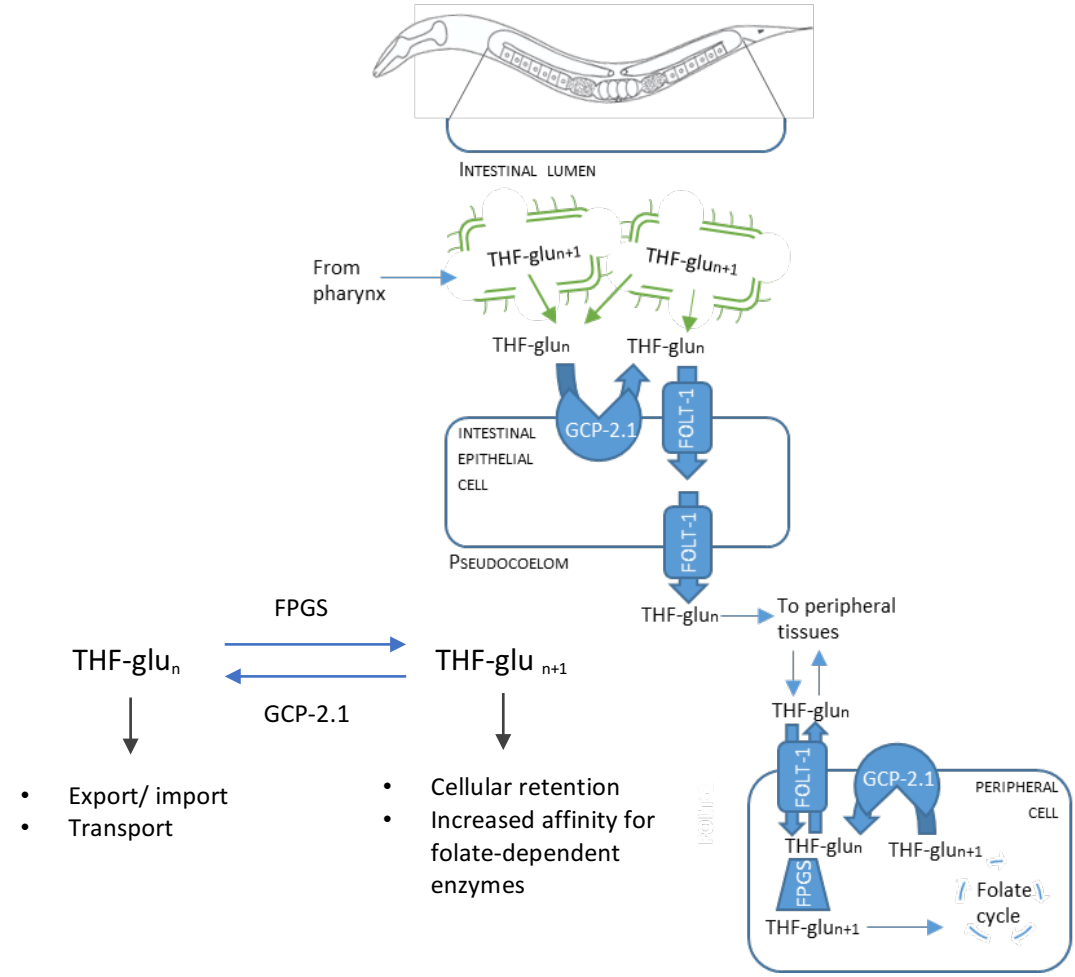

Figure 4. 6 A model representing the predicted roles of *C. elegans* GCP-2.1 in folate transport and metabolism. *E. coli* cells in the *C. elegans* intestine will be disintegrated by the grinding of the pharynx. *E. coli* provide both monoglutamated (THF-glu) and polyglutamated (THF-glu$_n$) THFs. THF-glu$_n$ are hydrolysed by GCP-2.1 expressed in the membrane of the intestinal epithelial cells for absorption as THF-glu by the reduced folate carrier, FOLT-1. THF-glu from *E. coli* can be absorbed directly, but these represent a low percentage of the total bacterial folate pool. Monoglutamated THFs are transported out of epithelial cells and to peripheral cells, where they are imported by the ubiquitously expressed FOLT-1. Polyglutamation of THFs is carried out by folyl-polyglutamate synthase (FPGS). THF-glu$_n$ are used by folate-dependent enzymes for one-carbon metabolism. In order to be exported, THF-glu$_n$ must be hydrolysed by GCP-2.1 to THF-glu$_1$. Loss of *gcp-2.1* is predicted to shift the glutamtion equilibrium towards polyglutamation, and thus 'trap' THF-glu$_n$ intracellularly.

Furthermore, the inability of folinic acid to increase *C. elegans* folate levels on wild-type *E. coli*, despite an accumulation of 5/10-formyl THF-glu$_{1,}$ may be due to a saturation of FPGS and/ or of the enzymes involved in one-carbon metabolism and THF interconversions. Indeed, the only effect of folate supplementation observed here is with 10 μM folinic acid in *gcp-2.1* mutants, where enzymes are likely to be less saturated. This is consistent with the ability of this concentration of folinic acid to rescue the *gcp-2.1* folate-deficient phenotype on *pabA* mutant *E. coli* (Chapter 7, figure 7.12). As a positive control, it would be interesting to test whether over-expression of *C. elegans* genes involved in folate metabolism can increase the folate status of the worm on wild-type *E. coli* in response to folinic acid.

Together, the data presented in this chapter provide several novel insights into the *C. elegans* folate uptake and metabolism and highlights several areas for further investigation. Although the LC-MS/MS measurements do not support the use of either the *gcp-2.1* mutant as a condition which specifically restricts worm folates, nor the supplementation of wild-type worms on *pabA* with folinic acid as a condition which specifically increases worm folates, overall the data indicates that the folate status of the worm is not a determinant of lifespan. Furthermore, the data also demonstrate that *E. coli* synthesizes folate in excess of that required by *C. elegans* and therefore prompts further investigation into the underlying mechanism responsible for apparent over production of folate. Finally, an insight is provided into the interplay between *E. coli* and *C. elegans* genotype in determining the response to folic acid supplementation.

CHAPTER 5: INVESTIGATING THE GROWTH PHASE DEPENDENCE OF *E. COLI* FOLATE SYNTHESIS

5.1 INTRODUCTION

It has been established that *E. coli* provides a source of THFs above the threshold required for sufficient one-carbon metabolism in both *E. coli* and *C. elegans.* It is clear that this activity negatively impacts *C. elegans* lifespan, however, it is unclear why *E. coli* appears to waste biosynthetic energy in this manner. Little is known about the regulation of bacterial folate synthesis; no transcription factors have been identified and it is not clear whether folates are synthesized constitutively or within a specific growth phase. This chapter aims to provide insight into this matter by investigating the growth phase dependence of *E. coli* folate synthesis at 25 °C on DM agar. Here, LC-MS/MS will be used to examine how THF levels fluctuate over time and this will be combined with an examination of longitudinal *pabA* gene expression under the same conditions, using qPCR. Lifespan analyses where *E. coli* folate synthesis is inhibited at different temporal stages will be carried out with the aim of identifying a target window for lifespan extension.

5.2 CHAPTER AIMS

- Aim 1: Examine *E. coli* growth and folate levels over time using LC-MS/MS
- Aim 2: Investigate the temporal expression of *pabA* using qPCR
- Aim 3: Investigate how inhibiting *E. coli* folate synthesis at different time-points impacts lifespan

5.3 RESULTS

5.3.1i Longitudinal LC-MS/MS detection of *E. coli* folate levels reveals a folate peak in exponential growth phase

E. coli growth and folate levels were monitored over a six day time course on conditions used for *C. elegans* experiments. WT and *pabA* mutant *E. coli* were seeded onto DM agar plates and incubated at 25 °C. WT was also seeded onto plates supplemented with 128 μg/ml SMX, as a negative control. All plates were supplemented with 0.1 μM PABA to ensure comparable growth between WT and *pabA* mutant *E. coli*. Optical density at 600 nM was used to measure bacterial growth and this was used to normalize the extraction volume. Extractions were performed in quadruplicate on consecutive days over six days. Extracts were subjected to LC-MS/MS and the levels of THF, 5/10-formyl TH, 5-methyl THF, 5,10-methenyl THF and 5,10-methylene THF $-glu_3$ derivatives were normalized to an internal MTX-glu_6 spike. WT *E. coli* and the *pabA* mutant showed similar growth kinetics and both reached stationary phase at day 5. The growth conditions of SMX-treated *E. coli* have not been optimized for growth on DM and it is clear from the growth curves in figure 5.1 (first panel) that 0.1 μM PABA is not sufficient to support normal wild-type growth. Nevertheless, extracts were normalized for growth and the SMX condition provides a negative control.

LC-MS/MS detection revealed that THF levels in WT *E. coli* extracts were higher than in *pabA* extracts, both of which were significantly higher than folates detected in SMX extracts (figure 5.1). In WT extracts, folate levels peaked at day 3 in THF, 5/10-formyl THF, 5,10-methylene THF ($P<0.001$, in all 3 cases) and day 2/3 in 5,10-

methenyl THF (P=0.023), where P values here indicate the result of a two-tailed, paired Student's *t*-test, comparing the stated day from day 1. The peak in 5-methylTHF at day 3 was not significant (P=0.065). After this peak, levels of THF and 5,10-methenyl THF exhibited a gradual decline, whereas levels of 5/10-formyl THF, 5,10-methylene THF and 5-methyl THF fluctuated, but remained constant. The decrease in 5-methyl THF at day 4 was significant (P<0.001), but remains unresolved. The difference in the consumption of these THFs may represent their different roles in one-carbon metabolism.

Folate levels in *pabA* extracts showed a gradual decline over the six day time course (figure 5.1). The lack of an early peak suggests that *pabA* activity is responsible for the high levels observed in WT extracts at days 2/3. This indicates that *pabA* is expressed and active during the first 48-72 hours of bacterial growth, coinciding with early exponential phase. The decline in folate levels after this period, despite continued bacterial growth in line with WT, suggests that *pabA* activity either declines after this initial period, as sufficient folate has been synthesized, or activity is maintained, but folate is used up for cellular biosynthetic reactions more rapidly than it is being synthesized. This discrepancy will be addressed by examining *pabA* expression under these conditions.

The folate levels at day 1 in *pabA* extracts were similar to those in WT extracts. This might be due to carryover of folate synthesized in *pabA* cells from exogenous PABA in the LB overnight culture. Despite 'washing' cells using a DM subculture as

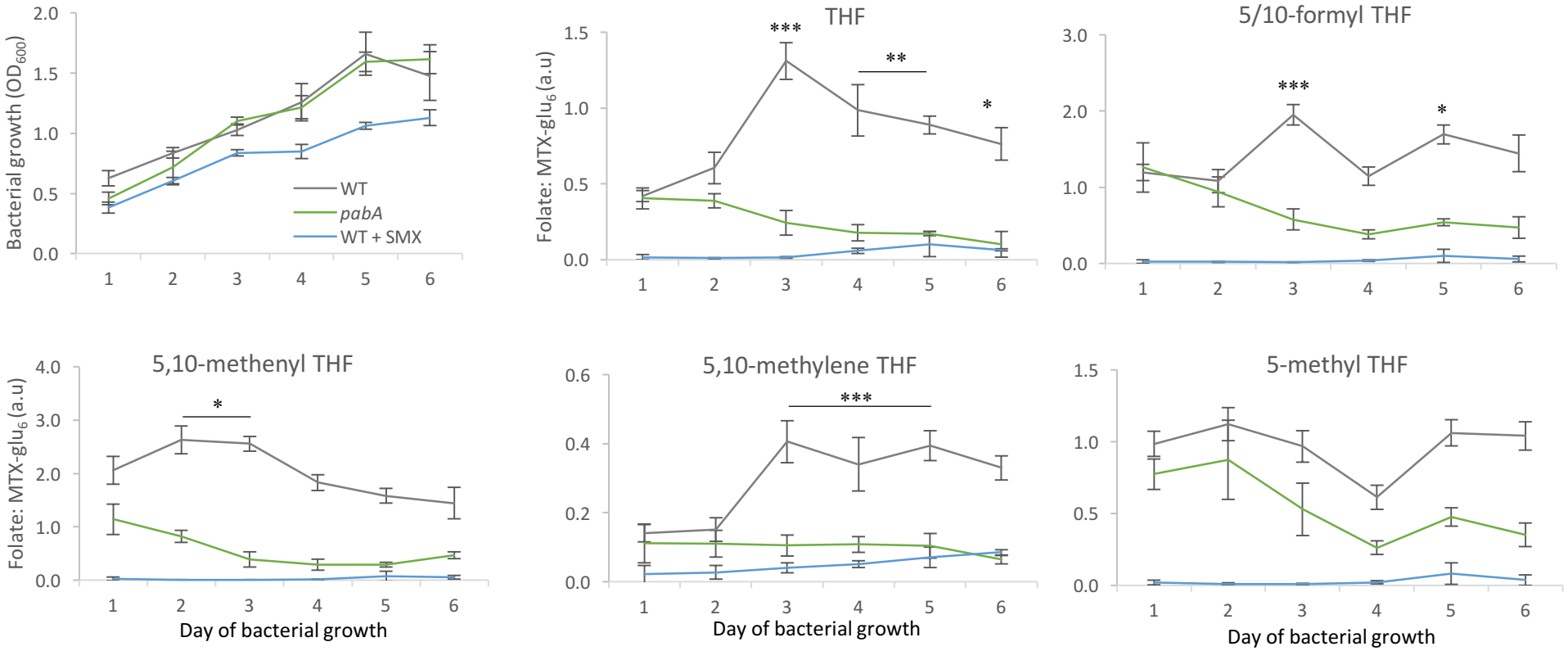

Figure 5.1 LC-MS/MS detects fluctuations in folate level in WT *E. coli* ± SMX and *pabA* mutant *E. coli* over six days of bacterial growth. Levels of THFs detected in extracts of WT, *pabA* mutant and WT + SMX *E. coli* over a six day time course were measured by LC-MS/MS. Folate level is displayed as a ratio of an internal MTX-glu$_6$ spike for normalization between samples. Top left panel shows bacterial growth over the six day time course. Error bars represent standard deviation. Asterisks denote the result of Student's *t*- tests of folate level on denoted condition compared to folate level on day 1, where ***P<0.001, **P<0.01 *<0.05.

outlined in Chapter 3, *E. coli* only requires nanomolar quantities of PABA to support folate synthesis (Chapter 3, figure 3.6). 0.1 μM PABA added to the DM plates is not sufficient to allow continued synthesis in *pabA* mutants, thus we see a decline in folate levels over the six day time course. In contrast, SMX blocks the ability of cells to use exogenous PABA, therefore, detectable levels of folate were low from day 1 in SMX-treated WT *E. coli* extracts (figure 5.1). As extracts were normalized for growth, the lower levels of folate in SMX-treated conditions cannot be attributed to the sub-optimal growth. Slight increases in all folate species in SMX-treated WT extracts were detected towards the end of the time course. This may be due to the degradation of SMX over time in the plates, or the accumulation of PABA over time, causing competition between PABA and SMX.

5.3.1 ii THF peak in exponential phase is accentuated with glucose

The impact of glucose on *E. coli* growth kinetics was first described by Monod in 1949 (Monod, 1949). The ability of *E. coli* (and many other bacteria) to preferentially use glucose as a carbon source is now referred to as carbon catabolite repression (Stulke and Hillen, 1999) where the use of other carbon sources is suppressed in favour of glucose metabolism. 0.1% glucose was added to the amino acid media here, post-autoclaving, in order to alter the growth kinetics of *E. coli.* Monitoring the temporal pattern of folate levels in response to glucose would therefore act as a positive control to determine whether folate is synthesized in association with a specific growth phase. Folate extractions of WT and *pabA E. coli* on glucose DM over a six-day time course were carried out and subjected to LC-MS/MS in parallel with the control non-supplemented extractions

already discussed. WT *E. coli* on SMX and glucose DM was included as a negative control condition (figure 5.2).

Consistent with glucose being a more readily utilizable carbon source than amino acids, 0.1% glucose increased exponential phase growth in all conditions as bacterial growth reached stationary phase at the same time-point as control conditions, but the final OD_{600} was significantly higher in all cases (figure 5.2, first panel). It was hypothesized that glucose would shift the peak in folate levels to the left of the graphs, but would not increase overall folate levels as the extraction volumes would be normalized for growth before LC-MS/MS detection. Indeed, in WT extracts on 0.1% glucose DM, the peak in all folate species was shifted to day 2, but unexpectedly, the level of this peak was significantly increased in all cases compared to the non-supplemented controls ($P<0.001$) (figure 5.2). After this peak, levels returned to those in line with the control extracts, with the exception of 5-methylTHF. It was ensured that glucose did not interfere with the MTX internal standard and that there were no peculiarities with day 2 extractions.

In *pabA* extracts on 0.1% glucose DM, a peak at day 2 was not observed. In a similar manner to the non-supplemented *pabA* extracts, folate levels declined for the remainder of the time course, again with the exception of 5-methyl THF, which was detected at increasingly higher levels from days 2-5, followed by a decrease on day 5. Similarly to the non-supplemented control extracts, folate levels in *pabA* extracts on 0.1% glucose DM were again detected at similar levels to those in WT extracts on day 1, likely owing to initial synthesis supported by trace PABA from

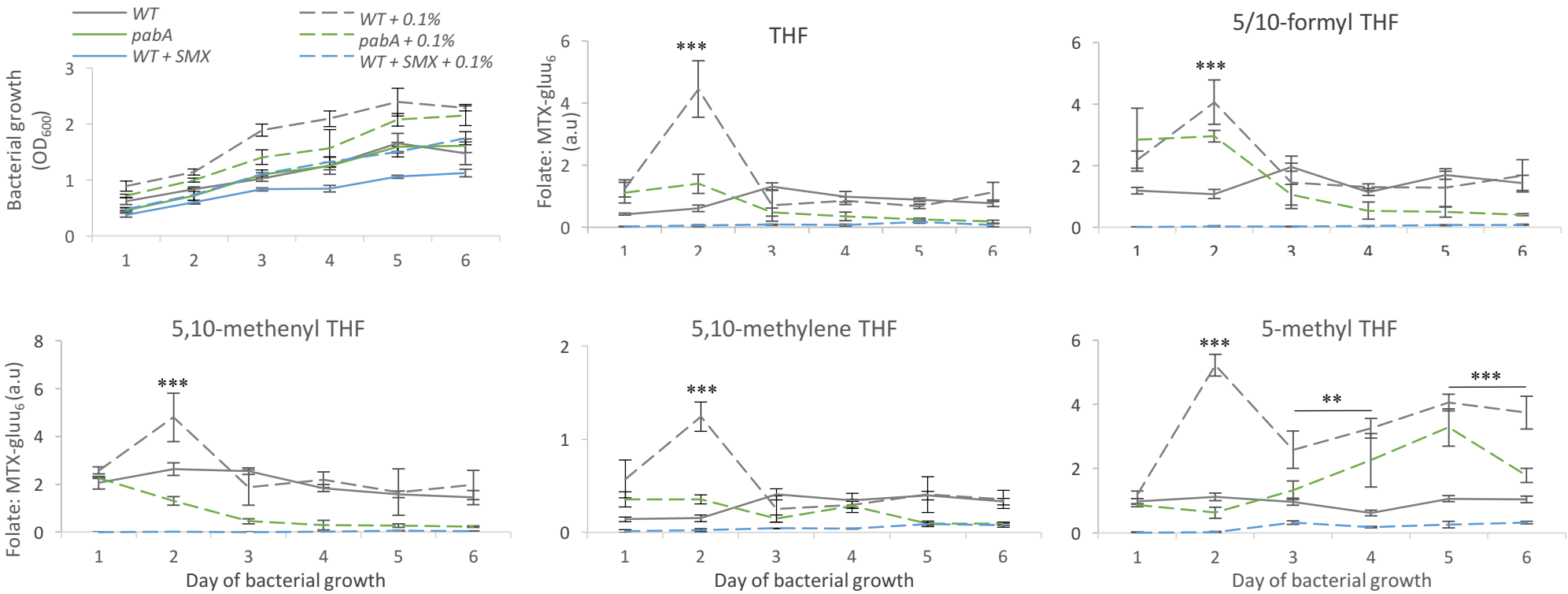

Figure 5.2 LC-MS/MS detects an increase in folate level in WT *E. coli* in response to 0.1% glucose. Levels of THFs detected in *E. coli* extracts of WT ± 0.1% glucose, *pabA* mutant + 0.1% glucose, and WT + SMX + 0.1% glucose measured by LC-MS/MS. Folate level is displayed as a ratio of an internal MTX-glu_6 spike for normalization between samples. 0.1% here represents 0.1% glucose added to the DM agar media post-autoclaving. Top left panel shows bacterial growth over the six day time course. Error bars represent standard deviation. Asterisks denote the result of Student's *t*- tests of folate level on denoted condition compared to on day 1 of the same condition, where ***P<0.001, **P<0.01 *<0.05.

LB. Overall, these data suggest that *E. coli* folate synthesis is temporally regulated, not constitutive, in our model system. Folates seem to be synthesized in excess in early exponential phase, and after this point in general, folate levels begin to gradually decline. Furthermore, the data here has revealed a novel association between glucose and folate synthesis, indicating that cells using glucose as a carbon source generate more folate. This will be discussed in more detail.

5.3.2 *pabA* expression peaks in exponential phase and decreases in stationary phase

In order to verify that folate synthesis is active in exponential phase, *pabA* gene expression in WT *E. coli* under the same conditions used for LC-MS/MS was examined using qPCR. WT *E. coli* was seeded onto DM agar plates (again supplemented with 0.1 μM PABA) and RNA extractions were carried out in quadruplicate after 6, 24, 48, 72 and 96 hours. Note the earlier time point in order to capture lag phase, which was missing from the previous folate extraction data. RNA extractions of 4 independent overnight DM liquid cultures were carried out before they were pooled and used to seed the plates. RNA was converted to cDNA and qPCR carried out as previously described (see methods). Normalized expression levels were obtained using the delta delta ct method, using *rrsA* as an internal reference gene and normalizing to expression in the overnight cultures.

As depicted in figure 5.3, *pabA* expression was increased during exponential growth, with a 6-fold increase after 24 hours and reaching a peak in expression after 48 hours growth, with a 22-fold increase compared to expression in the overnight culture. After this point, when cells began to enter stationary phase, *pabA* expression was reduced, however it was maintained 8-10-fold higher than in the overnight culture at 72 and 96 hours. As the time course did not continue past

4 days of bacterial growth, it is not clear how long *pabA* expression is maintained at this level. Overall, the temporal expression pattern of *pabA* is consistent with the temporal pattern of folate levels detected by LC-MS/MS.

5.3.3 Inhibiting folate synthesis has a partial protective effect on glucose-induced lifespan reduction

The Kenyon lab has demonstrated that 0.1% glucose negatively effects *C. elegans* lifespan by stimulating the insulin/ IGF-1 signalling pathway and thereby inhibiting the transcription of DAF-16/ FOXO downstream genes (Lee and Kenyon, 2009). As the data here suggests that glucose has a marked effect on *E. coli* folate levels, it was examined whether glucose may have an as of yet undetermined and indirect impact on *C. elegans* lifespan.

Lifespan assays were carried out on the same conditions used for the glucose LC-MS/MS extractions (figure 5.4). These lifespans were conducted by Lucy Lancaster (LL), a Masters student in the Weinkove laboratory working under my supervision. Figures 5.4 depicts the Kaplan Meier survival curves. The P values here are the test-statistic of Log-rank tests. Consistent with the peer-reviewed findings, 0.1 % glucose significantly reduced lifespan by 24% on WT *E. coli* ($P<0.0001$). In line with work presented in this thesis and that previously carried out in the lab, lifespans carried out by LL on *pabA* mutant and SMX-treated WT *E. coli* were significantly increased, by 45% and 47% respectively ($P<0.0001$, in both cases). In both these cases, glucose was found to decrease lifespan significantly, but to a lesser extent than on WT *E. coli.* Lifespan on the *pabA* mutant with glucose was 40% higher and on SMX-treated *E. coli* with glucose, 13% higher than lifespan on WT *E. coli* with glucose (figure 5.4). This suggests that there is a partially

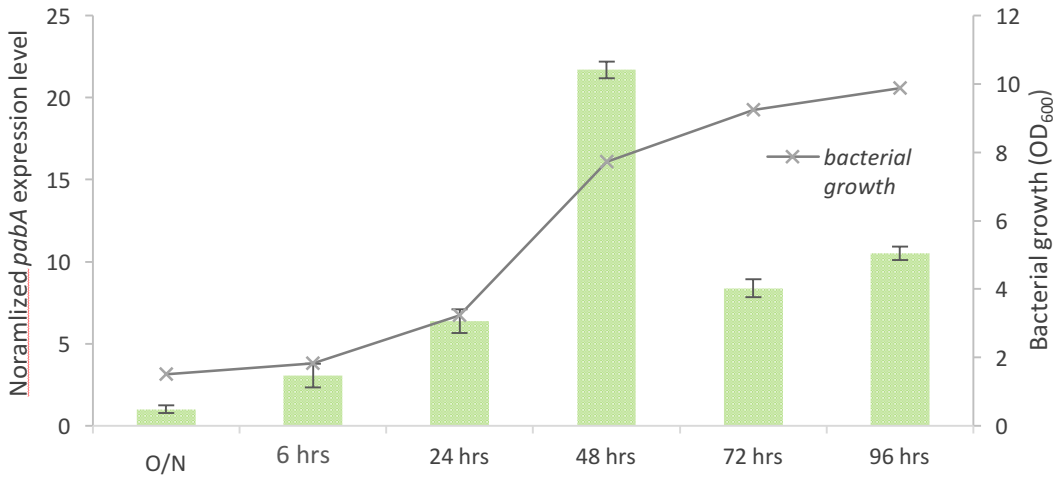

Figure 5.3 Normalized mRNA expression level of *pabA* in WT *E. coli* over a 96 hour time course. RNA extractions were performed on agar DM seeded with WT *E. coli.* Expression here represents the fold change normalized to expression measured the DM overnight culture used to seed the plates, and to the internal reference gene, *rrsA,* as determined by qPCR. Error bars represent standard deviation over 4 biological replicates. Bacterial growth is plotted on the y axis.

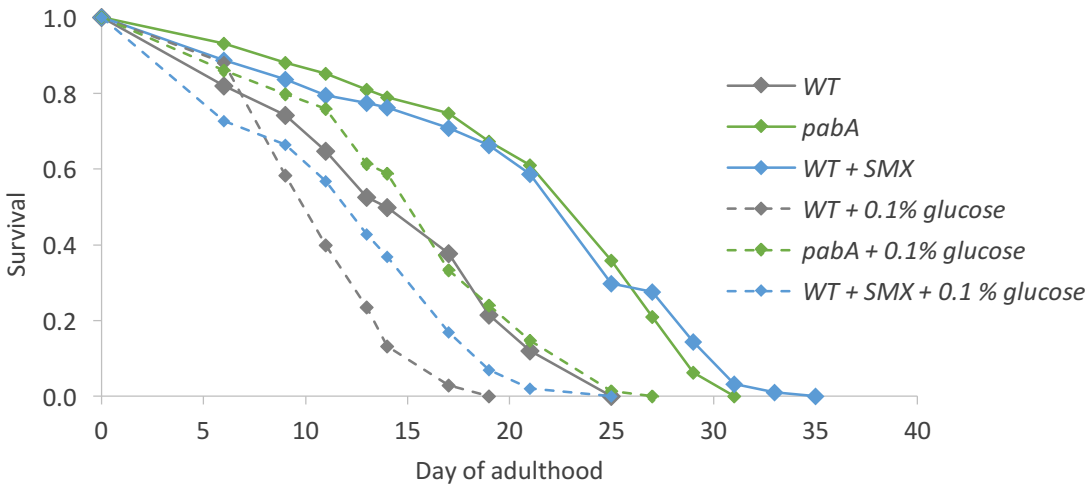

Figure 5.4 SMX and the *pabA* mutant are partially protective of the negative impact of 0.1% glucose on *C. elegans* lifespan. Kaplan-Meier survival curves of *C. elegans* on WT, WT + SMX, *pabA* mutant ± 0.1% glucose (added into DM post-autoclaving). Worms were added onto the experimental condition at day 1 of adulthood. [SMX] = 128 µg/ml.

protective effect of inhibiting folate synthesis on glucose-induced lifespan reduction. This is in line with the observation that glucose increases *E. coli* folate synthesis, and demonstrates that this has an indirect and previously unaccounted for impact on lifespan.

5.3.4 SMX extends lifespan most effectively when the first 2 days of bacterial growth are targeted

In order to confirm that the folate synthesized during early exponential phase is responsible for folate-induced lifespan modulation, folate synthesis was inhibited with SMX at different time points within the first 4 days of bacterial growth and lifespans were carried out. Conventionally, 128 μg/ml SMX is added to the agar media post-autoclaving (after cooling to 50 °C) before pouring the plates (see methods). *E. coli* is cultured in LB overnight and then sub-cultured into DM overnight before 'seeding' onto DM agar plates and incubated at 25°C for 48 hours. L4/ young adult *C. elegans* are then transferred onto the plates for aversion and lifespan assays, where this represents day 1 of adulthood (figure 5.5). As bacteria are subjected to SMX for the entirety of their growth on the agar plates, it is not clear at what stage SMX is acting. It was hypothesized that SMX may have less of an effect on *C. elegans* lifespan if it is added after exponential growth phase.

Lifespans in the Weinkove laboratory are conducted by transferring worms at days 7 and 14 of adulthood onto 'freshly' seeded (48 hours previously) *E. coli* plates. This is done to prevent worms from starving and to reduce plate-drying and cracking which can lead to *C. elegans* desiccation and censorship. However, this procedure will triple the exposure of *C. elegans* to exponential phase *E. coli* during the course of their lifespan. It was hypothesized that lifespan may be

increased if worms are not transferred to fresh *E. coli* during their lifespan. These two hypotheses were tested using the experimental set-up as depicted in figure 5.5. Eight lifespan conditions were set up, where half would be the 'transfer' cohort and transferred to freshly seeded *E. coli* plates on day 7 and day 14 of their adult lifespan (as standard procedure) and the other half would remain on the same plate from day 1 of adulthood, the 'non-transfer' cohort. Within each cohort, there were 4 conditions: control, non-supplemented; SMX control, added directly after autoclaving; SMX added after 2 days of bacterial growth; SMX added after 4 days of bacterial growth. No additional SMX would be added to the non-transfer cohort, but SMX would be added to the transfer cohort after transfer on days 2 and 4 of bacterial growth, respectively (see Figure 5.5 for experimental set-up).

Figure 5.6 depicts the Kaplan Meier survival curves (5.6a, 5.6b) and the mean lifespans (5.6c) on each condition. P values here indicate the result of Log-rank statistical analysis. On control SMX plates, lifespan was extended by 54% in the transfer cohort and 43% in the non-transfer cohort ($P<0.0001$, in both cases) compared to their respective non-supplemented controls, where the difference between these two lifespans was not significant. Likewise, there was no significant difference in lifespan between the two non-supplemented conditions.

In the transfer cohort (figure 5.6a), when SMX was added after 2 days of bacterial growth, lifespan extension increased by only 15.24%. When added after 4 days of bacterial growth, SMX failed to have any effect on lifespan. In contrast, in the non-transfer cohort (figure 5.6b), lifespans were significantly higher compared to their relative transfer cohort lifespans ($P<0.0001$, in both cases), where lifespan was increased by 33% when SMX was added after 2 days of bacterial growth and 11%

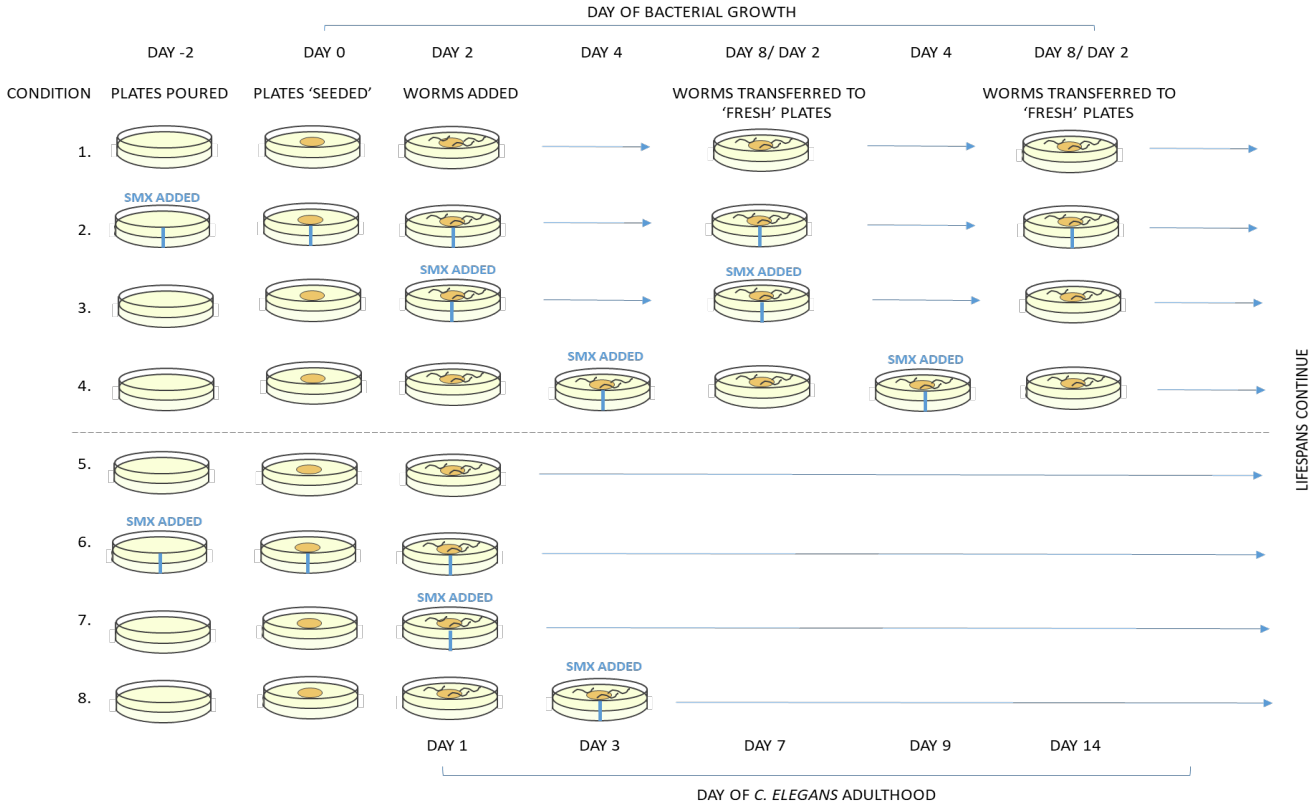

Figure 5.5 Experimental schematic for examining the impact of SMX at different stages of bacterial growth on *C. elegans* lifespan. Plates were seeded, as standard, 2 days before *C. elegans* are added. Conditions (1, 2) are control plates; (2, 6) SMX control (128 μg/ml SMX added after autoclaving); (3, 7) SMX added at day 2; and (4, 8) SMX added at day 4 of bacterial growth. Worms are added onto plates at day 2 of bacterial growth (at day 1 of adulthood). At day 7 and 14 of adulthood, worms on conditions 1-4 are transferred onto fresh plates (and receive SMX again at days 2 or 4 of bacterial growth). Worms on conditions 5-8 remain on same plates and do not receive additional SMX.

when added after 4 days. This may seem initially counter intuitive as the worms which lived the longest were on *E. coli* conditions which received less SMX throughout their lifespan, however these worms were only exposed to exponential phase *E. coli* once. Additionally, in both cohorts, worms lived longest on plates supplemented with SMX after 2 days of bacterial growth than 4, and longest on control SMX plates. Thus, the number and length of exposure to exponential phase non-SMX treated *E. coli* determines lifespan.

Together, this supports the hypothesis that folate synthesis within the first 48 hours of bacterial growth is responsible for *C. elegans* lifespan decrease. That lifespan is not further decreased in the transfer cohort on the non-supplemented control plates compared to the non-transfer conditions may represent a limit for lifespan decrease via this means.

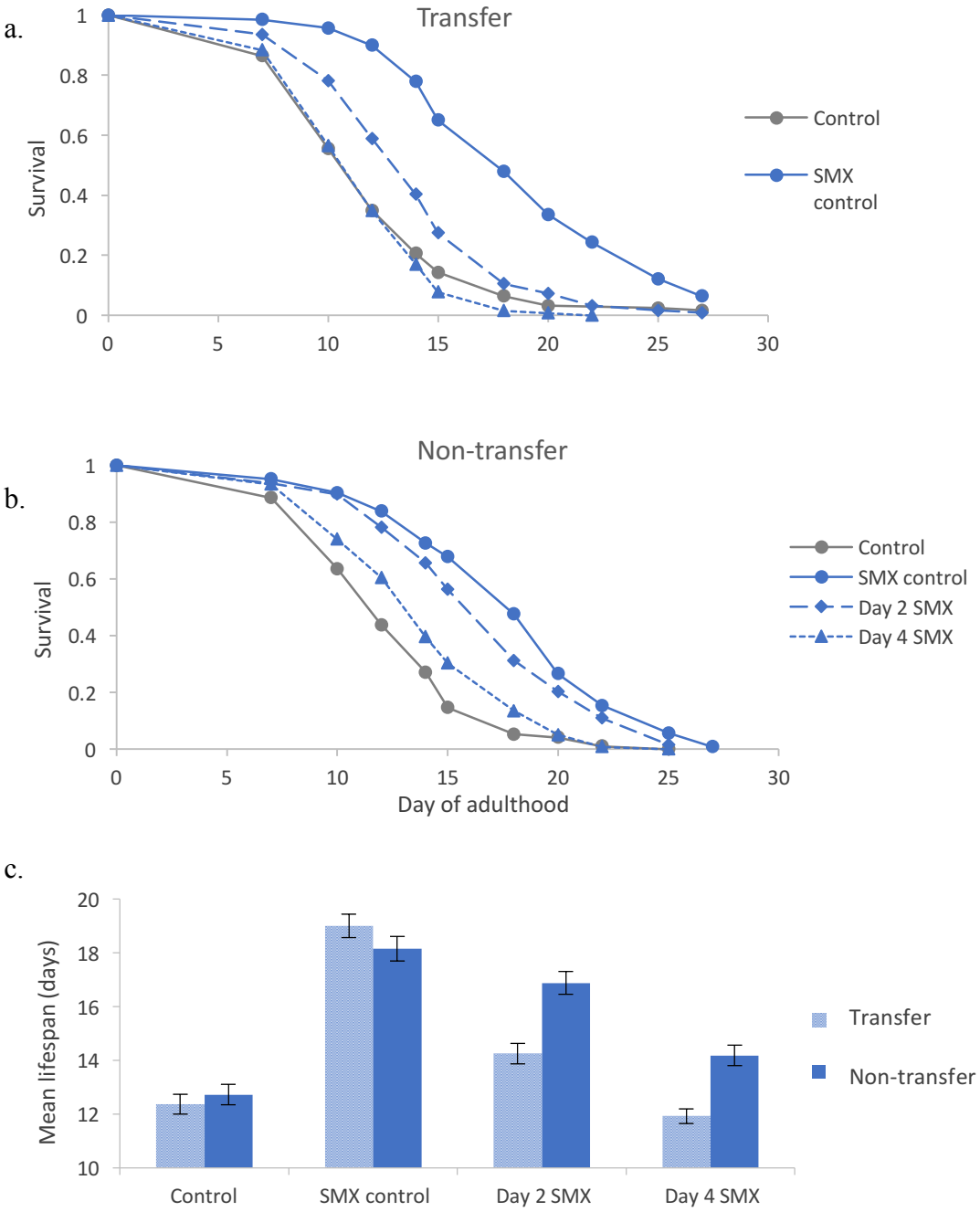

Figure 5.6. Addition of SMX within the first two days of bacterial growth is most effective at extending *C. elegans* lifespan a-b) Kaplan-Meier survival curves of *C. elegans* on WT *E. coli* supplemented with SMX either post-autoclaving or after 2 days or 4 days of bacterial growth where a) worms were transferred onto fresh *E. coli* at days 7 and 14 of adulthood and b) worms were not transferred c) mean lifespan on all conditions (error bars represent standard error).

5.4 DISCUSSION

5.4.1 Excess folate responsible for lifespan decrease is generated in early exponential phase

This chapter aimed to determine when *E. coli* synthesizes folate and how folate levels fluctuate over time, under conditions used for *C. elegans* experiments. Rather than continuous constitutive synthesis, both LC-MS/MS detection of folate levels (figure 5.1, 5.2) and qPCR analysis of *pabA* gene expression (figure 5.3) were consistent with a model whereby the majority of folate synthesis occurs during early exponential growth phase, after which point activity is decreased, but a basal level is maintained into stationary phase. In our model system, early exponential phase here coincides with 2/3 days after seeding the bacteria onto the DM agar plates, when plates are incubated at 25 °C. It is also shown here that inhibiting *E. coli* folate synthesis with SMX increases *C. elegans* lifespan most effectively when this early window is targeted (figure 5.6). Together, this work provides a novel insight into the temporality of bacterial folate synthesis and demonstrates that excessive folate synthesis occurs during early exponential phase growth.

5.4.2 A novel association between glucose and *E. coli* folate synthesis

Glucose is a readily utilizable carbon source and is well known to increase bacterial growth. 0.1% glucose was included here in order to shift the growth kinetics of *E. coli* compared to growth on amino acids, and therefore act as a positive control for the temporality of folate synthesis. Indeed, glucose did increase bacterial growth and this correlated to a left shift in the peak of folate levels (from day 3 to day 2). As the

extracts were normalized for growth, the effect of glucose on detectable folate levels was separated from increased cell number, but unexpectedly glucose markedly increased the levels of all folate species at day 2. Glucose is not a recognised extrinsic factor known to increase bacterial folate synthesis, and it has only previously been described anecdotally (Sybesma et al., 2003). The effect was not observed in *pabA* mutant or SMX-treated extracts, indicating that glucose increases folate levels by boosting bacterial folate synthesis. Unfortunately, *pabA* expression was not monitored in WT *E. coli* on 0.1% glucose media, but it is hypothesized that glucose would increase *pabA* expression and perhaps other genes involved in folate synthesis

The impact of glucose on bacterial folate synthesis was here found to be partially responsible for the negative impact of glucose on *C. elegans* longevity, which is regarded in the field to be mediated directly through *C. elegans*. Together this work reveals a novel role of glucose in boosting *E. coli* folate synthesis and thus indirectly modulating *C. elegans* lifespan. The mechanism underlying this phenomena was not further explored within the scope of this thesis, however, areas for further study and the translational implications of this work will be discussed in Chapter 8.

6.1 INTRODUCTION

As discussed in Chapter 1, studies have indicated that *E. coli* K12 and OP50 impact *C. elegans* lifespan in mechanisms independent of nutritional content, and consistent with a mild pathogenicity or toxicity (Kim, 2013). The data presented in this thesis have demonstrated that *E. coli* synthesizes folate above the threshold required for growth and biosynthesis and that this negatively affects *C. elegans* lifespan. This chapter investigates whether excessive bacterial folate synthesis is associated with a toxicity and explores a potential genetic mechanism via which this toxicity may occur.

6.1.1 *C. elegans* as sensors of toxicity

C. elegans encounter diverse microbes in the wild and must be able to differentiate between those that are beneficial and those that are harmful. As such, *C. elegans* have evolved mechanisms to escape and defend against pathogenic bacteria and toxic metabolites (Pujol et al., 2008; Schulenburg et al., 2008; Shtonda and Avery, 2006; Stupp et al., 2013; Zhang, 2008). *C. elegans* can be maintained in monoculture on a wide range of commensal and pathogenic bacteria and these mechanisms have been characterized in the laboratory (Clark and Hodgkin, 2014; Couillault and Ewbank, 2002). One of the most well established phenotypes is sensing and avoidance, termed aversion behaviour (Bargmann et al., 1993; Melo and Ruvkun, 2012). Furthermore, the sensitivity of *C. elegans* developmental and reproductive phenotypes to toxicity is also being used as a platform to screen for toxic chemicals (Hunt, 2017; Xiong et al., 2017). The first section of this chapter

will harness these phenotypes in order to assess folate-dependent bacterial toxicity.

6.1.2 The global stress response sigma factor, RpoS

Sigma factors are conserved bacterial proteins which associate with RNA polymerase and provide promoter specific recognition. They facilitate transcription by contributing to DNA strand separation and disassociate following transcription initiation. Prokaryotes have several sigma factors, each of which has a specific regulon, and therefore provide a means to simultaneously regulate the expression of a large subset of genes (Davis et al., 2017).

RpoS, or σ^S, is the global stress response sigma factor responsible for the transcription of genes involved in the response to external stimuli, such as: nutrient starvation, hyperosmolarity, low pH, low temperature and oxidative stress (Hengge-Aronis, 2002). In *E. coli,* the RpoS-regulon is predicted to positively regulate over 400 genes (Patten et al., 2004). RpoS was initially identified as a component necessary for survival in stationary phase (Tanaka et al., 1993), however, subsequent studies have found that RpoS function is not confined to stationary phase (Hengge-Aronis, 1996), with significant regulatory activity reported during exponential growth (Dong et al., 2008; Hengge-Aronis, 1996; Seputiene et al., 2006; Vijayakumar et al., 2004)

As discussed in Chapter 1, the *rpoS* gene is of interest as it was identified in the Weinkove laboratory during a screen of *E. coli* mutants for *C. elegans* longevity. *rpoS* has also been extensively linked to the expression of virulence factors and toxins in pathogenic bacteria (Bachman and Swanson, 2001; Dong et al., 2008;

Iriarte et al., 1995; Suh et al., 1999; Yildiz and Schoolnik, 1998). In *C. elegans*, *rpoS* deletion in *Serratia sp*. *ATCC 39006* (Wilf and Salmond, 2012) and *Salmonella typhimurium* (Labrousse et al., 2000) have been reported to reduce virulence and extend lifespan. *rpoS* expression has also been identified as a necessary factor for infection in mouse models (Allen-Vercoe et al., 1998; Banik et al., 2011; Lee et al., 2007) and human infections (Preziosi et al., 2012).

Furthermore, although *rpoS* has not explicitly been linked to folate synthesis, a literature search revealed two *E. coli* microarray data sets that pulled out *pabA* as significantly downregulated in an *rpoS* mutant (Ito et al., 2008; Weber et al., 2005). Combined with the finding in the Weinkove laboratory that the *E. coli* K12 *rpoS* mutant extends *C. elegans* lifespan (Virk et al. 2016), the hypothesis was made that excessive folate synthesis in *E. coli* K12 may be regulated by *rpoS* in a mechanism either directly or indirectly related to virulence and/ or toxicity. In this chapter, this hypothesis will be tested by examining whether *C*. *elegans* lifespan extension on the *rpoS* mutant is folate-dependent and screening for *rpoS* and folate-dependent mechanisms of toxicity.

6.2 CHAPTER AIMS

- Aim 1: Investigate the coincidence of bacterial folate synthesis and toxicity
  - -using *C. elegans* aversion to the bacterial lawn
  - -investigating the *Enterobacter cloacae* B29 strain
- Aim 2: Investigate the role of *rpoS* in folate-dependent bacterial toxicity

6.3 RESULTS

6.3.1 *C. elegans* aversion as a phenotypic readout of folate-dependent bacterial toxicity

Here, *C. elegans* aversion to *E. coli* is used as a proxy for bacterial toxicity and will be measured by calculating percentage aversion to the bacterial lawn, where:

$$\%\ \text{aversion} = \left(\frac{\text{N (off lawn)}}{\text{N (total)}}\right) \text{x } 100$$

6.3.1i. SMX decreases C. elegans aversive behaviour and increases lifespan on two E. coli strains

The impact of SMX on the aversive behaviour of two wild-type *C. elegans* strains (N2 and SS104) on agar seeded with either OP50 or K12 *E. coli* was measured. 128 µg/ ml SMX was used in all cases. Aversion was calculated 24 hours after transfer of 50 L4/ young adult worms onto each plate, with 5 replicates per condition. When SMX was present in the media, the percentage aversion of both SS104s and N2s was significantly lower compared to the non-supplemented control on both wild-type strains of *E. coli* ($P<0.001$ in all cases) (figure 1a). In the absence of SMX, the mean percentage aversion was significantly higher on K12 WT compared to OP50, in both SS104s ($P=0.017$) and N2s ($P=0.020$). Whilst this does not provide direct evidence of toxicity, the data is consistent with the hypothesis that inhibiting folate synthesis attenuates a folate-dependent activity that normally deters *C. elegans* from the bacterial lawn.

Using just the temperature sensitive sterile *C. elegans* strain, SS104 (*glp-4*(*bn2*)), lifespan assays were carried out on K12 and OP50 treated with SMX (figure 6.1b). In line with a higher percentage of aversion on K12 compared to OP50, *C. elegans*

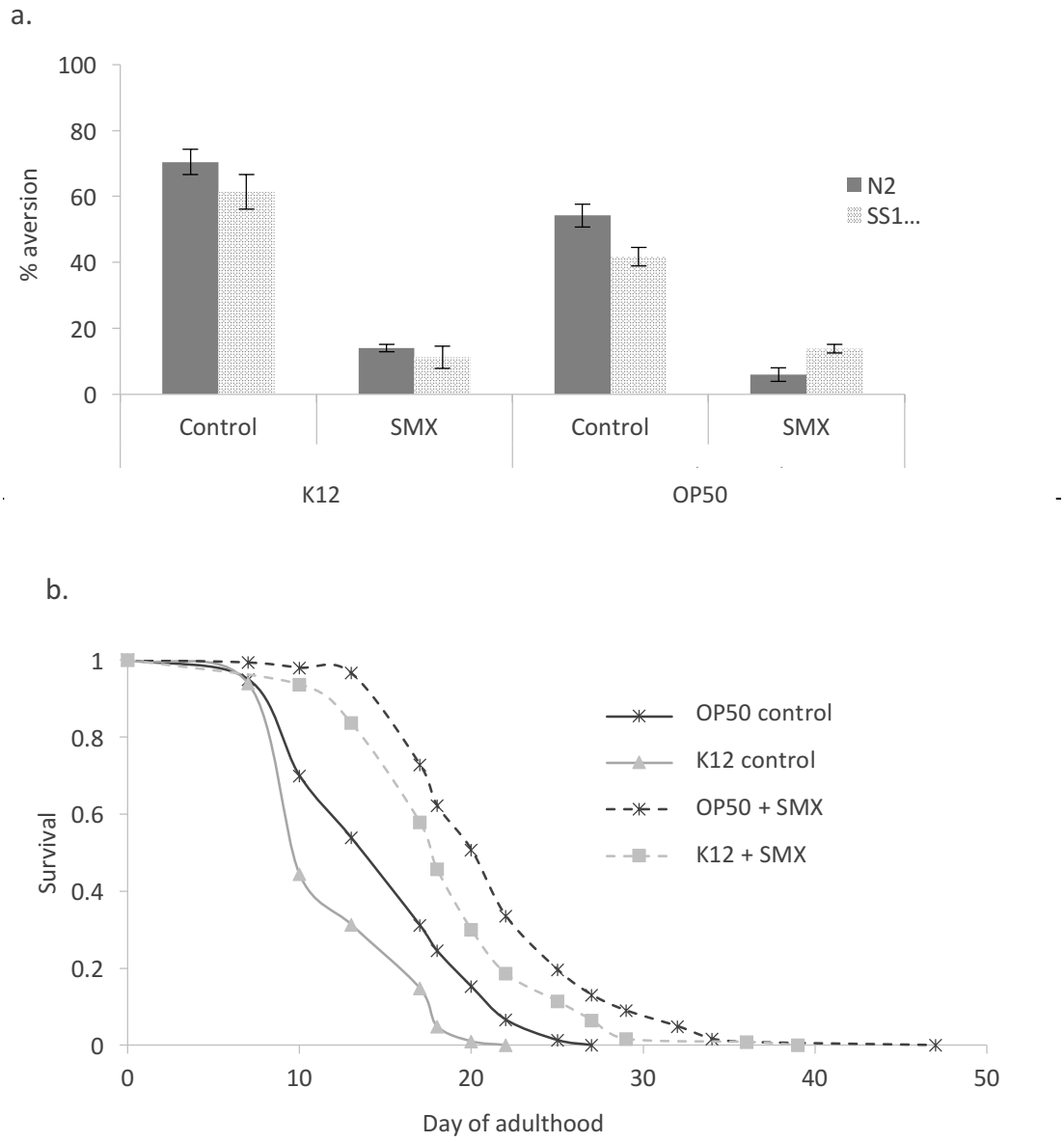

Figure 6.1 SMX decreases *C. elegans* aversion and increases lifespan on OP50 and K12 *E. coli* a) 50 worms were transferred onto each plate, with 5 replicates per condition, after 2 days of bacterial growth. Aversion of two wild-type *C. elegans* strains, N2 and SS104, was measured after 3 days of bacterial growth. Error bars represent standard deviation b) Kaplan-Meier survival curves of the SS104 strain on OP50 and K12 with and without SMX. Assays were carried out on NGM. Assays performed at 25°C. [SMX] = 128 µg/ml.

were also shorter lived on K12 (P<0.0001). Likewise, SMX increased survival of *C. elegans* on both *E. coli* strains compared to their untreated conditions (P<0.0001 in both cases), however survival of worms on K12 remained significantly shorter than worms on OP50.

6.3.2ii pabA and rpoS mutant E. coli decrease C. elegans aversion

In order to verify that the impact of SMX on *C. elegans* aversion is folate-dependent and not an artefact of a xenobiotic, aversion assays were carried out DM plates seeded with *pabA* mutant *E. coli,* with SMX included as a positive control (figure 6.2). Aversion was also measured on the *rpoS* mutant. Consistent with a folate-dependent activity mediating *C. elegans* aversion, the *pabA* mutation significantly decreased aversive behaviour of both N2 (P=0.004) and SS104s (P=0.001) compared to the WT *E. coli* control, verifying that aversion is folate-dependent. On *rpoS* mutant *E. coli,* both N2 (P<0.001) and SS104 (P=0.001) also showed significantly decreased aversive behaviour. The difference in aversion of N2 and SS104 worms on *rpoS* was not significant (P=0.092).

6.3.1iii SMX impacts C. elegans aversion most effectively in E. coli exponential phase

In order to investigate whether aversion and lifespan are affected by the same folate-dependent activity, aversion was measured on the conditions used for the lifespans in Chapter 6 (figure 6.6): SMX was either added into the media after autoclaving, or pipetted on top of the agar media at the appropriate concentration, after 2 or 4 days of bacterial growth. 25 L4/ young adult worms were transferred onto 10 plates per each condition, after the bacteria had been

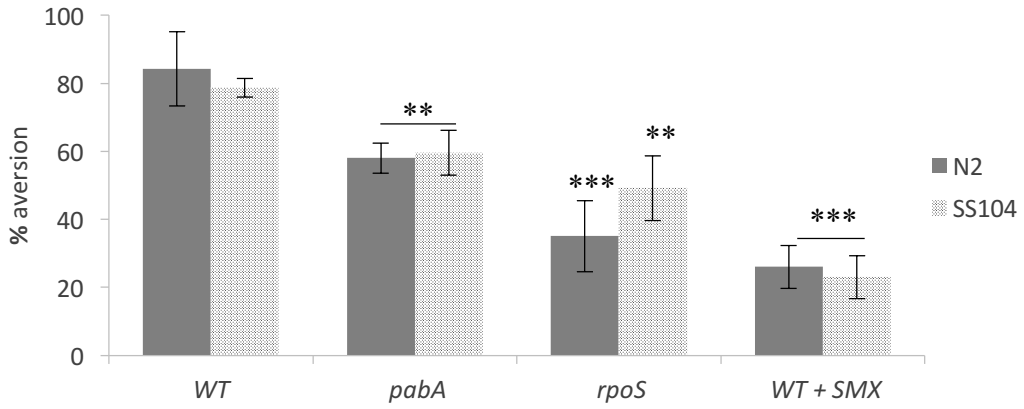

Figure 6.2 *C. elegans* aversion is decreased on *pabA* and *rpoS* mutants. *E. coli* strains were seeded onto DM plates. N2 and SS104 *C. elegans* strains were transferred onto each plate (n=50), with 5 replicates per condition, after 2 days of bacterial growth. Aversion was measured after 3 days of bacterial growth. [SMX] = 128 μg/ml. Error bars represent standard deviation. Asterisks denote the result of two-tailed Student's *t*-test's of denoted condition compared to on WT *E. coli* of the same *C. elegans* strain, where *P<0.05, **P<0.005, ***P<0.001

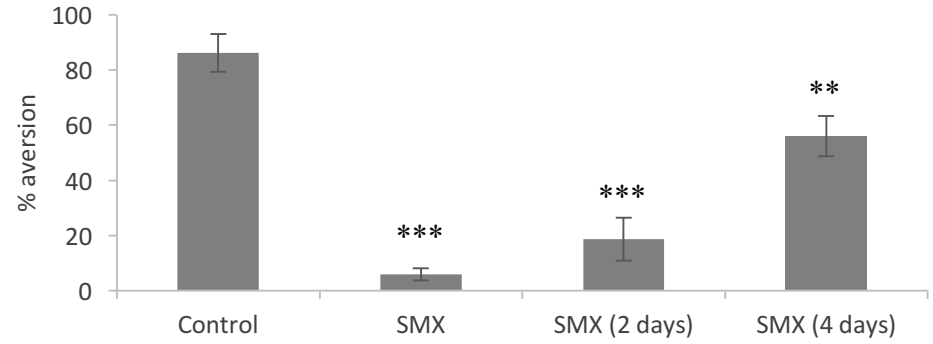

Figure 6.3 SMX is most effective at decreasing *C. elegans* aversion during early exponential phase growth. 128 μg/ml SMX was added to DM plates either post-autoclaving into cooled, liquid media, or pipetted on top of seeded plates in evenly distributed aliquots after either 2 or 4 days of bacterial growth. 50 worms were transferred onto each plate, with 5 replicates per condition, after 2 days of bacterial growth. Aversion was measured after 6 days of bacterial growth. Error bars represent standard deviation. Asterisks denote the result of two-tailed Student's *t*-test's of SMX condition compared to control condition, where *P<0.05, **P<0.005, ***P<0.001

seeded and incubated at 25 ˚C for 48 hours. On all conditions, aversion to the bacterial lawn was measured on the 6th day of bacterial growth (worms on plates for 4 days).

Consistent with the previous data, adding SMX to the liquid agar growth media post-autoclaving resulted in very low aversion (6%), markedly lower than the non-supplemented control (85%) (figure 6.3). Percentage aversion was significantly higher on plates supplemented after 2 days (18%) and higher again on plates supplemented at 4 days (56%) (figure 6.3). This data is consistent with the decreased efficacy of SMX as a means to extend lifespan, the later the phase of bacterial growth it is added. It also suggests that the same folate-dependent activity during exponential phase of bacterial growth is modulating *C. elegans* aversion and lifespan.

6.3.2 Folate-dependent toxicity in the *Enterobacter cloacae* strain, B29

The LPS endotoxin producing *Enterobacter cloacae* strain, B29 (Fei and Zhao, 2013), was used to investigate folate-dependent toxicity in a different bacterial species. Previous work carried out by B. Virk in collaboration with the Zhao lab at Shanghai Jiao Tong University (SJTU) found that *C. elegans* can be maintained on B29, but that worms display strong aversive behaviour, a reduced brood size and shortened lifespan. These phenotypes could not be rescued by knockout of two genes required for LPS biosynthesis, *waaG* and *wbbL* (Virk et al., unpublished). In this chapter, work carried out during a six-week visit to SJTU investigated whether this toxicity is folate-dependent. Due to time constraints, *C. elegans* aversion and reproductive fitness were focused on in preference to lifespan. Experiments were carried out on NGM due to the lack of amino acids and trace metals available at

SJTU.

6.3.2i SMX decreases C. elegans aversive behaviour on B29

Aversion of N2 worms on the B29 strain seeded onto plates supplemented with 128 μg/ml SMX was measured. SMX was not found to affect B29 growth at this concentration (data not shown). Percentage aversion was found to be significantly higher on B29 compared to OP50 (P=0.011) (figure 6.4a) When SMX was present in the media, aversion was significantly decreased on both OP50 and B29 (P<0.001) and nearly all worms were found on the bacterial lawn on both bacterial species (figure 6.4a).

6.3.1 ii SMX rescues defective reproductive phenotype on B29

Preliminary work indicated that *C. elegans* have a significantly reduced brood size on B29 compared to on OP50 or K12 *E. coli* (Virk et al., unpublished). Here, the folate-dependence of this phenotype was investigated further. Progeny production was monitored over a 4-day egg-laying period, where N2 *C. elegans* were transferred to fresh plates each day (see methods). Each experimental condition consisted of 5 biological replicates of 3 egg-laying gravid adults per plate. In the same procedure as described in Chapter 3, gravid adults were transferred onto fresh plates each day for 4 consecutive days. Hatched larvae and unhatched eggs were counted after the worms had been transferred onto fresh plates and the progeny plate had been incubated at 25°C for at least 24 hours (see methods). The phenomena of matricidal hatching or 'bagging' was observed in *C. elegans* on B29; although this is interesting as it is indicator of bacterial toxicity, (Mosser et al. 2011) these worms were censored and removed from the assay.

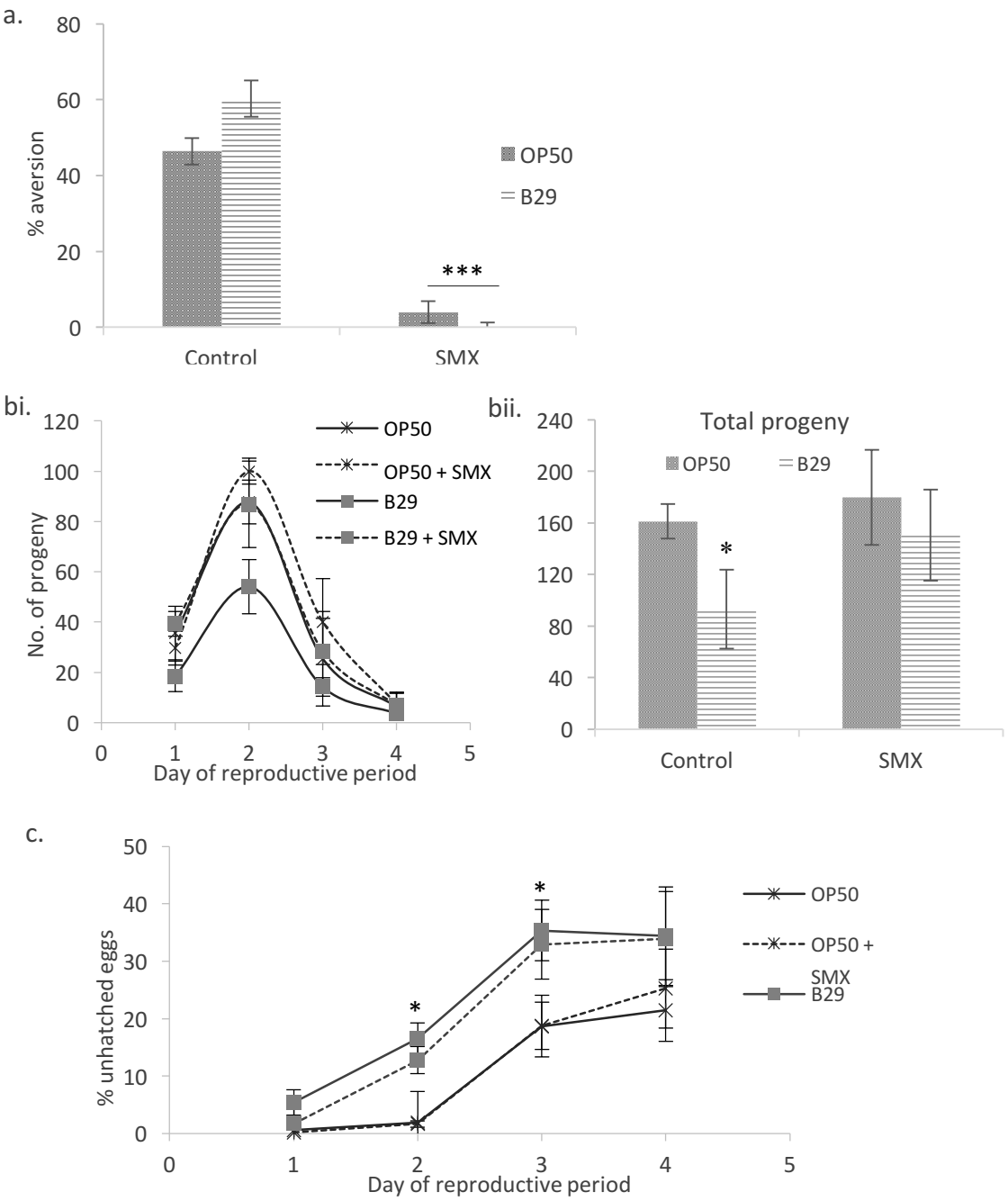

Figure 6.4 SMX rescues *C. elegans* aversion and reproductive phenotypes on B29 a) *C. elegans* aversion on OP50 and B29 ± SMX was carried out as previously described bi) number of viable progeny produced by *C. elegans* on OP50 and B29 ± SMX during a 4 day window bii) total number of viable progeny produced c) unhatched eggs produced by *C. elegans* on OP50 and B29 ± SMX within 4 day window. [SMX] = 128 μg/ml. Error bars represent standard deviation. Asterisks denote the result of two-tailed Student's *t*-test's of SMX condition compared to control condition, where *P<0.05, **P<0.005, ***P<0.001

The reproductive schedule of *C. elegans* on B29 was consistent with that observed on OP50, however the total number of viable progeny was significantly less on B29 compared to OP50 (P=0.0131) (figure 6.4b). When SMX was present in the plates, progeny production on B29 was restored to OP50 levels (P= 0.1236), suggesting that the impaired reproductive phenotype of *C. elegans* on B29 is folate-dependent. On both OP50 and B29, the number of unhatched eggs was seen to increase over the 4 day period (figure 6.4c). On days 2 and 3, this percentage was markedly higher on B29 than on OP50. The number of unhatched eggs was not affected by SMX and therefore cannot account for the decreased brood size on B29. This indicates a separate folate-independent bacterial effect on *C. elegans.*

Together, this work has found that the inhibition of folate synthesis in *Enterobacter cloacae* B29 with SMX decreases *C. elegans* aversive behaviour and restores reproductive fitness. Previous work also found that SMX increases lifespan on B29 (Virk et al., unpublished). Aversion and lifespan have also been identified here as conserved folate-dependent *C. elegans* phenotypes in *E. coli* K12 and OP50. The data is consistent with a model whereby a broad-scale folate-dependent toxicity in *E. coli* K12 and OP50 affects several *C. elegans* life-traits, where this toxicity is amplified in *Enterobacter cloacae*, B29.

6.3.3 Candidate mutant gene screen of the RpoS regulon for genes which modulate lifespan and decrease folate levels

As discussed, the sigma factor encoded for by *rpoS* transcribes hundreds of genes in response to stress, many of which are involved in toxicity and virulence in pathogenic bacteria. Deletion of *rpoS* has previously been found to extend *C.*

elegans lifespan (Virk et al. 2016) and here, decrease aversive behaviour (figure 6.2). In order to investigate whether *rpoS* is involved in folate-dependent toxicity, a candidate screen of *rpoS* downstream genes cited to be involved in toxicity and/ or virulence was set up, where mutants would be tested for their impact on *C. elegans* lifespan, and if positive, carried forward and tested for their folate status using the *gcp-2.1* assay.

There is significant variation in the number of genes cited in the literature to be under *rpoS* regulatory control, likely due to differences between studies in the growth media used and the stage of bacterial growth at which RNA extracts were made. As not all of the RpoS regulon could be screened within the scope of this PhD, interesting candidate genes involved in toxicity or virulence mechanisms were chosen from the studies where *pabA* had been identified as a downstream target (Weber et al. 2005; Ito et al. 2008). In addition, three global transcriptional regulators, *crp, lrhA* and *relA* were also included for their reported associations and transcriptional cross-over with *rpoS. rpoS* was included as a positive control and all experiments were carried out on DM unless otherwise stated.

6.3.3ii Candidate mutant screen for downstream RpoS genes that modulate lifespan

15 *E. coli* deletion mutant strains were tested in the first screen and five significantly increased *C. elegans* survival, namely: *astA, bipA, , crp* and *lrhA* (figure 6.5a). These genes were carried forward into a second lifespan screen (figure 6.5b). Four more genes were identified to significantly extend lifespan, namely, *relA, sodA, otsB* and *fic* ($P<0.005$). *cfa* did not have as much of a significant effect on lifespan ($P<0.05$),

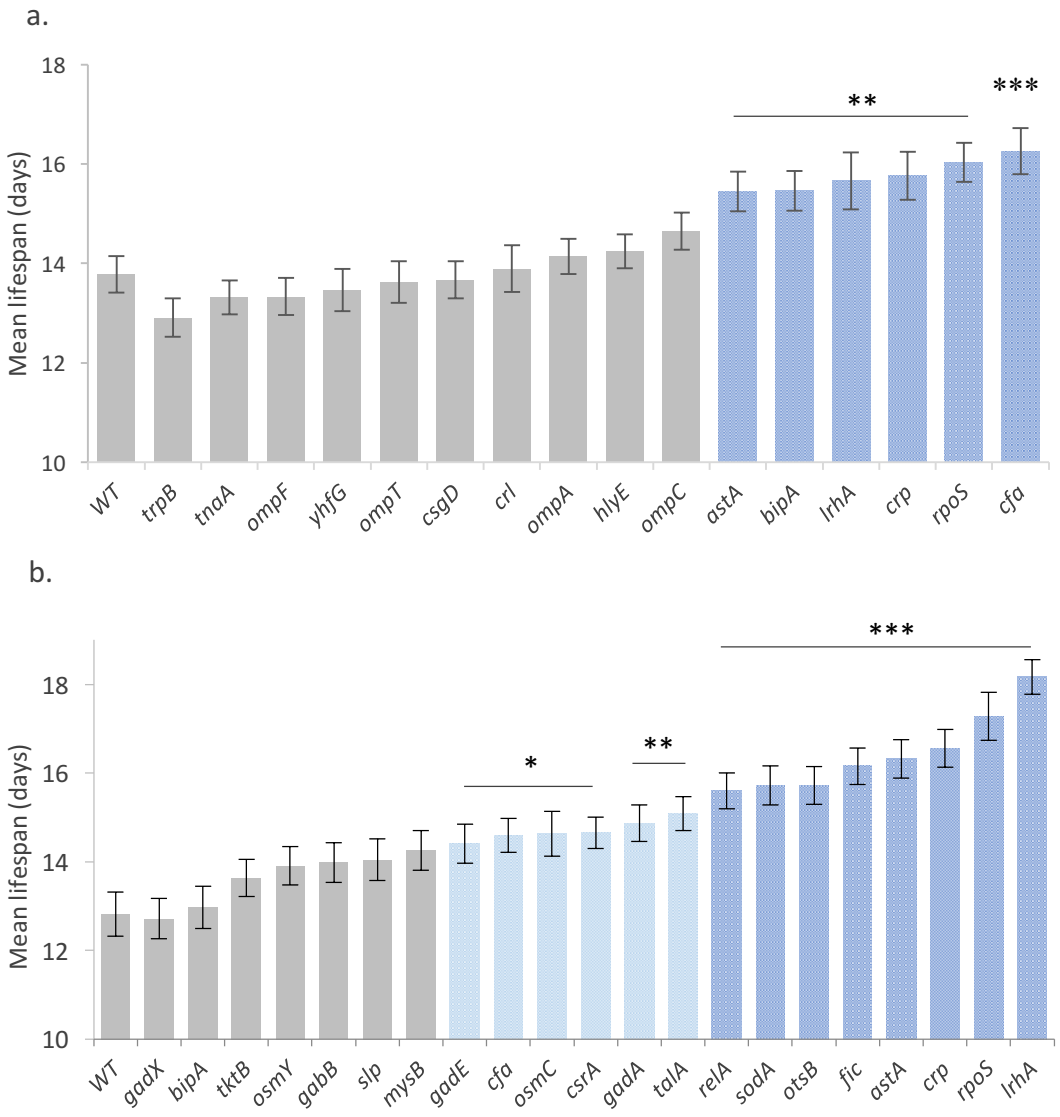

Figure 6.5 Candidate gene screen for mutants in the RpoS regulon that increase *C. elegans* lifespan. Lifespans were conducted in two separate rounds. Positive mutants from the first round (a) were tested again in the second round (b) along with additional candidates. Error bars represent standard error. Dark blue bars indicate mutants carried forward to the next round of the screen. Light blue bars indicate significance compared to WT but were not carried forward. Asterisks denote result of Log-rank statistical analyses of Kaplan-Meier survival curves, where ***P<0.001, **P<0.01, *P<0.05. See supplementary table 1 for full outline of conditions, statistical analysis and n numbers.

and *bipA* did not significantly extend lifespan here. Genes involved in classical virulence mechanisms, such as *hlyE* (Kerenyi et al., 2005), *crl* (Dudin et al., 2013) and *csgD* (Uhlich et al., 2002) (figure 6.5a) were not found to increase lifespan, thus eliminating several hypotheses.

6.3.3ii gcp-2.1 bioassay to examine the folate status of rpoS and downstream rpoS positive lifespan mutants

The folate status of these positive lifespan mutants was examined using the *gcp-2.1* mutant bioassay, as previously described. *pabA* mutant and SMX-treated WT *E. coli* were included as positive controls and the wild-type *C. elegans* strain was used to control for folate-independent effects on worm development. On both *rpoS* and *fic* mutants, *gcp-2.1* body length was significantly shortened at L4 stage compared to on WT *E. coli* ($P<0.001$, in both cases), where neither mutant exerted any effect on the wild-type *C. elegans* strain (figure 6.6a). The *lrhA* mutant significantly reduced body length of both *gcp-2.1* mutants and the wild-type strain. No effect on *gcp-2.1* body length was measured for any of the other mutants.

This assay was repeated with just the *gcp-2.1* mutants on WT *E. coli*, *pabA, rpoS, fic* and a negative control mutant, *ygfA.* All mutants were also tested on SMX supplemented plates. Consistent with previous findings, *gcp-2.1* mutant growth at L4 stage was significantly stunted on *pabA, rpoS* and *fic* mutants and on all conditions with SMX ($P<0.001$, in all cases) (figure 6.6b). Interestingly, SMX did not significantly further decrease body length on *pabA, rpoS* or *fic,* suggesting that these two interventions may be working in the same pathway (figure 6.6b). Together, this points to a novel role of both *rpoS* and *fic* in bacterial folate synthesis

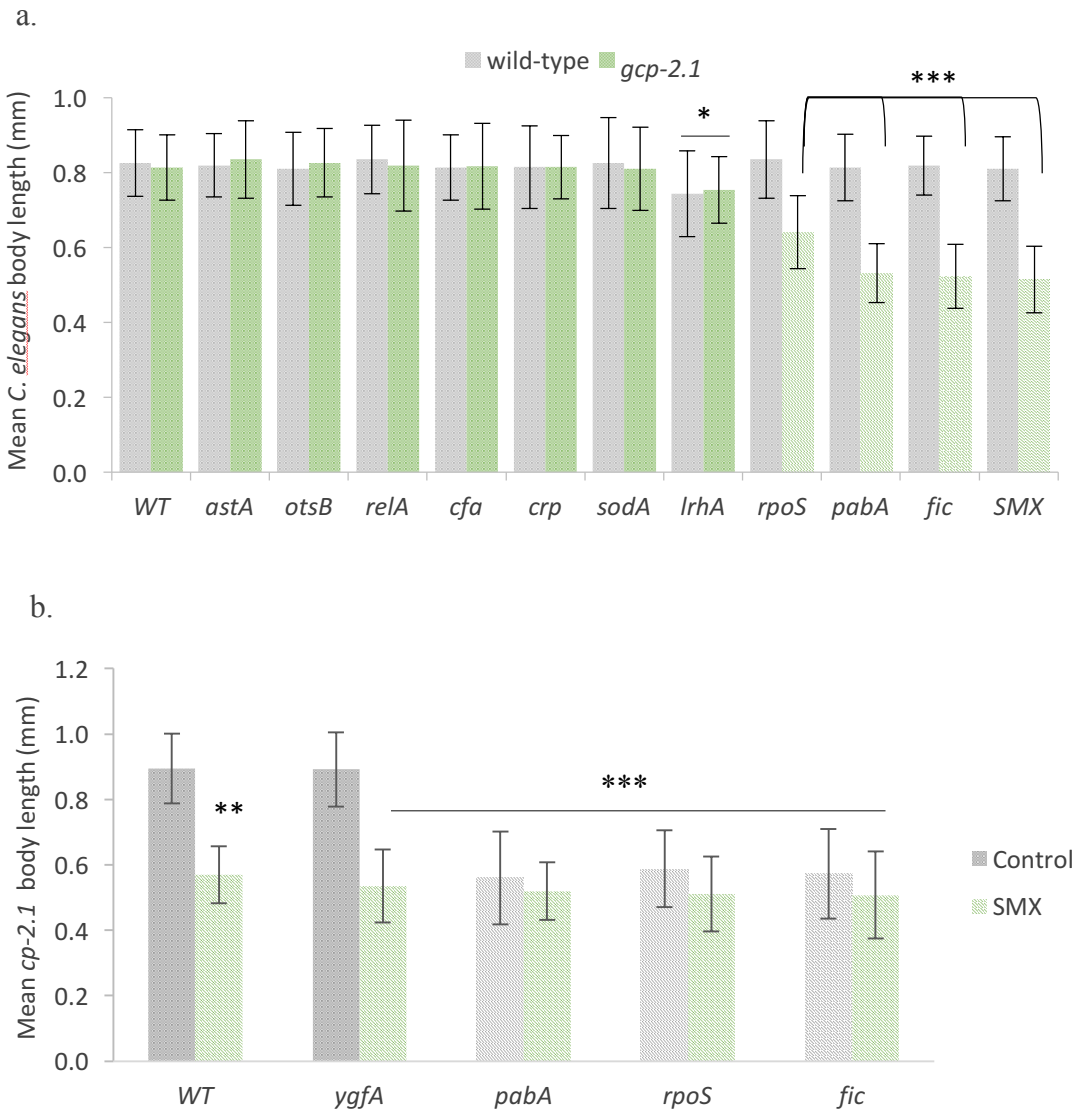

Figure 6.6 *gcp-2.1* mutants exhibit developmental folate deficiency on *rpoS* and *fic* mutants. a) *gcp-2.1* mutant body length at L4 stage on all positive *E. coli* mutants identified in the candidate gene screen, ordered by decreasing mean body length, left to right b) *gcp-2.1* body length on just positive mutants from (a) including a negative control (*ygfA)* ± 128 μg/ml SMX. Error bars represent standard deviation, where n≥ 40 in all cases. Asterisks denote the results of Student's *t*-tests, where *P<0.05 **P<0.01 ***P<0.001 of denoted condition compared to WT *E. coli.*

and/ or metabolism. This is interesting considering the recently elucidated role of Fic proteins in bacterial toxicity, which will be discussed in more detail in Chapter 8.

6.3.4 Examining the folate status of *rpoS* and *fic* mutants

The data above indicates that *rpoS* and *fic* mutants have a lowered levels of folate, however, it is not clear whether these genes are mediating this via altered folate synthesis and/ or one-carbon metabolism. In order to clarify how *rpoS* and *fic* interact with *E. coli* folate, and thus *C. elegans* lifespan, the folate status of these mutants was examined more sensitively and specifically using LC-MS/MS detection.

6.3.4i LC-MS/MS verifies the low folate status of rpoS and fic mutants

Folate extractions were carried out on WT*, rpoS, fic, pabA* and *lrhA* mutant *E. coli* which had been seeded onto DM agar plates and for 4 days at 25°C, as is standard procedure. *lrhA* was included for interest due to its reported regulation of *rpoS* expression. As the focus of the experiment was not *pabA,* and the folate requirements of the strains in question were unclear, 0.1 μM PABA was not supplemented into the DM so as not to confound results. Only the *pabA* strain showed a growth defect on DM without PABA (figure 6.7b). Nevertheless, as standard with all folate extraction procedures, samples were normalized for bacterial growth and folate levels are displayed as a ratio of an internal MTX-glu_6 spike.

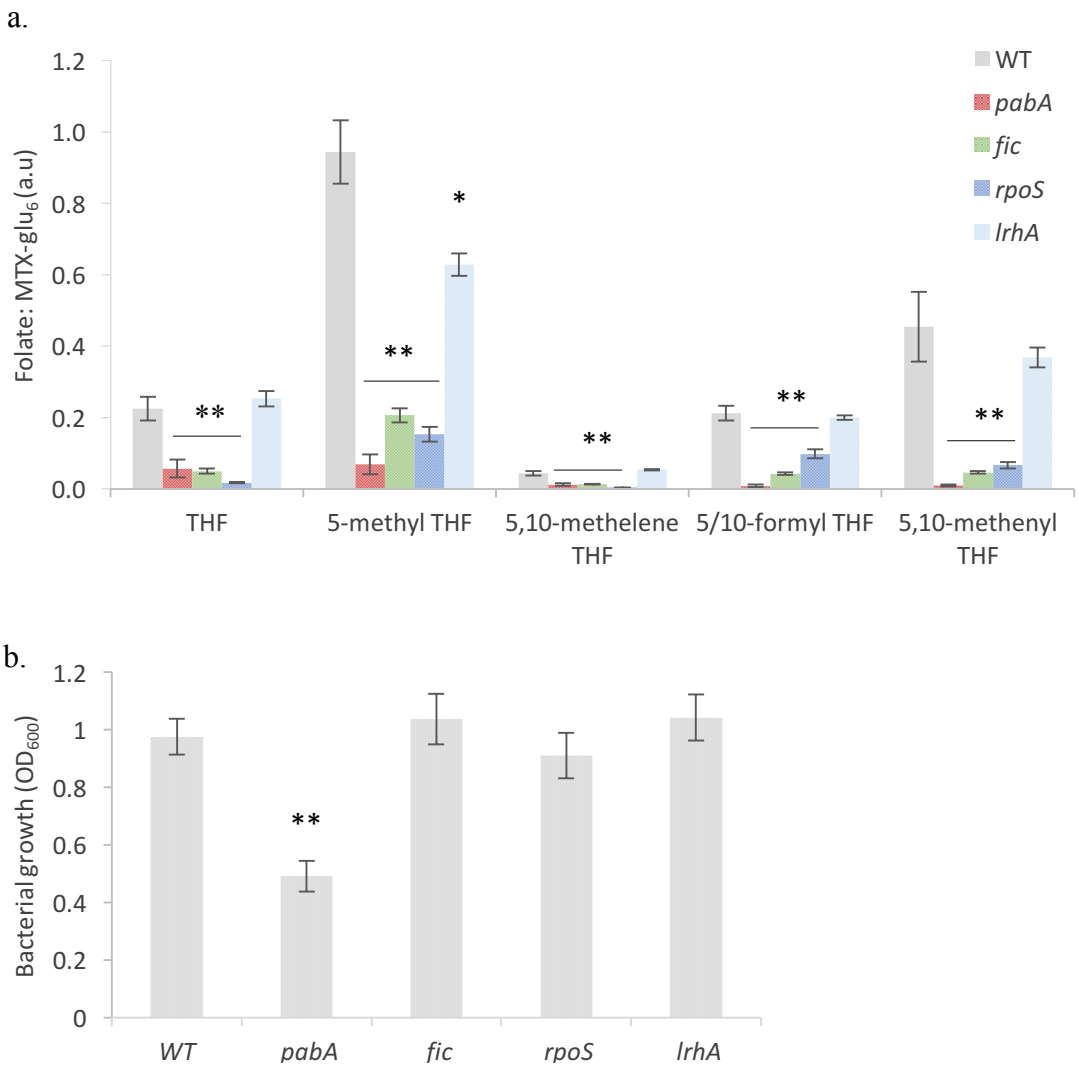

Figure 6.7 LC-MS/MS reveals low folate levels in *E. coli pabA*, *rpoS* and *fic* mutants a) levels of THFs detected in extracts of WT *E. coli* and *pabA, fic, rpoS, lrhA* mutants displayed as a ratio of an internal MTX-glu$_6$ spike for normalization between samples. Extracts were made after 4 days of bacterial growth at 25°C b) growth of strains used for this assay as measured by OD_{600} before extractions were made. Extractions were normalized for growth. Error bars represent standard deviation. Asterisks denote the test statistic from Student's *t* test comparison of means, where *P<0.05; **P<0.01.

All detectable folate species were significantly lower in *rpoS, fic* and *pabA* extracts compared to WT ($P<0.01$) and only 5-methyl THF-glu_3 was significantly lower in *lrhA* ($P<0.05$) (figure 6.7). Thus, LC-MS/MS analysis of *rpoS* and *fic* mutants is consistent with the results of the *gcp-2.1* bioassay and supports the hypothesis that these genes are involved in folate synthesis and/ or one-carbon metabolism.

6.3.4ii PABA supplementation reveals altered one-carbon metabolism in rpoS mutant as detected by LC-MS/MS

In order to understand if *rpoS* and *fic* regulate folate synthesis or one-carbon metabolism, the impact of the folate precursor, PABA, on the folate profile of these strains was examined. Folate extractions were carried out as above and on plates supplemented with 0.1 µM and 1 µM PABA. Consistent with figure 6.7, levels of all folate species were significantly lower than WT in *rpoS*, *pabA* and *fic* mutant extracts on non-supplemented control plates, with the exception of DHF in *pabA* and *fic* and 5/10-formyl THF in *rpoS* (figure 6.8). PABA increased folate levels in the WT and *pabA* extracts, where folates in *pabA* extracts were detected at lower levels than in the relative WT condition (with the exception of DHF and THF at 0.1 µM PABA). At 1 µM PABA, folate levels in *pabA* extracts were detected at similar levels to those in WT extracts at 0.1 µM PABA (with the exception of THF at 1 µM PABA). Folate levels in *fic* mutant extracts showed a similar profile and response to PABA as seen in *pabA* extracts, consistent with a role of *fic* in folate synthesis, acting upstream of *pabA.*

Folate levels in *rpoS* mutant extracts showed a more complex response to PABA: levels of 5-methyl THF and 5,10-methenyl THF increased in response to PABA in

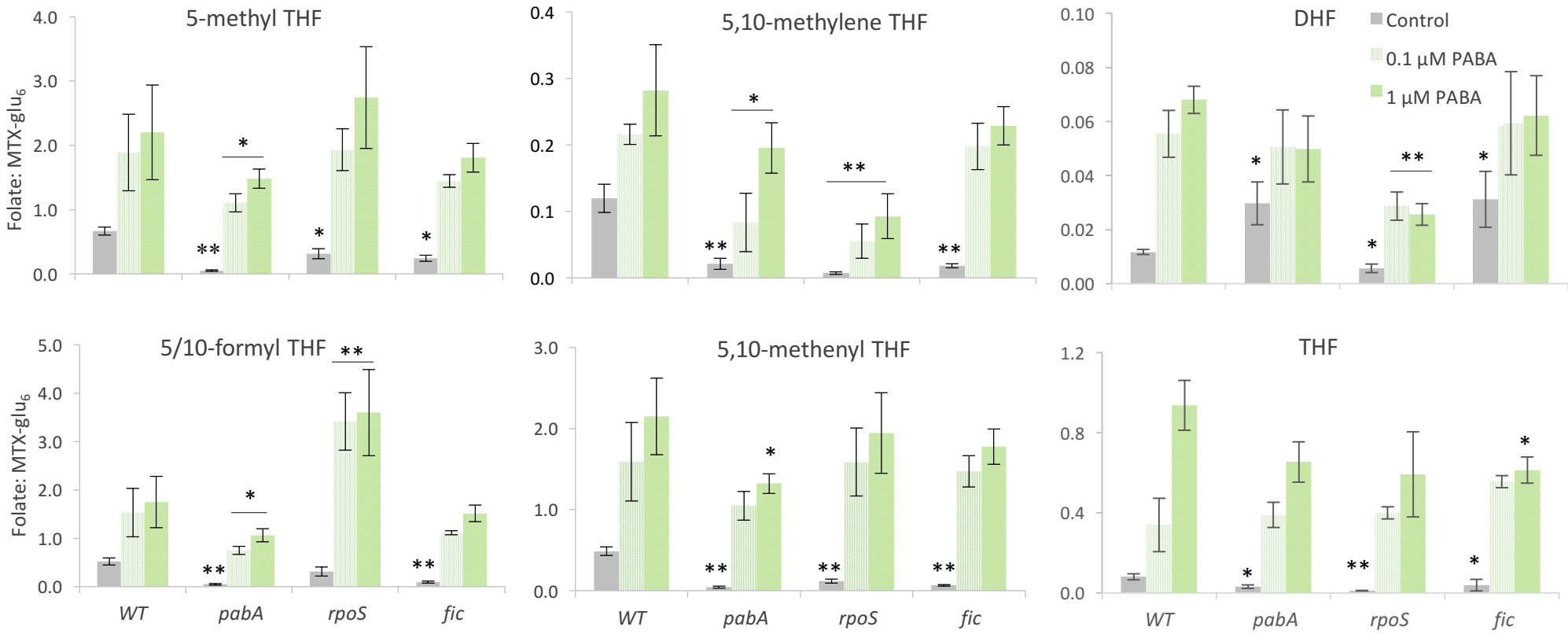

Figure 6.8 LC/MS-MS reveals differential impact of PABA on folate levels in *E. coli* WT, *pabA*, *rpoS* and *fic* mutants. Folate levels in extracts of WT, *pabA, rpoS* and *fic* mutant *E. coli* were analysed by LC-MS/MS. Extracts were made after 4 days of bacterial growth on DM at 25°C. Samples were normalized for growth before extractions. Levels of tri-glutamated THFs detected in extracts are displayed as a ratio of an internal MTX-glu_6 spike for normalization between samples. Error bars represent standard deviation. Asterisks denote the test statistic from Student's *t* test of folate level in denoted condition compared to the WT *E. coli* extract of the same condition, where * = P<0.05; **= P<0.01.

line with the comparative WT condition and 5/10-formyl THF was detected at significantly higher levels at both 0.1 and 1 μM PABA compared to the relative WT Conditions (figure 6.8). In contrast, levels of 5,10-methylene and DHF in *rpoS* were significantly lower than WT on all conditions. 5,10-methylene levels in *rpoS* extracts were significantly lower than in *pabA* extracts at 1 μM PABA. DHF levels were significantly lower in *rpoS* than *pabA* at both 0.1 μM and 1 μM PABA.

Folate extractions of *rpoS* mutants were repeated on non-supplemented and 1 μM PABA supplemented conditions (figure 6.9). The impact of the *rpoS* mutation and its response to PABA was consistent between these two experiments: all folates were at lower levels in *rpoS* mutant extracts than WT extracts on non-supplemented conditions, again with the exception of 5-formyl THF. In response to PABA, 5/10-formyl THF and 5-methyl THF was significantly higher than in WT extracts and 5-10-methylene THF and DHF were significantly lower. Toegther this indicates that *rpoS* may have a role in both folate synthesis and one-carbon metabolism.

6.3.4iii E. coli rpoS mutants have low levels of the pterin branch intermediate, 7,8-Dihydro-D-neopterin, and accumulate PABA

The low level of most folate species in non-supplemented control extracts of *rpoS* and *fic* mutants was consistent with a role of these genes in folate synthesis. In order to examine this further, the pterin branch intermediate, 7,8-Dihydro-D-neopterin (DHNP) (Chapter 1, figure 1.2) and PABA were obtained from Schircks laboratories and standard solutions were injected into the LC-MS/MS to

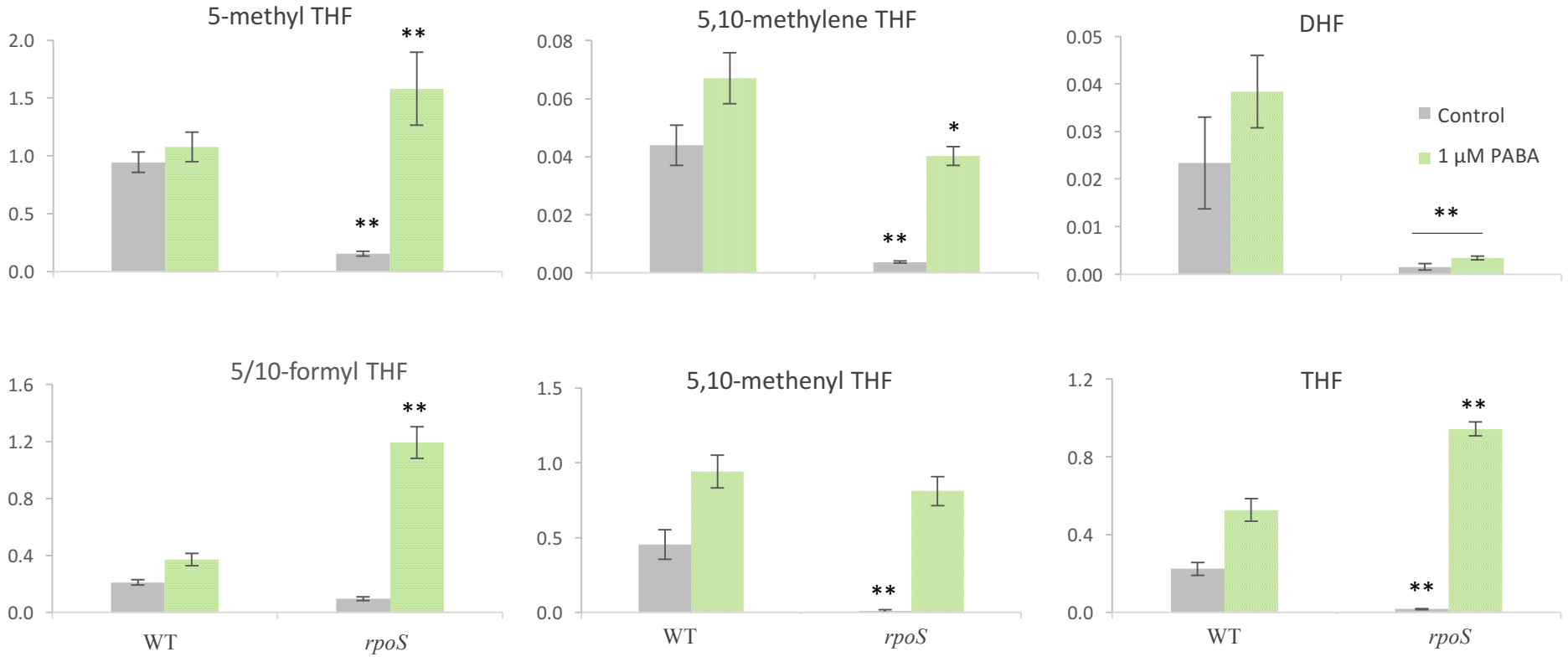

Figure 6.9 LC-MS/MS confirms altered folate profile of the *E. coli rpoS* mutant. Folate levels in extracts of WT, *pabA, rpoS* and *fic* mutant *E. coli* was analysed by LC-MS/MS. Extracts were made after 4 days of bacterial growth on DM at 25°C. Samples were normalized for growth before extractions. Levels of tri-glutamated THFs detected in extracts are displayed as a ratio of an internal MTX-glu_6 spike for normalization between samples. Asterisks denote the test statistic from Student's *t* test of folate level in *rpoS* mutant extract compared to in to the WT extract of the same condition, where * = P<0.05; **= P<0.01. Error bars represent standard deviation.

determine retention times. Other pterin intermediates were not tested due to their inhibitory costs. Levels of both of these compounds were detected by LC-MS/MS in the first folate extraction experiment (figure 6.8), but have been presented subsequently for data clarity.

In WT, *pabA* and *fic E. coli* extracts, DHNP was detected at similar levels, where a significant decrease was observed in all extracts at 1 μM PABA ($P<0.05$, in all cases). This may indicate an increased consumption of DHNP when cells have excess PABA. However, in *rpoS* extracts, DHNP levels were significantly lower on control ($P<0.001$), 0.1 μM PABA ($P=0.005$) and 1 μM PABA ($P=0.029$) supplemented conditions compared to relative WT extracts. This suggests that either *rpoS* mutant cells are less able to synthesize or stabilize DHNP, or it is being used up more efficiently.

PABA levels in all *E. coli* mutants on non-supplemented conditions were markedly lower than in WT *E. coli* extracts; *pabA* ($P=0.005$), *fic* ($P=0.002$) *rpoS* extracts ($P=0.018$), consistent with a role of these genes in PABA synthesis. In response to 0.1 μM PABA, levels of intracellular PABA were significantly higher in the *rpoS* mutant ($P=0.005$) compared to WT at this concentration; levels in *pabA* and *fic* were similar to WT. At 1 μM PABA, PABA levels were consistent across strains and were detected at least 50-fold higher in *pabA, fic* and WT extracts (and 10-fold higher in *rpoS*) compared to at 0.1 μM PABA, despite only a 10-fold increase in PABA concentration. This is suggestive of PABA accumulation, which occurs at a lower concentration in *rpoS* mutants. Combined with the low levels of DHNP in *rpoS* mutants, this data indicates that folate synthesis is inhibited in *rpoS* mutants

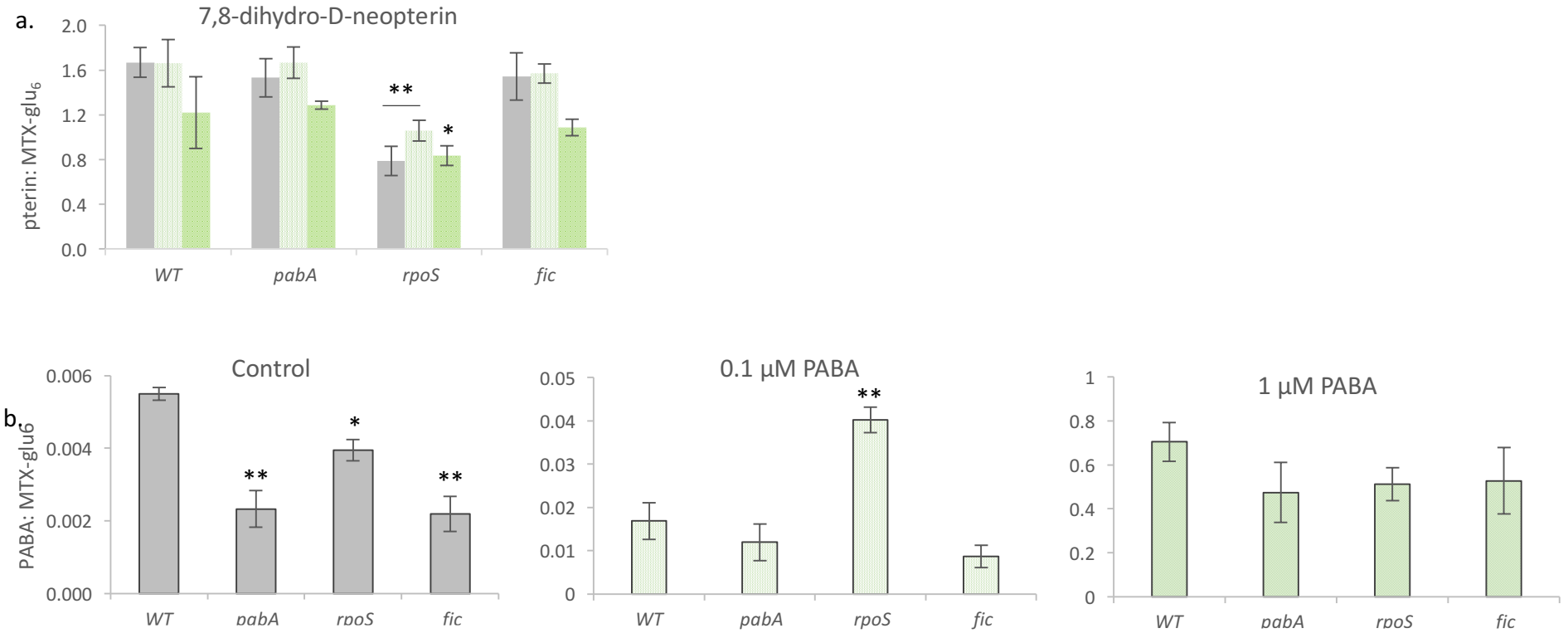

Figure 6.10 LC-MS/MS reveals low levels of a pterin intermediate and accumulation of PABA in the *rpos* mutant. Levels of PABA and 7,8-dihydro-D-neopterin (DHNP) in extracts of WT, *pabA, rpoS* and *fic* mutant *E. coli* were analysed by LC-MS/MS. Extracts were made after 4 days of bacterial growth on DM at 25°C. Samples were normalized for growth before extractions. Levels are displayed as a ratio of an internal MTX-glu_6 spike for normalization between samples. Error bars represent standard deviation. Asterisks denote the significance of Student's *t* test of folate level in denoted condition compared to the WT extract, where * = P<0.05; **= P<0.01.

due to lack of 7,8-dihydropterin to conjugate with PABA to form dihydropteroate. These data reveal that *rpoS* has a complex regulatory role over both the PABA and GTP/ pterin branches of folate synthesis and on enzymes involved in one-carbon metabolism; this will be discussed in more detail in section 6.4. On the other hand, folate levels in *fic* mutants are similar to those detected in *pabA* mutants, suggesting that *fic* is involved only in the PABA branch of folate synthesis.

6.3.3i rpoS expression correlates with pabA expression in exponential phase

The data in Chapter 6 indicates that *pabA* is expressed most highly during exponential phase of bacterial growth (day 2) and that this corresponds to the window of toxicity which is responsible for lifespan decrease. In order to examine the interaction of *rpoS* and *pabA,* here, the same cDNA used to monitor longitudinal *pabA* expression in WT *E. coli* (Chapter 6, figure 6.3) was used to probe for *rpoS* expression.

Expression of *rpoS* was found to mirror *pabA*: expression peaked at 48 hours by 12.5-fold compared to expression in the overnight culture, and decreased after this peak, with a 4-fold increase after 72 and 96 hours. In order to eliminate the speculation that the similar pattern may arise from differential RNA integrity at the different time points, attention should be drawn to figure 7.9, Chapter 7, in which the same cDNA was used to probe *abgT* expression: high *abgT* expression was detected after 6 hours, with maximal expression at 24 hours. This data indicates that *rpoS* and *pabA* are at least co-expressed.

6.3.4 iv pabA expression is downregulated in rpoS and fic mutants

pabA, fic and *rpoS* gene expression was examined in WT *E. coli* and in mutants of *pabA,*

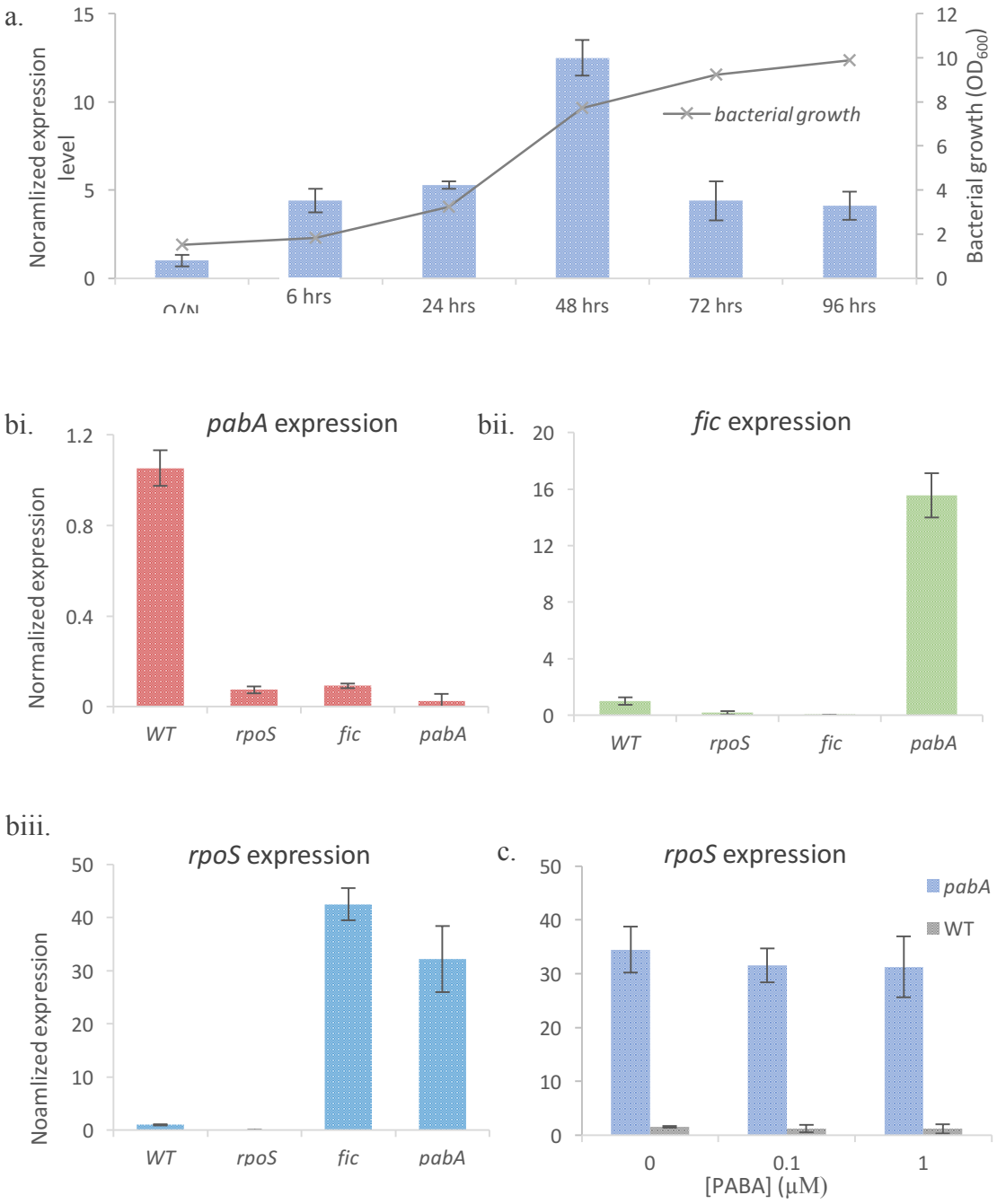

Figure 6.11 Normalized mRNA expression level of *E. coli pabA, rpoS* and *fic* genes as determined by qPCR. Expression in mutants here represents the fold change compared to expression in WT and normalized to the internal reference gene, *rrsA* a) *rpoS* expression in WT *E. coli* mRNA over a 96 hour time course. Expression of bi) *pabA* , bii) *fic* and biii) *rpoS* in *pabA, fic* and *rpoS* mutants c) the impact of PABA on *rpoS* expression in *pabA* mutant mRNA.

rpoS and *fic.* RNA extractions were carried out on non-supplemented DM agar plates after 4 days of bacterial growth at 25 °C. This was followed by DNase treatment and cDNA synthesis (see methods). Gene specific internal primers were designed and used to probe gene expression via quantitative PCR. Normalized expression levels were calculated using the delta delta ct method, using *rrsA* as an internal reference gene and normalizing to expression in WT extracts.

Consistent with the predicted gene interactions, *pabA* expression was downregulated in both *rpoS* and *fic* mutants (figure 6.11ai) and *fic* expression was downregulated in the *rpoS* mutant (figure 6.11aii). Unexpectedly, *fic* expression was 16-fold higher in the *pabA* mutant, indicating that *fic* may be negatively regulated when *pabA* is active. *rpoS* expression was significantly higher in both *pabA* and *fic* mutants (figure 6.11aiii), suggestive of the activation of an RpoS stress response, likely due to low folate levels. In response to PABA supplementation, *rpoS* expression in the *pabA* mutant did not change (figure 6.11b).

6.3.4 vi Lifespan on rpoS is not shortened by PABA supplementation

The data in this section has painted a complex picture of the interaction of *rpoS* with folate synthesis, one-carbon metabolism and folate-dependent toxicity. RpoS seems to have regulatory control over both *fic* and *pabA,* and thus the PABA branch of folate synthesis. Moreover, the data suggests that RpoS also regulates the activity of the pterin branch and the altered folate profile of the *rpoS* mutant in response to PABA suggests RpoS may also regulate folate-dependent enzymes involved in the folate cycle. However, the finding that *rpoS* expression does not respond to PABA was surprising. It is not clear whether these predicted RpoS-gene interactions are direct

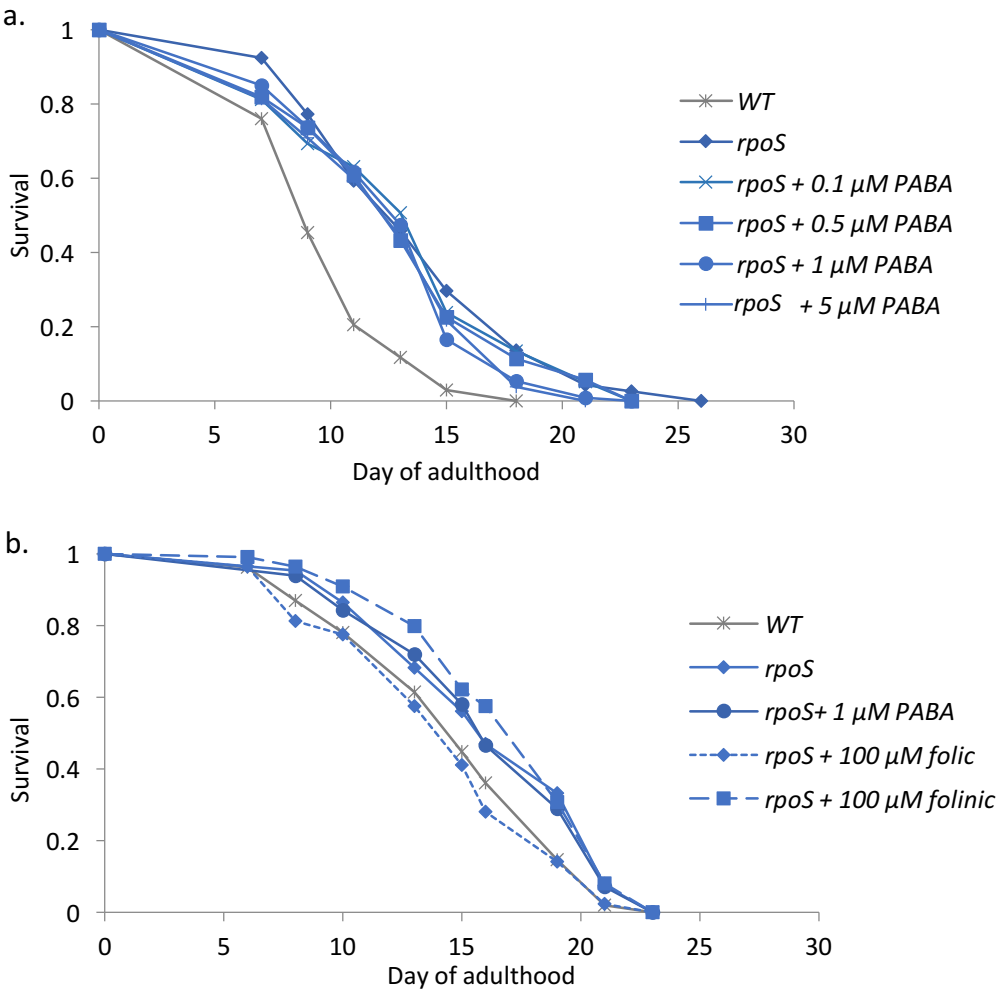

Figure 6.12 *C. elegans* lifespan on *E. coli rpoS* mutant is not affected by PABA supplementation a) *C. elegans* lifespans carried out from day 1 of adulthoof on DM plates seeded with the *rpoS* mutant and supplemented with varying concentrations of PABA b) lifespans carried out on DM plates seeded with the *rpoS* mutant and supplemented with folic and folinic acid, with PABA as a control. See supplementary table 1 for full outline of conditions, statistical analysis and n numbers.

or indirect. In order to clarify whether these interactions are associated with the toxic activity that shortens *C. elegans* lifespan, lifespan assays were carried out on *rpoS* mutants on DM supplemented with PABA, folic acid and folinic acid. Unlike on the *pabA* mutant (Chapter 3, figure 3.7), PABA was not found to have an effect on *C. elegans* lifespan on the *rpoS* mutant at a range of concentrations (figure 6.12a). This experiment was carried out in conjunction with the *pabA* lifespan (Chapter 3, figure 3.7), which acted as a positive control, ruling out the possibility that the PABA stock was degraded/ inactive. In contrast, similarly to the *pabA* mutant, folic acid significantly reduced lifespan on *rpoS* by 12% (P=0.0041), and folinic acid had no effect (figure 6.12b). Together, this suggests that the mechanism by which RpoS modulates lifespan is not dependent on its regulation of *fic* or *pabA,* but on its regulation of one-carbon metabolism. This is consistent with the sustained high expression of *rpoS* in the *pabA* mutant despite PABA supplementation (figure 6.11b)

6.3.4vii gcp-2.1 phenotype on rpoS is not rescued by PABA supplementation

The impact of PABA supplementation on the sensitivity of the *gcp-2.1* mutant strain to *rpoS* was examined. DM agar plates supplemented with varying concentrations of PABA and were seeded with the *rpoS* mutant. WT and *pabA* mutant conditions were included as controls and plates supplemented with varying concentrations of folinic acid were also included as controls, as folinic acid supplementation rescues *gcp-2.1* folate deficiency directly (Chapter 7, figure 7.12).

Consistent with Chapter 3, figure 9, a dose-dependent rescue of *gcp-2.1* body length

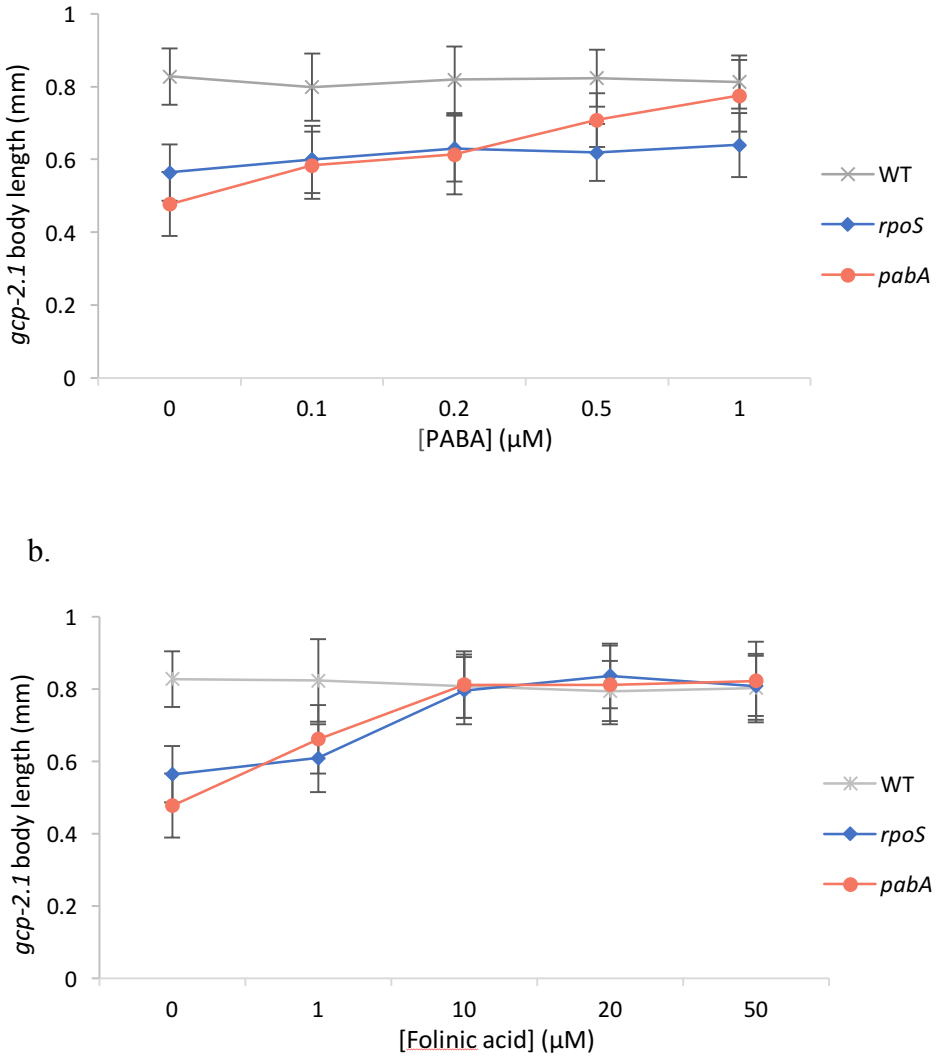

Figure 6.13 *C. elegans gcp-2.1* mutant developmental folate deficiency on the *E. coli rpoS* mutant is not rescued by PABA. *gcp-2.1* mutants were raised from egg on WT, *rpoS* or *pabA* mutant on DM plates supplemented with varying concentrations of a) PABA or b) folinic acid. Plates were incubated at 25 °C and body length measured at L4 stage (n>40). Error bars represent standard deviation.

a. With PABA was observed on the *pabA* mutant, with complete restoration of body length at 1μM PABA (figure 6.13a). On the *rpoS* mutant, *gcp-2.1* body length was significantly increased at 0.2 μM (P=0.0085), 0.5 μM (P=0.031) and 1.0 μM PABA (P<0.001), however, compared to on WT *E. coli,* body length remained significantly lower on all conditions (P<0.001, in all cases). Similar responses to folinic acid in *gcp-2.1* mutants on *pabA* and *rpoS* were observed; wild-type body length was reached at 10 μM folinic acid in both cases (figure 6.13b). The inability of PABA to effect the *gcp-2.1* phenotype and lifespan, despite this strain being able to use PABA for folate synthesis, suggests that the impact of *rpoS* on specific folates or the pterin branch, as observed by LC-MS/MS (figure 6.8-6.10) may be accountable for the two observed phenotypes.

6.4 DISCUSSION

6.4.1 Inhibiting bacterial folate synthesis may remove a toxicity

C. elegans aversion behaviour was here used as a phenotypic readout of bacterial toxicity. On *E. coli* (K12 and OP50) (figure 6.1) and the *Enterobacter cloacae* strain, B29 (figure 6.4a), inhibiting folate synthesis was found to markedly decrease aversive behaviour. The unique B29 phenotype of reduced progeny production was also found to be rescued following the inhibition of folate synthesis (figure 6.4b). This latter observation is in line with the finding that programmed cell-death in the *C. elegans*

germline resulting in reduced progeny production occurs in response to bacterial toxicity (Aballay & Ausubel et al., 2001). Moreover, aversion was also significantly decreased on the *pabA* and *rpoS* mutants, both of which have been shown here to have low folate levels (figure 6.2). Together, the data presented in this chapter supports the hypothesis that inhibiting bacterial folate synthesis removes a broad-scale toxicity, although further work is required to verify this hypothesis.

6.4.2 *rpoS* may regulate *fic*-dependent folate toxicity

In an attempt to understand how folate synthesis may be related to toxicity in *E. coli* K12, research became focused on the *E. coli* stress response sigma factor, *rpoS.* RpoS regulates the expression of genes involved in toxicity and virulence, and its deletion has previously been found to increase *C. elegans* lifespan (Virk et al. 2016). As mentioned, the *rpoS* mutant was found to decrease *C. elegans* aversion (figure 6.2) and its impact on lifespan was verified (figure 6. 5). The *gcp-2.1* bioassay (figure 6.13) and LC-MS/MS detection revealed that the *rpoS* mutant has low folate levels (figure 6.7-6.9) and qPCR analysis of *rpoS* gene expression revealed a temporal pattern consistent with co-expression with *pabA* (figure 6.11a) Indeed, *pabA* expression was significantly lower in the *rpoS* mutant (figure 6.11bi). Together, this demonstrated that the *rpoS* mutant has a role in folate synthesis.

A candidate gene screen was conducted to identify RpoS-downstream genes involved in toxicity that are also folate-dependent (figures 6.5-6.6): out of 31 mutants screened, only 1 candidate gene, *fic,* was identified which both extended lifespan and decreased *E. coli* folate levels, similarly to the *rpoS* mutant (as assayed by the *gcp-2.1* mutant).

LC-MS/MS detection of *E. coli* folates combined with qPCR analysis of gene expression confirmed a novel role of both *rpoS* and *fic* as positive regulators of *pabA* and thus folate synthesis (figure 6.11). These interactions should be tested using DNAse footprinting or chromatin immunoprecipitation with microarray hybridization (ChIP-chip). The *fic* gene is interesting for two reasons: its coding region ends 31 nucleotides upstream of *pabA* and the protein it encodes has recently been identified in pathogenic bacteria as a toxin. The potential role of *fic* in folate-dependent toxicity will be discussed in more detail in Chapter 8.

6.4.3 *rpoS* is a novel regulator of folate synthesis and one-carbon metabolism

The regulatory role of *rpoS* was found to extend beyond folate synthesis as the folate profile in *rpoS* mutant *E. coli* was not restored to wild-type with the addition of PABA, as was observed in *fic* and *pabA* mutants (figure 6.8-6.9). Moreover, high *rpoS* expression in the *pabA* mutant could not be decreased with PABA (figure 6.11) and PABA could not reverse lifespan on *rpoS* (figure 6.12) or relieve *gcp-2.1* folate deficiency (figure 6.13). Together, this indicates that *rpoS* has a role in *E. coli* folate which is independent of its interaction with *pabA.*

In response to PABA in *rpoS* mutants, 5,10-methyelene THF and DHF remained low, whereas 5/10-formyl THF and 5-methylTHF were higher than detected in WT extracts (figure 6.8-6.9). Furthermore, *rpoS* mutants had low levels of the pterin pathway intermediate, 7,8-dihydro-D-neopterin, and abnormal accumulation of PABA in response to PABA supplementation. Together, these data suggest *rpoS* has positive regulatory control over the pterin branch of folate synthesis *and* over

interconversions between THFs in the folate cycle.

A recent metabolic modelling study has highlighted a link between 5,10-methylene THF and the pterin branch of folate synthesis, based on the initial observation of strong chromosomal clustering of *folK* with *panB* in several bacterial genomes

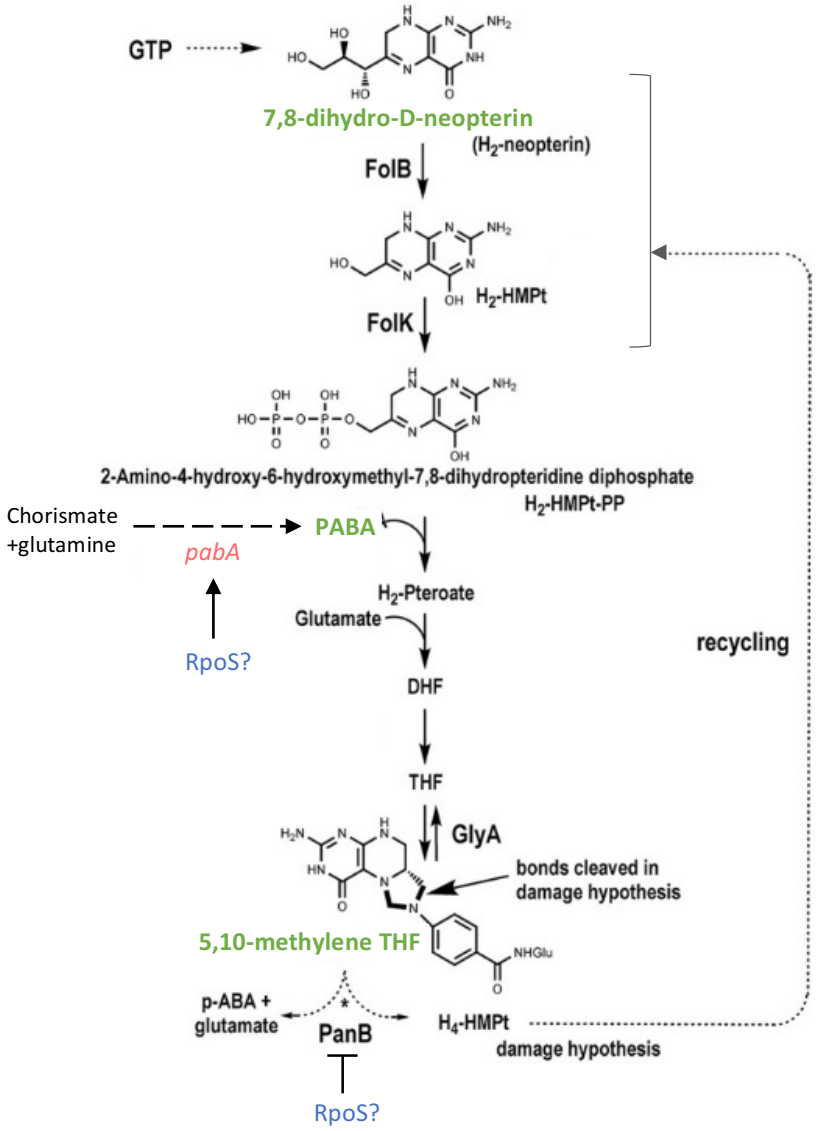

Figure 6.14 Pterin pathway of THF synthesis, the 5,10-methylene THF damage hypothesis and the regulatory roles of RpoS. 5,10-methylene is damaged by a side-reaction catalyzed by PanB. The pterin moeity is recycled in a mechanism dependent on FolK. RpoS may negatively regulate PanB, and therefore act to maintain 5,10-methylene THF levels. This work indicates that RpoS also regulates *pabA.* It is not clear if these interactions are direct or indirect. Adapted from Thiaville et al. 2016.

(Thiaville et al., 2016). The authors revealed that in *E. coli* K12, the pantothenate (vitamin B5) biosynthesis enzyme, PanB, damages 5,10-methylene THF in a side reaction and cells recycle the pterin moeity by an activity dependent on the pterin branch enzyme, FolK (figure 6.14) (Thiaville et al. 2016). FolK works downstream of DHNP. From the data presented here, it is postulated that RpoS may negatively regulate *panB*, thus offering a potential explanation as to why specifically 5,10-methylene THF and 7,8-dihydro-D-neopterin (upstream of FolK) are low in *rpoS* mutants in response to PABA. Indeed, in the same *E. coli* K12 microarray dataset that indicated decreased *pabA* expression in an *rpoS* mutant, *panB* showed increased expression (Ito et al. 2008). Gene expression analysis in *rpoS* mutants with primers specific to genes involved in these pathways will help to clarify these interactions.

6.4.4 Levels of *E. coli* 5,10-methylene THF correlate to *C. elegans* lifespan

Interestingly, neither *C. elegans* lifespan nor *gcp-2.1* developmental folate deficiency on the *rpoS* mutant was signifiacntly altered by PABA supplementation, yet these phenotypes responded similarly to folic and folinic acid as in the *pabA* mutant. This acted to rule out the possibility of excess PABA as a mediator of folate-dependent toxicity and combined with the LC-MS/MS data, also provided insights into possible mechanisms of lifespan extension. In *rpoS* mutants, even with 1 μM PABA (where *C. elegans* are still long-lived) 5,10-methylene THF remained below levels detected in WT *E. coli* and similar to levels detected in *pabA* mutants with 0.1 μM PABA (where *C. elegans* are long-lived). In *pabA* mutants supplemented with 1 μM PABA (where *C. elegans* are short-lived), levels of 5,10-methylene THF were in line with WT

supplemented with 0.1 μM PABA. Thus, low levels of 5,10-methylene may be responsible for lifespan increase on these mutants. This counters the previous work in the Weinkove lab which had suggested that individual folates were not determinants of longevity and therefore prompts a re-evaluation of this hypothesis.

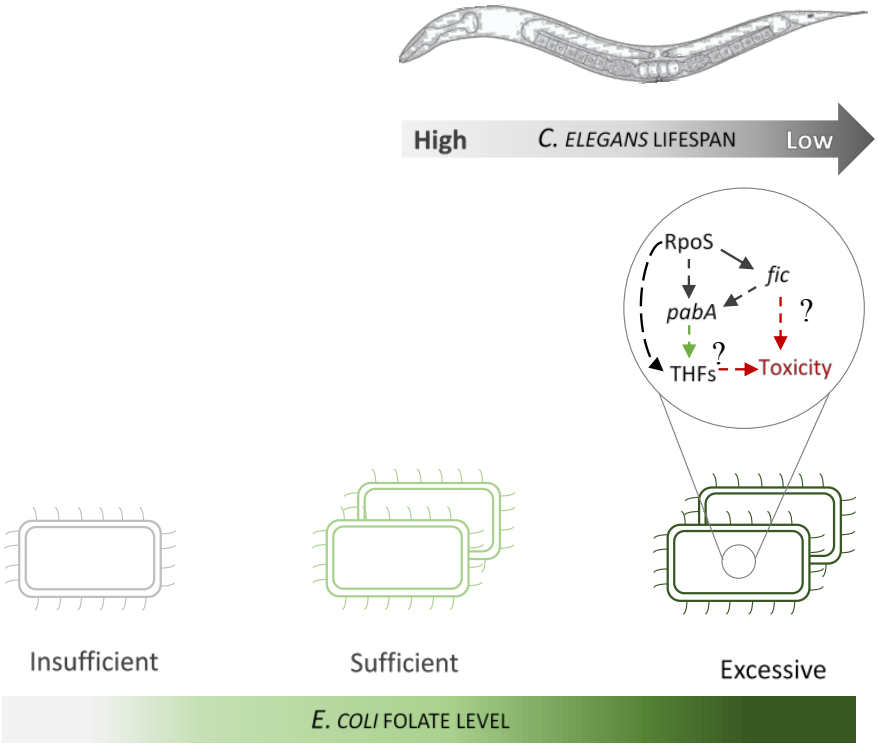

Figure 6.15 Diagram illustrating the model of excessive *E. coli* folate synthesis, RpoS-dependent bacterial toxicity and *C. elegans* lifespan. Bacterial folate levels above the 'sufficient' threshold for bacterial growth are associated with a toxicity which shortens *C. elegans* lifespan. Gene expression analysis has here shown that *pabA* is downstream of both *rpoS* and *fic* and that *fic* is downstream of *rpoS.* Possible mechanisms via which this pathway may lead to toxicity are outline in Chapter 8. Black arrors represent gene regulation (dotted= indirect); green arrow represents folate synthesis pathway; Red dotted arrows represent possible mechanisms of toxicity; THFs represents tetrahydrofolates.

CHAPTER 7. INVESTIGATING THE IMPACT OF FOLIC ACID ON *E. COLI* FOLATE SYNTHESIS AND *C. ELEGANS* LIFESPAN

7.1 INTRODUCTION

Previous work in the Weinkove lab found that 500 μM folic acid reversed lifespan on the *aroD* mutant, but further work was not carried out to determine whether this was acting via *E. coli* or having a direct effect on *C. elegans.* This chapter investigates whether folic acid impacts *E. coli* folate synthesis and thus if it increases bacterial folate levels above the threshold for *C. elegans* lifespan modulation. As folic acid cannot be transported directly by *E. coli,* a route dependent on salvage of the folate degradation product, PABA-glu, by the *E. coli* transporter, AbgT, will be investigated. Several folic acid sources, including a commercial over-the-counter supplement, will be examined for their quality, degradation and impact on *C. elegans* lifespan. This work was prompted by the growing concerns over the safety of folic acid as a supplement and the lack of research over its interaction with the microbiota.

7.2 CHAPTER AIMS

- Aim 1: Investigate whether folic acid impacts *E. coli* folate synthesis and thus *C. elegans* lifespan
    - create constructs to examine the role of *abgT*
    - examine the degradation of folic acid in our model system
- Aim 2: Examine whether folinic acid is an appropriate alternative supplement

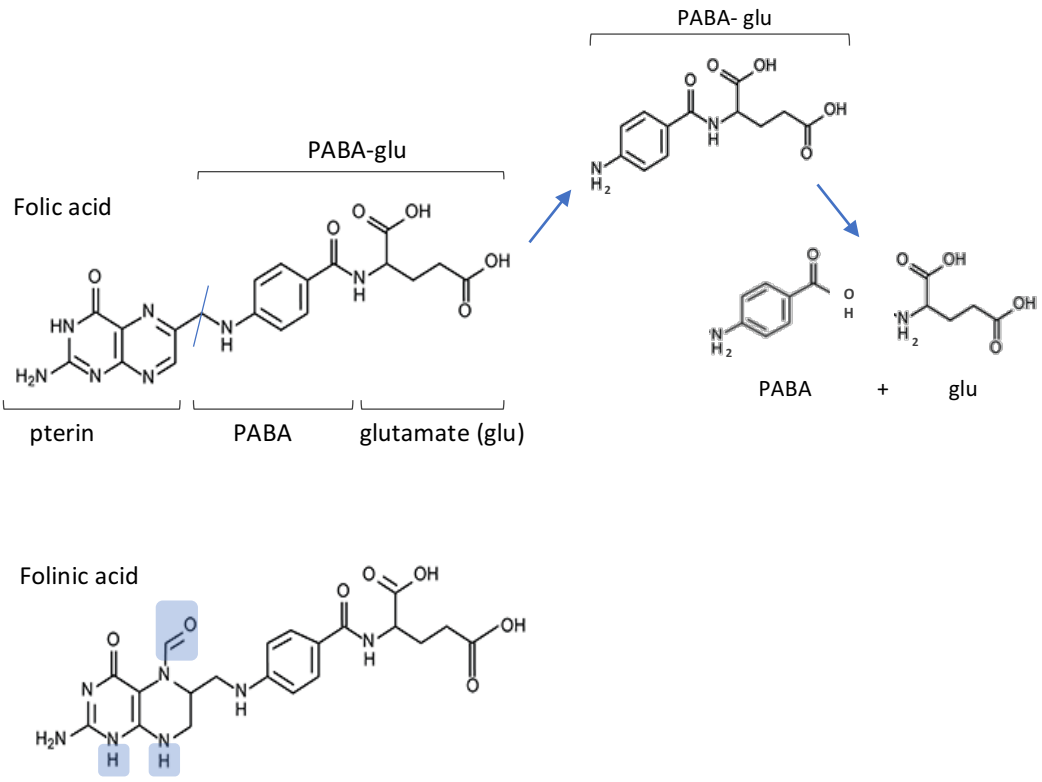

Figure 7.1 Chemical structures of folic and folinic acid. Folic acid is oxidized on its pterin ring. It is a synthetic folate not found in nature. It requires two reduction reactions, catalysed by dihydrofolate reductase, to be converted first to dihydrofolate and then tetrahydrofolate before it can be incorporated into the folate cycle. The methylene bridge of folic acid is unstable and can spontaneously disassociate to generate PABA-glu and PABA. Folinic acid is otherwise known as 5-formyl tetrahydrofolate, so called as it carries a formyl group on its pterin N5 atom. Folinic acid is the most stable of naturally occurring folates.

7.3 RESULTS

7.3.1 Examining the role of *E. coli abgT* on *E. coli* folate synthesis and *C. elegans* lifespan following folic acid supplementation

As folic acid cannot be taken up directly by *E. coli,* PABA-glu and PABA are the only means by which folic acid can impact *E. coli* metabolism. As discussed in Chapter 1, PABA can freely diffuse into cells, but PABA-glu requires the transporter, AbgT (Carter et al., 2007) (see Chapter 1, figure 1.3). Constructs were created to examine the effect of PABA-glu on *E. coli* folate synthesis. An *abgT pabA* double mutant was made by P1 transduction and a high copy number plasmid (pJ128) over-expressing *abgT* was transformed into WT, *pabA* and *abgT pabA* mutants. Strains with the pJ128 plasmid shall be denoted (*abgT* OE). The appropriate control strains were transformed with an empty vector (pUC19), but this has not been denoted in the text. See Chapter 2 for full outline of microbiological procedures.

7.3.1i 100 µM folic acid reverses C. elegans lifespan on pabA at 100 µM

Preliminary work was carried out to determine concentrations of folic acid that impact *C. elegans* lifespan on DM. Lower concentrations of folic acid (1 µM, 5 µM) did not have any impact on lifespan on the *pabA* mutant (data not shown; see lifespan supplementary data), whereas 10 µM had a partial effect and 100 µM folic acid fully reversed lifespan on *pabA* by 16.58% lifespan ($P<0.0001$) (figure 4.2). Lifespan was not significantly affected by folic acid on WT *E. coli*. 10 µM and 100 µM folic acid were used for further experiments. All lifespan conditions here (including control) contain 0.1 µM PABA to ensure sufficient bacterial growth, unless otherwise stated.

7.3.1i Folic acid shortens C. elegans lifespan in an abgT-dependent mechanism

In order to examine the role of the *abgT* gene in *C. elegans* lifespan following folic acid supplementation, lifespans were carried out on DM seeded with WT, *pabA, abgTpabA* and *pabA* (*abgT* OE) (figure 7.3), supplemented with 10 and 100μM folic acid. Mean lifespans are displayed here, but P values refer to Log-rank statistical analysis of the Kaplan Meier survival curves. As before (figure 7.1), folic acid was not found to have any impact on *C. elegans* longevity on WT *E. coli* at either concentration. In contrast, lifespan on the *pabA* mutant in response to folic acid was dependent on *abgT* expression: 10 μM folic acid did not significantly impact lifespan on *pabA* (Log-rank, P=0.7322) or *abgTpabA* (P=0.4026), but did significantly shorten lifespan on the *pabA* (*abgT* OE) strain by 14.00% (P=0.0053); 100 μM folic acid significantly shortened lifespan on both *pabA* and *pabA* (*abgT* OE) strains compared to their non-supplemented controls, by 13.57% (P<0.0001), and 14.36%, respectively (P<0.0003), but did not affect lifespan on *abgTpabA* (P=0.719). *abgT* mutant had no impact on longevity (see supplementary table 1).

This indicates that the over-expression of *abgT* sensitizes *C. elegans* lifespan on the *pabA* mutant to 10 μM folic acid, and knockout of *abgT* eliminates the effect of folic acid on lifespan. It is concluded that *abgT* expression mediates the negative impact of folic acid on *C. elegans* lifespan. This infers that PABA-glu is available following folic acid supplementation and that AbgT uptake of PABA-glu boosts *E. coli* folate synthesis and thus shortens lifespan.

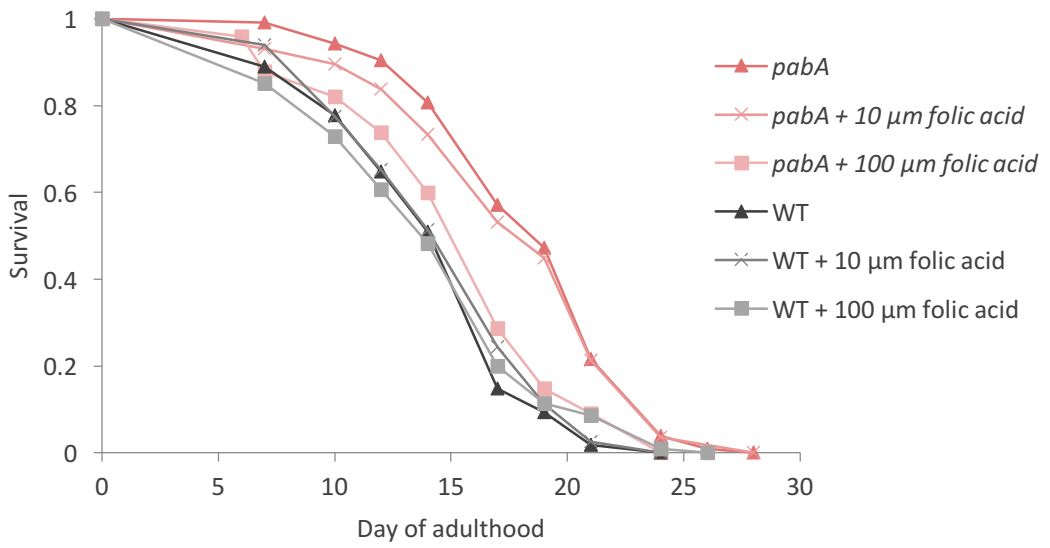

Figure 7.2 Lifespan analysis reveals 100 µM folic acid reverses *C. elegans* longevity on *pabA* mutant. Kaplan-Meier survival curves of *C. elegans* transferred onto WT or *pabA* mutant *E. coli* ± 10, 100 µM folic acid at day 1 of adulthood. See supplementary table 1 for full statistical analysis, n numbers and experimental conditions.

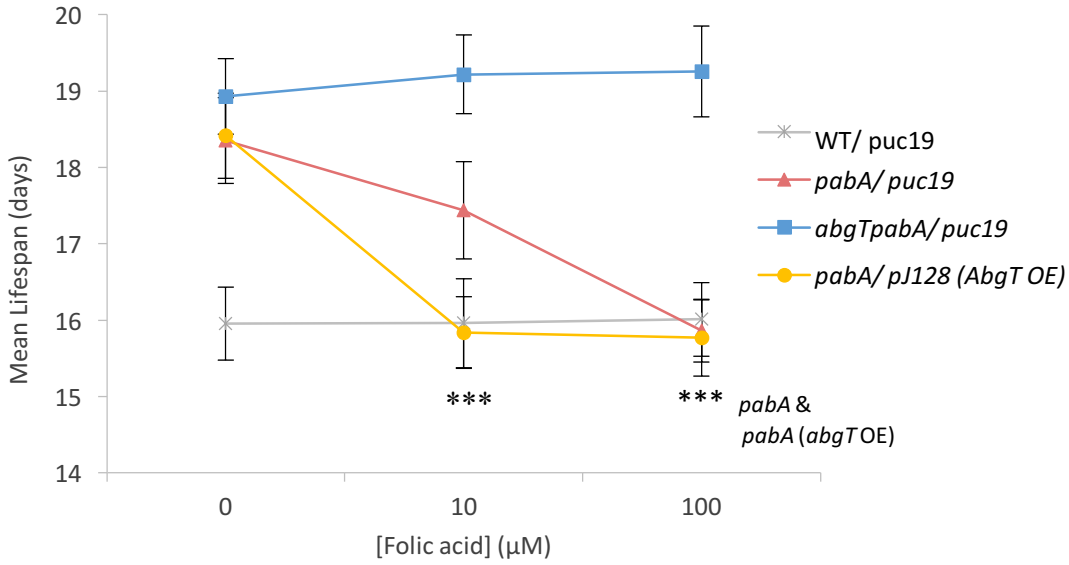

Figure 7.3 Lifespan analysis reveals *E. coli abgT* determines lifespan in response to folic acid. Mean lifespans of *C. elegans* transferred onto WT, *pabA, abgTpabA, pabA* (*abgT* OE) mutant *E. coli* ± 10, 100 µM folic acid at day 1 of adulthood. Error bars represent standard error. Asterisks denote the result of Log-rank statistical tests, where ***P<0.005

7.3.1ii pabA mutant growth is dependent on abgT following PABA-glu supplementation

In order to test these hypotheses, the following will be carried out: 1. LC-MS/MS detection of PABA-glu in folic acid; 2. Lifespan analysis with PABA-glu; 3. LC/MS-MS detection of *E. coli* folate levels following folic acid supplementation. It was necessary to initially determine concentrations of PABA-glu equivalent to 10 μM and 100 μM folic acid. The growth of the *pabA* strain in the liquid DM 96-well plate assay was used to test a large range of concentrations. Results are plotted on a log-scale in figure 7.4a. PABA-glu rescued *pabA* growth with similar kinetics to folic acid, but at ~10-fold lower concentrations, where growth was similar at 100 μM growth PABA-glu and folic acid. 1 μM and 10 μM PABA-glu were taken as equivalent concentrations as 10 μM and 100 μM folic acid. These concentrations were tested for growth on conditions used for *C. elegans* lifespans. DM agar plates were seeded with WT, *pabA, abgTpabA* and *pabA* (*abgT* OE). 0.1 μM and 1 μM PABA conditions were included as controls. OD_{600} was measured 96 hours after seeding. P values here indicate the result of paired, two-tailed Student's *t*-tests.

At the lower concentrations of both PABA-glu and folic acid (figure 4.4bi, ii), growth was dictated by *abgT* expression: the *pabA* mutant showed growth comparable to WT levels on both conditions; *abgTpabA* growth was significantly lower than WT with 1 μM PABA-glu (P=0.016) and 10 μM folic acid (P=0.005); and *pabA* (*abgT* OE) growth was slightly significantly higher with 1 μM PABA-glu (P=0.047) and 10 μM folic acid (P=0.040) than WT. At the higher concentration, all strains showed similar levels of growth, with the exception of a slightly higher

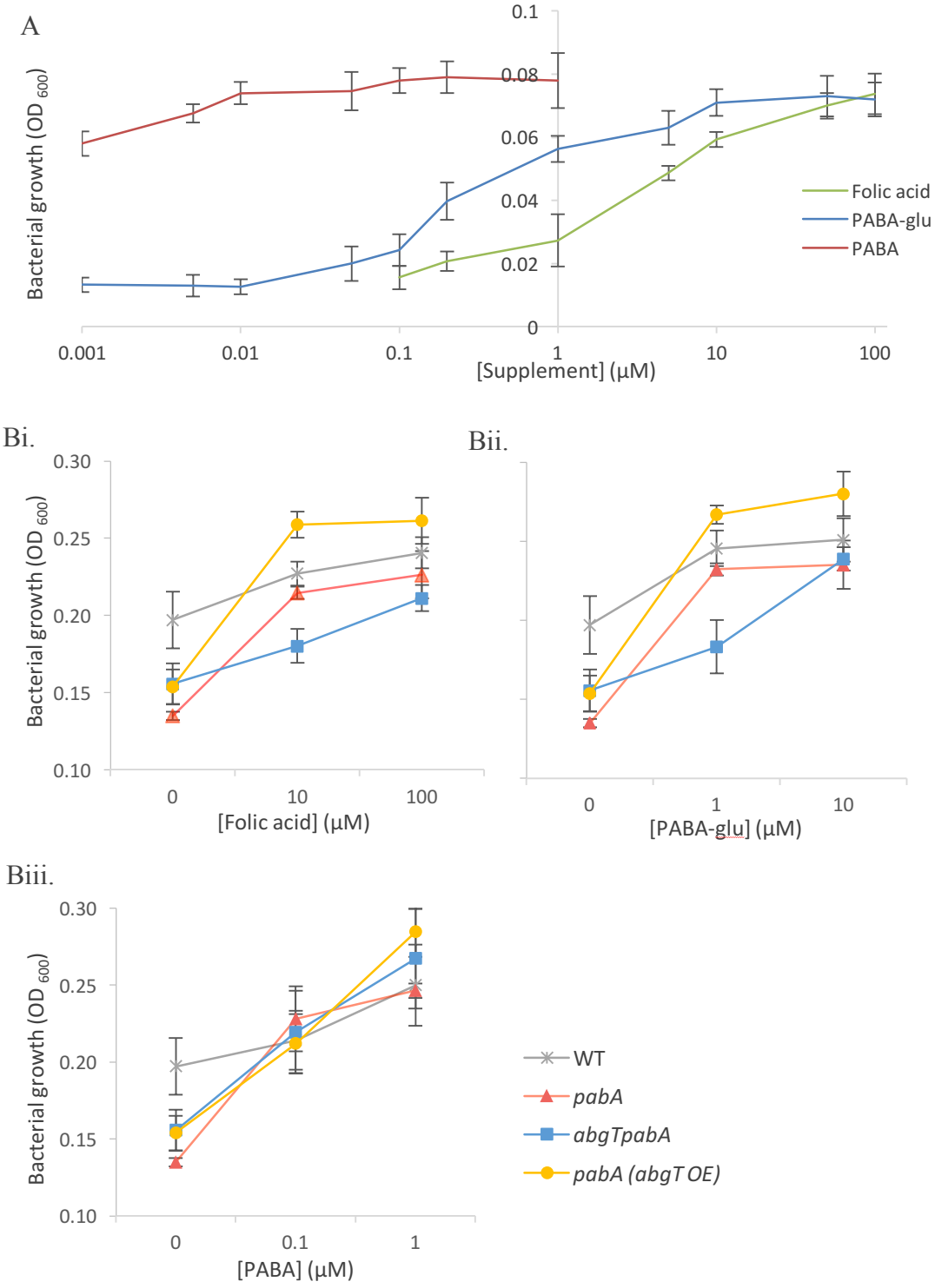

Figure 7.4 Folic acid and PABA-glu rescue of *pabA* growth is dependent on *abgT* a) determining equivalent concentrations of PABA-glu and folic acid required for *pabA* growth in liquid DM in 96-well plate assay at 37 ˚C for 22 hours. Growth of WT, *pabA, abgTpabA, pabA* (*abgT* OE) on DM agar plates supplemented with bi) 10 µM and 100 µM folic acid ii) 1 µM and 10 µM PABA-glu iii) 0.1 µM and 1 µM PABA and incubated at 25 ˚C for 4 days. Error bars represent standard deviation.

OD_{600} of the *pabA* (*abgT* OE) strain on PABA-glu (P=0.049). In contrast, in response to PABA, growth of all strains was comparable (figure 7.3c), consistent with the ability of PABA to freely diffuse across biological membranes, independently of AbgT. These data are consistent with the hypothesis that PABA-glu is transported by AbgT. At high concentrations of folic acid and PABA-glu, it is likely that this pathway is superseded by nanomolar quantities of PABA which are able to freely diffuse into bacterial cells, thus explaining why growth of all strains is similar.

7.3.1 iv LC-MS/MS detects PABA-glu and PABA in folic acid supplements

In order to determine whether folic acid does indeed degrade to PABA-glu in our model system, standard solutions of folic acid, PABA-glu and PABA were analysed by LC-MS/MS and standard curves created to determine concentration. The folic acid used in this study is a high-grade compound obtained from a specialized manufacturer in Switzerland, Schricks laboratories. Here, the purity of this compound was tested in solution and in extractions made from DM agar plates after 4 days incubation at 25˚C (conditions used for *C. elegans- E. coli* assays). Two other folic acid sources were also tested, namely, from Sigma Aldrich and a UK high-street retailer, Boots. Folic acid preparations were solubilised in weak sodium hydroxide, with 5 technical replicates for each solution.

PABA-glu was detected in all three folic acid sources (figure 7.5), where concentration was lowest in the Schircks folic acid solution and highest in the Boots folic acid solution. Percentage degradation of PABA-glu was as follows: 4% in Boots folic acid, 1.2% in Sigma folic acid and 0.3% in Schircks folic acid. PABA was detected at 0.058%, 0.033% and 0.009% in Boots, Sigma and Shircks folic acid,

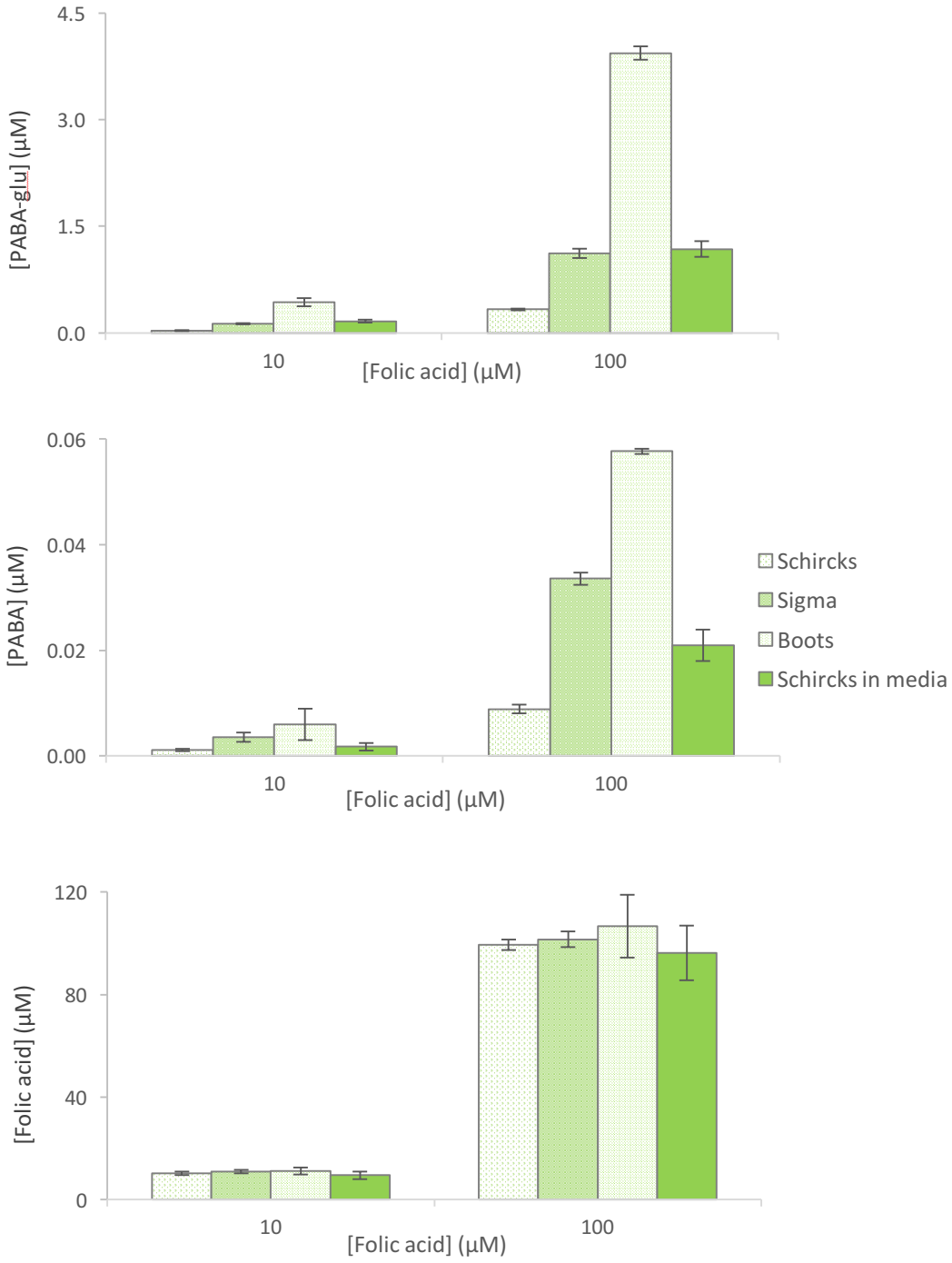

Figure 7.5 LC-MS/MS detects PABA-glu and PABA in three folic acid sources. 10 µM and 100 µM solutions of Schircks, Sigma and Boots folic acid were prepared in weak NaOH, with 3 technical replicates per solution. Solutions was analysed by LC-MS/MS and concentrations of PABA-glu, PABA and folic acid were calculated by analysing known concentrations of these compounds. Schircks folic acid was also supplemented into DM plates and incubated for 4 days at 25˚C before extraction and LC-MS/MS detection. Error bars represent standard deviation.

respectively. Percentages of PABA-glu and PABA in Schircks folic acid from DM indicate that agar plates increased to 1.2% and 0.02%, respectively. This is the first study to PABA-glu is present in folic acid at physiological concentrations relevant to bacterial growth. It is shows that further breakdown occurs during the course of a lifespan experiment.

7.3.1v PABA-glu shortens C. elegans lifespan in an abgT-dependent mechanism

Lifespan analysis were carried out on *pabA, abgTpabA, pabA (abgT* OE) and *abgTpabA (abgT* OE) strains on DM agar plates supplemented with 1 μM and 10 μM PABA-glu, 10 μM and 100 μM folic acid and 1 μM PABA. WT *E. coli* was included only as a non-supplemented control due to confidence from previous experiments that *C. elegans* lifespan on WT *E. coli* would not be affected by further supplementation. Mean lifespans are displayed in figure 7.6 instead of Kaplan-Meier survival curves due to the large number of lifespans conducted here. P values here refer to Log-rank statistical analysis of the Kaplan-Meier survival curves (see full lifespan analysis in supplementary table 1).

Consistent with previous findings, *C. elegans* maintained on any *E. coli pabA* mutant were long-lived compared to *C. elegans* fed wild type *E. coli* in the absence of supplementation ($P<0.001$, in all cases). Similarly to the initial findings (figure 4.3), the response to folic acid was dependent on *abgT* expression: 10 μM folic acid partially reversed *C. elegans* longevity on *pabA* by 9.36 % ($P=0.0052$); no significant reversal was observed on *abgTpabA* ($P=0.1817$); and a complete reversal of lifespan on *pabA* (*abgT* OE) was seen ($P<0.0001$) (figure 7.6a). At 100

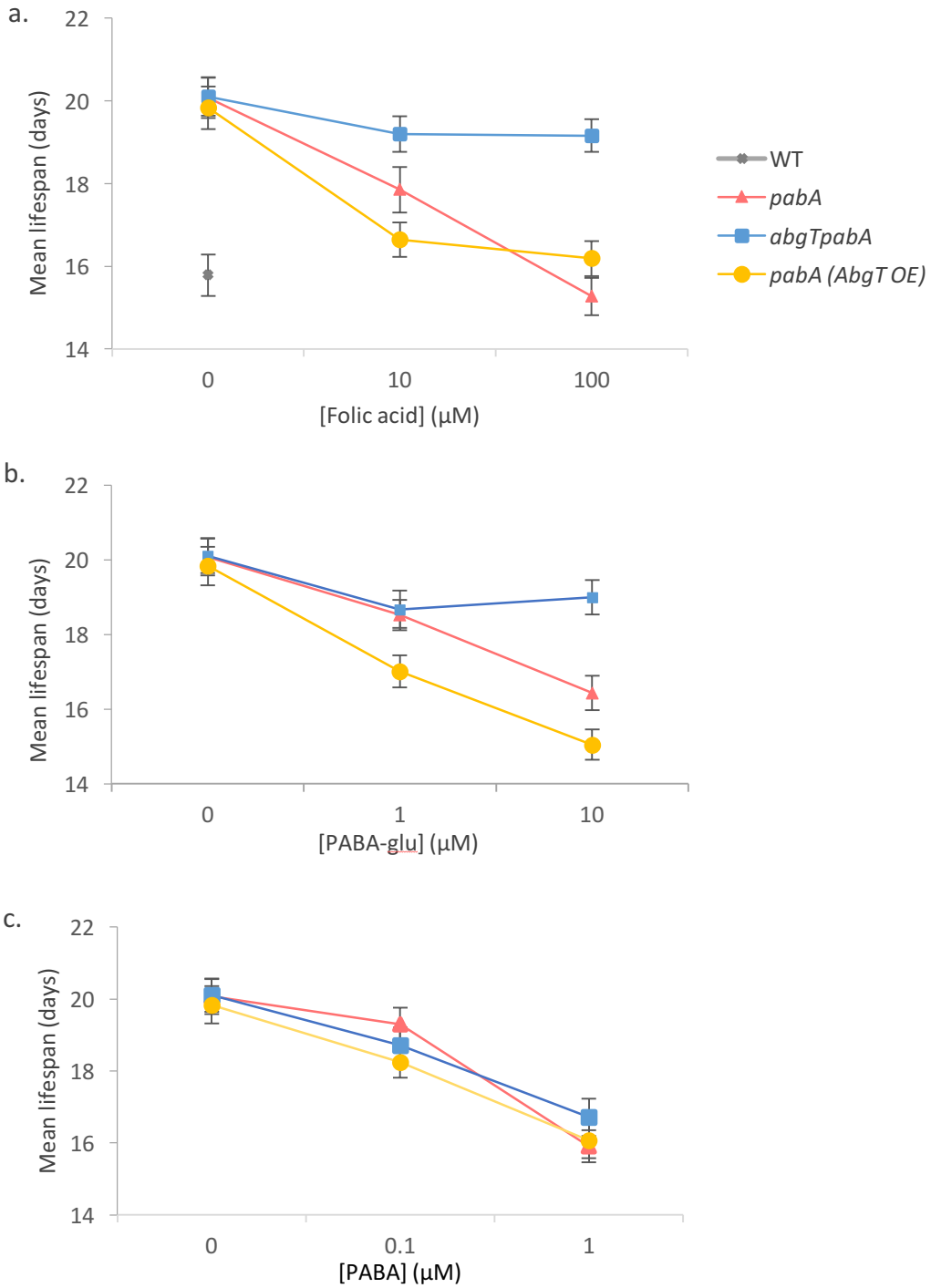

Figure 7.6 Lifespan analysis reveals *E. coli abgT* determines lifespan in response to both folic acid and PABA-glu. Mean lifespans of *C. elegans* transferred at day 1 of adulthood onto WT, *pabA, abgTpabA, pabA* (*abgT* OE) mutant *E. coli* ± a) 10, 100 µM folic acid b) 1, 10 µM PABA-glu and c) 0.1, 1 µM PABA. Error bars represent standard error.

μM folic acid, lifespan was completely reversed on *pabA,* (P<0.0001), but still had no significant impact on *C. elegans* lifespan on *abgT pabA* (P=0.1901). These data consistent with the previous lifespan analysis (figure 7.3) and indicate that *E. coli abgT* deletion is protective against folic acid-induced lifespan reduction.

The response of lifespan to PABA-glu mirrored the response to folic acid (figure 7.6b) where lifespan was dictated by *abgT* expression. In contrast, PABA supplementation reversed *C. elegans* lifespan to WT in all cases and was independent of *abgT* expression (figure 7.6c). Together, these results suggest that AbgT-dependent uptake of PABA-glu by *E. coli* following folic acid supplementation is responsible for the negative impact folic acid has on *C. elegans* lifespan maintained on folate-deficient *E. coli.*

7.3.1 iii LC-MS/MS detects that folic acid increases E. coli folate levels in an abgT-dependent mechanism

In order to test whether *abgT* expression, and thus *C. elegans* survival, correlates to *E. coli* folate status following folic acid supplementation, folate extractions were carried out on WT, *pabA, abgTpabA* and *pabA (abgT* OE) strains which had been incubated on DM agar plates at 25 ˚C for 4 days supplemented with 10 and 100 μM folic acid. Extraction volumes were normalized for growth and extracts subjected to LC-MS/MS. Tri-glutamated folate species were detected and normalized to the signal of an MTX-glu_6 internal standard. Two-tailed paired student's *t*-tests have been carried out to determine significance difference in counts of a single folate species between conditions; asterisks are indicated on the graphs, where P<0.05 compared to counts detected in the WT extract of the same condition (figure 7.7)

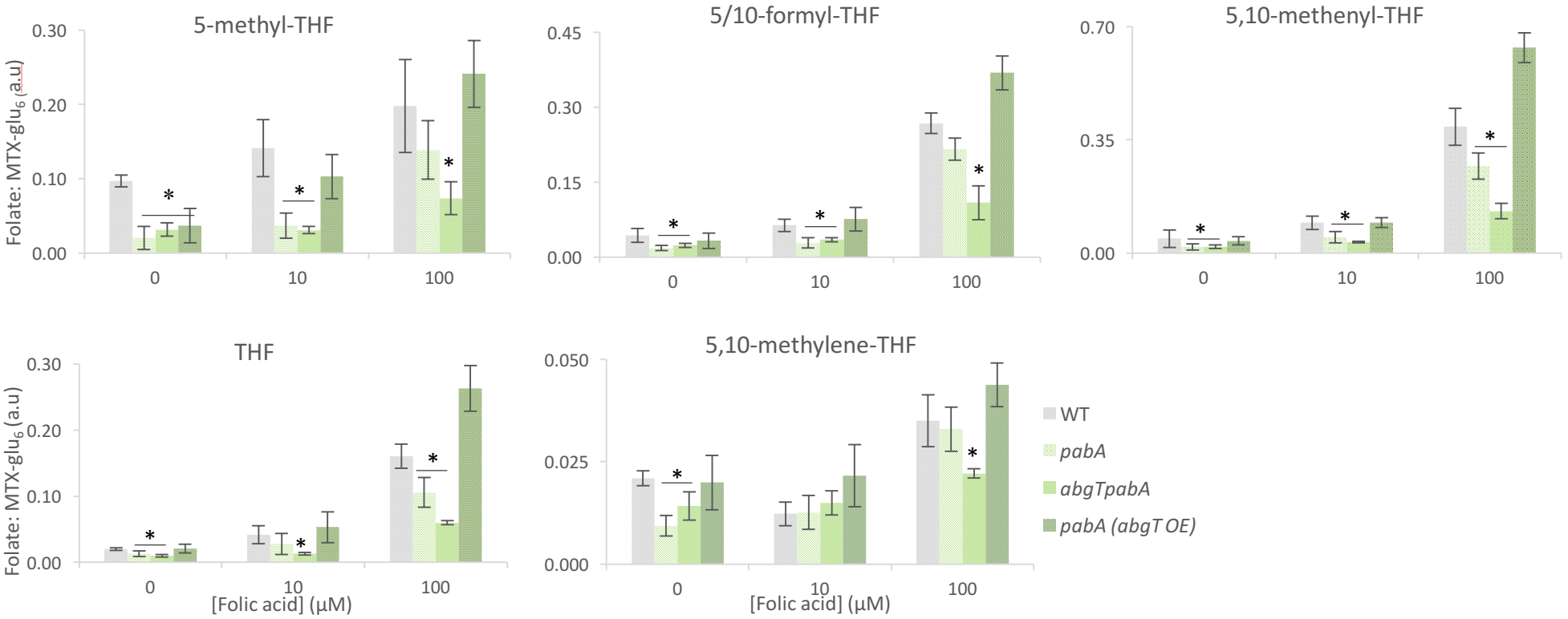

Figure 7.7 LC-MS/MS detects lower levels of THFs in *pabA* mutants, where *abgT* determines response to folic acid. Levels of THFs detected in extracts of *E. coli* WT, *pabA, abgTpabA, pabA* (*abgT* OE) were analysed by LC-MS/MS. Folate levels were displayed as a ratio of an internal MTX-glu$_6$ spike for normalization between samples. Extracts were made after 4 days of bacterial growth at 25°C. Asterisks denote the result of Student's *t*- tests of folate level in *pabA, abgTpabA* or *pabA* (abgT OE) mutant extract on denoted condition compared to in WT extract of the same condition, where, **P<0.01 *<0.05. Error bars represent standard deviation.

In the absence of folic acid, levels of all folate species were significantly lower in *pabA* and *abgTpabA* mutant extracts compared to WT; only 5-methyl THF was lower in *pabA* (*abgT* OE) (figure 4.7). In response to 10 μM folic acid, folate levels in WT and *pabA* (*abgT* OE) increased and were detected at comparable levels (with the exception of 5,10-methylene THF). Folate levels in *pabA* and *abgTpabA* extracts were significantly lower compared to WT in response to 10 μM folic acid, again with the exception of 5,10-methylene THF and THF in *pabA.* In response to 100 μM folic acid, folate levels were increased in *all* extracts compared to non-supplemented controls, however, levels detected with respect to WT were dependent on *abgT* expression: folate species in extracts of *abgTpabA* remained significantly lower; levels in *pabA* extracts were comparable; and levels in *abgTpabA* extracts were higher.

The marked difference in folate levels between these strains (despite comparable growth) correlates to the impact of these conditions on *C. elegans* lifespan. Where folate levels are comparable to WT, such as in the *pabA* mutant at 100 μM and on the *pabA* (*abgT* OE) mutant strain at 10 μM folic acid, lifespan is reversed to WT. The low levels of folates in *abgTpabA* mutant extracts compared to all other strains is consistent with its protective effect on lifespan in response to folic acid.

7.3.2 Examining *abgT* expression

7.3.2 pabA is required for wild-type abgT expression

The data thus far have implicated *abgT* expression as a requirement for folic-acid induced lifespan reduction. Here, the expression pattern of *abgT* is examined using qPCR under the conditions used for *C. elegans* experiments. RNA extractions were

carried out on WT and *pabA E. coli* seeded onto DM plates supplemented with 0.1 µM PABA, after 96 hours (day 4) incubation at 25 ˚C .This was followed by DNase treatment, cDNA synthesis and qPCR. RNA extractions were normalized for bacterial growth based on OD_{600} and cell number. These procedures had not been carried out in the Weinkove laboratory previously and therefore several steps required optimisation. See Chapter 2 for full outline of methods. Two reference genes, *rrsA* and *mdoG* were initially analysed for their suitability for normalization in WT and *pabA* mutant cDNA. These genes were chosen based on peer-reviewed literature (Heng et al., 2011; Rocha et al., 2015). *rrsA* codes for the 16S-RNA ribosomal subunit, and *mdoG* for an enzyme involved in glucan biosynthesis.

Figure 7.8 depicts *abgT* expression normalized to both *rrsA* and *mdoG* reference genes in WT and *pabA E. coli* at the day 4 time point. Expression levels of *abgT* normalized to either reference gene were consistent and indicated a significantly lower expression in *pabA* compared to WT *E. coli.* The *rrsA* gene was selected as a suitable reference gene for further qPCR analysis due to a smaller standard deviation compared to *mdoG* over the four biological replicates (see Chapter 2, figure 2. 4 for analysis of primer efficiency). The low expression of *abgT* in *pabA* is consistent with the lower response of the *pabA* mutant to folic acid compared to the WT, as detected by LC-MS/MS. It is concluded that *abgT* expression in wild-type *E. coli* is dependent on *pabA.*

7.3.2i abgT is highly expressed in lag and early exponential phase growth

RNA was extracted from WT *E. coli* at different stages of bacterial growth on DM

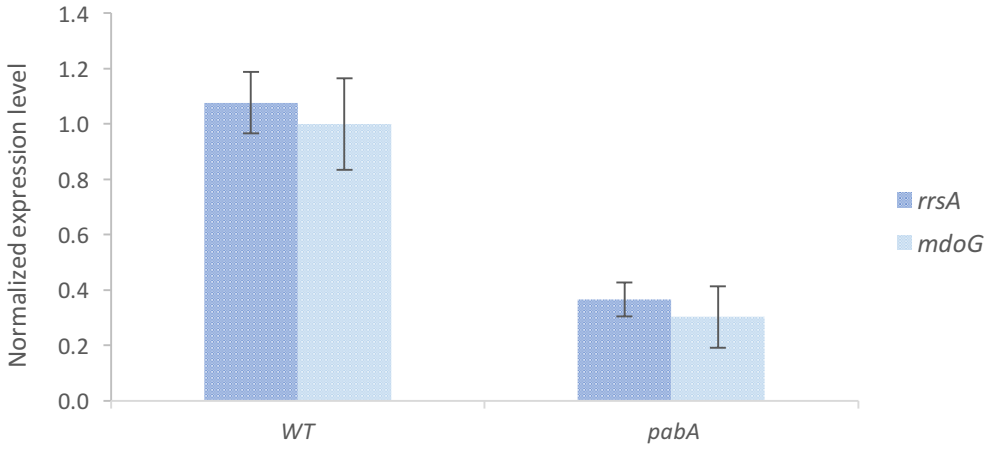

Figure 7.8 Quantitative PCR reveals decreased *abgT* expression in *pabA* mutant. RNA extractions were performed on DM agar plates seeded with WT and *pabA E. coli. abgT* mRNA levels in the *pabA* mutant are normalized to expression in the WT strain and to two reference genes. See Chapter 2, section 2.14 for full outline of procedure. Error bars represent standard deviation.

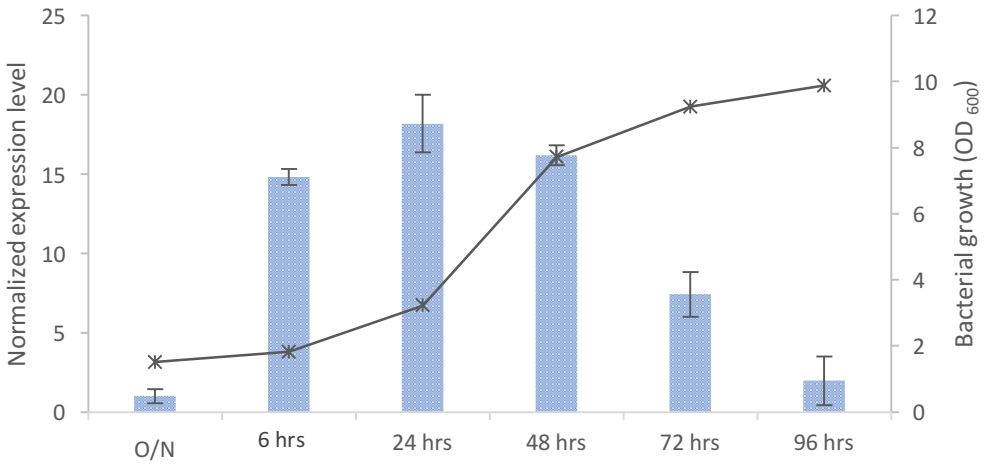

Figure 7.9 Quantitative PCR reveals expression of *abgT* in WT *E. coli* peaks during lag and exponential growth. RNA extractions were performed on DM agar plates seeded with WT *E. coli* over the course of 96 hours**.** *abgT* mRNA levels are normalized to expression in the overnight (O/N) cultures which were pooled before used to seed the plates, and to the *rrsA* reference genes. Error bars represent standard deviation. Bacterial growth is plotted on the secondary y axis.

agar plates (log phase, 24, 48, 72, 96 hours). Extractions of 4 replicate overnight cultures were made before the cultures were pooled and used to seed the plates. *abgT* expression was examined in these extracts by qPCR, where expression was normalized to expression in O/N liquid cultures. The primary y axis in figure 4.9 indicates normalized expression level or 'fold-change' and the secondary y axis plots bacterial growth. *abgT* expression increased by 15-fold in log-phase, increasing to an 18-fold expression change at 24 hours and 16-fold at 48 hours. Normalized expression lowered to a 7-fold increase at 72 hours and a 2-fold increase at 96 hours. This indicated that *abgT* is temporally expressed in accordance with bacterial growth phase, where expression is highest during lag and early exponential growth and lower in stationary phase (O/N culture and 96 hour time-point). Extractions were not carried out longitudinally in the *pabA* mutant, so it is unclear how expression differs here.

7.3.3 Investigating how folinic acid interacts with *C. elegans* and *E. coli*

The previous section demonstrated that folic acid restores bacterial folate synthesis in folate deficient bacteria via AbgT uptake of PABA-glu and that this pathway is responsible for shortening *C. elegans* lifespan. This section examines the impact of the naturally occurring reduced monoglutamated folate, folinic acid, (5-formyl THF), on *C. elegans* lifespan. Like folic acid, folinic acid cannot be taken up by *E. coli* directly.

7.3.3i Folinic acid does not reverse C. elegans lifespan on pabA mutant E. coli

Lifespan assays on DM supplemented with 100 μM folic and folinic acid were carried out on *pabA, abgTpabA* mutant and WT *E. coli*, with non-supplemented

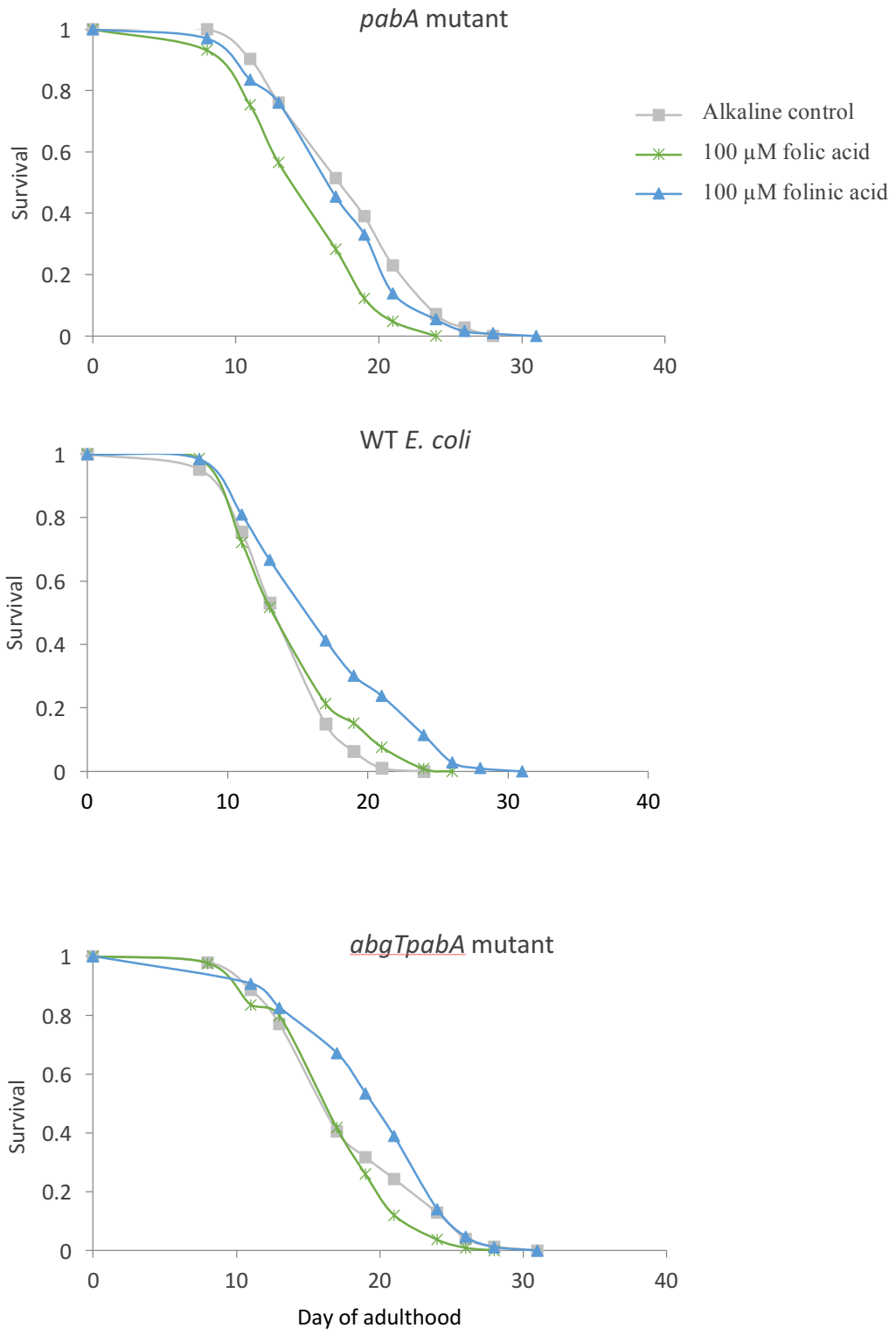

Figure 7.10 Lifespan analysis reveals 100 µM folinic acid extends *C. elegans* lifespan on WT and *abgTpabA* mutant *E. coli.* Kaplan-Meier survival curves of *C. elegans* transferred onto WT, *pabA, abgTpabA* mutant *E. coli* at day 1 of adulthood, on DM plates supplemented with 100 µM folic and folinic acid.

plates included as controls. Consistent with previous findings (figure 7.3, 7.6), 100 μM folic acid shortened lifespan significantly on the *pabA* mutant by 15.37% (P<0.001), but not on *abgTpabA E. coli* (P=0.0719) (figure 7.10). In contrast, folinic acid did not affect lifespan of *C. elegans* on *pabA E. coli* (P=0.2046). Surprisingly, folinic acid was found to increase lifespan on WT *E. coli* by 18.4% (P<0.001), on *abgTpabA E. coli* by 9.61% (P=0.0188), and on *abgT* single mutant by 10.31% (P=0.0040) compared to their respective non-supplemented controls (figure 7.10).

7.3.3 ii Folinic acid is less effective at rescuing pabA mutant growth than folic acid

The data predicts that folinic acid does not interact with *E. coli* in the same way as folic acid. In order to understand this interaction, growth assays of *pabA* and *abgTpabA* mutants in liquid DM supplemented with folic and folinic acid were carried out in 96-well microtiter plates, as previously described. Growth curves are shown in figure 4.11 and are the average of triplicate technical wells. Mean end point growth from these wells is also (figure 7.11).

At 5 μM and 10 μM, folinic acid was found to be less effective at rescuing both *pabA* and *abgTpabA* growth than equivalent concentrations of folic acid, where bacterial genotype did not significantly impact growth in response to folinic acid. Consistent with the previous findings, at 100 μM, growth of both strains was comparable regardless of supplement or bacterial genotype. This assay was repeated several times with varying concentrations of supplements and the same trends were observed (data not shown). This data suggests that folinic acid is less effective at

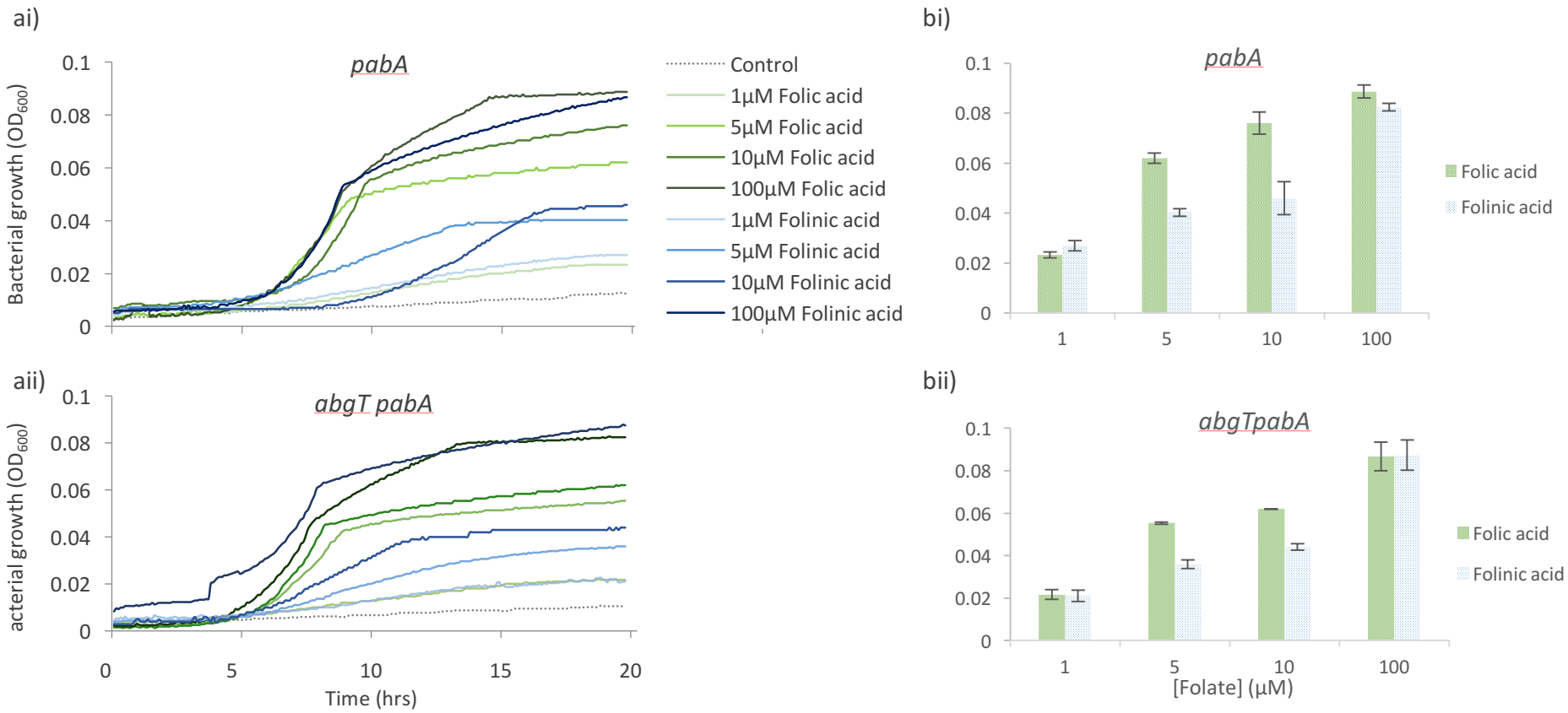

Figure 7.11 Folinic acid is less effective at supplementing *pabA* growth than folic acid. Growth assays of *pabA* and *abgTpabA* mutants were condiucted in liquid 96-well plates. Wells were supplemented with 1, 5, 10, 100 µM folic or folinic acid and growth was measured every 5 minutes for 20 hours in a plate reader (see Chapter 2, section 2.7.2) a) growth curves of i) *pabA* and ii) *abgTpabA* over 20 hours b) end point growth of i) *pabA* and ii) *abgTpabA.* Error bars represent standard deviation.

restoring bacterial growth than folic acid, and unlike with folic acid, this is independent of abgT expression.

7.3.3iii Folinic acid rescue of the gcp-2.1 mutant is not dependent on abgT expression

In order to understand how folinic acid interacts with *E. coli* folate levels, the *gcp-2.1* mutant bioassay was carried out. Synchronous populations of *gcp-2.1* mutant worms were raised from egg on *pabA, abgTpabA* or *pabA* (*abgT* OE) mutant *E. coli* on DM agar plates supplemented with varying concentrations of folic and folinic acid (plotted on a log scale in figure 7.12). Plates were incubated at 25 ˚C and body length at L4 stage was measured as previously described. All plates were supplemented with 0.1 μM PABA.

A stark contrast was observed between the efficacies of folic and folinic acid to rescue *gcp-2.1* body length. 2.5 μM folinic acid completely rescued *gcp-2.1* body length regardless of bacterial genotype, whereas 200 μM folic acid was required for equivalent rescue on all strains. *gcp-2.1* body length was dictated by *abgT* expression in response to folic acid: over-expression of *abgT* increased the responsiveness to folic acid, whereas *abgT* deletion rendered *gcp-2.1* mutants less responsive. This indicates that, unlike folic acid, folinic acid is taken up directly by *C. elegans* and is not dependent on bacterial *abgT* expression. A two-way ANOVA analysis finds significant interaction effect of strain type ($F=102.67$, $p<0.0001$) and folic acid concentration ($F=123.55$, $p<0.0001$) on *C. elegans gcp-2.1* body length.

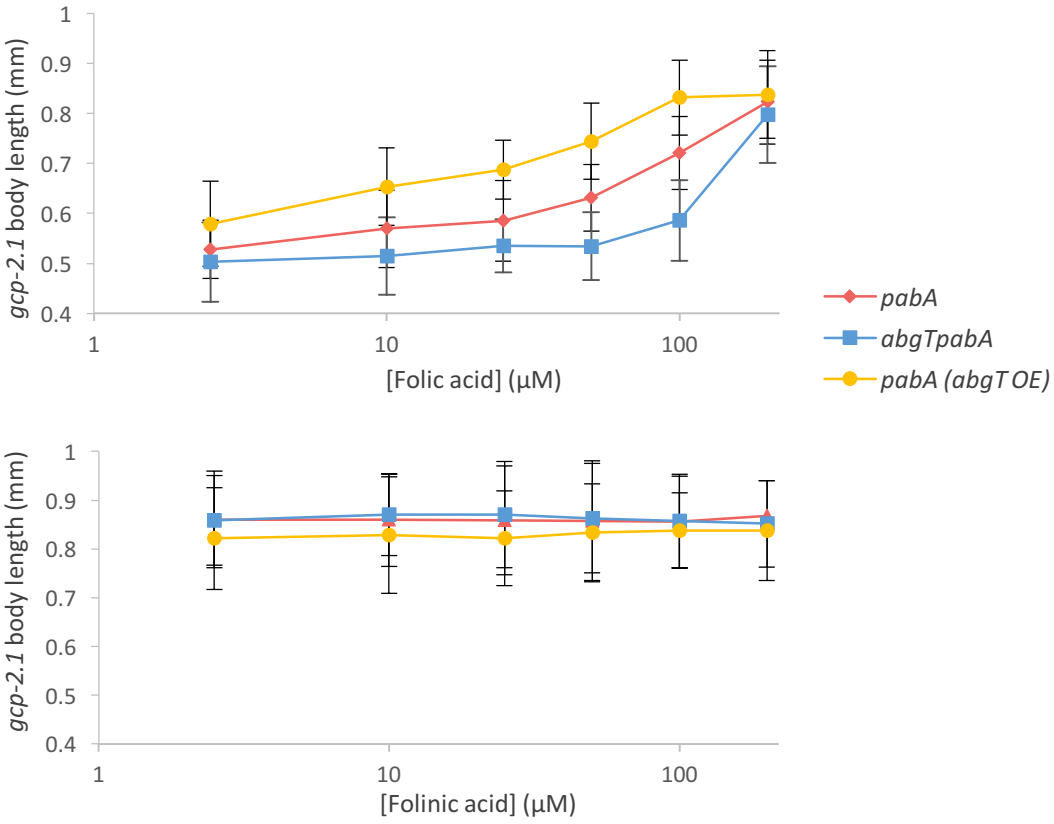

Figure 7.12. Folic acid supplements *C. elegans* via an *E. coli abgT*-dependent route during development. Body length of *gcp-2.1* mutant *C. elegans* at L4 stage raised on DM agar plates seeded with *pabA* mutant, *abgTpabA* double mutant or *pabA* mutant over-expressing *abgT* with increasing concentrations of a) folic acid and b) folinic acid. Two-way ANOVA analyses finds a significant interaction effect of strain type ($F=102.67$, $p<0.0001$) and folic acid concentration ($F=123.55$, $p<0.0001$) on *C. elegans gcp-2.1* body length. Over-expression is conferred by transformation with a high copy number plasmid, pJ128. *pabA* and *abgTpabA* strain are transformed with the empty vector, pUC19. Error bars represent standard deviation of *C. elegans* body length; $n \geq 40$.

7.4 DISCUSSION

7.4.1 Folic acid supplements contain degradation products which boost bacterial folate synthesis and decrease *C. elegans* lifespan

The first section of this chapter addressed the initial aim of determining how folic acid impacts *C. elegans* lifespan. Folic acid was here found to impact *C. elegans* lifespan in a mechanism dependent on *E. coli* AbgT uptake of PABA-glu. Indeed, LC-MS/MS detected PABA-glu in the folic acid used for this study at physiological concentrations. Although this data cannot determine whether PABA-glu is a contaminant or a degradation product, the further degradation of folic acid when supplemented into the media suggests that it may be the latter. Folic acid was found to boost *E. coli* folate synthesis in both WT and *pabA* mutant *E. coli,* where folate levels and lifespan in the latter were dependent on *abgT* expression.

However, as indicated by the *gcp-2.1* mutant bioassay, the ability of folic acid to boost *E. coli* folate synthesis may be beneficial during development. In this genetically susceptible folate-deficient model, the impact of folic acid on bacterial folate synthesis was able to rescue *gcp-2.1* developmental folate deficiency on the *pabA* mutant albeit at high concentrations. Together, this points to a novel role of folic acid supplements as suppliers of precursors (both PABA-glu and PABA) for bacterial folate synthesis and thus modulators of host health during development and adulthood. The translational implications of these data within the context of the debate on the safety of folic acid, and its impact on the microbiota and ageing will be discussed in more detail in Chapter 8.

7.4.2 AbgT as a novel antibacterial target

A Blastn search reveals that *abgT* is also found in the genomes of several pathogenic members of the human gut microbiota, including *Shigella boydii, Kelbsiella phenumonia* and *Enterobacter cloacae*, in addition to *E. coli*. Indeed, *E. coli* AbgT has recently been identified as a member of a conserved superfamily of antimetabolite transporters (Delmar and Yu, 2016). Members of this family are capable of both import and export of folate precursors and antimetabolites, such as sulfonamides. In light of this recent literature and the data presented here, AbgT may represent a novel target for antibiotics. The finding that *abgT* is downregulated in the *pabA* strain is consistent with analysis of RNA sequencing data collected in the Weinkove laboratory, which found that AbgT was downregulated in response to SMX treatment on OP50 *E. coli*. It seems that *abgT* expression is folate-dependent. Further work is required in order to characterize this association.

7.4.3 Folinic acid increase *C. elegans* lifespan and may be a suitable alternative to folic acid as a folate supplement

This chapter also aimed to investigate the impact of the alternative folate supplement, folinic acid, on *C. elegans* lifespan. In contrast to folic acid, folinic acid was here found to increase lifespan. Folinic acid rescued the developmental folate deficiency of the *gcp-2.1* strain at almost 200-fold lower concentration (2.5 μM) than folic acid, in a mechanism independent of *abgT* expression. Together, these data indicate that folinic acid is taken up directly by *C. elegans* and it does not boost *E. coli* folate synthesis above the threshold which negatively effects lifespan. Folinic acid therefore represents a more suitable folate supplement for

maintaining the longevity of *C. elegans* on low folate *E. coli,* than folic acid. This may be useful in a translational capacity, where folate supplementation should accompany an intervention that targets bacterial folate synthesis to extend lifespan, in order to prevent folate deficiency. Indeed, folate deficiency has been reported in certain patients receiving the sulphonamide drug, sulfasalazine, to treat Crohn's disease (Goldberg, 1983; Nemes et al., 2016; Swinson et al., 1981). In these cases, folic acid is administered as treatment. It is noted that the conclusions here are limited by the lack of LC-MS/MS data regarding folinic acid degradation and of the impact of folinic acid on *E. coli* folate levels. Further work should address these limitations. Possible mechanisms underpinning the positive impact of folinic acid on *C. elegans* lifespan will be discussed in Chapter 8.

The uptake of folinic acid by *C. elegans* is consistent with the reported high affinity of the *C. elegans* reduced folate carrier (RFC), FOLT-1, for folinic acid (5-formyl THF); 5-formyl THF was found to impair folic acid uptake (Balamurugan et al., 2007). However, owing to the pH-dependence of RFCs (see Chapter 1), it is unclear whether the pH of the DM (pH 6.0) biases this model system in favour of THF uptake over oxidized folates. Studies suggest that *C. elegans* do however, differentially regulate the pH of their intestinal lumen (Chauhan et al., 2013). A *C. elegans* proton-coupled folate transporter (PCFT) has not been characterized, but a gene encoding for a PCFT-like protein has recently been identified (Ortbauer et al., 2016). Further study would use RNAi to knock-down *folt-1* and *pcft* and monitor folic and folinic acid uptake by *C. elegans* under varying pHs. It is likely that this will also have an effect on the stability of folic and folinic acid, which should be monitored by LC-MS/MS.

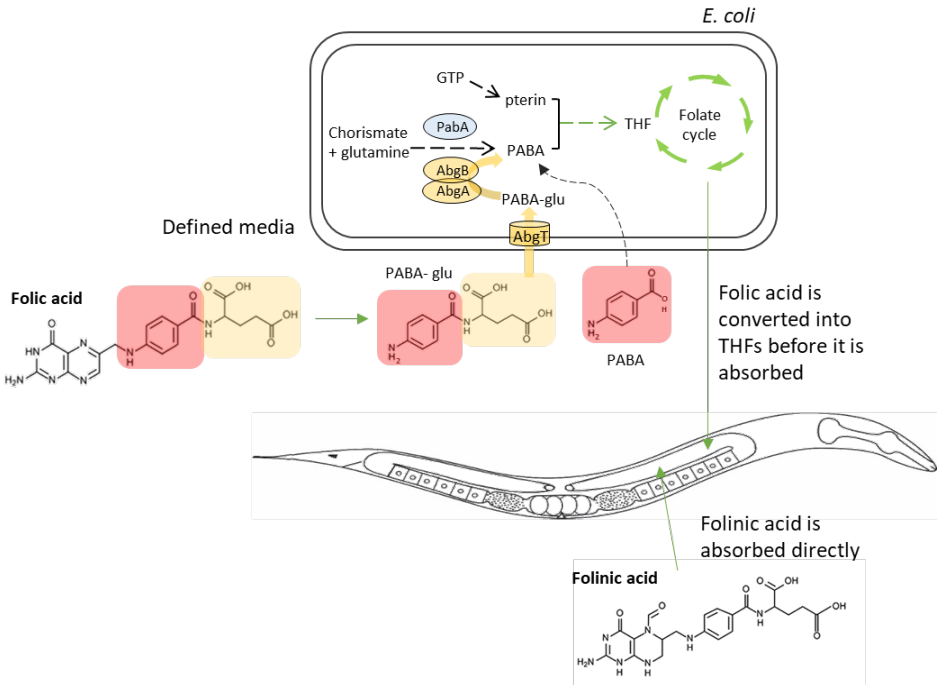

Figure 7.13: Diagrammatic representation of the routes of uptake of folic and folinic acid by *C. elegans*. Folic acid degrades to PABA-glu and PABA. PABA-glu is imported by *E. coli* AbgT and cleaved intracellularly by AbgA/B to generate PABA. PABA can freely diffuse into *E. coli.* This supply of PABA boosts bacterial folate synthesis and generates THFs**.** Following ingestion of *E. coli, C. elegans* is supplied with THFs via this route. Folinic acid is absorbed directly in the intestine following ingestion of *E. coli.*

CHAPTER 8. DISCUSSION

8.1 SUMMARY OF MAIN FINDINGS

The main aim of this thesis was to develop a defined system (where *E. coli* folate levels could be controlled and accurately measured) in order to investigate the factors that influence bacterial folate synthesis and thus *C. elegans* lifespan. Firstly, a folate-free and chemically defined media (DM) was optimised to support both *E. coli* and *C. elegans* similarly to on NGM. Using DM and sensitive LC-MS/MS detection, the bacterial folate threshold that supports bacterial growth was distinguished from the higher bacterial folate threshold that negatively affects lifespan.

This defined system was then used to investigate the impact of several extrinsic and intrinsic genetic factors on these parameters; folic acid and glucose and the genes, *rpoS* and *fic,* were identified as novel mediators of bacterial folate synthesis and modulators of *C. elegans* lifespan. Investigation into the timing of bacterial folate synthesis revealed a novel association with exponential growth phase. Based on the characterisation of *C. elegans* phenotypes on a pathogenic bacterial strain, it was hypothesized that bacterial folate synthesis is linked to a mild toxicity which is responsible for *C. elegans* ageing. The implications of these and other emerging findings from this work will be discussed below.

8.2 IMPLICATIONS OF THIS WORK

8.2.1 Excessive bacterial folate synthesis

Using LC-MS/MS, it has been clearly demonstrated here that *E. coli* synthesizes folate above the threshold required to support bacterial growth. This excessive synthesis was found to be temporally regulated in exponential growth phase and was amplified by glucose. Increased bacterial folate production in glucose supplemented media has only been mentioned anecdotally (Sybesma et al., 2003). In mammalian cells, however, a pathway known as serine-driven one-carbon metabolism is upregulated in cancer cell lines (Labuschagne et al., 2014) and in response to glucose (Tedeschi et al., 2013). This pathway catabolizes serine to glycine using THF as a one-carbon acceptor to form 5,10-methylene THF, in a reaction catabolized by serine hydroxymethyltransferase (SHMT) (Lunt and Vander Heiden, 2011) (figure 8.2). Interestingly, studies have suggested that the provision of THFs as cofactors to support biosynthesis in these rapidly dividing cells is secondary to the production of ATP and NADPH via this pathway (Fan et al., 2014; Meiser et al., 2016; Tedeschi et al., 2013). Indeed, Meiser and colleagues demonstrated that a significant proportion of the one-carbon units derived from this pathway are excreted (as formate).

This pathway has not been elucidated in prokaryotic cells, however, it may underpin why *E. coli* here synthesizes excess folate during exponential growth phase. Further work would investigate this hypothesis by monitoring whether the expression of genes involved in this pathway are upregulated in exponential phase and in response to glucose. Meiser and colleagues observed an inverse

relationship between serine concentration in the media and the amount of formate excreted by dividing cells, both *in vitro* and *in vivo* (Meiser et al., 2016). In our model system, the serine concentration in DM can easily be altered and the impact on *E. coli* gene expression, folate and formate levels and *C. elegans* lifespan could be monitored; serine concentration would be expected to inversely correlate to longevity and positively correlate to bacterial folate levels.

Intriguingly, the mitochondria complex-1 inhibitor, metformin, was found to moderate serine-driven one-carbon metabolism in mammalian cells, likely due to the mitochondrial localization of the enzymes involved in this pathway (Meiser et al., 2016). This is of note as metformin has also been shown to increase *C. elegans* lifespan in an unclarified, but *E. coli* folate-dependent mechanism (Cabreiro et al., 2013). This adds weight to the hypothesis that serine-driven one-carbon metabolism during bacterial exponential growth phase may be modulating *C. elegans* lifespan, and therefore warrants further study.

The obvious dichotomy here is that serine-driven one-carbon metabolism does not rely on folate *synthesis*, but the increase in *E. coli* folate levels in response to glucose was found here to be dependent on *pabA* expression (Chapter 6). It is likely, however, that inhibiting bacterial folate synthesis limits serine-driven one-carbon metabolism, as the latter does require a source of THF as a one-carbon acceptor for serine catabolism. This pathway therefore offers a model which may account for excessive folate production in exponential phase growth.

8.2.2 Folate-dependent bacterial toxicity

The data presented in Chapter 7 was supportive, but not conclusive, of the hypothesis that bacterial folate synthesis is associated with a toxicity. Further work would harness the genetic tractability of the worm to test this hypothesis. The expression of *C. elegans* genes involved in detoxification pathways, such as *skn-1,* should be examined using qPCR or reporter constructs under the *E. coli* conditions found here to decrease bacterial folate levels. It is hypothesized that *C. elegans* mutants involved in detoxification pathways would be hyper-sensitive under conditions which increase bacterial folate levels, such as PABA, folic acid or glucose supplementation. Further work would also examine the source of this bacterial toxicity; two avenues for further work are outlined below.

8.2.2i fic-folate-dependent toxicity

Following the isolation of the *rpoS* gene as a modulator of *C. elegans* lifespan (Virk et al. 2016), it was investigated here as a possible mediator of folate-dependent toxicity due to its role in virulence in pathogenic bacteria and the identification of *pabA* and *pabB* as downstream targets (Ito et al., 2008; Weber et al., 2005). A candidate mutant gene screen of the RpoS regulon revealed that the *fic* mutant both increased *C. elegans* lifespan and decreased *E. coli* folate levels.

fic was included as a candidate gene in the screen for two reasons: it lies directly upstream of *pabA* and it has recently been implicated in toxicity pathogenic bacteria. Fic proteins are a conserved family of eukaryotic and prokaryotic toxins (Harms et al., 2016), where Fic acts as the toxin subunit of a toxin-antitoxin system (Engel et al., 2012; Kinch et al., 2009). Fic proteins have AMP transferase activity

and mediate AMPylation of target proteins when not inhibited by its antitoxin (Itzen et al., 2011; Woolery et al., 2010). Fic proteins have recently been identified in several Proteobacteria, including species of *Enterobacter*, *Salmonella, Shigella, Klebsiella, Yersinia* and *Pseuodamonas* (Stanger et al., 2016). *In vitro* infection models of mammalian cells have revealed that pathogenic bacteria secrete Fic toxins which AMPylate target proteins and cause cytoskeletal collapse and cell death (Worby et al., 2009). AMPylation of Fic target proteins in *C. elegans* was recently found to increase susceptibility to killing by *Pseuodamonas auerginosa* by dampening innate immunity and promoting pathogen proliferation (Truttmann et al., 2016).

The crystal structure of the *E. coli* K12 Fic protein in complex with its antitoxin was solved in 2016 and the *E. coli fic* gene was renamed *ecficT* and the *yhfG* gene encoding the antitoxin, *ecficA* (Stanger et al., 2016). The role of *ecficT* in toxicity, however, is unclear due to a lack of *in vivo* studies. However, the data presented in Chapter 7 supports the hypothesis that *fic* (*ecficT*) may be mediating a folate-dependent toxicity responsible for *C. elegans* ageing. Further work is required to investigate possible mechanisms of this toxicity and whether it is dependent on, or just coincident with folate synthesis.

In order to design experiments to test the above hypothesis, the chromosomal arrangement of *fic* and *pabA* must be understood (figure 8.1). The *fic* gene ends 31 nucleotides upstream of *pabA* and contains within its coding region the *pabA* P1 promoter (Komano et al., 1991; Tran et al., 1990). It is therefore possible that decreased folate levels and lifespan modulation in the *fic* (in-frame) mutant

observed in this work may be due to lack of transcription from the *pabA* P1 promoter. In order to delineate the effect of *fic* on *E. coli* folate levels and *C. elegans* lifespan, we must knockout *fic* whilst preserving expression of *pabA.* This could be achieved by transforming the *fic* mutant with a plasmid containing a fusion construct of the P1 promoter and the *pabA* gene, or alternatively by creating a targeted knockout of the *fic* gene by homologous recombination.

However, it is also possible that *fic*-mediated toxicity is co-dependent on folate synthesis. Indeed, a secondary *pabA* promoter, P2, is located upstream of *fic.* Transcription from this site generates polycistronic mRNA including both *fic* and *pabA* and only occurs when an mRNA stem-loop structure, which forms in the intergenic region between *fic* and *pabA*, is disrupted (Tran et al., 1990; Tran and Nichols, 1991). It is not clear why these two genes are transcribed together, or what regulatory elements stimulate transcription from this site, however, it has been suggested that *fic-pabA* co-transcription facilitates cell division (Komano et al., 1991), owing to the initial observation that *fic* in *E. coli* mediates cell filimentation induced by cAMP (Utsumi et al., 1982). In light of the more recently elucidated role of Fic proteins in toxicity, and the role of *pabA* and *pabB* in the virulence of pathogenic bacteria (Brown and Stocker, 1987; Chimalapati et al., 2011), this co-transcription may facilitate invasion and colonization of a host.

E. coli K12, however, is a lab-adapted strain and not classically considered a pathogen. Based on the data in this thesis, a model is proposed whereby the co-transcription of *fic* and *pabA* from P2 facilitates cell division during exponential phase, where this transcription is likely to be promoted by RpoS. The coincident

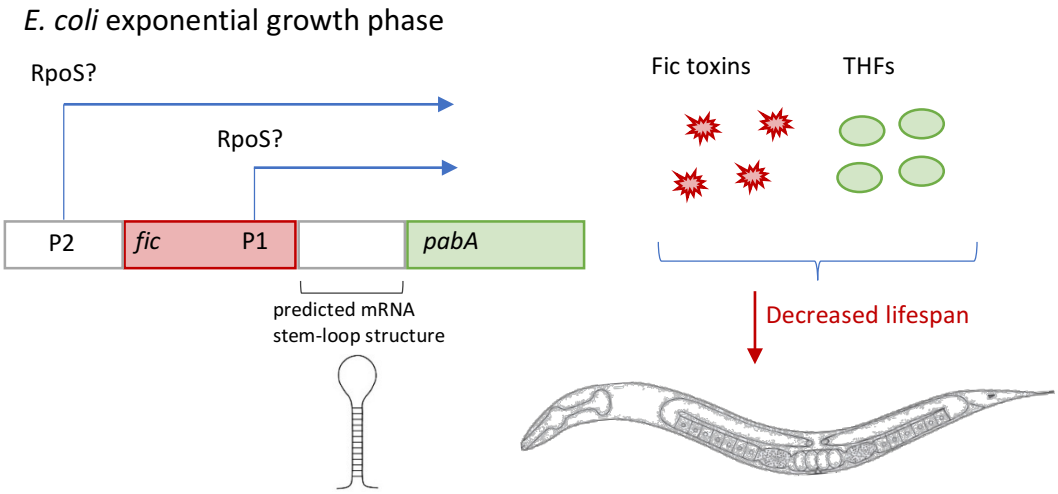

Figure 8.1. Diagrammatic representation of *fic-pabA* chromosomal organisation and a mechanism of Fic-dependent lifespan reduction. The *fic* coding region ends 31 nucleotides upstream of *pabA. pabA* has two known promoters, P1, which is located within the *fic* coding region, and P2, located upstream of *fic.* Transcription from P2 transcribes polycistronic mRNA containing both *fic* and *pabA* (Tran et al. 1991). The intragenic region between *fic* and *pabA* forms an mRNA stem-loop structure, which is disrupted following transcription from P2. A mechanism is proposed whereby RpoS activates *fic* and *pabA* transcription from P2 during exponential growth phase. This generates both the Fic toxin and tetrahydrofolates following folate synthesis which together decrease *C. elegans* lifespan.

secretion of Fic toxins may AMPylate *C. elegans* target proteins and cause an accumulation of damage which accelerates *C. elegans* ageing. It would be interesting to examine *fic*- dependent toxicity on *C. elegans* in the O-antigen restored K12 strain, which is reported to kill *C. elegans* at rates similar to those observed with pathogenic bacterial species (Browning et al., 2013) and also in the *Enterobacter cloacae* strain, B29. Monitoring changes in *C. elegans* protein AMPylation under these conditions may provide insights into the mechanism of *fic*-folate-dependent toxicity. The interaction of RpoS with these genes should be tested by DNAse footprinting or chromatin immunoprecipitation with microarray hybridization (ChIP-chip).

8.2.2ii Folate degradation and formaldehyde toxicity

Previous work in the Weinkove laboratory hypothesized that folates themselves are not toxic to *C. elegans*, as *E. coli* gene mutants involved in interconversions of THFs in the folate cycle did not have any effect on lifespan (Virk et al. 2016). However, the work here identified a correlation between low *E. coli* 5,10-methylene THF and increased *C. elegans* lifespan (outlined in Chapter 7, section 7.4.4) which challenged this original hypothesis.

A study published this year has highlighted a direct link between 5,10-methylene THF and toxicity in mammalian cells (Burgos-Barragan et al., 2017). The authors reported that oxidative degradation of endogenous THFs generates a ubiquitous source of the potent genotoxin, formaldehyde; 5,10-methylene was the most prone to oxidation and release of formaldehyde, followed by THF and DHF, but 5-methyl THF and 5-formyl THF (folinic acid) were resistant (Burgos-Barragan et al., 2017).

It is known that both eukaryotic and prokaryotic cells have mechanisms of detoxifying formaldehyde, by using THF as a one-carbon acceptor of formaldehyde to generate 5,10-methylene THF (Chen et al., 2016). This reaction is catalysed by SHMT during the conversion of serine to glycine (as described in section 8.1) (Burgos-Barragan et al., 2017). Indeed 5,10-methylene has been coined 'active formaldehyde' as it is known to degrade spontaneously to generate formaldehyde *in vitro* (Osborn et al., 1960).

In prokaryotic cells, folate-dependent formaldehyde production is not a widespread or renowned phenomena and the detoxification pathway is thought to compensate only for host-derived formaldehyde (Chen et al. 2016). However, in light of this recent discovery of mammalian folate-dependent formaldehyde release, and given the same biochemistry of eukaryotic and prokaryotic folates, it is not unlikely that bacterial folates are also a source of formaldehyde. This may underpin the association of excessive bacterial folate synthesis, and indeed 5,10-methylene THF, in our model system with *C. elegans* ageing.

Further work would test this hypothesis by monitoring formaldehyde concentrations in response to the factors identified in this work that influence both *E. coli* folate levels and *C. elegans* lifespan. It is hypothesized that formaldehyde would decrease in response to SMX and on *pabA, rpoS* and *fic* mutants, and concentrations would be expected to increase in response to PABA in *pabA* and *fic* mutants but not in the *rpoS*

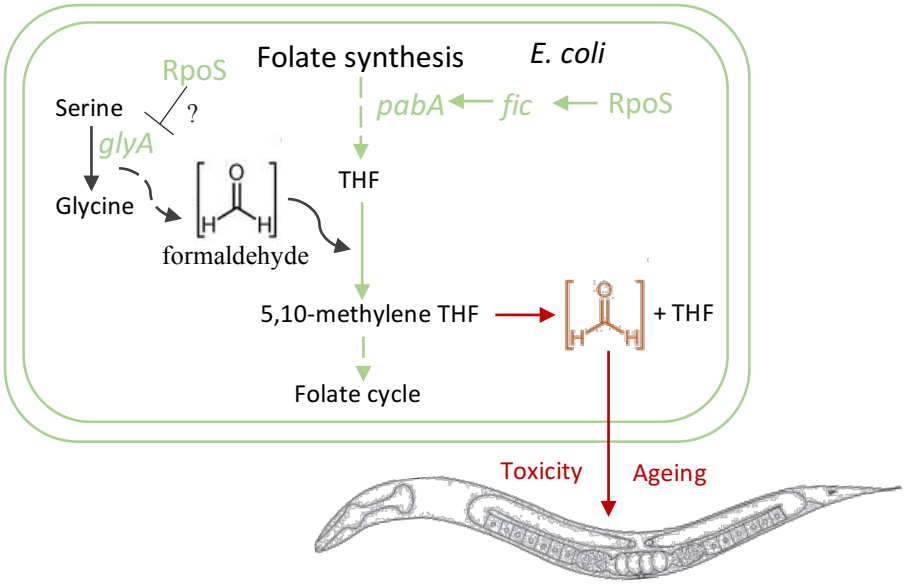

Figure 8.2 Hypothetical model of folate-dependent formaldehyde toxicity in *E. coli*

The conversion of serine to glycine liberates a transient molecule of formaldehyde, which reacts with THF to generate 5,10-methylene THF. 5,10-methylene THF can spontaneously degrade to release formaldehyde. Formaldehyde can diffuse across biological membranes and is a genotoxic compound, where it may disrupt *C. elegans* DNA and decrease lifespan. SHMT: serine hydroxymethyl transferase; THF: tetrahydrofolate. Adapted from Burgos- Burgos-Barragan et al, 2017.

mutant. This could be sensitively measured using LC-MS/MS or an *E. coli* reporter strain. See figure 8.2 for a model of folate-dependent formaldehyde toxicity.

A mechanism for RpoS regulation of 5,10-methylene stability was proposed in light of the co-incidence of altered pterin levels in the *rpoS* mutant (Chapter 7, section 7.14). It would be interesting to also examine whether RpoS regulates expression of *glyA,* the gene that encodes SHMT and therefore regulates 5,10-methylene levels (Tibbetts and Appling, 2010). Interestingly, deletion of the *glyA* gene was found to have a small (~8% increase) significant effect on lifespan in the screen conducted by Virk et al (Virk et al. 2016) but was disregarded for further study as its lifespan effect was small.

8.2.3 Regulation of *E. coli* folate synthesis

8.2.3i Temporal regulation

Given the importance of bacterial folate synthesis as an antibiotic target, surprisingly little is known about the genetic regulation of this process and there have been no transcription factors identified to date which regulate genes involved in either folate synthesis or one-carbon metabolism. The work presented in Chapter 6 suggested that folate synthesis is not constitutive, but regulated temporally, as folate levels and *pabA* expression were found to peak during early exponential growth phase. The coincidence of this peak with *rpoS* expression, and the decreased expression of *pabA* in the *rpoS* mutant, highlighted a novel role of RpoS, as a regulator of *pabA* and therefore bacterial folate synthesis. This has important implications for antibiotics which target bacterial folate synthesis, indicating that maximum efficacy may only be achieved when bacterial cells are dividing.

8.2.3ii THF riboswitch

Further work would also investigate the role of the THF riboswitch in *E. coli*. This is an mRNA motif which was identified in 2010 and found upstream of the folate transporter *folT* and several other genes involved in folate synthesis (*folC*,*Q, P, B, K*), but not in the PABA branch (Ames et al., 2010). The motif was also found in the human gut metagenome. This motif was found to bind to the pterin moiety of THFs, but not PABA, PABA-glu or pterin alone (Ames et al., 2010). The crystal structure of 5-formyl THF revealed that binding to the ligand-specific 'aptamer' domain changed the secondary structure of the 'expression platform' domain (Trausch et al., 2011). This conformational change supposedly regulates gene expression by either promoting or preventing access of the RNA polymerase holoenzyme (Wakeman et al., 2007), however *in vivo* studies on the regulatory control of the THF riboswitch have not been published.

The stem-loop secondary mRNA structure which forms in the intragenic region between *fic* and *pabA* as discussed (figure 8.2.1), was identified in 1991 (Tran and Nichols, 1991). This structure is consistent with that of a riboswitch, although it has not been identified as one to date. *fic* expression was upregulated in the *pabA* mutant and *pabA* expression was downregulated in the *fic* mutant (Chapter 7, figure 7.11) indicating possible negative feedback of a downstream *pabA* process on *fic* expression i.e a folate or folate-dependent metabolite. Further work would carry out *in vivo* analyses of the impact of this mRNA motif on transcription/ translation of *pabA* and *fic* in *E. coli* and examine the conditions that affect its secondary structure.

8.2.4 Folinic acid-dependent lifespan extension

In Chapter 7, a marked difference between the impact of folic and folinic acid on *C. elegans* lifespan was observed: whilst folic acid decreased lifespan on *pabA E. coli*, folinic acid markedly increased lifespan on WT and the *abgTpabA* mutant, but did not further increase the lifespan of the *pabA* mutant. Further work would investigate this interaction, especially given the detrimental impact of folic acid on *C. elegans* longevity.

Folinic acid is the monoglutamated derivative of 5-formyl THF and the only folate species which does not serve as a co-factor for one-carbon metabolism. 5-formyl THF is formed solely from a side-reaction mediated by SMHT, where 5,10-methenyltetrahydrofolate is converted to 5-formyl THF in the presence of glycine (Stover and Schirch, 1991). The only known metabolic roles of 5-formyl THF are inhibition of various enzymes involved in one-carbon metabolism, including SHMT (Stover and Schirch, 1991, 1993). As discussed, folinic acid has been shown to bind the THF riboswitches (Trausch et al., 2011), and although this mechanism of gene expression has not been demonstrated *in vivo,* it is likely that this is how folinic acid inhibits gene expression.

This suggests a possible mechanism whereby folinic acid supplementation may be increasing *C. elegans* lifespan by lowering *E. coli* folate levels. LC-MS/MS analysis of bacterial folate levels following folinic acid supplementation would be useful to clarify this hypothesis. Specifically, we may expect to see decreased levels of 5,10-

methyelene THF, due to the inhibitory action of folinic acid on SHMT. Intriguingly, whilst 5,10-methylene THF was identified as the most potent source of formaldehyde in the Burgos-Barragan study, 5-formyl THF was not found to generate detectable levels of formaldehyde (Burgos-Barragan et al., 2017). This is consistent with the hypothesis that bacterial levels of 5,10-methylene THF correlate to *C. elegans* lifespan.

Alternatively, lifespan extension in response to folinic acid may be mediated by a direct effect on *C. elegans.* Indeed, folinic acid was shown to supplement the *gcp-2.1* strain at low concentrations and independently of bacterial genotype (Chapter 7). Furthermore, *gcp-2.1* folate levels as detected by LC-MS/MS were increased with folinic acid (Chapter 5). Further work would examine the expression of *C. elegans* genes involved in longevity pathways in response to folinic acid supplementation; combined with lifespan analysis of known long-lived *C. elegans* mutants on folinic acid supplemented DM. In light of the negative health associations of folic acid, this work may provide the basis for the development of folinic acid as a widespread dietary supplement.

8.2.5 Does folic acid supplementation boost folate synthesis in the gut microbiota?

The work presented in Chapter 7 demonstrated that folic acid supplementation boosts both wild-type and *pabA* mutant *E. coli* folate synthesis. This was found to be dependent on the degradation of folic acid into PABA-glu, which was detected in three independent folic acid sources, solubilized in weak sodium hydroxide, by LC-MS/MS. The commercially available folic acid supplement contained the highest proportion of PABA-glu and PABA. The uptake of PABA-glu by *E. coli* AbgT was found to be

responsible for shortening *C. elegans* lifespan on *pabA E. coli* following folic acid supplementation. These data therefore highlight an indirect pathway whereby folic acid interacts with bacterial folate synthesis and negatively impacts animal long-term health.

As discussed, several pathogenic species of the gut microbiota possess AbgT (Blastn search) and are therefore able to transport PABA-glu, and many others are able to use PABA for folate synthesis. It is likely that PABA-glu and PABA will be available to the gut microbiota following folic acid supplementation, given the instability of folic acid at low pH (such as in the stomach and the upper small intestine). Furthermore, a US study investigating the quality of commercial folic acid supplements reported that only three out of nine multivitamin products tested met US Pharmacopeia standards for folic acid dissolution (Hoag et al., 1997). A study in the UK reported that only seven out of 11 commercial folic acid supplements met the British Pharmacopeia dissolution specifications (Sculthorpe et al., 2001). It has recently been revealed that due to issues with folic acid instability, manufactures have adopted a policy of 'overages', where folic acid supplements may contain up to 150% of the stated dose; indeed, in this study, Boots folic acid was found to contain 107% of the stated dose (Flynn et al., 2016; Mudryj et al., 2016).

Together, this indicates that folic acid supplements may supply the microbiota with precursors for folate synthesis. In light of the associations of folic acid supplementation with negative health consequences (as discussed in Chapter 1), the work here suggests that the quality of folic acid supplements should be reviewed and

the role of the microbiota following folic acid supplementation should be investigated (Andrews et al., 2017). Indeed, work presented in Chapter 5 demonstrated a complex interplay between bacterial folate status, folic acid supplementation, and animal folate, where *C. elegans* folate levels *decreased* in response to folic acid supplementation on *pabA E. coli.* It is hypothesized that the patient specific microbiota may be a confounding variable underlying the inability of meta-analyses to agree on the outcome of folic acid supplementation on human health. It would be interesting to conduct clinical trials examining gut microbiota composition following folic acid supplementation and monitor long-term health. Preliminary studies could also be carried out using *Drosophila* or mice.

8.2.6 Sulfonamides and ageing in higher model organisms

The *C. elegans- E. coli* simplified system was used here to investigate the parameters that influence bacterial folate synthesis in order to better define how this process affects animal ageing. The logical progression of this work is to test whether inhibiting bacterial folate synthesis is a viable means to extend lifespan, and importantly healthspan, in higher model organisms with established microbiotas. Preliminary work in collaboration with the Clark laboratory at Durham University indicates that SMX may also increase the lifespan of *Drosophila.* It is hoped that perseverance with this genetically tractable model organism with its relatively simplified microbiota will further our understanding of how this intervention extends lifespan.

An interesting insight from a rodent study conducted in the 1950s showed that the sulfonamide drug, sulfadiazine, significantly increased the health and lifespan of both rats and mice. Longevity was not achieved in a cohort supplemented with both sulfadiazine and PABA (Hackmann, 1958). As the researchers here were primarily concerned with the animal side-effects of sulfonamides, there was no acknowledgement of the impact on the gut microbiota. Conducting rodent studies and analysing longitudinal changes in microbiota composition over time, in response to an intervention that targets bacterial folate synthesis, would provide useful insights into how this intervention promotes longevity.

8.3 BACTERIAL FOLATE SYNTHESIS IN THE MICROBIOTA: A CAUSE OF AGEING?

Dysbiosis, in both ageing and disease, is often associated with an increased abundance of Proteobacteria (Hughes et al., 2017; Shin et al., 2015). Magnusodottir et al. reported that 71% of Proteobacteria in the human gut microbiota are able to synthesize folate *de novo* (Magnusdottir et al., 2015). It is hypothesized here that folate-synthesizing Proteobacteria in the intestine may generate a folate-dependent toxicity that promotes the host inflammatory response and thus drives dysbiosis. Thus, the factors identified here to promote bacterial folate synthesis, such as folic acid and glucose, may promote dysbiosis and thus alter host health via the gut microbiota.

Evidence for this model comes from the use of the sulfonamide drug, sulfasalazine for patient's with inflammatory disorders, such as Crohn's disease, ulcerative colitis and rheumatoid arthritis. Sulfasalazine is a two-part molecule whose action is dependent

on cleavage by intestinal bacteria into 5-aminosalicylate and sulfapyridine (Sack and Peppercorn, 1983). The efficacy of sulfasalazine is widely attributed to the unclarified function of 5-aminosalicylate on host cells and the action of sulfapyridine on bacterial folate synthesis is overlooked. It is not unlikely that sulfasalazine tempers inflammation by inhibiting bacterial folate synthesis. Further clinical evidence comes from the association of small intestinal bacterial overgrowth with both inflammation and increased serum folate levels (Camilo et al., 1996). Mechanistic work in model organisms is required in order to determine whether bacterial folate synthesis is a causative agent of inflammation.

In a normal 'healthy' microbiota, a model is proposed whereby bacterial folate synthesis throughout one's lifetime contributes to a chronic toxicity that accelerates ageing. This is perhaps best considered within the framework of the antagonistic pleiotropy theory of ageing, proposed in 1957 by George Williams (Williams, 1957). Williams reasoned that a gene with a detrimental impact on host fitness post reproductive age will be selected for by natural selection if it has a fitness advantage during development. Applied to the microbiota and ageing, this theory may underpin why the bacterial synthesis of folate, which is beneficial as a micronutrient during development, is sustained as an activity in the adult microbiota, despite its negative impact on long-term host health. This continued synthesis of folate, above the biosynthetic demands of the host, is consistent with the studies which have identified a large depository of folate in the human colon (Kim et al., 2004). It is therefore hypothesized that bacterial folate synthesis in the microbiota may be a double-edged sword for human health and longevity.

Supplementary Table 1. Details of all lifespan experiments conducted

All lifespans were carried out at 25 °C using the SS104 (*glp4(bn2)*) temperature-sensitive strain according to the protocol outlined in Chapter 2, section 2.12

* Data not shown in text

Chapter	Fig.	Group name	n	Censor	Mean lifespan	Std. error	% change	p value (Log rank)	p value (Wilcoxon)	Supplement	Bacterial genotype/ strain	Plasmid	Antibiotics
3	**3.3**	NGM, NGM	153	7	14.523	0.35956	Control	n/a	n/a	n/a	WT/ BW25113	pGreen 0029	25 µg/ml kan
		NGM, DM	150	0	15.800	0.38472	8.80%	0.0254*	0.0352*	n/a	WT/ BW25113	pGreen 0029	25 µg/ml kan
		NGM, DM + B12	133	13	16.894	0.46279	16.33%	<.0001	**0.0003**	10 nM B12	WT/ BW25113	pGreen 0029	25 µg/ml kan
		DM, NGM	129	0	14.388	0.39549	Control	n/a	n/a	n/a	WT/ BW25113	pGreen 0029	25 µg/ml kan
		DM, DM	113	27	15.621	0.41116	8.57%	0.0351	0.0177	n/a	WT/ BW25113	pGreen 0029	25 µg/ml kan
		DM, DM + B12	113	8	16.181	0.44747	12.46%	0.0067	0.0051	10 nM B12	WT/ BW25113	pGreen 0029	25 µg/ml kan
		DM + B12, NGM	91	3	14.422	0.43774	Control	n/a	n/a	n/a	WT/ BW25113	pGreen 0029	25 µg/ml kan
		DM + B12, DM	147	6	16.901	0.3662	17.19%	<.0001	<.0001	n/a	WT/ BW25113	pGreen 0029	25 µg/ml kan
		DM + B12, DM + B12	165	10	18.575	0.49146	28.79%	<.0001	<.0001	10 nM B12	WT/ BW25113	pGreen 0029	25 µg/ml kan
3	**3.6**	WT + 0.1 µM PABA	143	0	10.636	0.25487	Control	n/a	n/a	0.1 µM PABA	WT/ BW25113	pGreen 0029	25 µg/ml kan
		WT + 0.2 µM PABA	106	0	10.689	0.27938	0.49%	0.99	0.7301	0.2 µM PABA	WT/ BW25113	pGreen 0029	25 µg/ml kan
		WT + 0.5 µM PABA	150	0	10.500	0.2387	-1.28%	0.6339	0.7709	0.5 µM PABA	WT/ BW25113	pGreen 0029	25 µg/ml kan
		WT + 1 µM PABA	108	0	10.694	0.27167	0.55%	0.9792	0.6495	1 µM PABA	WT/ BW25113	pGreen 0029	25 µg/ml kan
		WT + 5 µM PABA	168	0	10.833	0.23469	1.85%	0.5777	0.4938	5 µM PABA	WT/ BW25113	pGreen 0029	25 µg/ml kan

		pabA + 0.1 µM PABA	131	0	14.214	0.39403	33.63%	<0.0001*	<0.0001*	0.1 µM PABA	*ΔpabA*/ JW3323-1	n/a	25 µg/ml kan
		pabA + 0.2 µM PABA	125	0	13.152	0.39383	23.65%	<0.0001*	<0.0001*	0.2 µM PABA	*ΔpabA*/ JW3323-1	n/a	25 µg/ml kan
		pabA + 0.5 µM PABA	100	0	12.320	0.3339	15.83%	<0.0002*	<0.0001*	0.5 µM PABA	*ΔpabA*/ JW3323-1	n/a	25 µg/ml kan
		pabA + 1 µM PABA	155	0	10.568	0.25052	-0.65%	0.8769	0.7959	1 µM PABA	*ΔpabA*/ JW3323-1	n/a	25 µg/ml kan
		pabA + 5 µM PABA	139	0	11.022	0.264	3.62%	0.489	0.3319	5 µM PABA	*ΔpabA*/ JW3323-1	n/a	25 µg/ml kan
4	*	WT	118	2	12.529	0.38704	Control	n/a	n/a	Alkaline control	WT/ BW25113	pGreen 0029	25 µg/ml kan
		WT + 10µM folic acid	125	6	12.588	0.45631	0.47%	0.8981	0.9513	10 µM folic acid	WT/ BW25113	pGreen 0029	25 µg/ml kan
		pabA	130	1	15.425	0.45812	Control	n/a	n/a	Alkaline control	*ΔpabA*/ JW3323-1	n/a	25 µg/ml kan
		pabA + 1µM folic acid	117	1	15.928	0.47219	3.26%	0.4924	0.2536	1 µM folic acid	*ΔpabA*/ JW3323-1	n/a	25 µg/ml kan
		pabA + 5µM folic acid	103	0	15.340	0.51321	-0.55%	0.8751	0.9723	5 µM folic acid	*ΔpabA*/ JW3323-1	n/a	25 µg/ml kan
		pabA + 10µM folic acid	132	1	14.181	0.33544	-8.06%	0.0121*	0.1849	10 µM folic acid	*ΔpabA*/ JW3323-1	n/a	25 µg/ml kan
4	**4.2**	WT	108	0	14.583	0.40466	Control	n/a	n/a	Alkaline control	WT/ BW25113	pGreen 0029	25 µg/ ml kan
		WT + 10 µm folic acid	115	0	15.000	0.3937	2.86%	0.4448	0.4588	10 µM folic acid	WT/ BW25113	pGreen 0029	25 µg/ ml kan
		WT + 100 µm folic acid	106	1	14.569	0.48154	-0.10%	0.566	0.844	100 µM folic acid	WT/ BW25113	pGreen 0029	25 µg/ ml kan
		pabA	102	2	18.914	0.4233	Control	n/a	n/a	Alkaline control	*ΔpabA*/ JW3323-1	n/a	25 µg/ ml kan
		pabA + 10 µm folic acid	84	2	18.195	0.56211	-3.80%	0.7322	0.43	10 µM folic acid	*ΔpabA*/ JW3323-1	n/a	25 µg/ ml kan
		pabA + 100 µm folic acid	122	0	15.967	0.43551	-15.58%	<.0001*	<.0001*	100 µM folic acid	*ΔpabA*/ JW3323-1	n/a	25 µg/ ml kan
4	*	WT	91	9	13.849	0.44	Control	n/a	n/a	n/a	WT/ BW25113	pGreen 0029	25 µg/ml kan

		abgT	114	3	12.675	0.35	-8.48%	0.4312	0.0963	n/a	*ΔabgT/* JW5822-1	n/a	25 µg/ml kan
4	**4.3**	WT	102	9	15.956	0.47723	Control	n/a	n/a	Alkaline control	CM1/puc19	pUC19	50 µg/ml carb, 25 µg/ ml kan
		WT + 10 µM folic	98	12	15.961	0.58353	0.03%	0.8268	0.4283	10 µM folic acid	CM1/puc19	pUC19	50 µg/ml carb, 25 µg/ ml kan
		WT 100 µM folic	102	18	16.014	0.48219	0.36%	0.866	0.7792	100 µM folic acid	CM1/puc19	pUC19	50 µg/ml carb, 25 µg/ ml kan
		pabA	113	10	18.351	0.55995	Control	n/a	n/a	Alkaline control	CM1/puc19	pUC19	50 µg/ml carb, 25 µg/ ml kan
		pabA 10 µM folic	90	11	17.442	0.63673	-4.95%	0.2527	0.2605	10 µM folic acid	CM1/puc19	pUC19	50 µg/ml carb, 25 µg/ ml kan
		pabA 100 µM folic	122	3	15.860	0.4041	-13.57%	<.0001*	0.0019*	100 µM folic acid	CM1/puc19	pUC19	50 µg/ml carb, 25 µg/ ml kan
		abgTpabA	136	14	18.932	0.49624	Control	n/a	n/a	Alkaline control	CM1/puc19	pUC19	50 µg/ml carb, 25 µg/ ml kan
		abgTpabA + 10 µM folic	115	26	19.217	0.5155	1.51%	0.6416	0.5684	10 µM folic acid	CM1/puc19	pUC19	50 µg/ml carb, 25 µg/ ml kan
		abgTpabA + 100 µM folic	93	11	19.255	0.59683	1.71%	0.5868	0.4482	100 µM folic acid	CM1/puc19	pUC19	50 µg/ml carb, 25 µg/ ml kan
		pabA (abgT OE)	101	23	18.416	0.55641	Control	n/a	n/a	Alkaline control	CM2/pJ128*	pJ128	50 µg/ml carb, 25 µg/ ml kan
		pabA (abgT OE) + 10 µM folic	124	0	15.839	0.46927	-14.00%	0.0005*	0.0035*	10 µM folic acid	CM2/pJ128*	pJ128	50 µg/ml carb, 25 µg/ ml kan
		pabA (abgT OE) 100 µM folic	105	0	15.771	0.49895	-14.36%	0.0003*	0.0041*	100 µM folic acid	CM2/pJ128*	pJ128	50 µg/ml carb, 25 µg/ ml kan

		WT *(abgT* OE)	110	9	16.109	0.49644	Control	n/a	n/a	Alkaline control	CM1/pJ128*	pJ128	50 µg/ml carb, 25 µg/ ml kan
		WT *(abgT* OE) + 10 µM folic	99	4	16.050	0.57274	-0.37%	0.9479	0.8905	10 µM folic acid	CM1/pJ128*	pJ128	50 µg/ml carb, 25 µg/ ml kan
		WT *(abgT* OE) + 100 µM folic	127	4	15.783	0.38634	-2.02%	0.3698	0.8168	100 µM folic acid	CM1/pJ128*	pJ128	50 µg/ml carb, 25 µg/ ml kan
4	**4.6**	WT	108	0	15.790	0.53	n/a	n/a	n/a	Alkaline control	CM1/puc19	pUC19	50 µg/ml carb, 25 µg/ ml kan
		pabA	94	3	20.076	0.52	Control	n/a	n/a	Alkaline control	CM2/puc19	pUC19	50 µg/ml carb, 25 µg/ ml kan
		pabA + 0.1 µM PABA	107	0	19.299	0.46	-3.89%	0.0973	0.3296	0.1 µM pABA	CM1/puc19	pUC19	50 µg/ml carb, 25 µg/ ml kan
		pabA + 1 µM PABA	118	0	15.907	0.45	-20.78%	<.0001*	<.0001*	1 µM pABA	CM2/puc19	pUC19	50 µg/ml carb, 25 µg/ ml kan
		pabA + 1 µM pAB-glu	110	2	18.575	0.40	-7.49%	0.0030*	0.0277*	1 µM pAB-glu	CM2/puc19	pUC19	50 µg/ml carb, 25 µg/ ml kan
		pabA + 10 µM pAB-glu	125	10	16.433	0.46	-18.16%	<.0001*	<.0001*	10 µM pAB-glu	CM2/puc19	pUC19	50 µg/ml carb, 25 µg/ ml kan
		pabA + 10 µM folic acid	93	5	18.201	0.55	-9.36%	0.0052*	0.0061*	10 µM Schircks folic acid	CM2/puc19	pUC19	50 µg/ml carb, 25 µg/ ml kan
		pabA + 100 µM folic acid	112	1	15.275	0.45	-23.93%	<.0001*	<.0001*	100 µM Schircks folic acid	CM2/puc19	pUC19	50 µg/ml carb, 25 µg/ ml kan
		**pabA* + 10 uM Boots	126	1	15.939	0.48256	-20.61%	<.0001*	<.0001*	10 µM Boots folic acid	CM2/puc19	pUC19	50 µg/ml carb, 25 µg/ ml kan

**pabA* + 10 uM Sigma	110	0	17.727	0.50764	-8.14%	0.0005*	0.0053*	10 µM Sigma folic acid	CM2/puc19	pUC19	50 µg/ml carb, 25 µg/ ml kan
abgTpabA	91	3	20.103	0.44	Control	n/a	n/a	Alkaline control	CM3/puc19	pUC19	50 µg/ml carb, 25 µg/ ml kan
abgTpabA + 0.1 µM PABA	91	6	18.716	0.49	-6.88%	0.0631	0.0477*	0.1 µM pABA	CM3/puc19	pUC19	50 µg/ml carb, 25 µg/ ml kan
abgTpabA + 1 µM PABA	102	1	16.711	0.45	-16.86%	<.0001*	<.0001*	1 µM pABA	CM3/puc19	pUC19	50 µg/ml carb, 25 µg/ ml kan
abgTpabA + 1 pAB-glu	101	11	18.105	0.52421	-9.94%	0.0698	0.0333*	1 µM pAB-glu	CM3/puc19	pUC19	50 µg/ml carb, 25 µg/ ml kan
abgTpabA + 10 µM pAB-glu	106	4	18.996	0.46	-5.49%	0.1817	0.0512	10 µM pAB-glu	CM3/puc19	pUC19	50 µg/ml carb, 25 µg/ ml kan
abgTpabA + 10 µM folic acid	110	1	19.198	0.43	-4.49%	0.1901	0.114	10 µM Schircks folic acid	CM3/puc19	pUC19	50 µg/ml carb, 25 µg/ ml kan
abgTpabA + 100 µM folic acid	100	3	19.160	0.40	-4.67%	0.0476*	0.0743	100 µM Schircks folic acid	CM1/puc19	pUC19	50 µg/ml carb, 25 µg/ ml kan
**abgTpabA* + 10 uM Boots	92	3	19.634	0.44283	-2.33%	0.3997	0.5249	10 µM Boots folic acid	CM3/puc19	pUC19	50 µg/ml carb, 25 µg/ ml kan
**abgTpabA* + 10 uM Sigma	92	0	20.457	0.47624	9.30%	0.2876	0.4599	10 µM Sigma folic acid	CM3/puc19	pUC19	50 µg/ml carb, 25 µg/ ml kan
pabA (abgT OE)	62	10	19.895	0.52	Contol	n/a	n/a	Alkaline control	CM2/pJ128	pJ128	50 µg/ml carb, 25 µg/ ml kan
pabA (abgT OE) + 0.1 µM PABA	121	1	18.552	0.45	-6.72%	0.0049*	0.0184*	0.1 µM pABA	CM2/pJ128	pJ128	50 µg/ml carb, 25 µg/ ml kan
pabA (abgT OE) + 1 µM PABA	104	2	16.072	0.50	-19.19%	<.0001*	<.0001*	1 µM pABA	CM2/pJ128	pJ128	50 µg/ml carb, 25 µg/ ml kan

		pabA (abgT OE) + 1 µM pAB-glu	104	1	17.012	0.43	-14.47%	<.0001*	<.0001*	1 µM pAB-glu	CM2/pJ128	pJ128	50 µg/ml carb, 25 µg/ ml kan
		pabA (abgT OE) + 10 µM pAB-glu	117	0	15.051	0.41	-24.33%	<.0001*	<.0001*	10 µM pAB-glu	CM2/pJ128	pJ128	50 µg/ml carb, 25 µg/ ml kan
		pabA (abgT OE) + 10 µM folic acid	119	0	16.647	0.42	-16.30%	<.0001*	<.0001*	10 µM Schircks folic acid	CM2/pJ128	pJ128	50 µg/ml carb, 25 µg/ ml kan
		pabA (abgT OE) + 100 µM folic acid	117	0	16.188	0.42	-18.61%	<.0001*	<.0001*	100 µM Schircks folic acid	CM2/pJ128	pJ128	50 µg/ml carb, 25 µg/ ml kan
		**pabA (abgT* OE) + 10 uM Boots	105	0	17.648	0.50799	-11.29%	0.0032*	0.0067*	10 µM Boots folic acid	CM2/pJ128	pJ128	50 µg/ml carb, 25 µg/ ml kan
		**pabA (abgT* OE) + 10 uM Sigma	108	0	16.167	0.47479	-18.74%	<.0001*	<.0001*	10 µM Sigma folic acid	CM2/pJ128	pJ128	50 µg/ml carb, 25 µg/ ml kan
4	**4.1**	WT	99	26	14.947	0.33973	Control	n/a	n/a	Alkaline control	WT/ BW25113	pGreen 0029	25 µg/ml kan
		WT + 100 µM folic acid	132	3	15.439	0.35922	3.30%	0.1964	0.6903	100 µM folic acid	WT/ BW25113	pGreen 0029	25 µg/ml kan
		WT + 100 µM folinic acid	120	9	17.697	0.47526	18.40%	<.0001*	0.0003*	100 µM folinic acid	WT/ BW25113	pGreen 0029	25 µg/ml kan
		pabA	113	1	18.540	0.43348	Control	n/a	n/a	Alkaline control	*ΔpabA*/ JW3323-1	n/a	25 µg/ml kan
		pabA + 100 µM folic acid	107	9	15.505	0.39687	-16.37%	<.0001*	<.0001*	100 µM folic acid	*ΔpabA*/ JW3323-1	n/a	25 µg/ml kan
		pabA + 100 µM folinic acid	131	3	17.768	0.4008	-4.17%	0.2046	0.2109	100 µM folinic acid	*ΔpabA*/ JW3323-1	n/a	25 µg/ml kan
		abgT	130	2	15.309	0.36093	Control	n/a	n/a	Alkaline control	*ΔabgT*/ JW5822-1	n/a	25 µg/ml kan
		abgT + 100 µM folic acid	137	5	15.018	0.40015	-1.90%	0.9233	0.6568	100 µM folic acid	*ΔabgT*/ JW5822-1	n/a	25 µg/ml kan
		abgT + 100 µM folinic acid	120	1	16.886	0.47067	10.31%	0.0040*	0.0176*	100 µM folinic acid	*ΔabgT*/ JW5822-1	n/a	25 µg/ml kan

		abgTpabA	148	1	18.352	0.4141	Control	n/a	n/a	Alkaline control	CMabgTpabA	n/a	25 µg/ml kan
		abgTpabA + 100µM folic acid	111	17	17.608	0.38666	-4.05%	0.0719	0.4487	100 µM folic acid	CMabgTpabA	n/a	25 µg/ml kan
		abgTpabA + 100µM folinic acid	101	29	20.115	0.46278	9.61%	0.0188*	0.0021*	100 µM folinic acid	CMabgTpabA	n/a	25 µg/ml kan
6	**6.4**	WT	80	9	14.929	0.67224	Control	n/a	n/a	Volume control	WT/ BW25113	pGreen 0029	25 µg/ml kan
		WT + SMX	92	6	21.603	0.85748	44.71%	<.0001*	<.0001*	Volume control	WT/ BW25113	pGreen 0029	25 µg/ml kan
		pabA	96	5	21.983	0.74544	47.25%	<.0001*	<.0001*	Volume control	*ΔpabA/* JW3323-1	n/a	25 µg/ml kan
		WT + 0.1 % glucose	74	10	11.300	0.38043	Control	n/a	n/a	0.1 % glucose	WT/ BW25113	pGreen 0029	25 µg/ml kan
		WT + SMX + 0.1% glucose	104	6	12.735	0.509	12.70%	0.003*	0.137	0.1 % glucose	WT/ BW25113	pGreen 0029	25 µg/ml kan
		pabA + 0.1% glucose	76	3	15.861	0.68494	40.37%	<.0001*	<.0001*	0.1 % glucose	*ΔpabA/* JW3323-1	n/a	25 µg/ml kan
6	**6.6**	Control transfer	124	2	12.373	0.37099	Control	n/a	n/a	Alkaline control	WT/ BW25113	pGreen 0029	25 µg/ml kan
		SMX transfer	131	9	19	0.4289	53.56%	<.0001*	<.0001*	128 µg/ml SMX	WT/ BW25113	pGreen 0029	25 µg/ml kan
		Day 2 SMX transfer	123	1	14.2581	0.37805	15.24%	0.0012*	<.0001*	128 µg/ml SMX	WT/ BW25113	pGreen 0029	25 µg/ml kan
		Day 4 SMX transfer	129	0	11.9302	0.2685	-3.58%	0.2748	0.8838	128 µg/ml SMX	WT/ BW25113	pGreen 0029	25 µg/ml kan
		Control non-transfer	96	0	12.7292	0.38459	Control	n/a	n/a	Alkaline control	WT/ BW25113	pGreen 0029	25 µg/ml kan
		SMX non-transfer	123	1	18.1532	0.45491	42.61%	<.0001*	<.0001*	128 µg/ml SMX	WT/ BW25113	pGreen 0029	25 µg/ml kan
		Day 2 SMX non-transfer	126	2	16.875	0.42703	32.57%	<.0001*	<.0001*	128 µg/ml SMX	WT/ BW25113	pGreen 0029	25 µg/ml kan
		Day 4 SMX non-transfer	119	0	14.1849	0.37284	11.44%	0.0117*	0.0086*	128 µg/ml SMX	WT/ BW25113	pGreen 0029	25 µg/ml kan

7	**7.1**	OP50	154	6	15.442	0.40087	Control	n/a	n/a	Alkaline control	WT/ OP50	n/a	No kan
		OP50 + SMX	123	26	21.9287	0.51584	(from OP50) 42.01%	<0.0001*	<0.0001*	128µg/ml SMX	WT/ OP50	n/a	No kan
		WT	114	3	12.6754	0.35294	(from OP50) - 17.92%	<0.0001*	<0.0001*	Alkaline control	WT/ BW25113	pGreen 0029	No kan
		WT + SMX	138	4	19.307	0.44371	(from WT) 52.32%	<0.0001*	<0.0001*	128µg/ml SMX	WT/ BW25113	pGreen 0029	No kan
7	*	WT	150	3	12.8878	0.29364	Control	n/a	n/a	Alkaline control	WT/ BW25113	pGreen 0029	25 µg/ml kan
		WT + SMX	139	4	16.8407	0.41393	30.67%	<0.0001*	<0.0001*	128 µg/ml SMX	WT/ BW25113	pGreen 0029	25 µg/ml kan
		pabA	127	2	15.1621	0.38482	17.65%	<0.0001*	<0.0001*	Alkaline control	*ΔpabA/* JW3323-1	n/a	25 µg/ml kan
		pabA + SMX	124	3	16.01	0.43418	(from WT + SMX) - 4.93%	0.2121	0.1918	128 µg/ml SMX	*ΔpabA/* JW3323-1	n/a	25 µg/ml kan
		rpoS	65	0	14.9538	0.58975	16.03%	0.0003*	0.0025*	Alkaline control	*ΔrpoS/* JW5437-1	n/a	25 µg/ml kan
		rpoS + SMX	150	2	17.6372	0.38484	(from WT + SMX) 4.73%	0.2189	0.1214	128 µg/ml SMX	*ΔrpoS/* JW5437-1	n/a	25 µg/ml kan
7	**7.5a**	WT	112	0	13.7768	0.36513	Control	n/a	n/a	n/a	WT/ BW25113	pGreen 0029	25 µg/ml kan
		trpB	82	6	12.9083	0.3865	-6.30%	0.1002	0.195	n/a	*ΔtrpB/* JW1253-1	n/a	25 µg/ml kan
		tnaA	99	4	13.3178	0.33556	-3.33%	0.356	0.5006	n/a	*ΔtnaA/* JW3686-7	n/a	25 µg/ml kan
		ompF	79	7	13.3357	0.36955	-3.20%	0.3095	0.6389	n/a	*ΔompF/* JW0912-1	n/a	25 µg/ml kan
		yhfG	84	8	13.4665	0.42254	-2.25%	0.6263	0.575	n/a	*ΔyhfG/* JW3325-1	n/a	25 µg/ml kan
		ompT	104	0	13.625	0.41359	-1.10%	0.9282	0.5002	n/a	*ΔompT/* JW0554-1	n/a	25 µg/ml kan

		csgD	106	0	13.6698	0.37167	-0.78%	0.6796	0.7029	n/a	*ΔcsgD/* JW1023-1	n/a	25 µg/ml kan
		crl	93	6	13.8953	0.46595	0.86%	0.5229	0.8497	n/a	*Δcrl/* JW0230-1	n/a	25 µg/ml kan
		ompA	98	0	14.1429	0.35618	2.66%	0.0905	0.4742	n/a	*ΔompA/* JW0940-6	n/a	25 µg/ml kan
		hlyE	100	4	14.2409	0.34054	3.37%	0.6171	0.3494	n/a	*ΔhlyE/* JW5181-1	n/a	25 µg/ml kan
		ompC	78	5	14.651	0.37566	6.35%	0.1647	0.0504	n/a	*ΔompC/* JW2203-1	n/a	25 µg/ml kan
		astA	111	1	15.4485	0.39575	12.13%	0.0019*	0.0038*	n/a	*ΔastA/* JW1736-1	n/a	25 µg/ml kan
		bipA	98	3	15.4648	0.4014	12.25%	0.0026*	0.0018*	n/a	*ΔbipA/* JW5571-1	n/a	25 µg/ml kan
		lrhA	83	4	15.6581	0.57238	13.66%	0.0007*	0.0108*	n/a	*ΔlrhA/* JW2284-6	n/a	25 µg/ml kan
		crp	95	0	15.7684	0.48342	14.46%	0.0003*	0.0017*	n/a	*Δcrp/* JW5702-4	n/a	25 µg/ml kan
		cfa	97	0	16.2577	0.46466	18.01%	<.0001*	<.0001*	n/a	*Δcfa/* JW1653-1	n/a	25 µg/ml kan
7	**7.5b**	WT	95	11	12.8174	0.50518	Control	n/a	n/a	n/a	WT/ BW25113	pGreen 0029	25 µg/ml kan
		gadX	104	1	12.7146	0.45509	-0.80%	0.7316	0.9559	n/a	*ΔgadX/* JW3484-1	n/a	25 µg/ml kan
		bipA	109	4	12.9689	0.47313	1.18%	0.6526	0.717	n/a	*ΔbipA/* JW5571-1	n/a	25 µg/ml kan
		tktB	119	1	13.6318	0.41869	6.35%	0.3347	0.1482	n/a	*ΔtktB/* JW2449-4	n/a	25 µg/ml kan
		osmY	110	5	13.9034	0.43454	8.47%	0.2018	0.0828	n/a	*ΔosmY/* JW4338-1	n/a	25 µg/ml kan
		gabB	123	0	13.9756	0.44868	9.04%	0.0813	0.0818	n/a	*ΔgadB/* JW1488-7	n/a	25 µg/ml kan
		slp	109	12	14.0418	0.471	9.55%	0.0574	0.0628	n/a	*Δslp/* JW3474-5	n/a	25 µg/ml kan
		mysB	96	3	14.2527	0.4484	11.20%	0.1451	0.0278*	n/a	*ΔmysB/* JW1912-1	n/a	25 µg/ml kan
		gadE	121	3	14.4077	0.44506	12.41%	0.0217*	0.0175*	n/a	*ΔgadE/* JW3480-2	n/a	25 µg/ml kan

		cfa	121	6	14.5964	0.38252	13.88%	0.0281*	0.0025*	n/a	*Δcfa/* JW1653-1	n/a	25 µg/ml kan
		osmC	94	2	14.6298	0.50133	14.14%	0.0154*	0.0105*	n/a	*ΔosmC/* JW1477-1	n/a	25 µg/ml kan
		csrA	128	0	14.6563	0.35502	14.35%	0.0312*	0.0017*	n/a	*ΔcsrA/* JW3221-5	n/a	25 µg/ml kan
		gadA	114	6	14.8649	0.40842	15.97%	0.0079*	0.0011*	n/a	*ΔgadA/* JW3485-1	n/a	25 µg/ml kan
		talA	119	0	15.084	0.3859	17.68%	0.0037*	0.0003*	n/a	*ΔtalA/* JW2448-4	n/a	25 µg/ml kan
		relA	123	2	15.6017	0.40588	21.72%	<.0001*	<.0001*	n/a	*ΔrelA/* JW2755-3	n/a	25 µg/ml kan
		sodA	120	1	15.7144	0.44081	22.60%	<.0001*	<.0001*	n/a	*ΔsodA/* JW3879-1	n/a	25 µg/ml kan
		otsB	112	9	15.7178	0.42563	22.63%	<.0001*	<.0001*	n/a	*ΔotsB/* JW1886-1	n/a	25 µg/ml kan
		fic	122	6	16.1549	0.41128	26.04%	<.0001*	<.0001*	n/a	*Δfic/* JW3323-1	n/a	25 µg/ml kan
		astA	107	7	16.317	0.4366	27.30%	<.0001*	<.0001*	n/a	*ΔastA/* JW1736-1	n/a	25 µg/ml kan
		crp	120	1	16.5538	0.42341	29.15%	<.0001*	<.0001*	n/a	*Δcrp/* JW5702-4	n/a	25 µg/ml kan
		rpoS	83	9	17.2864	0.54141	34.87%	<.0001*	<.0001*	n/a	*ΔrpoS/* JW5437-1	n/a	25 µg/ml kan
		lrhA	121	2	18.1628	0.39001	41.70%	<.0001*	<.0001*	n/a	*ΔlrhA/* JW2284-6	n/a	25 µg/ml kan
7	**7.12a**	*rpoS* + 0.1 µM PABA	98	3	13.5063	0.48124	Control	n/a	n/a	0.1 µM PABA	*ΔrpoS/* JW5437-1	n/a	25 µg/ml kan
		rpoS + 0.2 µM PABA	115	5	14.9349	0.43591	10.58%	0.0004*	0.0031*	0.2 µM PABA	*ΔrpoS/* JW5437-1	n/a	25 µg/ml kan
		rpoS + 0.5 µM PABA	108	2	13.3179	0.44282	-1.39%	0.3738	0.9232	0.5 µM PABA	*ΔrpoS/* JW5437-1	n/a	25 µg/ml kan
		rpoS + 1 µM PABA	133	0	13.0226	0.34146	-3.58%	0.1482	0.5852	1 µM PABA	*ΔrpoS/* JW5437-1	n/a	25 µg/ml kan
		rpoS + 5 µM PABA	134	0	12.8806	0.3531	-4.63%	0.8655	0.8009	5 µM PABA	*ΔrpoS/* JW5437-1	n/a	25 µg/ml kan

7	**7.12b**	WT	102	5	15.1059	0.43811	Control	n/a	n/a	Alkaline control	WT/ BW25113	pGreen 0029	25 µg/ml kan
		WT + 1 µM PABA	121	0	15.1653	0.31739	0.39%	0.3299	0.9042	1 µM PABA	WT/ BW25113	pGreen 0029	25 µg/ml kan
		WT + 100 µM folic	97	6	14.5767	0.3859	-3.88%	0.1289	0.3348	100 µM folic acid	WT/ BW25113	pGreen 0029	25 µg/ml kan
		WT + 100 µM folinic	79	24	15.9143	0.50855	9.18%	0.0639	0.2332	100 µM folinic acid	WT/ BW25113	pGreen 0029	25 µg/ml kan
		rpoS	66	0	16.6515	0.53914	Control	n/a	n/a	Alkaline control	*ΔrpoS/* JW5437-1	n/a	25 µg/ml kan
		rpoS+ 1 µM PABA	106	17	16.5113	0.38532	-0.84%	0.1647	0.432	1 µM PABA	*ΔrpoS/* JW5437-1	n/a	25 µg/ml kan
		rpoS + 100 µM folic	100	12	14.6164	0.43298	-12.22%	0.0041*	0.0091*	100 µM folic acid	*ΔrpoS/* JW5437-1	n/a	25 µg/ml kan
		rpoS + 100 µM folinic	93	17	17.3562	0.38808	4.23%	0.5785	0.3742	100 µM folinic acid	ΔrpoS/ JW5437-1	n/a	25 µg/ml kan
7	*****	*pabA*	73	10	16.5554	0.4857	Control	n/a	n/a	Alkaline control	*ΔpabA/* JW3323-1	n/a	25 µg/ml kan
		pabA + 1 µM PABA	125	10	14.6716	0.34406	-11.38%	0.0003*	0.0021*	1 µM PABA	*ΔpabA/* JW3323-1	n/a	25 µg/ml kan
		pabA + 100 µM folic	85	24	14.1619	0.42421	-14.46%	<.0001*	0.0006*	100 µM folic acid	*ΔpabA/* JW3323-1	n/a	25 µg/ml kan
		pabA + 100 µM folinic	103	13	16.0138	0.42221	-3.27%	0.5331	0.42	100 µM folinic acid	*ΔpabA/* JW3323-1	n/a	25 µg/ml kan

Uncategorized References

(1991). Prevention of neural tube defects: results of the Medical Research Council Vitamin Study. MRC Vitamin Study Research Group. Lancet *338*, 131-137.

Allegra, C.J., Baram, J., Chabner, B.A., Yeh, G.C., Aiba, K., and Curt, G.A. (1987). Antimetabolites. Cancer Chemother Biol Response Modif *9*, 1-22.

Allegra, C.J., Chabner, B.A., Drake, J.C., Lutz, R., Rodbard, D., and Jolivet, J. (1985). Enhanced inhibition of thymidylate synthase by methotrexate polyglutamates. J Biol Chem *260*, 9720-9726.

Allen-Vercoe, E., Collighan, R., and Woodward, M.J. (1998). The variant rpoS allele of S. enteritidis strain 27655R does not affect virulence in a chick model nor constitutive curliation but does generate a cold-sensitive phenotype. FEMS Microbiol Lett *167*, 245-253.

Ames, T.D., Rodionov, D.A., Weinberg, Z., and Breaker, R.R. (2010). A eubacterial riboswitch class that senses the coenzyme tetrahydrofolate. Chem Biol *17*, 681-685.

Andrews, K.W., Roseland, J.M., Gusev, P.A., Palachuvattil, J., Dang, P.T., Savarala, S., Han, F., Pehrsson, P.R., Douglass, L.W., Dwyer, J.T.*, et al.* (2017). Analytical ingredient content and variability of adult multivitamin/mineral products: national estimates for the Dietary Supplement Ingredient Database. Am J Clin Nutr *105*, 526-539.

Angier, R.B., Boothe, J.H., Hutchings, B.L., Mowat, J.H., Semb, J., Stokstad, E.L., Subbarow, Y., Waller, C.W., Cosulich, D.B., Fahrenbach, M.J.*, et al.* (1945). Synthesis of a Compound Identical with the L. Casei Factor Isolated from Liver. Science *102*, 227-228.

Angier, R.B., Stokstad, E.L., and et al. (1948). Synthesis of pteroylglutamic acid. J Am Chem Soc *70*, 25.

Appling, D.R. (1991). Compartmentation of folate-mediated one-carbon metabolism in eukaryotes. FASEB J *5*, 2645-2651.

Asrar, F.M., and O'Connor, D.L. (2005). Bacterially synthesized folate and supplemental folic acid are absorbed across the large intestine of piglets. J Nutr Biochem *16*, 587-593.

Aufreiter, S., Gregory, J.F., 3rd, Pfeiffer, C.M., Fazili, Z., Kim, Y.I., Marcon, N., Kamalaporn, P., Pencharz, P.B., and O'Connor, D.L. (2009). Folate is absorbed across the colon of adults: evidence from cecal infusion of (13)C-labeled [6S]-5-formyltetrahydrofolic acid. Am J Clin Nutr *90*, 116-123.

Augustine, S., and Bonomo, R.A. (2011). Taking stock of infections and antibiotic resistance in the elderly and long-term care facilities: A survey of existing and upcoming challenges. Eur J Microbiol Immunol (Bp) *1*, 190-197.

Avery, L., and Shtonda, B.B. (2003). Food transport in the C. elegans pharynx. J Exp Biol *206*, 2441-2457.

Baba, T., Ara, T., Hasegawa, M., Takai, Y., Okumura, Y., Baba, M., Datsenko, K.A., Tomita, M., Wanner, B.L., and Mori, H. (2006). Construction of Escherichia coli K-12 in-frame, single-gene knockout mutants: the Keio collection. Mol Syst Biol *2*, 2006 0008.

Bachman, M.A., and Swanson, M.S. (2001). RpoS co-operates with other factors to induce Legionella pneumophila virulence in the stationary phase. Mol Microbiol *40*, 1201-1214.

Backhed, F., Ding, H., Wang, T., Hooper, L.V., Koh, G.Y., Nagy, A., Semenkovich, C.F., and Gordon, J.I. (2004). The gut microbiota as an environmental factor that regulates fat storage. Proc Natl Acad Sci U S A *101*, 15718-15723.

Backhed, F., Manchester, J.K., Semenkovich, C.F., and Gordon, J.I. (2007). Mechanisms underlying the resistance to diet-induced obesity in germ-free mice. Proc Natl Acad Sci U S A *104*, 979-984.

Bailey, L.B., Stover, P.J., McNulty, H., Fenech, M.F., Gregory, J.F., 3rd, Mills, J.L., Pfeiffer, C.M., Fazili, Z., Zhang, M., Ueland, P.M.*, et al.* (2015). Biomarkers of Nutrition for Development-Folate Review. J Nutr *145*, 1636S-1680S.

Baker, H., Herbert, V., Frank, O., Pasher, I., Hutner, S.H., Wasserman, L.R., and Sobotka, H. (1959). A microbiologic method for detecting folic acid deficiency in man. Clin Chem *5*, 275-280.

Balamurugan, K., Ashokkumar, B., Moussaif, M., Sze, J.Y., and Said, H.M. (2007). Cloning and functional characterization of a folate transporter from the nematode Caenorhabditis elegans. Am J Physiol Cell Physiol *293*, C670-681.

Balamurugan, K., and Said, H.M. (2006). Role of reduced folate carrier in intestinal folate uptake. Am J Physiol Cell Physiol *291*, C189-193.

Banik, S., Terekhova, D., Iyer, R., Pappas, C.J., Caimano, M.J., Radolf, J.D., and Schwartz, I. (2011). BB0844, an RpoS-regulated protein, is dispensable for Borrelia burgdorferi infectivity and maintenance in the mouse-tick infectious cycle. Infect Immun *79*, 1208-1217.

Bargmann, C.I., Hartwieg, E., and Horvitz, H.R. (1993). Odorant-selective genes and neurons mediate olfaction in C. elegans. Cell *74*, 515-527.

Barriere, A., and Felix, M.A. (2005). Natural variation and population genetics of Caenorhabditis elegans. WormBook, 1-19.

Baugh, C.M., Krumdieck, C.L., Baker, H.J., and Butterworth, C.E., Jr. (1971). Studies on the absorption and metabolism of folic acid. I. Folate absorption in the dog after exposure of isolated intestinal segments to synthetic pteroylpolyglutamates of various chain lengths. J Clin Invest *50*, 2009-2021.

Beanan, M.J., and Strome, S. (1992). Characterization of a Germ-Line Proliferation Mutation in C-Elegans. Development *116*, 755-766.

Berg, M., Stenuit, B., Ho, J., Wang, A., Parke, C., Knight, M., Alvarez-Cohen, L., and Shapira, M. (2016). Assembly of the Caenorhabditis elegans gut microbiota from diverse soil microbial environments. ISME J *10*, 1998-2009.

Berry, R.J., Li, Z., Erickson, J.D., Li, S., Moore, C.A., Wang, H., Mulinare, J., Zhao, P., Wong, L.Y., Gindler, J.*, et al.* (1999). Prevention of neural-tube defects with folic acid in China. China-U.S. Collaborative Project for Neural Tube Defect Prevention. N Engl J Med *341*, 1485-1490.

Biagi, E., Franceschi, C., Rampelli, S., Severgnini, M., Ostan, R., Turroni, S., Consolandi, C., Quercia, S., Scurti, M., Monti, D.*, et al.* (2016). Gut Microbiota and Extreme Longevity. Curr Biol *26*, 1480-1485.

Biagi, E., Nylund, L., Candela, M., Ostan, R., Bucci, L., Pini, E., Nikkila, J., Monti, D., Satokari, R., Franceschi, C.*, et al.* (2010). Through ageing, and beyond: gut microbiota and inflammatory status in seniors and centenarians. PLoS One *5*, e10667.

Bluher, M., Kahn, B.B., and Kahn, C.R. (2003). Extended longevity in mice lacking the insulin receptor in adipose tissue. Science *299*, 572-574.

Booijink, C.C., El-Aidy, S., Rajilic-Stojanovic, M., Heilig, H.G., Troost, F.J., Smidt, H., Kleerebezem, M., De Vos, W.M., and Zoetendal, E.G. (2010). High temporal and inter-individual variation detected in the human ileal microbiota. Environ Microbiol *12*, 3213-3227.

Borst, S.E., and Conover, C.F. (2005). High-fat diet induces increased tissue expression of TNF-alpha. Life Sci *77*, 2156-2165.

Bouter, B., Geary, N., Langhans, W., and Asarian, L. (2010). Diet-genotype interactions in the early development of obesity and insulin resistance in mice with a genetic deficiency in tumor necrosis factor-alpha. Metabolism *59*, 1065-1073.

Boyles, A.L., Billups, A.V., Deak, K.L., Siegel, D.G., Mehltretter, L., Slifer, S.H., Bassuk, A.G., Kessler, J.A., Reed, M.C., Nijhout, H.F.*, et al.* (2006). Neural tube defects and folate pathway genes: family-based association tests of gene-gene and gene-environment interactions. Environ Health Perspect *114*, 1547-1552.

Brenner, S. (1974). The genetics of Caenorhabditis elegans. Genetics *77*, 71-94.

Broderick, N.A., Buchon, N., and Lemaitre, B. (2014). Microbiota-induced changes in drosophila melanogaster host gene expression and gut morphology. MBio *5*, e01117-01114.

Broderick, N.A., and Lemaitre, B. (2012). Gut-associated microbes of Drosophila melanogaster. Gut Microbes *3*, 307-321.

Brown, R.F., and Stocker, B.A. (1987). Salmonella typhi 205aTy, a strain with two attenuating auxotrophic characters, for use in laboratory teaching. Infect Immun *55*, 892-898.

Browning, D.F., Wells, T.J., Franca, F.L., Morris, F.C., Sevastsyanovich, Y.R., Bryant, J.A., Johnson, M.D., Lund, P.A., Cunningham, A.F., Hobman, J.L.*, et al.* (2013). Laboratory adapted Escherichia coli K-12 becomes a pathogen of Caenorhabditis elegans upon restoration of O antigen biosynthesis. Mol Microbiol *87*, 939-950.

Buchon, N., Broderick, N.A., Poidevin, M., Pradervand, S., and Lemaitre, B. (2009). Drosophila intestinal response to bacterial infection: activation of host defense and stem cell proliferation. Cell Host Microbe *5*, 200-211.

Buford, T.W. (2017). (Dis)Trust your gut: the gut microbiome in age-related inflammation, health, and disease. Microbiome *5*, 80.

Burgos-Barragan, G., Wit, N., Meiser, J., Dingler, F.A., Pietzke, M., Mulderrig, L., Pontel, L.B., Rosado, I.V., Brewer, T.F., Cordell, R.L.*, et al.* (2017). Mammals divert endogenous genotoxic formaldehyde into one-carbon metabolism. Nature *548*, 549-554.

Butterworth, C.E., Jr., and Tamura, T. (1989). Folic acid safety and toxicity: a brief review. Am J Clin Nutr *50*, 353-358.

Cabreiro, F., Au, C., Leung, K.Y., Vergara-Irigaray, N., Cocheme, H.M., Noori, T., Weinkove, D., Schuster, E., Greene, N.D., and Gems, D. (2013). Metformin retards aging

in C. elegans by altering microbial folate and methionine metabolism. Cell *153*, 228-239.

Cabreiro, F., and Gems, D. (2013). Worms need microbes too: microbiota, health and aging in Caenorhabditis elegans. EMBO Mol Med *5*, 1300-1310.

Camilo, E., Zimmerman, J., Mason, J.B., Golner, B., Russell, R., Selhub, J., and Rosenberg, I.H. (1996). Folate synthesized by bacteria in the human upper small intestine is assimilated by the host. Gastroenterology *110*, 991-998.

Cani, P.D., Amar, J., Iglesias, M.A., Poggi, M., Knauf, C., Bastelica, D., Neyrinck, A.M., Fava, F., Tuohy, K.M., Chabo, C.*, et al.* (2007). Metabolic endotoxemia initiates obesity and insulin resistance. Diabetes *56*, 1761-1772.

Cani, P.D., Bibiloni, R., Knauf, C., Waget, A., Neyrinck, A.M., Delzenne, N.M., and Burcelin, R. (2008). Changes in gut microbiota control metabolic endotoxemia-induced inflammation in high-fat diet-induced obesity and diabetes in mice. Diabetes *57*, 1470-1481.

Carding, S., Verbeke, K., Vipond, D.T., Corfe, B.M., and Owen, L.J. (2015). Dysbiosis of the gut microbiota in disease. Microb Ecol Health Dis *26*, 26191.

Carroll, C., Cooper, K., Papaioannou, D., Hind, D., Tappenden, P., Pilgrim, H., and Booth, A. (2010). Meta-analysis: folic acid in the chemoprevention of colorectal adenomas and colorectal cancer. Aliment Pharmacol Ther *31*, 708-718.

Carter, E.L., Jager, L., Gardner, L., Hall, C.C., Willis, S., and Green, J.M. (2007). Escherichia coli abg genes enable uptake and cleavage of the folate catabolite p-aminobenzoyl-glutamate. J Bacteriol *189*, 3329-3334.

Chauhan, V.M., Orsi, G., Brown, A., Pritchard, D.I., and Aylott, J.W. (2013). Mapping the pharyngeal and intestinal pH of Caenorhabditis elegans and real-time luminal pH oscillations using extended dynamic range pH-sensitive nanosensors. ACS Nano *7*, 5577-5587.

Chen, N.H., Djoko, K.Y., Veyrier, F.J., and McEwan, A.G. (2016). Formaldehyde Stress Responses in Bacterial Pathogens. Front Microbiol *7*, 257.

Chimalapati, S., Cohen, J., Camberlein, E., Durmort, C., Baxendale, H., de Vogel, C., van Belkum, A., and Brown, J.S. (2011). Infection with conditionally virulent Streptococcus pneumoniae Deltapab strains induces antibody to conserved protein antigens but does not protect against systemic infection with heterologous strains. Infect Immun *79*, 4965-4976.

Claesson, M.J., Cusack, S., O'Sullivan, O., Greene-Diniz, R., de Weerd, H., Flannery, E., Marchesi, J.R., Falush, D., Dinan, T., Fitzgerald, G.*, et al.* (2011). Composition, variability, and temporal stability of the intestinal microbiota of the elderly. Proc Natl Acad Sci U S A *108 Suppl 1*, 4586-4591.

Claesson, M.J., Jeffery, I.B., Conde, S., Power, S.E., O'Connor, E.M., Cusack, S., Harris, H.M., Coakley, M., Lakshminarayanan, B., O'Sullivan, O.*, et al.* (2012). Gut microbiota composition correlates with diet and health in the elderly. Nature *488*, 178-184.

Clancy, D.J., Gems, D., Harshman, L.G., Oldham, S., Stocker, H., Hafen, E., Leevers, S.J., and Partridge, L. (2001). Extension of life-span by loss of CHICO, a Drosophila insulin receptor substrate protein. Science *292*, 104-106.

Clark, L.C., and Hodgkin, J. (2014). Commensals, probiotics and pathogens in the Caenorhabditis elegans model. Cell Microbiol *16*, 27-38.

Clark, R.I., Salazar, A., Yamada, R., Fitz-Gibbon, S., Morselli, M., Alcaraz, J., Rana, A., Rera, M., Pellegrini, M., Ja, W.W.*, et al.* (2015). Distinct Shifts in Microbiota Composition during Drosophila Aging Impair Intestinal Function and Drive Mortality. Cell Rep *12*, 1656-1667.

Cole, B.F., Baron, J.A., Sandler, R.S., Haile, R.W., Ahnen, D.J., Bresalier, R.S., McKeown-Eyssen, G., Summers, R.W., Rothstein, R.I., Burke, C.A.*, et al.* (2007). Folic acid for the prevention of colorectal adenomas: a randomized clinical trial. JAMA *297*, 2351-2359.

Couillault, C., and Ewbank, J.J. (2002). Diverse bacteria are pathogens of Caenorhabditis elegans. Infect Immun *70*, 4705-4707.

Croll, N.A., Smith, J.M., and Zuckerman, B.M. (1977). The aging process of the nematode Caenorhabditis elegans in bacterial and axenic culture. Exp Aging Res *3*, 175-189.

Czeizel, A.E., Dudas, I., Fritz, G., Tecsoi, A., Hanck, A., and Kunovits, G. (1992). The effect of periconceptional multivitamin-mineral supplementation on vertigo, nausea and vomiting in the first trimester of pregnancy. Arch Gynecol Obstet *251*, 181-185.

Daft, F.S., Mc, D.E., Herman, L.G., Romine, M.K., and Hegner, J.R. (1963). Role of coprophagy in utilization of B vitamins synthesized by intestinal bacteria. Fed Proc *22*, 129-133.

Davis, M.C., Kesthely, C.A., Franklin, E.A., and MacLellan, S.R. (2017). The essential activities of the bacterial sigma factor. Can J Microbiol *63*, 89-99.

De Brouwer, V., Zhang, G.F., Storozhenko, S., Straeten, D.V., and Lambert, W.E. (2007). pH stability of individual folates during critical sample preparation steps in prevision of the analysis of plant folates. Phytochem Anal *18*, 496-508.

Delmar, J.A., and Yu, E.W. (2016). The AbgT family: A novel class of antimetabolite transporters. Protein Sci *25*, 322-337.

Denko, C.W., Grundy, W.E., and et al. (1946). The excretion of B-complex vitamins by normal adults on a restricted intake. Arch Biochem *11*, 109-117.

Der-Petrossian, M., Fodinger, M., Knobler, R., Honigsmann, H., and Trautinger, F. (2007). Photodegradation of folic acid during extracorporeal photopheresis. Br J Dermatol *156*, 117-121.

Devlin, A.M., Clarke, R., Birks, J., Evans, J.G., and Halsted, C.H. (2006). Interactions among polymorphisms in folate-metabolizing genes and serum total homocysteine concentrations in a healthy elderly population. Am J Clin Nutr *83*, 708-713.

Dirksen, P., Marsh, S.A., Braker, I., Heitland, N., Wagner, S., Nakad, R., Mader, S., Petersen, C., Kowallik, V., Rosenstiel, P.*, et al.* (2016). The native microbiome of the nematode Caenorhabditis elegans: gateway to a new host-microbiome model. BMC Biol *14*, 38.

Dixon, K.H., Lanpher, B.C., Chiu, J., Kelley, K., and Cowan, K.H. (1994). A novel cDNA restores reduced folate carrier activity and methotrexate sensitivity to transport deficient cells. J Biol Chem *269*, 17-20.

Donaldson, G.P., Lee, S.M., and Mazmanian, S.K. (2016). Gut biogeography of the bacterial microbiota. Nat Rev Microbiol *14*, 20-32.

Dong, T., Kirchhof, M.G., and Schellhorn, H.E. (2008). RpoS regulation of gene expression during exponential growth of Escherichia coli K12. Mol Genet Genomics *279*, 267-277.

Dong, T., and Schellhorn, H.E. (2010). Role of RpoS in virulence of pathogens. Infect Immun *78*, 887-897.

Dudeja, P.K., Kode, A., Alnounou, M., Tyagi, S., Torania, S., Subramanian, V.S., and Said, H.M. (2001). Mechanism of folate transport across the human colonic basolateral membrane. Am J Physiol Gastrointest Liver Physiol *281*, G54-60.

Dudeja, P.K., Torania, S.A., and Said, H.M. (1997). Evidence for the existence of a carrier-mediated folate uptake mechanism in human colonic luminal membranes. Am J Physiol *272*, G1408-1415.

Dudin, O., Lacour, S., and Geiselmann, J. (2013). Expression dynamics of RpoS/Crl-dependent genes in Escherichia coli. Res Microbiol *164*, 838-847.

Dupuy, D., Bertin, N., Hidalgo, C.A., Venkatesan, K., Tu, D., Lee, D., Rosenberg, J., Svrzikapa, N., Blanc, A., Carnec, A.*, et al.* (2007). Genome-scale analysis of in vivo spatiotemporal promoter activity in Caenorhabditis elegans. Nat Biotechnol *25*, 663-668.

Ebbing, M., Bonaa, K.H., Nygard, O., Arnesen, E., Ueland, P.M., Nordrehaug, J.E., Rasmussen, K., Njolstad, I., Refsum, H., Nilsen, D.W.*, et al.* (2009). Cancer incidence and mortality after treatment with folic acid and vitamin B12. JAMA *302*, 2119-2126.

Edwards, B.K., Ward, E., Kohler, B.A., Eheman, C., Zauber, A.G., Anderson, R.N., Jemal, A., Schymura, M.J., Lansdorp-Vogelaar, I., Seeff, L.C.*, et al.* (2010). Annual report to the nation on the status of cancer, 1975-2006, featuring colorectal cancer trends and impact of interventions (risk factors, screening, and treatment) to reduce future rates. Cancer *116*, 544-573.

Egan, M.G., Sirlin, S., Rumberger, B.G., Garrow, T.A., Shane, B., and Sirotnak, F.M. (1995). Rapid decline in folylpolyglutamate synthetase activity and gene expression during maturation of HL-60 cells. Nature of the effect, impact on folate compound polyglutamate pools, and evidence for programmed down-regulation during maturation. J Biol Chem *270*, 5462-5468.

Engel, P., Goepfert, A., Stanger, F.V., Harms, A., Schmidt, A., Schirmer, T., and Dehio, C. (2012). Adenylylation control by intra- or intermolecular active-site obstruction in Fic proteins. Nature *482*, 107-110.

Fan, J., Ye, J., Kamphorst, J.J., Shlomi, T., Thompson, C.B., and Rabinowitz, J.D. (2014). Quantitative flux analysis reveals folate-dependent NADPH production. Nature *510*, 298-302.

Fava, F., Lovegrove, J.A., Gitau, R., Jackson, K.G., and Tuohy, K.M. (2006). The gut microbiota and lipid metabolism: implications for human health and coronary heart disease. Curr Med Chem *13*, 3005-3021.

Fei, N., and Zhao, L. (2013). An opportunistic pathogen isolated from the gut of an obese human causes obesity in germfree mice. ISME J *7*, 880-884.

Felix, M.A., and Braendle, C. (2010). The natural history of Caenorhabditis elegans. Curr Biol *20*, R965-969.

Fife, J., Raniga, S., Hider, P.N., and Frizelle, F.A. (2011). Folic acid supplementation and colorectal cancer risk: a meta-analysis. Colorectal Dis *13*, 132-137.

Fire, A., Albertson, D., Harrison, S.W., and Moerman, D.G. (1991). Production of antisense RNA leads to effective and specific inhibition of gene expression in C. elegans muscle. Development *113*, 503-514.

Flint, H.J. (2012). The impact of nutrition on the human microbiome. Nutr Rev *70 Suppl 1*, S10-13.

Flint, K.M., Van Walleghen, E.L., Kealey, E.H., VonKaenel, S., Bessesen, D.H., and Davy, B.M. (2008). Differences in eating behaviors between nonobese, weight stable young and older adults. Eat Behav *9*, 370-375.

Flynn, A., Kehoe, L., Hennessy, A., and Walton, J. (2016). Estimating safe maximum levels of vitamins and minerals in fortified foods and food supplements. Eur J Nutr.

Fodinger, M., Buchmayer, H., Heinz, G., Papagiannopoulos, M., Kletzmayr, J., Perschl, A., Vychytil, A., Horl, W.H., and Sunder-Plassmann, G. (2001). Association of two MTHFR polymorphisms with total homocysteine plasma levels in dialysis patients. Am J Kidney Dis *38*, 77-84.

Fox, J.T., and Stover, P.J. (2008). Folate-mediated one-carbon metabolism. Vitam Horm *79*, 1-44.

Franceschi, C. (2007). Inflammaging as a major characteristic of old people: can it be prevented or cured? Nutr Rev *65*, S173-176.

Franceschi, C., and Campisi, J. (2014). Chronic inflammation (inflammaging) and its potential contribution to age-associated diseases. J Gerontol A Biol Sci Med Sci *69 Suppl 1*, S4-9.

Friedman, D.B., and Johnson, T.E. (1988a). 3 Mutants That Extend Both Mean and Maximum Life-Span of the Nematode, Caenorhabditis-Elegans, Define the Age-1 Gene. J Gerontol *43*, B102-B109.

Friedman, D.B., and Johnson, T.E. (1988b). A Mutation in the Age-1 Gene in Caenorhabditis-Elegans Lengthens Life and Reduces Hermaphrodite Fertility. Genetics *118*, 75-86.

Gabbianelli, R., Scotti, R., Ammendola, S., Petrarca, P., Nicolini, L., and Battistoni, A. (2011). Role of ZnuABC and ZinT in Escherichia coli O157:H7 zinc acquisition and interaction with epithelial cells. BMC Microbiol *11*, 36.

Garigan, D., Hsu, A.L., Fraser, A.G., Kamath, R.S., Ahringer, J., and Kenyon, C. (2002). Genetic analysis of tissue aging in Caenorhabditis elegans: a role for heat-shock factor and bacterial proliferation. Genetics *161*, 1101-1112.

Garratt, L.C., Ortori, C.A., Tucker, G.A., Sablitzky, F., Bennett, M.J., and Barrett, D.A. (2005). Comprehensive metabolic profiling of mono- and polyglutamated folates and their precursors in plant and animal tissue using liquid chromatography/negative ion electrospray ionisation tandem mass spectrometry. Rapid Commun Mass Spectrom *19*, 2390-2398.

Garrow, T.A., and Shane, B. (1993). Purification and general properties of human folylpolyglutamate synthetase. Adv Exp Med Biol *338*, 659-662.

Garsin, D.A., Sifri, C.D., Mylonakis, E., Qin, X., Singh, K.V., Murray, B.E., Calderwood, S.B., and Ausubel, F.M. (2001). A simple model host for identifying Gram-positive virulence factors. Proc Natl Acad Sci U S A *98*, 10892-10897.

Garsin, D.A., Villanueva, J.M., Begun, J., Kim, D.H., Sifri, C.D., Calderwood, S.B., Ruvkun, G., and Ausubel, F.M. (2003). Long-lived C. elegans daf-2 mutants are resistant to bacterial pathogens. Science *300*, 1921.

Gazzali, A.M., Lobry, M., Colombeau, L., Acherar, S., Azais, H., Mordon, S., Arnoux, P., Baros, F., Vanderesse, R., and Frochot, C. (2016). Stability of folic acid under several parameters. Eur J Pharm Sci *93*, 419-430.

Gems, D., and Riddle, D.L. (2000). Defining wild-type life span in Caenorhabditis elegans. J Gerontol A Biol Sci Med Sci *55*, B215-219.

Ghoshal, U.C., Sengar, V., and Srivastava, D. (2012). Colonic Transit Study Technique and Interpretation: Can These Be Uniform Globally in Different Populations With Non-uniform Colon Transit Time? J Neurogastroenterol Motil *18*, 227-228.

Goldberg, J. (1983). Sulfasalazine and folate deficiency. JAMA *249*, 729.

Green, J.M., and Matthews, R.G. (2007). Folate Biosynthesis, Reduction, and Polyglutamylation and the Interconversion of Folate Derivatives. EcoSal Plus *2*.

Green, J.M., Merkel, W.K., and Nichols, B.P. (1992). Characterization and sequence of Escherichia coli pabC, the gene encoding aminodeoxychorismate lyase, a pyridoxal phosphate-containing enzyme. J Bacteriol *174*, 5317-5323.

Green, J.M., and Nichols, B.P. (1991). p-Aminobenzoate biosynthesis in Escherichia coli. Purification of aminodeoxychorismate lyase and cloning of pabC. J Biol Chem *266*, 12971-12975.

Gregory, J.F., 3rd (1982). Denaturation of the folacin-binding protein in pasteurized milk products. J Nutr *112*, 1329-1338.

Gregory, J.F., 3rd (1989). Chemical and nutritional aspects of folate research: analytical procedures, methods of folate synthesis, stability, and bioavailability of dietary folates. Adv Food Nutr Res *33*, 1-101.

Guigoz, Y., Dore, J., and Schiffrin, E.J. (2008). The inflammatory status of old age can be nurtured from the intestinal environment. Curr Opin Clin Nutr Metab Care *11*, 13-20.

Hackmann, C. (1958). [Observations on influenceability of age phenomena in experimental animals by peroral administration of combinations of 2-(p-aminobenzolsulfonamide)-pyrimidin]. Munch Med Wochenschr *100*, 1814-1817.

Hahm, J.H., Kim, S., and Paik, Y.K. (2011). GPA-9 is a novel regulator of innate immunity against Escherichia coli foods in adult Caenorhabditis elegans. Aging Cell *10*, 208-219.

Halsted, C.H., Beer, W.H., Chandler, C.J., Ross, K., Wolfe, B.M., Bailey, L., and Cerda, J.J. (1986). Clinical studies of intestinal folate conjugases. J Lab Clin Med *107*, 228-232.

Halsted, C.H., Gandhi, G., and Tamura, T. (1981). Sulfasalazine inhibits the absorption of folates in ulcerative colitis. N Engl J Med *305*, 1513-1517.

Halsted, C.H., Ling, E.H., Luthi-Carter, R., Villanueva, J.A., Gardner, J.M., and Coyle, J.T. (1998). Folylpoly-gamma-glutamate carboxypeptidase from pig jejunum. Molecular characterization and relation to glutamate carboxypeptidase II. J Biol Chem *273*, 20417-20424.

Han, B., Sivaramakrishnan, P., Lin, C.J., Neve, I.A.A., He, J., Tay, L.W.R., Sowa, J.N., Sizovs, A., Du, G., Wang, J.*, et al.* (2017). Microbial Genetic Composition Tunes Host Longevity. Cell *169*, 1249-1262 e1213.

Hanson, A.D., and Gregory, J.F., 3rd (2011). Folate biosynthesis, turnover, and transport in plants. Annu Rev Plant Biol *62*, 105-125.

Harms, A., Stanger, F.V., and Dehio, C. (2016). Biological Diversity and Molecular Plasticity of FIC Domain Proteins. Annu Rev Microbiol *70*, 341-360.

Hawkes, J.G., and Villota, R. (1989). Folates in foods: reactivity, stability during processing, and nutritional implications. Crit Rev Food Sci Nutr *28*, 439-538.

Heng, S.S., Chan, O.Y., Keng, B.M., and Ling, M.H. (2011). Glucan Biosynthesis Protein G Is a Suitable Reference Gene in Escherichia coli K-12. ISRN Microbiol *2011*, 469053.

Hengge-Aronis, R. (1996). Back to log phase: sigma S as a global regulator in the osmotic control of gene expression in Escherichia coli. Mol Microbiol *21*, 887-893.

Hengge-Aronis, R. (2002). Recent insights into the general stress response regulatory network in Escherichia coli. J Mol Microbiol Biotechnol *4*, 341-346.

Hibbard, B.M. (1964). The Role of Folic Acid in Pregnancy; with Particular Reference to Anaemia, Abruption and Abortion. J Obstet Gynaecol Br Commonw *71*, 529-542.

Hibbard, B.M., Hibbard, E.D., and Jeffcoate, T.N. (1965). Folic acid and reproduction. Acta Obstet Gynecol Scand *44*, 375-400.

Hildebrandt, M.A., Hoffmann, C., Sherrill-Mix, S.A., Keilbaugh, S.A., Hamady, M., Chen, Y.Y., Knight, R., Ahima, R.S., Bushman, F., and Wu, G.D. (2009). High-fat diet determines the composition of the murine gut microbiome independently of obesity. Gastroenterology *137*, 1716-1724 e1711-1712.

Hoag, S.W., Ramachandruni, H., and Shangraw, R.F. (1997). Failure of prescription prenatal vitamin products to meet USP standards for folic acid dissolution. J Am Pharm Assoc (Wash) *NS37*, 397-400.

Hoffbrand, A.V. (1975). Synthesis and breakdown of natural folates (folate polyglutamates). Prog Hematol *9*, 85-105.

Hoffbrand, A.V., and Weir, D.G. (2001). The history of folic acid. Br J Haematol *113*, 579-589.

Hollander, D., and Tarnawski, H. (1985). Aging-associated increase in intestinal absorption of macromolecules. Gerontology *31*, 133-137.

Holzenberger, M., Dupont, J., Ducos, B., Leneuve, P., Geloen, A., Even, P.C., Cervera, P., and Le Bouc, Y. (2003). IGF-1 receptor regulates lifespan and resistance to oxidative stress in mice. Nature *421*, 182-187.

Hughes, E.R., Winter, M.G., Duerkop, B.A., Spiga, L., Furtado de Carvalho, T., Zhu, W., Gillis, C.C., Buttner, L., Smoot, M.P., Behrendt, C.L.*, et al.* (2017). Microbial Respiration and Formate Oxidation as Metabolic Signatures of Inflammation-Associated Dysbiosis. Cell Host Microbe *21*, 208-219.

Human Microbiome Project, C. (2012). Structure, function and diversity of the healthy human microbiome. Nature *486*, 207-214.

Hunt, P.R. (2017). The C. elegans model in toxicity testing. J Appl Toxicol *37*, 50-59.

Hussein, M.J., Green, J.M., and Nichols, B.P. (1998). Characterization of mutations that allow p-aminobenzoyl-glutamate utilization by Escherichia coli. J Bacteriol *180*, 6260-6268.

Hutchings, B.L., Bohonos, N., Hegsted, D.M., Elvehjem, C.A., and Peterson, W.H. (1941). Relation of a growth factor required by lactobacillus casei (is an element of) to the nutrition of the chick. Journal of Biological Chemistry *140*, 681-682.

Ifergan, I., and Assaraf, Y.G. (2008). Molecular mechanisms of adaptation to folate deficiency. Vitam Horm *79*, 99-143.

Imbard, A., Benoist, J.F., and Blom, H.J. (2013). Neural tube defects, folic acid and methylation. Int J Environ Res Public Health *10*, 4352-4389.

Iriarte, M., Stainier, I., and Cornelis, G.R. (1995). The rpoS gene from Yersinia enterocolitica and its influence on expression of virulence factors. Infect Immun *63*, 1840-1847.

Ito, A., May, T., Kawata, K., and Okabe, S. (2008). Significance of rpoS during maturation of Escherichia coli biofilms. Biotechnol Bioeng *99*, 1462-1471.

Itzen, A., Blankenfeldt, W., and Goody, R.S. (2011). Adenylylation: renaissance of a forgotten post-translational modification. Trends Biochem Sci *36*, 221-228.

Jukes, T.H., and Stokstad, E.L. (1948). Pteroylglutamic acid and related compounds. Physiol Rev *28*, 51-106.

Kaletta, T., and Hengartner, M.O. (2006). Finding function in novel targets: C. elegans as a model organism. Nat Rev Drug Discov *5*, 387-398.

Kamada, N., Chen, G.Y., Inohara, N., and Nunez, G. (2013). Control of pathogens and pathobionts by the gut microbiota. Nat Immunol *14*, 685-690.

Kenyon, C., Chang, J., Gensch, E., Rudner, A., and Tabtiang, R. (1993). A C. elegans mutant that lives twice as long as wild type. Nature *366*, 461-464.

Kenyon, C.J. (2010). The genetics of ageing. Nature *464*, 504-512.

Kerenyi, M., Allison, H.E., Batai, I., Sonnevend, A., Emody, L., Plaveczky, N., and Pal, T. (2005). Occurrence of hlyA and sheA genes in extraintestinal Escherichia coli strains. J Clin Microbiol *43*, 2965-2968.

Kim, D.H. (2013). Bacteria and the aging and longevity of Caenorhabditis elegans. Annu Rev Genet *47*, 233-246.

Kim, S.K. (1968). Small intestine transit time in the normal small bowel study. Am J Roentgenol Radium Ther Nucl Med *104*, 522-524.

Kim, T.H., Yang, J., Darling, P.B., and O'Connor, D.L. (2004). A large pool of available folate exists in the large intestine of human infants and piglets. J Nutr *134*, 1389-1394.

Kim, Y., and Mylonakis, E. (2012). Caenorhabditis elegans immune conditioning with the probiotic bacterium Lactobacillus acidophilus strain NCFM enhances gram-positive immune responses. Infect Immun *80*, 2500-2508.

Kim, Y.I. (2004). Will mandatory folic acid fortification prevent or promote cancer? Am J Clin Nutr *80*, 1123-1128.

Kinch, L.N., Yarbrough, M.L., Orth, K., and Grishin, N.V. (2009). Fido, a novel AMPylation domain common to fic, doc, and AvrB. PLoS One *4*, e5818.

Kirkwood, T.B., Feder, M., Finch, C.E., Franceschi, C., Globerson, A., Klingenberg, C.P., LaMarco, K., Omholt, S., and Westendorp, R.G. (2005). What accounts for the wide variation in life span of genetically identical organisms reared in a constant environment? Mech Ageing Dev *126*, 439-443.

Kirkwood, T.B., and Finch, C.E. (2002). Ageing: the old worm turns more slowly. Nature *419*, 794-795.

Klass, M.R. (1977). Aging in the nematode Caenorhabditis elegans: major biological and environmental factors influencing life span. Mech Ageing Dev *6*, 413-429.

Klass, M.R. (1983). A method for the isolation of longevity mutants in the nematode Caenorhabditis elegans and initial results. Mech Ageing Dev *22*, 279-286.

Kleiman, S.C., Carroll, I.M., Tarantino, L.M., and Bulik, C.M. (2015). Gut feelings: A role for the intestinal microbiota in anorexia nervosa? Int J Eat Disord *48*, 449-451.

Klipstein, F.A. (1967). Intestinal folate conjugase activity in tropical sprue. Am J Clin Nutr *20*, 1004-1009.

Komano, T., Utsumi, R., and Kawamukai, M. (1991). Functional analysis of the fic gene involved in regulation of cell division. Res Microbiol *142*, 269-277.

Kumar, C.K., Moyer, M.P., Dudeja, P.K., and Said, H.M. (1997). A protein-tyrosine kinase-regulated, pH-dependent, carrier-mediated uptake system for folate in human normal colonic epithelial cell line NCM460. J Biol Chem *272*, 6226-6231.

Labrousse, A., Chauvet, S., Couillault, C., Kurz, C.L., and Ewbank, J.J. (2000). Caenorhabditis elegans is a model host for Salmonella typhimurium. Curr Biol *10*, 1543-1545.

Labuschagne, C.F., van den Broek, N.J., Mackay, G.M., Vousden, K.H., and Maddocks, O.D. (2014). Serine, but not glycine, supports one-carbon metabolism and proliferation of cancer cells. Cell Rep *7*, 1248-1258.

Lai, C.H., Chou, C.Y., Ch'ang, L.Y., Liu, C.S., and Lin, W. (2000). Identification of novel human genes evolutionarily conserved in Caenorhabditis elegans by comparative proteomics. Genome Res *10*, 703-713.

Lakoff, A., Fazili, Z., Aufreiter, S., Pfeiffer, C.M., Connolly, B., Gregory, J.F., 3rd, Pencharz, P.B., and O'Connor, D.L. (2014). Folate is absorbed across the human colon: evidence by using enteric-coated caplets containing 13C-labeled [6S]-5-formyltetrahydrofolate. Am J Clin Nutr *100*, 1278-1286.

Larsen, P.L., and Clarke, C.F. (2002). Extension of life-span in Caenorhabditis elegans by a diet lacking coenzyme Q. Science *295*, 120-123.

Lascelles, J., and Woods, D.D. (1952). The synthesis of folic acid by Bacterium coll and Staphylococcus aureus and its inhibition by sulphonamides. Br J Exp Pathol *33*, 288-303.

Lassenius, M.I., Pietilainen, K.H., Kaartinen, K., Pussinen, P.J., Syrjanen, J., Forsblom, C., Porsti, I., Rissanen, A., Kaprio, J., Mustonen, J.*, et al.* (2011). Bacterial endotoxin activity in human serum is associated with dyslipidemia, insulin resistance, obesity, and chronic inflammation. Diabetes Care *34*, 1809-1815.

LeBlanc, J.G., Milani, C., de Giori, G.S., Sesma, F., van Sinderen, D., and Ventura, M. (2013). Bacteria as vitamin suppliers to their host: a gut microbiota perspective. Curr Opin Biotechnol *24*, 160-168.

Lederberg, J., and McCray, A.T. (2001). 'Ome sweet 'omics - A genealogical treasury of words. Scientist *15*, 8-8.

Lee, H.Y., Cho, S.A., Lee, I.S., Park, J.H., Seok, S.H., Baek, M.W., Kim, D.J., Lee, S.H., Hur, S.J., Ban, S.J.*, et al.* (2007). Evaluation of phoP and rpoS mutants of Salmonella enterica serovar Typhi as attenuated typhoid vaccine candidates: virulence and protective immune responses in intranasally immunized mice. FEMS Immunol Med Microbiol *51*, 310-318.

Lee, S.J., and Kenyon, C. (2009). Regulation of the longevity response to temperature by thermosensory neurons in Caenorhabditis elegans. Curr Biol *19*, 715-722.

Ley, R.E., Backhed, F., Turnbaugh, P., Lozupone, C.A., Knight, R.D., and Gordon, J.I. (2005). Obesity alters gut microbial ecology. Proc Natl Acad Sci U S A *102*, 11070-11075.

Ley, R.E., Turnbaugh, P.J., Klein, S., and Gordon, J.I. (2006). Microbial ecology: human gut microbes associated with obesity. Nature *444*, 1022-1023.

Lozupone, C.A., and Knight, R. (2007). Global patterns in bacterial diversity. Proc Natl Acad Sci U S A *104*, 11436-11440.

Lu, W., Kwon, Y.K., and Rabinowitz, J.D. (2007). Isotope ratio-based profiling of microbial folates. J Am Soc Mass Spectrom *18*, 898-909.

Lucock, M. (2000). Folic acid: nutritional biochemistry, molecular biology, and role in disease processes. Mol Genet Metab *71*, 121-138.

Lunt, S.Y., and Vander Heiden, M.G. (2011). Aerobic glycolysis: meeting the metabolic requirements of cell proliferation. Annu Rev Cell Dev Biol *27*, 441-464.

Ma, T.Y., Hollander, D., Dadufalza, V., and Krugliak, P. (1992). Effect of aging and caloric restriction on intestinal permeability. Exp Gerontol *27*, 321-333.

Macfarlane, S., and Macfarlane, G.T. (2003). Regulation of short-chain fatty acid production. Proc Nutr Soc *62*, 67-72.

Madsen, J.L., and Graff, J. (2004). Effects of ageing on gastrointestinal motor function. Age Ageing *33*, 154-159.

Magnusdottir, S., Ravcheev, D., de Crecy-Lagard, V., and Thiele, I. (2015). Systematic genome assessment of B-vitamin biosynthesis suggests co-operation among gut microbes. Front Genet *6*, 148.

Marchesi, J.R., Adams, D.H., Fava, F., Hermes, G.D., Hirschfield, G.M., Hold, G., Quraishi, M.N., Kinross, J., Smidt, H., Tuohy, K.M.*, et al.* (2016). The gut microbiota and host health: a new clinical frontier. Gut *65*, 330-339.

Marchesi, J.R., and Ravel, J. (2015). The vocabulary of microbiome research: a proposal. Microbiome *3*, 31.

Marean, A., Graf, A., Zhang, Y., and Niswander, L. (2011). Folic acid supplementation can adversely affect murine neural tube closure and embryonic survival. Hum Mol Genet *20*, 3678-3683.

Maruyama, T., Shiota, T., and Krumdieck, C.L. (1978). The oxidative cleavage of folates. A critical study. Anal Biochem *84*, 277-295.

Mason, J.B., Dickstein, A., Jacques, P.F., Haggarty, P., Selhub, J., Dallal, G., and Rosenberg, I.H. (2007). A temporal association between folic acid fortification and an increase in colorectal cancer rates may be illuminating important biological principles: a hypothesis. Cancer Epidemiol Biomarkers Prev *16*, 1325-1329.

Matherly, L.H., and Goldman, D.I. (2003). Membrane transport of folates. Vitam Horm *66*, 403-456.

McDowell, M.A., Lacher, D.A., Pfeiffer, C.M., Mulinare, J., Picciano, M.F., Rader, J.I., Yetley, E.A., Kennedy-Stephenson, J., and Johnson, C.L. (2008). Blood folate levels: the latest NHANES results. NCHS Data Brief, 1-8.

Meadows, S. (2017). Multiplex Measurement of Serum Folate Vitamers by UPLC-MS/MS. Methods Mol Biol *1546*, 245-256.

Meiser, J., Tumanov, S., Maddocks, O., Labuschagne, C.F., Athineos, D., Van Den Broek, N., Mackay, G.M., Gottlieb, E., Blyth, K., Vousden, K.*, et al.* (2016). Serine one-carbon catabolism with formate overflow. Sci Adv *2*, e1601273.

Melo, J.A., and Ruvkun, G. (2012). Inactivation of conserved C. elegans genes engages pathogen- and xenobiotic-associated defenses. Cell *149*, 452-466.

Mendelsohn, L.G., Gates, S.B., Habeck, L.L., Shackelford, K.A., Worzalla, J., Shih, C., and Grindey, G.B. (1996). The role of dietary folate in modulation of folate receptor

expression, folylpolyglutamate synthetase activity and the efficacy and toxicity of lometrexol. Adv Enzyme Regul *36*, 365-381.

Miller, D.K., and Rekate, A.C. (1944). Inhibition of Growth of Mycobacterium Tuberculosis by a Mold. Science *100*, 172-173.

Miller, H.T., and Luckey, T.D. (1963). Intestinal Synthesis of Folic Acid in Monoflora Chicks. Journal of Nutrition *80*, 236-&.

Milman, N. (2012). Intestinal absorption of folic acid - new physiologic & molecular aspects. Indian J Med Res *136*, 725-728.

Milne, D.B., Canfield, W.K., Mahalko, J.R., and Sandstead, H.H. (1984). Effect of oral folic acid supplements on zinc, copper, and iron absorption and excretion. Am J Clin Nutr *39*, 535-539.

Mitchell, H.K., Snell, E.E., and Williams, R.J. (1941). The concentration of "folic acid". Journal of the American Chemical Society *63*, 2284-2284.

Monod, J. (1949). The Growth of Bacterial Cultures. Annual Review of Microbiology *3*, 371-394.

Mudryj, A.N., de Groh, M., Aukema, H.M., and Yu, N. (2016). Folate intakes from diet and supplements may place certain Canadians at risk for folic acid toxicity. Br J Nutr *116*, 1236-1245.

Mukhopadhya, I., Hansen, R., El-Omar, E.M., and Hold, G.L. (2012). IBD-what role do Proteobacteria play? Nat Rev Gastroenterol Hepatol *9*, 219-230.

Murphy, E.F., Cotter, P.D., Healy, S., Marques, T.M., O'Sullivan, O., Fouhy, F., Clarke, S.F., O'Toole, P.W., Quigley, E.M., Stanton, C.*, et al.* (2010). Composition and energy harvesting capacity of the gut microbiota: relationship to diet, obesity and time in mouse models. Gut *59*, 1635-1642.

Nagao-Kitamoto, H., Shreiner, A.B., Gillilland, M.G., 3rd, Kitamoto, S., Ishii, C., Hirayama, A., Kuffa, P., El-Zaatari, M., Grasberger, H., Seekatz, A.M.*, et al.* (2016). Functional Characterization of Inflammatory Bowel Disease-Associated Gut Dysbiosis in Gnotobiotic Mice. Cell Mol Gastroenterol Hepatol *2*, 468-481.

Navab-Moghadam, F., Sedighi, M., Khamseh, M.E., Alaei-Shahmiri, F., Talebi, M., Razavi, S., and Amirmozafari, N. (2017). The association of type II diabetes with gut microbiota composition. Microb Pathog *110*, 630-636.

Nemes, R.M., Pop, C.S., Calagiu, D., Dobrin, D., Chetroiu, D., Jantea, P., and Postolache, P. (2016). Anemia in Inflammatory Bowel Disease More Than an Extraintestinal Complication. Rev Med Chir Soc Med Nat Iasi *120*, 34-39.

Niven, C.F., and Sherman, J.M. (1944). Nutrition of the Enterococci. J Bacteriol *47*, 335-342.

O'Keefe, S.J., Ou, J., Aufreiter, S., O'Connor, D., Sharma, S., Sepulveda, J., Fukuwatari, T., Shibata, K., and Mawhinney, T. (2009). Products of the colonic microbiota mediate the effects of diet on colon cancer risk. J Nutr *139*, 2044-2048.

Ochsner, U.A., Snyder, A., Vasil, A.I., and Vasil, M.L. (2002). Effects of the twin-arginine translocase on secretion of virulence factors, stress response, and pathogenesis. Proc Natl Acad Sci U S A *99*, 8312-8317.

Ortbauer, M., Ripper, D., Fuhrmann, T., Lassi, M., Auernigg-Haselmaier, S., Stiegler, C., and Konig, J. (2016). Folate deficiency and over-supplementation causes impaired folate metabolism: Regulation and adaptation mechanisms in Caenorhabditis elegans. Mol Nutr Food Res *60*, 949-956.

Osborn, M.J., Talbert, P.T., and Huennekens, F.M. (1960). The Structure of Active Formaldehyde (N-5,N-10-Methylene Tetrahydrofolic Acid). Journal of the American Chemical Society *82*, 4921-4927.

Patten, C.L., Kirchhof, M.G., Schertzberg, M.R., Morton, R.A., and Schellhorn, H.E. (2004). Microarray analysis of RpoS-mediated gene expression in Escherichia coli K-12. Mol Genet Genomics *272*, 580-591.

Patzer, S.I., and Hantke, K. (1998). The ZnuABC high-affinity zinc uptake system and its regulator Zur in Escherichia coli. Mol Microbiol *28*, 1199-1210.

Pauli, F., Liu, Y., Kim, Y.A., Chen, P.J., and Kim, S.K. (2006). Chromosomal clustering and GATA transcriptional regulation of intestine-expressed genes in C. elegans. Development *133*, 287-295.

Pereira, F.C., and Berry, D. (2017). Microbial nutrient niches in the gut. Environ Microbiol *19*, 1366-1378.

Pickell, L., Brown, K., Li, D., Wang, X.L., Deng, L., Wu, Q., Selhub, J., Luo, L., Jerome-Majewska, L., and Rozen, R. (2011). High intake of folic acid disrupts embryonic development in mice. Birth Defects Res A Clin Mol Teratol *91*, 8-19.

Pietrzik, K., Bailey, L., and Shane, B. (2010). Folic acid and L-5-methyltetrahydrofolate: comparison of clinical pharmacokinetics and pharmacodynamics. Clin Pharmacokinet *49*, 535-548.

Portal-Celhay, C., Bradley, E.R., and Blaser, M.J. (2012). Control of intestinal bacterial proliferation in regulation of lifespan in Caenorhabditis elegans. BMC Microbiol *12*, 49.

Preziosi, M.J., Kandel, S.M., Guiney, D.G., and Browne, S.H. (2012). Microbiological analysis of nontyphoidal Salmonella strains causing distinct syndromes of bacteremia or enteritis in HIV/AIDS patients in San Diego, California. J Clin Microbiol *50*, 3598-3603.

Pujol, N., Cypowyj, S., Ziegler, K., Millet, A., Astrain, A., Goncharov, A., Jin, Y., Chisholm, A.D., and Ewbank, J.J. (2008). Distinct innate immune responses to infection and wounding in the C. elegans epidermis. Curr Biol *18*, 481-489.

Qi, H., Atkinson, I., Xiao, S., Choi, Y.J., Tobimatsu, T., and Shane, B. (1999). Folylpoly-gamma-glutamate synthetase: generation of isozymes and the role in one carbon metabolism and antifolate cytotoxicity. Adv Enzyme Regul *39*, 263-273.

Qin, J., Li, R., Raes, J., Arumugam, M., Burgdorf, K.S., Manichanh, C., Nielsen, T., Pons, N., Levenez, F., Yamada, T.*, et al.* (2010). A human gut microbial gene catalogue established by metagenomic sequencing. Nature *464*, 59-65.

Qin, T., Du, M., Du, H., Shu, Y., Wang, M., and Zhu, L. (2015). Folic acid supplements and colorectal cancer risk: meta-analysis of randomized controlled trials. Sci Rep *5*, 12044.

Qiu, A., Jansen, M., Sakaris, A., Min, S.H., Chattopadhyay, S., Tsai, E., Sandoval, C., Zhao, R., Akabas, M.H., and Goldman, I.D. (2006). Identification of an intestinal folate transporter and the molecular basis for hereditary folate malabsorption. Cell *127*, 917-928.

Rabot, S., Membrez, M., Bruneau, A., Gerard, P., Harach, T., Moser, M., Raymond, F., Mansourian, R., and Chou, C.J. (2010). Germ-free C57BL/6J mice are resistant to high-fat-diet-induced insulin resistance and have altered cholesterol metabolism. FASEB J *24*, 4948-4959.

Rera, M., Bahadorani, S., Cho, J., Koehler, C.L., Ulgherait, M., Hur, J.H., Ansari, W.S., Lo, T., Jr., Jones, D.L., and Walker, D.W. (2011). Modulation of longevity and tissue homeostasis by the Drosophila PGC-1 homolog. Cell Metab *14*, 623-634.

Ringling, C., and Rychlik, M. (2017). Origins of the difference between food folate analysis results obtained by LC-MS/MS and microbiological assays. Anal Bioanal Chem *409*, 1815-1825.

Rocha, D.J., Santos, C.S., and Pacheco, L.G. (2015). Bacterial reference genes for gene expression studies by RT-qPCR: survey and analysis. Antonie Van Leeuwenhoek *108*, 685-693.

Rong, N., Selhub, J., Goldin, B.R., and Rosenberg, I.H. (1991). Bacterially synthesized folate in rat large intestine is incorporated into host tissue folyl polyglutamates. J Nutr *121*, 1955-1959.

Rossi, M., Amaretti, A., and Raimondi, S. (2011). Folate production by probiotic bacteria. Nutrients *3*, 118-134.

Sack, D.M., and Peppercorn, M.A. (1983). Drug therapy of inflammatory bowel disease. Pharmacotherapy *3*, 158-176.

Saiki, R., Lunceford, A.L., Bixler, T., Dang, P., Lee, W., Furukawa, S., Larsen, P.L., and Clarke, C.F. (2008). Altered bacterial metabolism, not coenzyme Q content, is responsible for the lifespan extension in Caenorhabditis elegans fed an Escherichia coli diet lacking coenzyme Q. Aging Cell *7*, 291-304.

Samuel, B.S., Rowedder, H., Braendle, C., Felix, M.A., and Ruvkun, G. (2016). Caenorhabditis elegans responses to bacteria from its natural habitats. Proc Natl Acad Sci U S A *113*, E3941-3949.

Sanchez-Blanco, A., and Kim, S.K. (2011). Variable pathogenicity determines individual lifespan in Caenorhabditis elegans. PLoS Genet *7*, e1002047.

Sargent, F., Gohlke, U., De Leeuw, E., Stanley, N.R., Palmer, T., Saibil, H.R., and Berks, B.C. (2001). Purified components of the Escherichia coli Tat protein transport system form a double-layered ring structure. Eur J Biochem *268*, 3361-3367.

Schirch, V., and Strong, W.B. (1989). Interaction of folylpolyglutamates with enzymes in one-carbon metabolism. Arch Biochem Biophys *269*, 371-380.

Schulenburg, H., Hoeppner, M.P., Weiner, J., 3rd, and Bornberg-Bauer, E. (2008). Specificity of the innate immune system and diversity of C-type lectin domain (CTLD) proteins in the nematode Caenorhabditis elegans. Immunobiology *213*, 237-250.

Sculthorpe, N.F., Davies, B., Ashton, T., Allison, S., McGuire, D.N., and Malhi, J.S. (2001). Commercially available folic acid supplements and their compliance with the British Pharmacopoeia test for dissolution. J Public Health Med *23*, 195-197.

Selhub, J., Morris, M.S., Jacques, P.F., and Rosenberg, I.H. (2009). Folate-vitamin B-12 interaction in relation to cognitive impairment, anemia, and biochemical indicators of vitamin B-12 deficiency. Am J Clin Nutr *89*, 702S-706S.

Seputiene, V., Daugelavicius, A., Suziedelis, K., and Suziedeliene, E. (2006). Acid response of exponentially growing Escherichia coli K-12. Microbiol Res *161*, 65-74.

Seydel, J.K. (1968). Sulfonamides, structure-activity relationship, and mode of action. Structural problems of the antibacterial action of 4-aminobenzoic acid (PABA) antagonists. J Pharm Sci *57*, 1455-1478.

Shafquat, A., Joice, R., Simmons, S.L., and Huttenhower, C. (2014). Functional and phylogenetic assembly of microbial communities in the human microbiome. Trends Microbiol *22*, 261-266.

Shane, B. (2003). Folate fortification: enough already? Am J Clin Nutr *77*, 8-9.

Shane, B., and Stokstad, E.L. (1975). Transport and metabolism of folates by bacteria. J Biol Chem *250*, 2243-2253.

Shane, B., Tamura, T., and Stokstad, E.L. (1980). Folate assay: a comparison of radioassay and microbiological methods. Clin Chim Acta *100*, 13-19.

Shen, T., Na, S., Yu, G., Xie, J., and Jia, P. (1997). [Cloning and expression of the E. coli serine hydroxymethyltransferase gene (glyA)]. Wei Sheng Wu Xue Bao *37*, 423-428.

Shin, N.R., Whon, T.W., and Bae, J.W. (2015). Proteobacteria: microbial signature of dysbiosis in gut microbiota. Trends Biotechnol *33*, 496-503.

Shtonda, B.B., and Avery, L. (2006). Dietary choice behavior in Caenorhabditis elegans. J Exp Biol *209*, 89-102.

Smith, S.G., Mahon, V., Lambert, M.A., and Fagan, R.P. (2007). A molecular Swiss army knife: OmpA structure, function and expression. FEMS Microbiol Lett *273*, 1-11.

Stanger, F.V., Harms, A., Dehio, C., and Schirmer, T. (2016). Crystal Structure of the Escherichia coli Fic Toxin-Like Protein in Complex with Its Cognate Antitoxin. PLoS One *11*, e0163654.

Stover, P., and Schirch, V. (1991). 5-Formyltetrahydrofolate polyglutamates are slow tight binding inhibitors of serine hydroxymethyltransferase. J Biol Chem *266*, 1543-1550.

Stover, P., and Schirch, V. (1993). The metabolic role of leucovorin. Trends Biochem Sci *18*, 102-106.

Strong, W.B., and Schirch, V. (1989). In vitro conversion of formate to serine: effect of tetrahydropteroylpolyglutamates and serine hydroxymethyltransferase on the rate of 10-formyltetrahydrofolate synthetase. Biochemistry *28*, 9430-9439.

Stulke, J., and Hillen, W. (1999). Carbon catabolite repression in bacteria. Curr Opin Microbiol *2*, 195-201.

Stupp, G.S., von Reuss, S.H., Izrayelit, Y., Ajredini, R., Schroeder, F.C., and Edison, A.S. (2013). Chemical detoxification of small molecules by Caenorhabditis elegans. ACS Chem Biol *8*, 309-313.

Suh, S.J., Silo-Suh, L., Woods, D.E., Hassett, D.J., West, S.E., and Ohman, D.E. (1999). Effect of rpoS mutation on the stress response and expression of virulence factors in Pseudomonas aeruginosa. J Bacteriol *181*, 3890-3897.

Suh, Y., Atzmon, G., Cho, M.O., Hwang, D., Liu, B., Leahy, D.J., Barzilai, N., and Cohen, P. (2008). Functionally significant insulin-like growth factor I receptor mutations in centenarians. Proc Natl Acad Sci U S A *105*, 3438-3442.

Swinson, C.M., Perry, J., Lumb, M., and Levi, A.J. (1981). Role of sulphasalazine in the aetiology of folate deficiency in ulcerative colitis. Gut *22*, 456-461.

Sybesma, W., Starrenburg, M., Tijsseling, L., Hoefnagel, M.H., and Hugenholtz, J. (2003). Effects of cultivation conditions on folate production by lactic acid bacteria. Appl Environ Microbiol *69*, 4542-4548.

Tamboli, C.P., Neut, C., Desreumaux, P., and Colombel, J.F. (2004). Dysbiosis in inflammatory bowel disease. Gut *53*, 1-4.

Tamura, T., Romero, J.J., Watson, J.E., Gong, E.J., and Halsted, C.H. (1981). Hepatic folate metabolism in the chronic alcoholic monkey. J Lab Clin Med *97*, 654-661.

Tanaka, K., Takayanagi, Y., Fujita, N., Ishihama, A., and Takahashi, H. (1993). Heterogeneity of the principal sigma factor in Escherichia coli: the rpoS gene product, sigma 38, is a second principal sigma factor of RNA polymerase in stationary-phase Escherichia coli. Proc Natl Acad Sci U S A *90*, 3511-3515.

Tedeschi, P.M., Markert, E.K., Gounder, M., Lin, H., Dvorzhinski, D., Dolfi, S.C., Chan, L.L., Qiu, J., DiPaola, R.S., Hirshfield, K.M.*, et al.* (2013). Contribution of serine, folate and glycine metabolism to the ATP, NADPH and purine requirements of cancer cells. Cell Death Dis *4*, e877.

Thiaville, J.J., Frelin, O., Garcia-Salinas, C., Harrison, K., Hasnain, G., Horenstein, N.A., Diaz de la Garza, R.I., Henry, C.S., Hanson, A.D., and de Crecy-Lagard, V. (2016). Experimental and Metabolic Modeling Evidence for a Folate-Cleaving Side-Activity of Ketopantoate Hydroxymethyltransferase (PanB). Front Microbiol *7*, 431.

Tibbetts, A.S., and Appling, D.R. (2010). Compartmentalization of Mammalian folate-mediated one-carbon metabolism. Annu Rev Nutr *30*, 57-81.

Tran, L., and Greenwood-Van Meerveld, B. (2013). Age-associated remodeling of the intestinal epithelial barrier. J Gerontol A Biol Sci Med Sci *68*, 1045-1056.

Tran, P.V., Bannor, T.A., Doktor, S.Z., and Nichols, B.P. (1990). Chromosomal organization and expression of Escherichia coli pabA. J Bacteriol *172*, 397-410.

Tran, P.V., and Nichols, B.P. (1991). Expression of Escherichia coli pabA. J Bacteriol *173*, 3680-3687.

Trausch, J.J., Ceres, P., Reyes, F.E., and Batey, R.T. (2011). The structure of a tetrahydrofolate-sensing riboswitch reveals two ligand binding sites in a single aptamer. Structure *19*, 1413-1423.

Tropini, C., Earle, K.A., Huang, K.C., and Sonnenburg, J.L. (2017). The Gut Microbiome: Connecting Spatial Organization to Function. Cell Host Microbe *21*, 433-442.

Truttmann, M.C., Cruz, V.E., Guo, X., Engert, C., Schwartz, T.U., and Ploegh, H.L. (2016). The Caenorhabditis elegans Protein FIC-1 Is an AMPylase That Covalently Modifies Heat-Shock 70 Family Proteins, Translation Elongation Factors and Histones. PLoS Genet *12*, e1006023.

Turnbaugh, P.J., Backhed, F., Fulton, L., and Gordon, J.I. (2008). Diet-induced obesity is linked to marked but reversible alterations in the mouse distal gut microbiome. Cell Host Microbe *3*, 213-223.

Turnbaugh, P.J., Hamady, M., Yatsunenko, T., Cantarel, B.L., Duncan, A., Ley, R.E., Sogin, M.L., Jones, W.J., Roe, B.A., Affourtit, J.P.*, et al.* (2009). A core gut microbiome in obese and lean twins. Nature *457*, 480-484.

Turner, F.B., Andreassi 2nd, J.L., Ferguson, J., Titus, S., Tse, A., Taylor, S.M., and Moran, R.G. (1999). Tissue-specific expression of functional isoforms of mouse folypoly-gamma-glutamae synthetase: a basis for targeting folate antimetabolites. Cancer Res *59*, 6074-6079.

Uhlich, G.A., Keen, J.E., and Elder, R.O. (2002). Variations in the csgD promoter of Escherichia coli O157:H7 associated with increased virulence in mice and increased invasion of HEp-2 cells. Infect Immun *70*, 395-399.

Uno, M., and Nishida, E. (2016). Lifespan-regulating genes in C. elegans. NPJ Aging Mech Dis *2*, 16010.

Utsumi, R., Nakamoto, Y., Kawamukai, M., Himeno, M., and Komano, T. (1982). Involvement of cyclic AMP and its receptor protein in filamentation of an Escherichia coli fic mutant. J Bacteriol *151*, 807-812.

Vijayakumar, S.R., Kirchhof, M.G., Patten, C.L., and Schellhorn, H.E. (2004). RpoS-regulated genes of Escherichia coli identified by random lacZ fusion mutagenesis. J Bacteriol *186*, 8499-8507.

Vindigni, S.M., Zisman, T.L., Suskind, D.L., and Damman, C.J. (2016). The intestinal microbiome, barrier function, and immune system in inflammatory bowel disease: a tripartite pathophysiological circuit with implications for new therapeutic directions. Therap Adv Gastroenterol *9*, 606-625.

Virk, B., Correia, G., Dixon, D.P., Feyst, I., Jia, J., Oberleitner, N., Briggs, Z., Hodge, E., Edwards, R., Ward, J.*, et al.* (2012). Excessive folate synthesis limits lifespan in the C. elegans: E. coli aging model. BMC Biol *10*, 67.

Virk, B., Jia, J., Maynard, C.A., Raimundo, A., Lefebvre, J., Richards, S.A., Chetina, N., Liang, Y., Helliwell, N., Cipinska, M.*, et al.* (2016). Folate Acts in E. coli to Accelerate C. elegans Aging Independently of Bacterial Biosynthesis. Cell Rep *14*, 1611-1620.

Visentin, M., Diop-Bove, N., Zhao, R., and Goldman, I.D. (2014). The intestinal absorption of folates. Annu Rev Physiol *76*, 251-274.

Wakeman, C.A., Winkler, W.C., and Dann, C.E., 3rd (2007). Structural features of metabolite-sensing riboswitches. Trends Biochem Sci *32*, 415-424.

Weber, H., Polen, T., Heuveling, J., Wendisch, V.F., and Hengge, R. (2005). Genome-wide analysis of the general stress response network in Escherichia coli: sigmaS-dependent genes, promoters, and sigma factor selectivity. J Bacteriol *187*, 1591-1603.

Whetstine, J.R., Flatley, R.M., and Matherly, L.H. (2002). The human reduced folate carrier gene is ubiquitously and differentially expressed in normal human tissues: identification of seven non-coding exons and characterization of a novel promoter. Biochem J *367*, 629-640.

Wilf, N.M., and Salmond, G.P. (2012). The stationary phase sigma factor, RpoS, regulates the production of a carbapenem antibiotic, a bioactive prodigiosin and virulence in the enterobacterial pathogen Serratia sp. ATCC 39006. Microbiology *158*, 648-658.

Williams, B.L., Hornig, M., Buie, T., Bauman, M.L., Cho Paik, M., Wick, I., Bennett, A., Jabado, O., Hirschberg, D.L., and Lipkin, W.I. (2011). Impaired carbohydrate digestion and transport and mucosal dysbiosis in the intestines of children with autism and gastrointestinal disturbances. PLoS One *6*, e24585.

Williams, G.C. (1957). Pleiotropy, Natural-Selection, and the Evolution of Senescence. Evolution *11*, 398-411.

Wills, L. (1931). Treatment of "Pernicious Anaemia of Pregnancy" and "Tropical Anaemia". Br Med J *1*, 1059-1064.

Winkelmayer, W.C., Eberle, C., Sunder-Plassmann, G., and Fodinger, M. (2003). Effects of the glutamate carboxypeptidase II (GCP2 1561C>T) and reduced folate carrier (RFC1 80G>A) allelic variants on folate and total homocysteine levels in kidney transplant patients. Kidney Int *63*, 2280-2285.

Woolery, A.R., Luong, P., Broberg, C.A., and Orth, K. (2010). AMPylation: Something Old is New Again. Front Microbiol *1*, 113.

Worby, C.A., Mattoo, S., Kruger, R.P., Corbeil, L.B., Koller, A., Mendez, J.C., Zekarias, B., Lazar, C., and Dixon, J.E. (2009). The fic domain: regulation of cell signaling by adenylylation. Mol Cell *34*, 93-103.

Wright, A.J., Finglas, P.M., Dainty, J.R., Hart, D.J., Wolfe, C.A., Southon, S., and Gregory, J.F. (2003). Single oral doses of 13C forms of pteroylmonoglutamic acid and 5-formyltetrahydrofolic acid elicit differences in short-term kinetics of labelled and unlabelled folates in plasma: potential problems in interpretation of folate bioavailability studies. Br J Nutr *90*, 363-371.

Wright, A.J., Finglas, P.M., Dainty, J.R., Wolfe, C.A., Hart, D.J., Wright, D.M., and Gregory, J.F. (2005). Differential kinetic behavior and distribution for pteroylglutamic acid and reduced folates: a revised hypothesis of the primary site of PteGlu metabolism in humans. J Nutr *135*, 619-623.

Xiong, H., Pears, C., and Woollard, A. (2017). An enhanced C. elegans based platform for toxicity assessment. Sci Rep *7*, 9839.

Yatsunenko, T., Rey, F.E., Manary, M.J., Trehan, I., Dominguez-Bello, M.G., Contreras, M., Magris, M., Hidalgo, G., Baldassano, R.N., Anokhin, A.P.*, et al.* (2012). Human gut microbiome viewed across age and geography. Nature *486*, 222-227.

Yildiz, F.H., and Schoolnik, G.K. (1998). Role of rpoS in stress survival and virulence of Vibrio cholerae. J Bacteriol *180*, 773-784.

Zakin, M.M., Duchange, N., Ferrara, P., and Cohen, G.N. (1983). Nucleotide sequence of the metL gene of Escherichia coli. Its product, the bifunctional aspartokinase ii-homoserine dehydrogenase II, and the bifunctional product of the thrA gene, aspartokinase I-homoserine dehydrogenase I, derive from a common ancestor. J Biol Chem *258*, 3028-3031.

Zhang, F., Berg, M., Dierking, K., Felix, M.A., Shapira, M., Samuel, B.S., and Schulenburg, H. (2017). Caenorhabditis elegans as a Model for Microbiome Research. Front Microbiol *8*, 485.

Zhang, Y. (2008). Neuronal mechanisms of Caenorhabditis elegans and pathogenic bacteria interactions. Curr Opin Microbiol *11*, 257-261.

Zhao, R., Min, S.H., Wang, Y., Campanella, E., Low, P.S., and Goldman, I.D. (2009). A role for the proton-coupled folate transporter (PCFT-SLC46A1) in folate receptor-mediated endocytosis. J Biol Chem *284*, 4267-4274.